Possibility of Measuring the CP of a Higgs Boson at the LHC

Kari Ertresvåg Myklevoll

Cand. Scient. Thesis in Theoretical Particle Physics

Department of Physics
University of Bergen

May 2002

Acknowledgements

First of all I would like to thank my supervisor Per Osland, for his invaluable help with all problems I encountered during the work with this thesis, be it related to physics, to computers or to English grammar.

Next I want to thank my supervisor during my stay of one month in Lund, Torbjörn Sjöstrand. This was a very instructive month for me, and I learned a lot about Monte Carlo simulation and programming, as well as physics. The stay in Lund was made possible through financial support from *Nordic network "Discovery Physics at the LHC"*.

I also have to thank Anne Grete Frodesen for helpful discussions concerning statistics.

Thank you very much to my fellow students, here in Bergen, and also to the people I got to know in Lund. They have helped with moral support and discussions concerning physics, as well as orthography and computer problems.

Last but not least, I want to thank my wonderful family, my friends and my boyfriend Mathias for their love and support.

Contents

Chapter 1

Introduction

The Standard Model of elementary particle physics (SM) has been experimentally confirmed to a very high degree of accuracy [1]. There are nevertheless still some sectors of it that have not been confirmed through experiments, and among these is the origin of electroweak symmetry breaking. In the Standard Electroweak Theory by Glashow, Salam and Weinberg [2, 3], the $\mathrm{SU}(2)_L \times \mathrm{U}(1)_Y$ symmetry is broken down to the electromagnetic $U(1)_{EM}$, and at the same time the weak gauge bosons $W^{\pm}$ and Z acquire masses, while the photon remains massless.

Electroweak symmetry is broken through spontaneous symmetry breaking. This is caused by a scalar field with nonzero vacuum expectation value. The scalar field is a complex SU(2) doublet which couples to electroweak gauge bosons and to fermions. The field has got four degrees of freedom. Three of these, representing so-called Goldstone bosons, are transformed into longitudinal components of the vector bosons $W^{\pm}$ and Z, and the vector bosons thereby acquire masses. Goldstone bosons are unphysical massless spin-zero bosons that are created by spontaneous symmetry breaking. The fourth degree of freedom is a real scalar field that represents a neutral spin-zero particle called the Higgs boson.

The SM Higgs boson has got the quantum numbers $J^{PC} = 0^{++}$. Here J is the total intrinsic spin of the particle, and C and P denote the transformation properties under charge conjugation, C, and space inversion or parity, P. Under a C transformation, all particles are exchanged with their antiparticles, and under a P transformation all vectors $\mathbf{x}$ are exchanged with $-\mathbf{x}$. We say that the SM Higgs is a scalar particle, or a CP-even particle, because it does not change sign under a combined CP transformation.

Electroweak theory does not conserve C and P separately when fermion terms are included in the Lagrangian density. This means that the Lagrangian *changes form*, under a C or P transformation. Under a combined CP transformation, on the other hand, the Lagrangian density is *almost* unchanged. We say that CP is weakly broken in the Standard Electroweak Theory. I will get back to CP violation in the next chapter.

The only free parameter of the SM Higgs sector is the mass m_h of the Higgs boson. If the mass of the Higgs boson is known, all its other properties are fixed. An upper limit on the Higgs mass can be deduced from the energy range Λ up to which the theory is valid

[4]. Beyond this energy, the perturbative expansion of the theory breaks down. If the mass of the Higgs boson is less than approximately 200 GeV the SM could be valid up to the energy $\Lambda \sim 10^{16}$ GeV, which is called the grand unified theory scale (GUT).

In addition, the LEP Electroweak working group has quoted an upper limit on the Higgs mass from a global SM fit to electroweak precision data as a function of the Higgs mass: $m_h < 196$ GeV at 95% confidence level (CL) [5]. The experimental lower limit on the SM Higgs mass is at the moment $m_h > 114.1$ GeV at 95% CL [5].

The Higgs sector of the SM is only the simplest example of a model for electroweak symmetry breaking. In extended models there can exist more than one Higgs boson [4], and in some models there is no fundamental Higgs boson at all, but composite Higgs particles. One group of extended models are the *Two-Higgs-Doublet Models* (2HDM). Here there are two complex scalar SU(2) doublets. The eight degrees of freedom give rise to three Goldstone bosons, two neutral Higgs bosons with $J^{PC} = 0^{++}$, h and H, one neutral Higgs bosons with $J^{PC} = 0^{+-}$, A, and two charged Higgs bosons $H^{\pm}$, all spin-zero particles [4]. The boson A is also denoted a pseudoscalar, or a CP-odd particle, because its wave function changes sign under a CP transformation. With a certain choice of the parameters of a 2HDM, the three neutral Higgs bosons will not be eigenstates of CP, but mixtures of CP-even and CP-odd states [6]. The Minimal Supersymmetric extension of the Standard Model (MSSM), which is the simplest example of a realistic supersymmetric theory, is an example of a 2HDM model.

One of the main goals of the next generation of accelerators is to investigate the Higgs sector. If a Higgs boson is discovered, it is important to examine its properties in addition to mass: production and decay rates, charge, spin, CP-properties, couplings to gauge bosons and fermions, and self couplings.

Several methods have been suggested in order to measure the CP-properties of a discovered Higgs boson. Depending on what model is assumed and the range of Higgs masses that is studied, different strategies have to be used.

CP-even and CP-odd Higgs bosons couple differently to vector bosons and fermions. Each CP-state leads to distinct polarisation and spin states for the decay products. The distributions of decay angles for secondary decay products also depend on the CP of the Higgs boson. This is similar to the classical method to determine the CP of the π^0 meson [7].

Angular distributions in the decay channel

$$H \to VV^{(*)} \to f_1\bar{f}_2 f_3 \bar{f}_4 \,, \tag{1.1}$$

for $VV = WW, ZZ$, and in decays to fermions, $H \to \tau^+\tau^- \to \pi^+\bar{\nu}\pi^-\nu$ and $H \to t\bar{t} \to (bW^+) + (\bar{b}W^-)$, have been suggested in order to measure the CP-state of a discovered Higgs boson [9–14]. Which decay mode is optimal depends on the Higgs mass and on the background. Hadron colliders have larger QCD backgrounds than e^+e^- colliders. The decay to weak vector bosons have a small rate for Higgs masses below the threshold for production of real vector bosons, $m_h \sim 160$ GeV.

The production process $\gamma\gamma \to H$ with polarised photon beams, and the Bjorken process

$e^+e^- \to HZ$ have also been suggested as suitable for determining the CP-property of a Higgs boson [13, 14].

In this thesis I have studied angular correlations in the decay (1.1) of a Higgs boson H, that can be either CP-even or CP-odd. This decay mode can be used to determine the CP-properties of a Higgs boson with mass larger than approximately $2m_W$, where m_W is the mass of the W boson, $m_W = 80.4$ GeV.

The upper limit on the Higgs mass quoted by the LEP Electroweak working group, shows that experimental data makes a Higgs boson lighter than 200 GeV most probable. On the other hand, a Higgs boson with mass larger than 200 GeV is not experimentally excluded. Until this is the case, it is still interesting to investigate how to study the properties also of a heavier Higgs boson.

Unfortunately, the decay mode (1.1) can not be used to determine the CP-state of a CP-odd Higgs boson in a model that conserves CP, due to the fact that the AV_1V_2 coupling does not exist at tree level but is induced only through a fermion loop. The decay rate for $A \to V_1V_2$ is thus very small in a CP-conserving theory.

In a theory with CP violation, on the other hand, it is possible to have Higgs bosons which are strongly mixed states of CP-even and CP-odd states [6]. The rate for a CP-odd decay of a mixed state might therefore be larger in such a model. As a first approximation to the study of a model with CP violation, I have performed background studies for the hadron collider LHC, for a simple model with CP conservation, where the decay rate for the decay $A \to V_1V_2$ is comparable to the decay rate for a CP-even Higgs boson.

Other background studies have been performed for the possibility of measuring the CP-properties of a Higgs boson, both for the LHC [15] as well as for an e^+e^- collider [10, 16, 17, 18]. At LHC the QCD background is very large, and this makes studies of many angular distributions difficult. An e^+e^- collider seems to be a better tool to measure the CP-properties of a Higgs boson.

Next, I give an overview of the following chapters in this thesis:

- **Theoretical Background:** The chapter starts with an introduction to the Standard Model. It goes on with describing gauge theories (short) and the Higgs mechanism. The chapter ends with an introduction to CP transformations.

- **The Higgs Decay:** The chapter contains the calculation of the decay rate $\mathrm{d}\Gamma/\mathrm{d}\phi$, for a CP-even and a CP-odd Higgs boson. The calculation involves numerical integration. At the end of the chapter, $\mathrm{d}\Gamma/\mathrm{d}\phi$ is plotted for several values of the Higgs mass.

- **Monte Carlo Studies:** The chapter contains Monte Carlo analyses for the possibility of measuring the CP-property of a Higgs boson at the LHC, assuming a simple model. The Monte Carlo studies are performed using the Monte Carlo program PYTHIA. Plots of several angular distributions for the decay $H \to ZZ \to 4l$ are shown, in addition to the results of the statistical analysis. Most of the plots are placed in an appendix though, due to the large number of them.

- **Conclusion:** The results obtained in the thesis are summarised.

- **Appendix A:** The first appendix contains plots of the correlations for several angular observables.
- **Appendix B:** This appendix contains plots of the results from the statistical analysis.
- **Appendix C:** The third appendix contains the source code of a fortran program which was used for the statistical analysis.

Chapter 2

Theoretical Background

What is the Higgs boson, and why do particle physicists so desperately want to find it? In this section I will give the reader an introduction to the so-called Standard Model of elementary particle physics, and try to explain the point of introducing a Higgs boson. But we will have to start with the beginning. So let us start with answering the question, what are elementary particles?

We believe today that the fundamental building blocks of nature are particles. There are two kinds, the matter particles fermions, and the force carrying particles bosons. Let us start with the matter particles. The best known example of a fermion is the electron, e^-. The electron is believed to be a point particle, which means that it can not be divided into smaller parts and that it has got zero diameter. It belongs to a group of fermions called leptons. There are six leptons in total. The electron neutrino, ν_e, an electrically neutral very light particle, is the other lepton most closely related to the electron. The other four leptons are copies of the electron and the electron neutrino respectively, only that they are heavier. They are called muon, μ, muon neutrino, ν_μ, tau, τ, and tau neutrino, ν_τ. The electron, muon and tau are electrically charged, with charge equal to -1.6×10^{-16} C, and the three neutrinos are all electrically neutral and have small masses compared to the other leptons.

The other group of fundamental fermions are the quarks. Quarks are the kind of particles that build up the protons and neutrons in an atomic nucleus. What separates quarks from leptons is the fact that quarks interact strongly. This means that the strong force, one of the four fundamental forces in nature, affects the quarks but not the leptons. I will get back to the strong force later in this section. There are six distinct quarks like there are six leptons, but in addition quarks have got a property called colour charge (which has nothing to do with the colours we can see). Each of the six quarks come in three different colours, which are often denoted by green, blue and red. Counting the different colours there is actually eighteen types of quarks, six by three. The six different quark types which we call flavour, have got the names down, up, strange, charm, bottom and top. For short we just say d, u, s, c, b and t quarks. Here the d and u quarks are the ones that make up protons and neutrons, and therefore all ordinary matter. The other four quarks are heavier, just as with the leptons. The heaviest quark, the top, has got a mass of about 170

times the mass of the hydrogen atom.

Quarks also have another property which makes them different from the leptons. They are confined. This means that a quark can never exist on its own, but must always be bound with other quarks (or antiquarks) in larger particles which are called hadrons. Protons and neutrons are examples of hadrons. In addition there exist a large number of more rare hadrons, which for instance are produced in particle accelerators or when cosmic radiation hits the earth atmosphere. These are sometimes referred to as the "hadronic zoo". It is the colour charge that makes the quarks confined. One red, one green and one blue quark together give a colour-neutral bound state, and can therefore exist on its own.

Next I introduce the antiparticles. We believe today that all fundamental particles must have a mirror-image antiparticle. There are some particles, though, that are their own antiparticles, for instance the photon. The antiparticle has the same mass as the particle, and it has positive energy, but all its different charges have the opposite sign. The antiparticle of the electron is the positron, e^+. The electron has negative electric charge $-e$, where e is the elementary charge, $e = 1.6 \times 10^{-19}$ Coulomb. The positron, on the other hand, has the electric charge $+e$. In the same manner there exist antiquarks for all quarks, for instance anti-u and anti-d. Antiparticles are often denoted by the name of the particle, but with a bar over it, like $\bar{u}$. The antiquarks can have the colours anti-red, anti-blue and anti-green. A green quark and an anti-green antiquark together give a colourless object, and can therefore exist on its own.

Having introduced the fermions, it is time to say something about the bosons, the force carriers. I will list what is believed to be the four fundamental forces in nature, and name the bosons which are mediating them.

The gravitational force is the most familiar one from daily life. It is described by The General Theory of Relativity, by Albert Einstein. The gravitational force is responsible for us having weight, and for the Earth circling around the Sun. It is the weakest of the four fundamental forces, and the only one which has so far not been described by a quantum field theory. Quantum field theories are the theories we use today to describe the elementary particles and the way they interact with each other via forces. We believe that the gravitational force is mediated by the graviton. This is a boson with spin 2, which has so far never been observed in experiments.

Before we go on I will shortly mention that particle spin is an intrinsic quality of the elementary particles, like for instance charge or mass. But to some degree it gives the particle the same properties as if it were rotating around its own axis, and therefore the name spin. All fermions have half-integer spin, the quarks and leptons have spin 1/2, and all bosons have integer spin.

Next I will say something about the electromagnetic force. The electromagnetic force is responsible for all electric and magnetic phenomena, like for instance electric current, the magnetic field of the earth, which is responsible for the way compasses works, or the forces that keep atoms together. This force is described by the theory Quantum Electrodynamics, short QED, which is a quantum field theory. I will say more about the properties of quantum field theories later in this chapter. For now I will mention that the electromagnetic force acts on all particles with electric charge, which is all quarks, the

charged leptons, and their antiparticles, and some of the bosons which will be introduced later. This force is mediated by photons, the particles which make up light and other electromagnetic waves like radio-waves. The theory QED has been tested to a very high level of precision in experiments, and we believe that it gives a very accurate description of electric and magnetic phenomena.

I will now introduce the strong force, which only affects quarks, as mentioned earlier. Actually, the strong force works on all particles with colour charge. The strong force binds quarks together in colourless hadrons, and it also binds protons and neutrons together in the atomic nuclei. The force is mediated by eight distinct bosons called gluons, which carry combinations of colour and anti-colour. This means of course, that the strong force also affects the gluons. That is, the gluons interact with each other. This is different from QED, where the photon neither carries electric charge nor interacts directly with other photons. The gluons are massless spin 1 bosons. The strong force is described by the quantum field theory Quantum Chromodynamics, short QCD. Chromo here stands for colour.

The last of the four fundamental forces, the weak force, is mediated by very heavy spin 1 bosons, called W^+, W^- and Z^0. As might be understood from the superscripts, the W bosons are electrically charged, and the Z boson is electrically neutral. The electromagnetic force and the weak force have been unified into the Standard Electroweak Theory, by Glashow, Salam and Weinberg [2]. This unification shows that the massless photon and the very massive $W^\pm$ and Z bosons are in some way related, and that electromagnetic interactions and weak interactions are only different aspects of the same fundamental force. There exists a symmetry between the heavy vector bosons $W^\pm$ and Z and the photon γ in the theory, but this symmetry is broken by the fact that the mass of the photon (which is equal to zero) is so different from the masses of the three other bosons. In order to make a theory for the electroweak interactions where the bosons W and Z are allowed to be massive, one must make use of a mechanism which is called the Higgs mechanism.

The Higgs mechanism makes use of a trick called spontaneous symmetry breaking, which allows one to introduce boson and fermion masses. But the trick also introduces a new boson, the Higgs boson, which has got spin 0. Spin 0 particles are called scalars. The Higgs boson has not been experimentally observed yet, so we do not know whether this is the right solution to the problem with the particle masses. It is believed though, that either a Higgs boson exists, or the theory we have today, The Standard Model, is not the complete theory, but there exists some "new physics" (phenomena in particle physics which are not described by The Standard Model). We will probably know which answer is right when the next generation of particle accelerators (the Large Hadron Collider (LHC) at CERN and Tesla at DESY) have been running for some years.

It is important to explore the properties of different proposed models for the Higgs mechanism, as a preparation for the planned experiments at the new accelerators. The Standard Model is only the simplest of many theories for the interactions described above. One important group of theories are the so-called supersymmetric theories, denoted so because they contain a higher degree of symmetry, which does not exist in the Standard Model. In supersymmetric theories there exist not only antiparticles for all particles, but also bosonic partners for all fermions, and fermionic partners for the bosons. In one specific

supersymmetric theory, The Minimal Supersymmetric extension of the Standard Model, short MSSM, there is not only one Higgs boson, but five distinct ones [4].

2.1 Relativistic Notation and Natural Units

In his Special Theory of Relativity, Albert Einstein introduced the idea that time is just another dimension of the universe, and that it should be treated similarly to the other three (space) dimensions. Working with objects that reach relativistic energies, like elementary particles, it is conventional to use four-vector notation [3]:

$$x^\mu = (ct, \mathbf{x}), \quad \mu = 0, 1, 2, 3\,. \tag{2.1}$$

Here the zeroth component contains the time dimension t, and the other three components contain the three space dimensions $\mathbf{x}$. The symbol c stands for the speed of light in vacuum. The vector x^μ with upper index, is called a contravariant vector. The covariant vector is defined by

$$x_\mu = \sum_{\nu=0}^{3} g_{\mu\nu} x^\nu = g_{\mu\nu} x^\nu\,. \tag{2.2}$$

Here we have used the summation convention, which states that an index that appears both as upper and lower index should be summed over. The metric tensor is defined by:

$$g_{\mu\nu} = \mathrm{diag}(1, -1, -1, -1)\,. \tag{2.3}$$

It has the following properties:

$$g^{\mu\nu} g_{\mu\lambda} = g^\nu_\lambda = \delta^\nu_\lambda\,, \tag{2.4}$$

and

$$g^{\mu\nu} = g_{\mu\nu}\,. \tag{2.5}$$

The scalar product of two four-vectors a and b is given by

$$ab = a^\mu b_\mu = a_\mu b^\mu = g_{\mu\nu} a^\mu b^\nu = a^0 b^0 - \mathbf{a}\cdot\mathbf{b}\,. \tag{2.6}$$

The scalar product of any two four-vectors is invariant under a Lorentz transformation. Specifically, the energy-momentum four-vector is equal to:

$$p^\mu = (E/c, \mathbf{p})\,. \tag{2.7}$$

When it contains the energy and momentum of a particle with mass m, we have the following relation:

$$p^2 = p_\mu p^\mu = E^2/c^2 - \mathbf{p}^2 = m^2 c^2\,. \tag{2.8}$$

The four-dimensional generalisation of the gradient ∇ is defined by:

$$\frac{\partial}{\partial x^\mu} = \partial_\mu = \left(\frac{1}{c}\frac{\partial}{\partial t}, \nabla\right)\,, \tag{2.9}$$

with

$$\partial_\mu \partial^\mu = \frac{1}{c^2}\frac{\partial^2}{\partial t^2} - \nabla^2 \,. \tag{2.10}$$

In high-energy physics it is conventional to work in the system of Natural Units, also called "God-given" units [19]. In this system the speed of light c, and the reduced Planck constant $\hbar = h/2\pi$ are chosen as the units of speed and action/angular momentum, respectively. This is the same as setting their values equal to one:

$$\hbar = c = 1 \,. \tag{2.11}$$

The result of this choice of units is that there only exists one dimension. It is common to choose this dimension as energy, or mass. With the relations below, any time or length can be expressed in units of mass or energy and vice versa

$$[\text{length}] = [\text{time}] = [\text{energy}]^{-1} = [\text{mass}]^{-1} \,. \tag{2.12}$$

For the rest of this thesis, I have worked in natural units unless otherwise stated.

2.2 Gauge Theories

The quantum field theory QED is the simplest example of a gauge theory. A quantum field theory is described by its Lagrangian density. The simplest form of a quantum field theory is a so-called free-field theory, where the fields (which represent different particle types) do not interact with each other at all. For one type of fermions, the free-field Lagrangian density has the following form:

$$\mathcal{L}_0(x) = \bar{\psi}(x)(i\gamma^\mu \partial_\mu - m)\psi(x) \,. \tag{2.13}$$

Here m is the mass of the fermion, $\psi(x)$ is the fermion field (a column "matrix" with 4 elements, also called a spinor field) and γ^μ is a 4×4 matrix. The field $\bar{\psi}(x) = \psi^\dagger(x)\gamma^0$ is the Hermitian conjugate of $\psi(x)$ times a 4×4 matrix γ^0.

In order to derive the interaction of the (electrically charged) fermion field $\psi(x)$ with photons, as in QED, we might demand that the Lagrangian density be invariant under a local U(1) phase transformation:

$$\begin{aligned} \psi(x) \to \psi'(x) &= \psi(x)e^{-iqf(x)} \\ \bar{\psi}(x) \to \bar{\psi}'(x) &= \bar{\psi}(x)e^{iqf(x)} \,. \end{aligned} \tag{2.14}$$

This is called a *local* phase transformation because the phase $qf(x)$ depends on the variable x, and therefore might have a different value at each point in space-time. It is a U(1) phase transformation because $e^{iqf(x)}$ is a 1×1 unitary matrix.

The Lagrangian density in the form (2.13) is not invariant under this local U(1) phase transformation, but if we replace the derivative ∂_μ with a so-called covariant derivative:

$$D_\mu \psi(x) = [\partial_\mu + iqA_\mu(x)]\psi(x) \,, \tag{2.15}$$

and define the transformation of the *gauge field* $A_\mu(x)$ under a local phase transformation as

$$A_\mu(x) \to A'_\mu(x) = A_\mu(x) + \partial_\mu f(x)\,, \tag{2.16}$$

where $f(x)$ can be any differentiable function of x, then one can show that the Lagrangian density

$$\mathcal{L}(x) = \bar{\psi}(x)(i\gamma^\mu D_\mu - m)\psi(x) \tag{2.17}$$

is invariant under the simultaneous transformations (2.14) and (2.16).

From the requirement that the free-field Lagrangian density $\mathcal{L}_0$ should be invariant under the local U(1) phase transformation (2.14), we have now obtained a Lagrangian density with an interaction term $\mathcal{L}_I$, which creates an interaction between the fermion field $\psi(x)$ and the gauge field A_μ:

$$\mathcal{L}(x) = \mathcal{L}_0(x) - q\bar{\psi}(x)\gamma^\mu\psi(x)A_\mu(x) = \mathcal{L}_0(x) + \mathcal{L}_I(x)\,. \tag{2.18}$$

Here $\mathcal{L}_I(x)$ is the interaction term in the Lagrangian density, and q is the electric charge of the fermion represented by the field $\psi(x)$. If we in addition added the free-field Lagrangian density of the field $A_\mu(x)$ to the Lagrangian in (2.17), we would have the QED Lagrangian for one type of fermion $\psi(x)$. The gauge field $A_\mu(x)$ would then represent photons.

This is not the way QED was historically developed, but it has turned out that the above prescription is a fruitful way of constructing new theories. The transformations (2.14) and (2.16) are U(1) gauge transformations, and a theory which is invariant under a set of gauge transformation is called a gauge theory. All the quantum field theories mentioned in the introduction of this chapter, QED, QCD and the Standard Electroweak Theory, are gauge theories.

2.3 The Higgs Mechanism

The Higgs mechanism is exploited in the Standard Electroweak Theory, in order to allow fermions and the heavy vector bosons $W^\pm$ and Z to have masses. Without a mechanism such as the Higgs mechanism, it is not possible to add mass terms to the Lagrangian density of electroweak theory and still retain the gauge invariance. In this section, except for the part about Two-Higgs-Doublet Models, I follow the presentation and notation of ref. [3].

I will start by explaining the mechanism of *spontaneous symmetry breaking*. As I have already mentioned, a quantum field theory is defined by its Lagrangian density. If the Lagrangian density is invariant under some transformation, like for instance a rotation in space or a gauge transformation, we say that this transformation is a symmetry of the Lagrangian.

In quantum mechanics one talks about *eigenstates* and *energy levels*. An eigenstate is simply some possible state of the system, and its energy level is the corresponding energy of the eigenstate. The eigenstates and energy levels of a system are given by the equation(s) of motion of the system together with initial conditions. The equation(s) of motion are

again given by the Lagrangian density. If there is more than one eigenstate which share the same energy level, we say that this energy level is *degenerate*.

When the Lagrangian density has got some symmetry transformation, the eigenstates of a degenerate energy level are not invariant under this symmetry transformation. Instead they transform into some linear combination of this group of eigenstates. If the lowest energy level is degenerate, the *ground state*, the state of lowest energy, is not unique, and we can choose any of the eigenstates of the lowest energy as the ground state.

The degeneracy of the lowest energy level thus gives a ground state of the system which is not invariant under a symmetry transformation of the Lagrangian density. This is the mechanism of spontaneous symmetry breaking.

One classic example of spontaneous symmetry breaking is ferromagnetic material. It is the direction of the spins of the electrons in the material which determines its magnetic properties. The electromagnetic forces which work on the spins are invariant under space rotations. Therefore rotations are symmetry transformations of the Lagrangian. When the ferromagnetic material is cooled down below the critical temperature however, it reaches its ground state where all electron spins point in the same direction. The choice of this direction is arbitrary, and the ground state is clearly not invariant under rotations.

In quantum field theory, a degenerate lowest energy level is equivalent to the fact that the vacuum is degenerate. The vacuum, the state where no particles exist, is the lowest energy level of a quantum field theory.

2.3.1 The Goldstone Model

The vacuum can only be degenerate if there is some quantity which is not equal to zero for the vacuum state. This quantity can be the vacuum expectation value of a scalar field $\phi(x)$:

$$<0|\phi(x)|0> = c \neq 0\,. \tag{2.19}$$

A scalar field $\phi(x)$ represents a spin 0 boson, which we call a scalar particle. The fact that the vacuum expectation value of $\phi(x)$ is a constant, means that no scalar particle exists in vacuum. The vacuum expectation values of spinor fields $\psi(x)$ (representing spin 1/2 fermions) and vector fields $A_\mu(x)$ (representing spin 1 bosons) must be equal to zero if we want the ground state to be invariant under Lorentz boosts and rotations

$$<0|\psi(x)|0> = 0\,, \qquad <0|A_\mu(x)|0> = 0\,. \tag{2.20}$$

The Goldstone model is the simplest example of a field theory with spontaneous symmetry breaking. Its Lagrangian density is given by

$$\mathcal{L}(x) = [\partial^\mu \phi^*(x)][\partial_\mu \phi(x)] - \mu^2 |\phi(x)|^2 - \lambda |\phi(x)|^4\,, \tag{2.21}$$

where

$$\phi(x) = \frac{1}{\sqrt{2}}[\phi_1(x) + i\phi_2(x)] \tag{2.22}$$

is a complex scalar field, and μ^2 and λ are real parameters.

The Hamiltonian density of the Goldstone model is given by

$$\mathcal{H}(x) = [\partial^0\phi^*(x)][\partial_0\phi(x)] + [\nabla\phi^*(x)] \cdot [\nabla\phi(x)] + \mu^2|\phi(x)|^2 + \lambda|\phi(x)|^4 \,. \tag{2.23}$$

Here the first two terms are the kinetic energy terms, and the last two terms represent the potential energy. We see that λ must be positive if there should exist a state with lowest energy, a ground state. If μ^2 is positive the potential energy will have its minimum value for $\phi(x) = 0$. The value of $\phi(x)$ which gives the minimum of the potential energy corresponds to the vacuum expectation value of $\phi(x)$ in the quantised theory. We can see that for positive μ^2 there is no spontaneous symmetry breaking.

If μ^2 is negative the potential energy will have a minimum value for

$$\phi(x) = \phi_0 = \left(\frac{-\mu^2}{2\lambda}\right)^{1/2} e^{i\theta} \,, \qquad 0 \leq \theta < 2\pi \,. \tag{2.24}$$

This is a whole circle of points in the $\phi_1\phi_2$-plane.

The Lagrangian density of the Goldstone model is invariant under a so-called global U(1) phase transformation

$$\phi(x) \to \phi'(x) = \phi(x)e^{i\alpha} \,, \qquad \phi^*(x) \to \phi^{*\prime}(x) = \phi^*(x)e^{-i\alpha} \,. \tag{2.25}$$

This is a U(1) transformation because $e^{-i\alpha}$ is a unitary 1×1 matrix. It is a global transformation because α does not depend on x.

From the circle of points in (2.24), we can choose any value of $\phi(x)$ as the ground state. It is practical to choose the real value

$$\phi_0 = \left(\frac{-\mu^2}{2\lambda}\right)^{1/2} = \frac{1}{\sqrt{2}}v \tag{2.26}$$

of $\phi(x)$. When we choose a certain value for $\phi(x)$ as the ground state, it is no longer invariant under the transformation (2.25), and we therefore have spontaneous symmetry breaking.

We can choose a new basis for $\phi(x)$ around the value of the ground state (2.26):

$$\phi(x) = \frac{1}{\sqrt{2}}[v + \sigma(x) + i\eta(x)] \,. \tag{2.27}$$

Here $\sigma(x)$ and $\eta(x)$ are two real-valued scalar fields. The Lagrangian density expressed in terms of the new basis is given by

$$\begin{aligned} \mathcal{L}(x) \;=\; & \frac{1}{2}[\partial^\mu\sigma(x)][\partial_\mu\sigma(x)] - \frac{1}{2}(2\lambda v^2)\sigma^2(x) + \frac{1}{2}[\partial^\mu\eta(x)][\partial_\mu\eta(x)] \\ & - \lambda v\sigma(x)[\sigma^2(x) + \eta^2(x)] - \frac{1}{4}\lambda[\sigma^2(x) + \eta^2(x)]^2 \,, \end{aligned} \tag{2.28}$$

where a constant term is omitted. The three first terms are the free-field terms of the fields $\sigma(x)$ and $\eta(x)$ whereas the two last terms are of order three or higher in the fields and

therefore represent interactions. From the free-field terms one can see that for negative μ^2 the Goldstone model gives rise to the neutral scalar bosons σ and η. The bosons σ have got mass with the value $m_\sigma = \sqrt{2\lambda v^2}$ whereas the bosons η are massless. The bosons η are referred to as Goldstone bosons. Goldstone bosons do not exist in nature, but they still play an important role in the Standard Electroweak Theory, as will be shown in the following.

2.3.2 The Higgs Model

The Goldstone model is a simple example of spontaneous symmetry breaking in a quantum field theory. We want to exploit this mechanism in order to give masses to the gauge bosons W and Z in the electroweak theory. The Higgs model is a simple example of how the mechanism of spontaneous symmetry breaking can give rise to massive gauge bosons without destroying the gauge invariance of the gauge theory.

We want to make the Lagrangian density of the Goldstone model (2.21) invariant under the U(1) gauge transformation

$$\begin{aligned} \phi(x) \to \phi'(x) &= \phi(x)e^{-iqf(x)} \\ \phi^*(x) \to \phi^{*\prime}(x) &= \phi^*(x)e^{iqf(x)} \\ A_\mu(x) \to A'_\mu(x) &= A_\mu(x) + \partial_\mu f(x)\,. \end{aligned} \tag{2.29}$$

From the previous section we know that this is possible if we replace the derivative ∂_μ by a covariant derivative

$$D_\mu\phi(x) = [\partial_\mu + iqA_\mu(x)]\phi(x)\,. \tag{2.30}$$

The Lagrangian density of the Higgs model can now be written as

$$\begin{aligned} \mathcal{L}(x) &= [D^\mu\phi(x)]^*[D_\mu\phi(x)] - \mu^2|\phi(x)|^2 - \lambda|\phi(x)|^4 \\ &\quad - \frac{1}{4}F_{\mu\nu}(x)F^{\mu\nu}(x)\,, \end{aligned} \tag{2.31}$$

where we have added a free-field term of the gauge field $A_\mu(x)$, and where

$$F_{\mu\nu}(x) = \partial_\nu A_\mu(x) - \partial_\mu A_\nu(x) \tag{2.32}$$

is the field tensor of the gauge field.

Now we proceed in the same way as for the Goldstone model. For μ^2 negative the vacuum is degenerate. The vacuum expectation value of $A_\mu(x)$ must be equal to zero, and minima of the potential energy are given by the circle (2.24). If we choose the ground state $\phi(x) = \phi_0$, where ϕ_0 is given by (2.26), and expand $\phi(x)$ according to (2.27), the Lagrangian density of the Higgs model can be written as

$$\begin{aligned} \mathcal{L}(x) &= \frac{1}{2}[\partial^\mu\sigma(x)][\partial_\mu\sigma(x)] - \frac{1}{2}(2\lambda v^2)\sigma^2(x) - \frac{1}{4}F_{\mu\nu}(x)F^{\mu\nu}(x) \\ &\quad + \frac{1}{2}(qv)A_\mu(x)A^\nu(x) + \frac{1}{2}[\partial^\mu\eta(x)][\partial_\mu\eta(x)] + qvA^\mu(x)\partial_\mu\eta(x) \\ &\quad + \text{`higher order terms'}\,. \end{aligned} \tag{2.33}$$

Here 'higher order terms' are terms which are of third order or higher in the fields, and therefore are interaction terms.

There is a problem with this expression for the Lagrangian density. In fact, the term $qvA^\mu(x)\partial_\mu\eta(x)$ contains both of the fields $\eta(x)$ and $A_\mu(x)$, but it is only of order two so it is no interaction term. This means that the fields $\eta(x)$ and $A_\mu(x)$ are not independent of each other.

This problem can be solved by noting that the field $\eta(x)$ can be transformed away by a U(1) gauge transformation (2.29), so that the field $\phi(x)$ can be written in the following form:

$$\phi(x) = \frac{1}{\sqrt{2}}[v + \sigma(x)] \tag{2.34}$$

This represents a choice of gauge, which means that the above expression for $\phi(x)$ is not invariant under U(1) gauge transformations. The chosen gauge is called the *unitary gauge*. In this gauge the free-field part of the Lagrangian density has the form

$$\begin{aligned} \mathcal{L}_0(x) &= \frac{1}{2}[\partial^\mu\sigma(x)][\partial_\mu\sigma(x)] - \frac{1}{2}(2\lambda v^2)\sigma^2(x) \\ &\quad - \frac{1}{4}F_{\mu\nu}(x)F^{\mu\nu}(x) + \frac{1}{2}(qv)^2 A_\mu(x)A^\nu(x)\,. \end{aligned} \tag{2.35}$$

In addition the total Lagrangian density contains interaction terms.

The above free-field Lagrangian density represents a massive scalar field $\sigma(x)$, which creates scalar particles with mass $m_\sigma = \sqrt{2\lambda v^2}$, and a massive vector field $A_\mu(x)$, which creates vector bosons with mass $m_A = |qv|$. Notice that the Goldstone boson η has disappeared, while the gauge field $A_\mu(x)$ has acquired a mass. We say that the extra degree of freedom of the Goldstone boson gives mass to the gauge boson. In some way the Goldstone boson and the massless gauge boson together give a massive gauge boson.

We have now demonstrated that the mechanism of spontaneous symmetry breaking can give masses to gauge bosons without ruining the gauge invariance of the theory. This is called the Higgs mechanism.

2.3.3 Standard Electroweak Theory

In the Standard Electroweak Theory, by Glashow, Salam and Weinberg [2], the Higgs mechanism must create masses for three gauge bosons, W^+, W^- and Z. It is therefore not enough with spontaneous breaking of the symmetry under U(1) gauge transformations. The symmetry under SU(2) gauge transformations has to be broken. The Standard Electroweak Theory is a $\mathrm{SU}(2)_L \times \mathrm{U}(1)_Y$ gauge theory, which means that its Lagrangian density is invariant under both $\mathrm{SU}(2)_L$ and $\mathrm{U}(1)_Y$ gauge transformations. Here L and Y stand for the kind of charges the gauge fields interact with (similar to electric charge q for QED). The SU(2) matrices are 2×2 unitary matrices which have unit determinants.

Instead of a complex scalar field $\phi(x)$, the field of the Lagrangian density (2.31) must be an $\mathrm{SU}(2)_L$ doublet:

$$\Phi(x) = \begin{pmatrix} \phi_a(x) \\ \phi_b(x) \end{pmatrix}\,. \tag{2.36}$$

Here the fields $\phi_a(x)$ and $\phi_a(x)$ are complex scalar fields. An SU(2) doublet has special transformation properties under SU(2) gauge transformations.

A Lagrangian density for $\Phi(x)$ which is invariant under $\mathrm{SU}(2)_L \times \mathrm{U}(1)_Y$ gauge transformations can be written as

$$\mathcal{L}_H(x) = [D^\mu \Phi(x)]^\dagger [D_\mu \Phi(x)] - \mu^2 \Phi^\dagger(x)\Phi(x) - \lambda[\Phi^\dagger(x)\Phi(x)]^2 \,. \tag{2.37}$$

Here

$$D^\mu \Phi(x) = [\partial^\mu + ig\tau_j W_j^\mu(x)/2 + ig' Y B^\mu(x)]\Phi(x) \,, \tag{2.38}$$

where $W_j^\mu(x)$ for $j = 1, 2, 3$, and $B^\mu(x)$ are the SU(2) and U(1) gauge fields. Linear combinations of these fields give rise to the four electroweak vector bosons W^+, W^-, Z and the photon γ. In addition τ_j for $j = 1, 2, 3$ are the SU(2) generators. They are 2×2 matrices which are the basis of all SU(2) transformations. The quantities g, g' and Y are coupling constants and hypercharge respectively. The coupling constants give the strengths of interactions between particles and the hypercharge is a charge similar to the electric charge.

As was the case for the simple Higgs model, the potential energy has a minimum value for a circle of points in the $\phi_a(x)\phi_b(x)$-plane:

$$\Phi_0^\dagger \Phi_0 = |\phi_a|^2 + |\phi_b|^2 = \frac{-\mu^2}{2\lambda} = \frac{v^2}{2} \,. \tag{2.39}$$

We can choose any of these points as the value of $\Phi(x)$ in the ground state, so we choose

$$\Phi_0 = \begin{pmatrix} 0 \\ v/\sqrt{2} \end{pmatrix} . \tag{2.40}$$

The doublet $\Phi(x)$ can be transformed to a different basis

$$\Phi(x) = \frac{1}{\sqrt{2}} \begin{pmatrix} \eta_1(x) + i\eta_2(x) \\ v + \sigma(x) + i\eta_3(x) \end{pmatrix} . \tag{2.41}$$

Here $\sigma(x)$ and $\eta_i(x)$ for $i = 1, 2, 3$, are real scalar fields. It turns out that the η_i fields are not independent of the gauge fields $W_j^\mu(x)$ and $B^\mu(x)$. They can be transformed away through an SU(2) gauge transformation. We are then left with three massive gauge fields, which represent the vector bosons W^+, W^- and Z, a massless gauge field which represents the photon γ, and a massive scalar field $\sigma(x)$, which represents a massive neutral spin 0 boson. This boson is the famous Higgs boson. The Standard Electroweak Theory predicts its existence, but the mass of the Higgs boson can not be predicted from the theory (though upper and lower limits have been deduced [4]).

2.3.4 Two-Higgs-Doublet Models, 2HDM

The SU(2) Higgs doublet in the Standard Electroweak Theory is the simplest mechanism for breaking of $\mathrm{SU}(2)_L \times \mathrm{U}(1)_Y$ symmetry into $\mathrm{U}(1)_{EM}$. We do not have any experimental

evidence that this is the correct model for electroweak symmetry breaking though. More complex models have therefore been suggested. One group of extended models are the so-called *Two-Higgs-Doublet Models*, 2HDM [4, 6]. Here there are two SU(2) Higgs doublets, as the name suggests

$$\Phi_1(x) = \begin{pmatrix} \phi_1^+(x) \\ \frac{1}{\sqrt{2}}(v_1 + \phi_1(x) + ia_1(x)) \end{pmatrix}, \tag{2.42}$$

and

$$\Phi_2(x) = \begin{pmatrix} \phi_2^+(x) \\ \frac{1}{\sqrt{2}}(v_2 + \phi_2(x) + ia_2(x)) \end{pmatrix}. \tag{2.43}$$

Here, $v_1/\sqrt{2}$ and $v_2/\sqrt{2}$ are the vacuum expectation values of the fields. By a suitable rotation they can both be taken to be real.

Instead of one scalar Higgs boson as in the Standard Electroweak Theory, five spin 0 bosons are predicted in a 2HDM. There are two charged bosons H^+ and H^-, which are linear combinations of the complex fields ϕ_1^+ and ϕ_2^+. There are two neutral CP-even bosons, a lighter h and a heavier H. These are linear combinations of the real fields ϕ_1 and ϕ_2. Last but not least, there is one neutral CP-odd Higgs boson A, which is a linear combination of the real fields a_1 and a_2.

2.4 The CP-Transformation

The transformations P, T and C are examples of discrete transformations, which means that they, unlike the continuous Lorentz transformations, can not be made arbitrarily small [19]. Continuous Lorentz transformations consist of rotations and boosts in space-time. A boost is a transformation to a different frame of reference, which is moving with a constant speed relative to the original frame.

Parity, denoted by P, exchanges $(t, \mathbf{x})$ by $(t, -\mathbf{x})$, as mentioned in the Introduction. Time reversal, T, exchanges $(t, \mathbf{x})$ by $(-t, \mathbf{x})$, and thereby the past and the future are interchanged. These are both space-time transformations. In addition, C is connected to P and T, even though it is not a space-time transformation. Charge conjugation, C, interchanges particles and antiparticles.

The different fields or products of fields in a Lagrangian density can be classified as scalars, pseudoscalars, vectors, pseudovectors and tensors, depending on how they transform under continuous Lorentz transformations and P.

Scalars and pseudoscalars are both invariant under continuous Lorentz transformations, but a scalar is invariant under P, whereas a pseudoscalar changes sign. Similarly, vectors and pseudovectors transform in the same way under continuous Lorentz transformations, but vectors transform according to $(V^0(x), \mathbf{V}(x)) \to (V^0(x), -\mathbf{V}(x))$ under P, whereas pseudovectors transform according to $(A^0(x), \mathbf{A}(x)) \to (-A^0(x), \mathbf{A}(x))$.

In a theory which conserves C, P or T, the Lagrangian density must be invariant under the corresponding transformation. It is possible to construct theories which violate any

of these three discrete symmetries, by adding a new term to the Lagrangian density that is not invariant. But we demand that all theories must be invariant under continuous Lorentz transformations. The laws of physics must be the same independent of which frame of reference we are in. This is the famous principle of relativity, which is the basis of the Special Theory of Relativity by A. Einstein.

Therefore we can not add terms to a Lagrangian density which are not Lorentz scalars (are not invariant under continuous Lorentz transformations). From this one can show that all quantum field theories must be invariant under the simultaneous transformation CPT. This is called the CPT-theorem.

The gauge theories QED and QCD are both invariant under C and P, separately. The Standard Electroweak Theory violates P, but it is almost invariant under CP. From the fact that much more matter than antimatter exists in the universe, one can deduce that CP must be violated. We do not know yet, though, what the origin of all of this CP-violation is. One part of the CP violation comes from the mixing of quarks of different types. A d quark can decay into a u quark and the other way around. This mixing is described by the so-called CKM-matrix, from Cabibbo-Kobayashi-Maskawa [20]. This can not explain all the difference we observe between matter an antimatter though. Therefore the origin of CP violation is still a mystery, and much effort is made to find the solution to this problem.

Chapter 3

The Higgs Decay

In this chapter I have studied distributions in the decay

$$H \to V_1 V_2 \to f_1 \bar{f}_2 f_3 \bar{f}_4 \,, \tag{3.1}$$

where H is either a CP-even h, or a CP-odd A, Higgs boson. Here, $V_1 V_2$ are a pair of heavy vector bosons, W^+W^- or ZZ, and $f_1\bar{f}_2 f_3 \bar{f}_4$ are two fermion-antifermion pairs. The fermion pair $f_1\bar{f}_2$ is the decay product of V_1 and the pair $f_3\bar{f}_4$ is the decay product of V_2.

The CP-state of the Higgs boson will here determine the polarisations of the two vector bosons, and the polarisations will in turn determine the distributions of the decay angles in the decays of the two vector bosons to fermions. Therefore the momenta of the four fermions contain information about the CP-state of the Higgs boson.

One of the interesting distributions is the observable ϕ, which is defined as follows [8–14]: The momenta of V_i, f_j and $\bar{f}_k$, for $(i,j,k) = (1,1,2), (2,3,4)$, all lie in the same plane (from momentum conservation in the decay), and this plane we might denote as the decay plane of the decay $V_i \to f_j \bar{f}_k$. The angle ϕ is the angle between the decay planes of V_1 and V_2:

$$\cos\phi = \frac{(\mathbf{q}_1 \times \mathbf{q}_2)\cdot(\mathbf{q}_3 \times \mathbf{q}_4)}{|\mathbf{q}_1 \times \mathbf{q}_2||\mathbf{q}_3 \times \mathbf{q}_4|} \,. \tag{3.2}$$

Here $\mathbf{q}_i$ is the momentum of the final state fermion or antifermion f_i.

This chapter contains the calculations of the differential decay rate $\mathrm{d}\Gamma/\mathrm{d}\phi$ for the above decay. The calculations confirm earlier obtained results [10]. As is the case in [10], the decay rate is calculated with finite widths for the vector bosons, so that the correlations also can be studied for Higgs masses below the threshold, $2m_V$.

3.1 The Differential Higgs Decay Rate

In this section I am going to calculate an expression for the squared matrix element and the fully differential decay rate $\mathrm{d}\Gamma$ for a CP-even Higgs boson h and a CP-odd Higgs boson A, in terms of products of the fermion momenta. See figure 3.1 for a Feynman diagram for the decay, with the notation used.

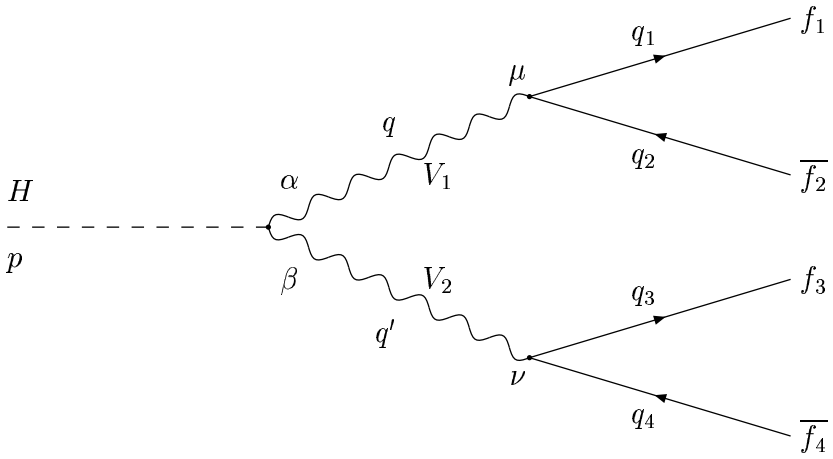

Figure 3.1: Decay of a CP-even or CP-odd Higgs boson into two fermion-antifermion pairs

The first part of this section contains the calculations for a CP-even Higgs boson h, and the second part contains the corresponding calculations for a CP-odd Higgs boson A.

The differential decay rate of a particle at rest into a final state of four particles is given by [19]:

$$\mathrm{d}\Gamma = (2\pi)^4 \delta^{(4)} \left(\sum_{f=1}^{4} q_f - p \right) \frac{1}{2m} |\mathcal{M}|^2 \left(\prod_{f=1}^{4} \frac{\mathrm{d}^3 \mathbf{q}_f}{(2\pi)^3 2E_f} \right) . \tag{3.3}$$

The momentum of the Higgs particle is equal to $p = (m, \mathbf{0})$ in its own rest frame.

3.1.1 Decay of a CP-even Higgs Boson h

For the CP-even Higgs boson the matrix element of the process can be written as:

$$\begin{aligned} \mathcal{M} \;=\; & \bar{u}(q_1) \left(\frac{-i}{2\sqrt{2}} \right) \gamma^\mu \, g_1 \, (\cos\chi_1 - \sin\chi_1 \, \gamma_5) \, v(q_2) \\ & \times \bar{u}(q_3) \left(\frac{-i}{2\sqrt{2}} \right) \gamma^\nu \, g_2 \, (\cos\chi_2 - \sin\chi_2 \, \gamma_5) \, v(q_4) \\ & \times \frac{i(-g_{\alpha\mu} + q_\alpha q_\mu / m_V^2)}{s_1 - m_V^2 + i m_V \Gamma_V} \, \frac{i(-g_{\beta\nu} + q'_\beta q'_\nu / m_V^2)}{s_2 - m_V^2 + i m_V \Gamma_V} \\ & \times i(2 \cdot 2^{1/4}) \sqrt{G_F} \, m_V^2 \, g^{\alpha\beta} \, . \end{aligned} \tag{3.4}$$

This can be seen from the Feynman diagram in figure 3.1 and from the Feynman rules [3]. Here s_1 and s_2 are the squared invariant masses of the vector bosons, defined by $s_1 = q^2 = (q_1 + q_2)^2$ and $s_2 = q'^2 = (q_3 + q_4)^2$, and m_V and Γ_V are the mass and width of the vector bosons.

The coupling of the standard-model Higgs to vector bosons is given by

$$i(2\cdot 2^{1/4})\sqrt{G_F}\, m_V^2 g^{\mu\nu}\,, \tag{3.5}$$

where G_F is the Fermi constant. The couplings between the vector bosons and the fermion-antifermion pairs can be written as

$$\frac{-i}{2\sqrt{2}}\,\gamma^\mu\,(g_V^{(i)} - g_A^{(i)}\,\gamma_5) \quad i = 1, 2\,. \tag{3.6}$$

I will use the following parametrisation for the vector and axial couplings:

$$g_V^{(i)} \equiv g_i \cos\chi_i\,, \quad g_A^{(i)} \equiv g_i \sin\chi_i\,, \quad i = 1, 2\,. \tag{3.7}$$

The angles χ_1 and χ_2 only appear in the expression $\sin 2\chi_i$ in the decay rate. Relevant values of $\sin 2\chi_i$ and the coupling constants g_i can be found in table 3.1 [21].

V_j	f	$\sin 2\chi_j$	g_j
W	leptons	1	$\sqrt{2}\,g$
W	quarks	1	$\sqrt{2}\,V_{ud}\,g$
Z	ν	1	$\dfrac{g}{\cos\theta_W}$
Z	$e,\ \mu,\ \tau$	$\dfrac{2(1-4\sin^2\theta_W)}{1+(1-4\sin^2\theta_W)^2} = 0.1498$	$\dfrac{g}{\sqrt{2}\cos\theta_W}[1+(1-4\sin^2\theta_W)^2]^{1/2}$
Z	$u,\ c,\ t$	$\dfrac{2(1-8/3\,\sin^2\theta_W)}{1+(1-8/3\,\sin^2\theta_W)^2} = 0.6687$	$\dfrac{g}{\sqrt{2}\cos\theta_W}[1+(1-8/3\,\sin^2\theta_W)^2]^{1/2}$
Z	$d,\ s,\ b$	$\dfrac{2(1-4/3\,\sin^2\theta_W)}{1+(1-4/3\,\sin^2\theta_W)^2} = 0.9358$	$\dfrac{g}{\sqrt{2}\cos\theta_W}[1+(1-4/3\,\sin^2\theta_W)^2]^{1/2}$

Table 3.1: $\sin 2\chi$ and g_j for the different $Vf\bar{f}$ couplings

I am now going to simplify the expression (3.4) for the matrix element. In the vector boson propagators the terms $q_\alpha q_\mu/m_V^2$ and $q'_\beta q'_\nu/m_V^2$ can be discarded in the approximation that the fermions are massless. This can be seen from the Dirac equation,

$$\bar{u}(p)\not{p} = \bar{u}(p)m\,, \quad \not{p}v(p) = -mv(p)\,,$$

and from a part of the matrix element

$$\begin{aligned}
& \bar{u}(q_1)\not{q}(\cos\chi_1 - \sin\chi_1\,\gamma_5)v(q_2)\,\frac{q_\alpha}{m_V^2} \\
= \;& \bar{u}(q_1)(\not{q}_1 + \not{q}_2)(\cos\chi_1 - \sin\chi_1\,\gamma_5)v(q_2)\,\frac{q_\alpha}{m_V^2} \\
= \;& \bar{u}(q_1)m_1(\cos\chi_1 - \sin\chi_1\,\gamma_5)v(q_2)\,\frac{q_\alpha}{m_V^2} \\
- \;& \bar{u}(q_1)(\cos\chi_1 + \sin\chi_1\,\gamma_5)\,m_2 v(q_2)\,\frac{q_\alpha}{m_V^2}\,. \qquad (3.8)
\end{aligned}$$

We see that the terms can be discarded because they are proportional to m_1/m_V and m_2/m_V.

In the approximation of massless fermions the matrix element can therefore be written as:

$$\begin{aligned}
\mathcal{M} \;=\; & \frac{i}{2^2}2^{1/4}\sqrt{G_F}m_V^2\left(\prod_{j=1}^{2}\frac{g_j}{s_j - m_V^2 + im_V\Gamma_V}\right) \\
& \times \bar{u}(q_1)\gamma^\mu(\cos\chi_1 - \sin\chi_1\,\gamma_5)v(q_2) \\
& \times \bar{u}(q_3)\gamma_\mu(\cos\chi_2 - \sin\chi_2\,\gamma_5)v(q_4)\,. \qquad (3.9)
\end{aligned}$$

I am now going to calculate the square of the matrix element. The expression we find is:

$$\begin{aligned}
|\mathcal{M}|^2 \;=\; & \frac{\sqrt{2}G_F m_V^4}{2^4}\left(\prod_{j=1}^{2}\frac{g_j^2 N_j}{(s_j - m_V^2)^2 + m_V^2\Gamma_V^2}\right) \\
& \times \bar{u}(q_1)\gamma^\mu(\cos\chi_1 - \sin\chi_1\,\gamma_5)v(q_2)\bar{v}(q_2)\gamma^\nu(\cos\chi_1 - \sin\chi_1\,\gamma_5)u(q_1) \\
& \times \bar{u}(q_3)\gamma_\mu(\cos\chi_2 - \sin\chi_2\,\gamma_5)v(q_4)\bar{v}(q_4)\gamma_\nu(\cos\chi_2 - \sin\chi_2\,\gamma_5)u(q_3) \qquad (3.10)
\end{aligned}$$

Here, N_i is equal to 1 if V_i couples to leptons, and equal to 3 if V_i couples to quarks. The extra factor 3 for quarks represents a sum over the colour degrees of freedom.

This is the squared matrix element for specific momentum and spin states of the final state fermions. We are not interested in the spin states of the fermions, and therefore sum the squared matrix element over all fermion spin states. This is called the spin sum. In the approximation of massless fermions we now get:

$$\begin{aligned}
\frac{1}{2m}\sum_{\text{spin}}|\mathcal{M}|^2 \;=\; & \frac{\sqrt{2}G_F m_V^4}{2^5 m}\left(\prod_{j=1}^{2}\frac{g_j^2}{(s_j - m_V^2)^2 + m_V^2\Gamma_V^2}\,N_j\right) \\
& \times \mathrm{Tr}[\not{q}_1\gamma^\mu(\cos\chi_1 - \sin\chi_1\gamma_5)\not{q}_2\gamma^\nu(\cos\chi_1 - \sin\chi_1\gamma_5)] \\
& \times \mathrm{Tr}[\not{q}_3\gamma_\mu(\cos\chi_2 - \sin\chi_2\gamma_5)\not{q}_4\gamma_\nu(\cos\chi_2 - \sin\chi_2\gamma_5)]\,. \qquad (3.11)
\end{aligned}$$

Here I have used the following normalisation for the spin sums of the fermions [19]:

$$\sum_{r=1}^{2} u_r(p)\bar{u}_r(p) = \not{p} + m\,, \qquad (3.12)$$

and

$$\sum_{r=1}^{2} v_r(p)\bar{v}_r(p) = \not{p} - m\,. \tag{3.13}$$

In order to evaluate the traces of Dirac γ-matrices, we will need some results concerning these matrices [19]. The matrix γ_5 is the product of four "normal" γ-matrices:

$$\gamma_5 = i\gamma^0\gamma^1\gamma^2\gamma^3 = -\frac{i}{4!}\epsilon^{\mu\nu\rho\sigma}\gamma_\mu\gamma_\nu\gamma_\rho\gamma_\sigma\,. \tag{3.14}$$

It anticommutes with the other γ-matrices, and the square of it is equal to one:

$$[\gamma^\mu, \gamma_5]_+ = 0\,, \quad (\gamma_5)^2 = 1\,. \tag{3.15}$$

The results concerning traces that are relevant for these calculations are:

$$\begin{aligned} \mathrm{Tr}(\gamma^\alpha\gamma^\beta\gamma^\gamma\gamma^\delta) &= 4(g^{\alpha\beta}g^{\gamma\delta} - g^{\alpha\gamma}g^{\beta\delta} + g^{\alpha\delta}g^{\beta\gamma}) \\ \mathrm{Tr}(\gamma_5\gamma^\alpha\gamma^\beta\gamma^\gamma\gamma^\delta) &= 4i\epsilon^{\alpha\beta\gamma\delta}\,. \end{aligned} \tag{3.16}$$

Here the completely antisymmetric tensor $\epsilon^{\alpha\beta\gamma\delta}$ is equal to $+1$ for $(\alpha,\beta,\gamma,\delta)$ an even permutation of $(0,1,2,3)$, equal to -1 for an odd permutation, and vanishes if two or more indices are the same. Contractions of the tensor can be simplified according to the following formulae:

$$\epsilon^{\alpha\beta\mu\nu}\epsilon_{\alpha\beta\mu\nu} = -24\,, \tag{3.17}$$

$$\epsilon^{\alpha\beta\gamma\mu}\epsilon_{\alpha\beta\gamma\nu} = -6\delta^\mu_\nu \tag{3.18}$$

and

$$\epsilon^{\alpha\beta\mu\nu}\epsilon_{\alpha\beta\sigma\tau} = -2(g^\mu_\sigma g^\nu_\tau - g^\mu_\tau g^\nu_\sigma)\,. \tag{3.19}$$

The metric tensor $g_{\mu\nu}$ is diagonal, see (2.3):

$$g_{\mu\nu} = \mathrm{diag}(1,-1,-1,-1)\,. \tag{3.20}$$

It can also be contracted over repeated indices, see (2.4):

$$g^{\lambda\mu}g_{\mu\nu} = g^\lambda_\nu = \delta^\lambda_\nu. \tag{3.21}$$

By use of the above results, we are now able to simplify the traces:

$$\begin{aligned} \mathrm{Tr}[\not{q}_1\gamma^\mu(\cos\chi_1 - \sin\chi_1\,\gamma_5)\not{q}_2\gamma^\nu(\cos\chi_1 - \sin\chi_1\,\gamma_5)] &= \mathrm{Tr}[\not{q}_1\gamma^\mu\not{q}_2\gamma^\nu(1 - \sin(2\chi_1)\,\gamma_5)] \\ &= 4q_{1\alpha}q_{2\beta}\; x_1^{\alpha\mu\beta\nu}\,, \\ \mathrm{Tr}[\not{q}_3\gamma_\mu(\cos\chi_2 - \sin\chi_2\,\gamma_5)\not{q}_4\gamma_\nu(\cos\chi_2 - \sin\chi_2\,\gamma_5)] &= \mathrm{Tr}[\not{q}_3\gamma_\mu\not{q}_4\gamma_\nu(1 - \sin(2\chi_2)\,\gamma_5)] \\ &= 4q_3^\rho q_4^\sigma\; x_{2\;\rho\mu\sigma\nu}\,, \end{aligned} \tag{3.22}$$

where

$$x_j^{\alpha\mu\beta\nu} = (g^{\alpha\mu}g^{\beta\nu} - g^{\alpha\beta}g^{\mu\nu} + g^{\alpha\nu}g^{\beta\mu} - i\sin(2\chi_j)\,\epsilon^{\alpha\mu\beta\nu})\,. \tag{3.23}$$

One can see that ${x_1}^{\alpha\mu\beta\nu}$ and $x_{2\,\rho\mu\sigma\nu}$ each consists of one part which is symmetric under interchange of μ and ν, and one part which is antisymmetric. Therefore, the product of ${x_1}^{\alpha\mu\beta\nu}$ and $x_{2\,\rho\mu\sigma\nu}$ only contains the product of the symmetric parts, and the product of the antisymmetric parts, but no mixed terms. This enables us to calculate the product:

$$ {x_1}^{\alpha\mu\beta\nu} x_{2\,\rho\mu\sigma\nu} = 2[(g^\alpha_\rho g^\beta_\sigma + g^\alpha_\sigma g^\beta_\rho) + \sin(2\chi_1)\,\sin(2\chi_2)\,(g^\alpha_\rho g^\beta_\sigma - g^\alpha_\sigma g^\beta_\rho)]\,. \tag{3.24} $$

With the above expression for the product of the traces, we can now write down the squared matrix element, in terms of the momenta of the final state fermions:

$$ \begin{aligned} \frac{1}{2m}\sum_{\text{spin}} |\mathcal{M}|^2 &= \frac{\sqrt{2}G_F m_V^4}{m}\left(\prod_{j=1}^{2}\frac{g_j^2 N_j}{(s_j - m_V^2)^2 + m_V^2\Gamma_V^2}\right) \\ &\quad \times \{(q_1\cdot q_3)(q_2\cdot q_4) + (q_1\cdot q_4)(q_2\cdot q_3) \\ &\quad + \sin(2\chi_1)\,\sin(2\chi_2)\,[(q_1\cdot q_3)(q_2\cdot q_4) - (q_1\cdot q_4)(q_2\cdot q_3)]\}\,. \end{aligned} \tag{3.25} $$

With this expression for the matrix element, it is easy to write down the desired expression for the fully differential decay rate for the decay of the CP-even Higgs boson. The result in [10] is confirmed:

$$ \begin{aligned} \mathrm{d}\Gamma &= (2\pi)^4\delta^{(4)}\left(\sum_{f=1}^{4} q_f - p\right)\left(\prod_{f=1}^{4}\frac{\mathrm{d}^3\mathbf{q}_f}{(2\pi)^3 2E_f}\right) \\ &\quad \times \frac{\sqrt{2}G_F m_V^4}{m}\left(\prod_{j=1}^{2}\frac{g_j^2 N_j}{(s_j - m_V^2)^2 + m_V^2\Gamma_V^2}\right) \\ &\quad \times \{(q_1\cdot q_3)(q_2\cdot q_4) + (q_1\cdot q_4)(q_2\cdot q_3) \\ &\quad + \sin(2\chi_1)\,\sin(2\chi_2)\,[(q_1\cdot q_3)(q_2\cdot q_4) - (q_1\cdot q_4)(q_2\cdot q_3)]\}\,. \end{aligned} \tag{3.26} $$

3.1.2 Decay of a CP-odd Higgs Boson A

The only new Feynman rule needed in order to calculate the matrix element for the decay of a CP-odd Higgs boson, is the coupling of a CP-odd Higgs boson to vector bosons V_1V_2. Here V_1V_2 denote, as before, W^+W^- or ZZ. The coupling comes from the Lagrangian density term [10, 12, 13]:

$$ \mathcal{L}_{AVV} = \frac{1}{4}\eta\epsilon^{\mu\nu\rho\sigma}V_{\mu\nu}V_{\rho\sigma}A\,. \tag{3.27} $$

Here $V_{\mu\nu}$ is the field tensor of the vector boson V, defined by $V_{\mu\nu} = \partial_\nu V_\mu - \partial_\mu V_\nu$, and A is the CP-odd Higgs field. In a renormalisable quantum field theory this coupling can only be induced at the loop level. This can be seen from the fact that η will have dimension $[\text{mass}]^{-1}$ for this term [19] (page 80). A term with a coupling constant with a negative mass dimension ruins the renormalisability of the theory if it occurs at tree level [19]. In a realistic CP-conserving theory, η is expected to be small, since the associated mass scale is assumed to be high.

This Lagrangian density term gives the coupling

$$i\eta\epsilon^{\mu\nu\rho\sigma}q_\rho q'_\sigma\,, \tag{3.28}$$

where q and q' are the momenta of the vector bosons V_1 and V_2, respectively.

With this Feynman rule for the coupling, it is now possible to write down the matrix element for the decay from the Feynman diagram in figure 3.1:

$$\begin{aligned}\mathcal{M} &= \frac{i}{2^3}\eta\prod_{j=1}^{2}\left(\frac{g_j}{s_j-m_V^2+im_V\Gamma_V}\right)\\ &\quad\times\bar{u}(q_1)\gamma^\mu(\cos\chi_1-\sin\chi_1\gamma_5)v(q_2)\\ &\quad\times\bar{u}(q_3)\gamma^\nu(\cos\chi_2-\sin\chi_2\gamma_5)v(q_4)\\ &\quad\times g_{\alpha\mu}g_{\beta\nu}\epsilon^{\alpha\beta\rho\sigma}q_\rho q'_\sigma\,,\end{aligned} \tag{3.29}$$

compare to (3.9) for the CP-even case. Here I have used the result from the calculation of the CP-even matrix element (3.8), that allows me to discard the terms $q_\alpha q_\mu/m_V^2$ and $q'_\beta q'_\nu/m_V^2$ in the numerator of the boson propagators, in the approximation that the fermions are massless.

The matrix element squared then equals:

$$\begin{aligned}|\mathcal{M}|^2 &= \frac{1}{2^6}|\eta|^2\prod_{j=1}^{2}\left(\frac{g_j^2N_j}{(s_j-m_V^2)^2+m_V^2\Gamma_V^2}\right)\\ &\quad\times\bar{u}(q_1)\gamma^\alpha(\cos\chi_1-\sin\chi_1\gamma_5)v(q_2)\bar{v}(q_2)\gamma^\mu(\cos\chi_1-\sin\chi_1\gamma_5)u(q_1)\\ &\quad\times\bar{u}(q_3)\gamma^\beta(\cos\chi_2-\sin\chi_2\gamma_5)v(q_4)\bar{v}(q_4)\gamma^\nu(\cos\chi_2-\sin\chi_2\gamma_5)u(q_3)\\ &\quad\times\epsilon_{\alpha\beta\gamma\delta}q^\gamma q'^\delta\epsilon_{\mu\nu\rho\sigma}q^\rho q'^\sigma\,.\end{aligned} \tag{3.30}$$

We take the spin sum, and similar to (3.11) we get:

$$\begin{aligned}\sum_{\text{spin}}|\mathcal{M}|^2 &= \frac{1}{2^6}|\eta|^2\prod_{j=1}^{2}\left(\frac{g_j^2N_j}{(s_j-m_V^2)^2+m_V^2\Gamma_V^2}\right)\\ &\quad\times\mathrm{Tr}[\not{q}_1\gamma^\alpha(\cos\chi_1-\sin\chi_1\gamma_5)\not{q}_2\gamma^\mu(\cos\chi_1-\sin\chi_1\gamma_5)]\\ &\quad\times\mathrm{Tr}[\not{q}_3\gamma^\beta(\cos\chi_2-\sin\chi_2\gamma_5)\not{q}_4\gamma^\nu(\cos\chi_2-\sin\chi_2\gamma_5)]\\ &\quad\times\epsilon_{\alpha\beta\gamma\delta}q^\gamma q'^\delta\epsilon_{\mu\nu\rho\sigma}q^\rho q'^\sigma\,.\end{aligned} \tag{3.31}$$

The traces over γ-matrices are, except for the Lorentz indices, identical to the traces we evaluated for the CP-even case. It is therefore easy to see from (3.22) that the traces are equal to

$$\begin{aligned}\mathrm{Tr}[1] &= \mathrm{Tr}[\not{q}_1\gamma^\alpha(\cos\chi_1-\sin\chi_1\gamma_5)\not{q}_2\gamma^\mu(\cos\chi_1-\sin\chi_1\gamma_5)]\\ &= 4q_{1\epsilon}q_{2\tau}(g^{\epsilon\alpha}g^{\tau\mu}-g^{\epsilon\tau}g^{\alpha\mu}+g^{\epsilon\mu}g^{\alpha\tau}-i\sin2\chi_1\epsilon^{\epsilon\alpha\tau\mu})\\ &= 4q_{1\epsilon}q_{2\tau}x_1^{\epsilon\alpha\tau\mu}\,,\end{aligned} \tag{3.32}$$

and

$$\begin{aligned}\mathrm{Tr}[2] &= \mathrm{Tr}[\not{q}_3\gamma^\beta(\cos\chi_2-\sin\chi_2\gamma_5)\not{q}_4\gamma^\nu(\cos\chi_2-\sin\chi_2\gamma_5)]\\ &= 4q_{3\phi}q_{4\theta}(g^{\phi\beta}g^{\theta\nu}-g^{\phi\theta}g^{\beta\nu}+g^{\phi\nu}g^{\beta\theta}-i\sin 2\chi_2\epsilon^{\phi\beta\theta\nu})\\ &= 4q_{3\phi}q_{4\theta}x_2^{\phi\beta\theta\nu}\,. \end{aligned} \tag{3.33}$$

With the above traces, we can write the squared matrix element in a more compact form:

$$\begin{aligned}\sum_{\text{spin}}|\mathcal{M}|^2 &= \frac{1}{2^2}|\eta|^2\prod_{j=1}^{2}\left(\frac{g_j^2}{(s_j-m_V^2)^2+m_V^2\Gamma_V^2}\right)\\ &\quad\times q_{1\epsilon}q_{2\tau}q_{3\phi}q_{4\theta}x_1^{\epsilon\alpha\tau\mu}x_2^{\phi\beta\theta\nu}\\ &\quad\times\epsilon_{\alpha\beta\gamma\delta}q^\gamma q'^\delta\epsilon_{\mu\nu\rho\sigma}q^\rho q'^\sigma\,. \end{aligned} \tag{3.34}$$

This is not the final expression for the squared matrix element, though. We want to write it in terms of products of the fermion momenta, as we did for the CP-even case. We have to find a way to simplify the above expression. This can be done by noting that it consists of some parts which are symmetric under interchange of certain indices, and some parts which are antisymmetric. Symbolically this can be written as

$$\begin{aligned}\sum_{\text{spin}}|\mathcal{M}|^2 &= \frac{1}{2^2}|\eta|^2\prod_{j=1}^{2}\left(\frac{g_j^2}{(s_j-m_V^2)^2+m_V^2\Gamma_V^2}\right)\\ &\quad\times(S_1^{\alpha\mu}+A_1^{\alpha\mu})(S_2^{\beta\nu}+A_2^{\beta\nu})N_{\alpha\beta\mu\nu}\,, \end{aligned} \tag{3.35}$$

where

$$S_1^{\alpha\mu}=q_1^\alpha q_2^\mu-(q_1\cdot q_2)g^{\alpha\mu}+q_1^\mu q_2^\alpha \tag{3.36}$$

and

$$S_2^{\beta\nu}=q_3^\beta q_4^\nu-(q_3\cdot q_4)g^{\beta\nu}+q_3^\nu q_4^\beta \tag{3.37}$$

are symmetric under interchange of the indices,

$$A_1^{\alpha\mu}=-i\sin 2\chi_1\epsilon^{\epsilon\alpha\tau\mu}q_{1\epsilon}q_{2\tau} \tag{3.38}$$

and

$$A_2^{\beta\nu}=-i\sin 2\chi_2\epsilon^{\phi\beta\theta\nu}q_{3\phi}q_{4\theta} \tag{3.39}$$

are antisymmetric, whereas

$$N_{\alpha\beta\mu\nu}=\epsilon_{\alpha\beta\gamma\delta}\epsilon_{\mu\nu\rho\sigma}q^\gamma q'^\delta q^\rho q'^\sigma=N_{\mu\nu\alpha\beta} \tag{3.40}$$

is symmetric under the simultaneous interchanges $\alpha\leftrightarrow\mu$ and $\beta\leftrightarrow\nu$. We can now show that some of the terms in (3.35) must be equal to zero:

$$\begin{aligned}S_1^{\alpha\mu}A_2^{\beta\nu}N_{\alpha\beta\mu\nu} &= S_1^{\mu\alpha}A_2^{\nu\beta}N_{\mu\nu\alpha\beta}\\ &= -S_1^{\alpha\mu}A_2^{\beta\nu}N_{\alpha\beta\mu\nu}\\ &= 0\,, \end{aligned} \tag{3.41}$$

and

$$\begin{aligned} S_2^{\beta\nu} A_1^{\alpha\mu} N_{\alpha\beta\mu\nu} &= S_2^{\nu\beta} A_1^{\mu\alpha} N_{\mu\nu\alpha\beta} \\ &= -S_2^{\beta\nu} A_1^{\alpha\mu} N_{\alpha\beta\mu\nu} \\ &= 0\,. \end{aligned} \tag{3.42}$$

This enables us to get rid of two terms, and the matrix element can now be written in the following form:

$$\begin{aligned} \sum_{\text{spin}} |\mathcal{M}|^2 &= \frac{1}{2^2}|\eta|^2 \prod_{j=1}^{2} \left(\frac{g_j^2 N_j}{(s_j - m_V^2)^2 + m_V^2 \Gamma_V^2} \right) \\ &\quad \times (S_1^{\alpha\mu} S_2^{\beta\nu} N_{\alpha\beta\mu\nu} + A_1^{\alpha\mu} A_2^{\beta\nu} N_{\alpha\beta\mu\nu})\,. \end{aligned} \tag{3.43}$$

We still have to calculate products involving two or four antisymmetric tensors $\epsilon^{\alpha\beta\mu\nu}$ though. It would be possible to contract two antisymmetric tensors over one common index. This gives six terms with three Kronecker delta each. Two antisymmetric tensors with no indices in common give twenty four terms with Kronecker deltas. The expressions become very long, and it would be quite a job to calculate it all by hand.

I have used the algebraic programming system REDUCE [22] to calculate these products. I obtained the following results:

$$\begin{aligned} S_1^{\alpha\mu} S_2^{\beta\nu} N_{\alpha\beta\mu\nu} &= 2\Big(-2[(q_1 \cdot q_2)(q_3 \cdot q_4)]^2 \\ &\quad - 2[(q_1 \cdot q_3)(q_2 \cdot q_4) - (q_1 \cdot q_4)(q_2 \cdot q_3)]^2 \\ &\quad + (q_1 \cdot q_2)(q_3 \cdot q_4) \\ &\quad \times \{[(q_1 \cdot q_3) + (q_2 \cdot q_4)]^2 + [(q_1 \cdot q_4) + (q_2 \cdot q_3)]^2\}\Big)\,, \end{aligned} \tag{3.44}$$

and

$$\begin{aligned} A_1^{\alpha\mu} A_2^{\beta\nu} N_{\alpha\beta\mu\nu} &= 2 \sin 2\chi_1 \sin 2\chi_2 (q_1 \cdot q_2)(q_3 \cdot q_4) \\ &\quad \times \{[(q_1 \cdot q_3) - (q_2 \cdot q_4)]^2 - [(q_1 \cdot q_4) - (q_2 \cdot q_3)]^2\} \\ &= 2 \sin 2\chi_1 \sin 2\chi_2 (q_1 \cdot q_2)(q_3 \cdot q_4) \\ &\quad \times [(q_1 - q_2) \cdot (q_3 + q_4)][(q_1 + q_2) \cdot (q_3 - q_4)]\,. \end{aligned} \tag{3.45}$$

Now we are finally able to write down an expression for the matrix element squared, summed over all spin states of final state fermions, in terms of the momenta of the final state fermions:

$$\sum_{\text{spin}} |\mathcal{M}|^2 = \frac{1}{2}|\eta|^2 \prod_{j=1}^{2} \left(\frac{g_j^2 N_j}{(s_j - m_V^2)^2 + m_V^2 \Gamma_V^2} \right) [X_A + \sin 2\chi_1 \sin 2\chi_2 Y_A]\,, \tag{3.46}$$

where

$$\begin{aligned} X_A &= -2[(q_1 \cdot q_2)(q_3 \cdot q_4)]^2 \\ &\quad - 2[(q_1 \cdot q_3)(q_2 \cdot q_4) - (q_1 \cdot q_4)(q_2 \cdot q_3)]^2 \\ &\quad + (q_1 \cdot q_2)(q_3 \cdot q_4) \\ &\quad \times \{[(q_1 \cdot q_3) + (q_2 \cdot q_4)]^2 + [(q_1 \cdot q_4) + (q_2 \cdot q_3)]^2\}\,, \end{aligned} \tag{3.47}$$

and

$$\begin{aligned} Y_A &= (q_1\cdot q_2)(q_3\cdot q_4)\{[(q_1\cdot q_3)-(q_2\cdot q_4)]^2-[(q_1\cdot q_4)-(q_2\cdot q_3)]^2\} \\ &= (q_1\cdot q_2)(q_3\cdot q_4)[(q_1-q_2)\cdot(q_3+q_4)][(q_1+q_2)\cdot(q_3-q_4)]\,. \end{aligned} \tag{3.48}$$

With the expression (3.3) for the differential decay rate, it is now easy to write down the fully differential decay rate for decay of a CP-odd Higgs boson, and the result in [10] is confirmed:

$$\begin{aligned} \mathrm{d}\Gamma &= (2\pi)^4\delta^{(4)}\left(\sum_{f=1}^{4} q_f - p\right)\left(\prod_{f=1}^{4}\frac{\mathrm{d}^3\mathbf{q}_f}{(2\pi)^3 2E_f}\right) \\ &\quad\times\frac{|\eta|^2}{4m}\left(\prod_{j=1}^{2}\frac{g_j^2 N_j}{(s_j-m_V^2)^2+m_V^2\Gamma_V^2}\right) \\ &\quad\times[X_A+\sin 2\chi_1\sin 2\chi_2 Y_A]\,. \end{aligned} \tag{3.49}$$

3.2 The Phase Space Factor

The next thing to do is to transform the differential to variables which are more practical to work with, one of which should be the observable ϕ. I want to keep the dependence of $\mathrm{d}\Gamma$ on ϕ, but integrate over all other kinematic variables.

In this section I will rewrite the phase space to a form which will make the integrations easier [23]. In the form of (3.3), the phase space contains the differentials of the fermion momenta, $\mathbf{q}_i$ for $i = 1,2,3,4$, and a delta function which enforces overall momentum conservation for the decay. In addition, momentum conservation at each vertex is implied.

As will be shown below, from momentum conservation at each vertex, it is possible to introduce new differentials and delta functions into the phase space factor. At the end of this section I will explain why this makes it easier to perform the integrations over the phase space.

I introduce four new differentials, and two new delta functions to the phase space. Let us start with definitions of some new notation [23]:

$$\mathrm{d}^{12}\xi(m^2;q_1,q_2,q_3,q_4) \equiv (2\pi)^4\,\delta^{(4)}(p-q_1-q_2-q_3-q_4)\left(\prod_{f=1}^{4}\frac{\mathrm{d}^3\mathbf{q}_f}{(2\pi)^3\,2E_f}\right)\,, \tag{3.50}$$

and

$$\tilde{\mathrm{d}}^{12}\xi(q_1,q_2,q_3,q_4) \equiv \left(\prod_{f=1}^{4}\frac{\mathrm{d}^3\mathbf{q}_f}{(2\pi)^3\,2E_f}\right)\,. \tag{3.51}$$

It can therefore be seen that

$$\mathrm{d}^{12}\xi(m^2;q_1,q_2,q_3,q_4) \equiv (2\pi)^4\delta^{(4)}(p-q_1-q_2-q_3-q_4)\,\tilde{\mathrm{d}}^{12}\xi(q_1,q_2,q_3,q_4)\,. \tag{3.52}$$

Following this pattern, we also define

$$\tilde{\mathrm{d}}^6\xi(q_1,q_2) \equiv \left(\prod_{f=1}^{2}\frac{\mathrm{d}^3\mathbf{q}_f}{(2\pi)^3\,2E_f}\right). \tag{3.53}$$

Now, for $s_1 = q^2$ we get

$$\mathrm{d}^6\xi(s_1;q_1,q_2) \equiv (2\pi)^4\delta^{(4)}(q-q_1-q_2)\,\tilde{\mathrm{d}}^6\xi(q_1,q_2)\,. \tag{3.54}$$

Because of conservation of energy and momentum at the $V_1 f_1 \bar{f}_2$ vertex, we can write

$$\int \mathrm{d}^4q\,\delta^{(4)}(q-q_1-q_2) = 1 \tag{3.55}$$

We can use this to introduce the differential d^4q and the delta function $\delta^{(4)}(q-q_1-q_2)$ to the phase space. The definition of the new phase space differential is:

$$\begin{aligned}\mathrm{d}^{16}\xi(m^2;q_1,q_2,q_3,q_4) &= (2\pi)^4\,\delta^{(4)}(p-q-q_3-q_4)\\ &\quad\times\mathrm{d}^4q\,\delta^{(4)}(q-q_1-q_2)\,\tilde{\mathrm{d}}^{12}\xi(q_1,q_2,q_3,q_4)\,.\end{aligned} \tag{3.56}$$

Similarly, from $s_1 = q^2$, we see that

$$\int \mathrm{d}s_1\,\delta(s_1-q^2) = 1\,. \tag{3.57}$$

This allows us to define:

$$\begin{aligned}\mathrm{d}^{17}\xi(m^2;q_1,q_2,q_3,q_4) &= (2\pi)^4\,\delta^{(4)}(q-q_1-q_2)\,\tilde{\mathrm{d}}^{12}\xi(q_1,q_2,q_3,q_4)\\ &\quad\times\delta^{(4)}(p-q-q_3-q_4)\,\mathrm{d}^4q\\ &\quad\times\delta(s_1-q^2)\,\mathrm{d}s_1\\ &= \mathrm{d}^6\xi(s_1;q_1,q_2)\,\tilde{\mathrm{d}}^6\xi(q_3,q_4)\,\delta^{(4)}(p-q-q_3-q_4)\\ &\quad\times\delta(s_1-q^2)\,\mathrm{d}q^0\,\mathrm{d}^3\mathbf{q}\,\mathrm{d}s_1\,.\end{aligned} \tag{3.58}$$

Now, we want to get rid of the differential $\mathrm{d}q^0$ again, so we perform the integral

$$\int \mathrm{d}q^0\,\delta(s_1-q^2) = \int \mathrm{d}q^0\,\delta[(q^0)^2-(\mathbf{q}^2+s_1)] = \frac{1}{2q^0}\,, \tag{3.59}$$

where

$$q^0 = \sqrt{\mathbf{q}^2+s_1}\,. \tag{3.60}$$

The expression for the differential phase space we end up with contains one new delta function and two new differentials:

$$\begin{aligned}\mathrm{d}^{16}\xi(m^2;q_1,q_2,q_3,q_4) &= \mathrm{d}^6\xi(s_1;q_1,q_2)\,\tilde{\mathrm{d}}^6\xi(q_3,q_4)\\ &\quad\times\delta^{(4)}(p-q-q_3-q_4)\frac{\mathrm{d}^3\mathbf{q}}{2q^0}\,\mathrm{d}s_1\\ &= \frac{1}{2\pi}\,\mathrm{d}^6\xi(s_1;q_1,q_2)\\ &\quad\times(2\pi)^4\,\delta^{(4)}(p-q-q_3-q_4)\\ &\quad\times\tilde{\mathrm{d}}^9\xi(q,q_3,q_4)\,\mathrm{d}s_1\\ &= \frac{1}{2\pi}\,\mathrm{d}^6\xi(s_1;q_1,q_2)\,\mathrm{d}^9\xi(m^2;q,q_3,q_4)\,\mathrm{d}s_1\,.\end{aligned} \tag{3.61}$$

So far, we have introduced into the phase space the differentials $\mathrm{d}^3\mathbf{q}$ and $\mathrm{d}s_1$, and the delta function $\delta^{(4)}(q - q_1 - q_2)$. In the following, we will do the same trick with the $V_2 f_3 \bar{f}_4$ vertex. We use the relations

$$q' = q_3 + q_4 \quad \text{and} \quad s_2 = q'^2\,, \tag{3.62}$$

and get the expression for the phase space which we want:

$$\begin{aligned} \mathrm{d}^{20}\xi(m^2; q_1, q_2, q_3, q_4) &= \frac{1}{(2\pi)^2}\,\mathrm{d}^6\xi(s_1; q_1, q_2)\,\mathrm{d}^6\xi(s_2; q_3, q_4) \\ &\quad \times \mathrm{d}^6\xi(m^2; q, q')\,\mathrm{d}s_1\,\mathrm{d}s_2\,, \end{aligned} \tag{3.63}$$

where

$$q'^0 = \sqrt{\mathbf{q}'^2 + s_2}\,. \tag{3.64}$$

From (3.50), we can write out the explicit expression for the phase space:

$$\begin{aligned} \mathrm{d}^{20}\xi(m^2; q_1, q_2, q_3, q_4) &= \frac{1}{(2\pi)^2}\,(2\pi)^4\,\delta^{(4)}(q - q_1 - q_2)\,\frac{\mathrm{d}^3\mathbf{q}_1}{(2\pi)^3\,2E_1}\,\frac{\mathrm{d}^3\mathbf{q}_2}{(2\pi)^3\,2E_2} \\ &\quad \times (2\pi)^4\,\delta^{(4)}(q' - q_3 - q_4)\,\frac{\mathrm{d}^3\mathbf{q}_3}{(2\pi)^3\,2E_3}\,\frac{\mathrm{d}^3\mathbf{q}_4}{(2\pi)^3\,2E_4} \\ &\quad \times (2\pi)^4\,\delta^{(4)}(p - q - q')\,\frac{\mathrm{d}^3\mathbf{q}}{(2\pi)^3\,2q^0}\,\frac{\mathrm{d}^3\mathbf{q}'}{(2\pi)^3\,2q'^0}\,\mathrm{d}s_1\,\mathrm{d}s_2\,. \end{aligned} \tag{3.65}$$

We are now ready to explain why this new form of the phase space factor (3.65) is better than the form (3.50) which we started with. The factor (3.65) can be divided into four Lorentz invariant parts, one for the decay of each of the three particles H, V_1 and V_2, and one extra factor $\mathrm{d}s_1\mathrm{d}s_2$ which is the differential of the squared invariant masses of the two vector bosons. Because the factors for the three decays are separately Lorentz invariant, the integral over the phase space of each decay can be performed in its own rest frame. The rest frame of a decay is the natural frame in which to study it. This can be seen from the fact that the polar and azimuthal decay angles will be isotropically distributed in this frame if the matrix element is constant. In this frame, any deviation from flat distributions must come from the matrix element. This is not the case for a boosted frame.

I am in the following calculations not going to evaluate each part of the phase space factor in its own frame, but in the rest frame of the Higgs boson. The form (3.65) of the phase space factor is still very practical to work with. This can be seen from the fact that there is one delta function for the decay of each vector boson, compared to one delta function for both decays in (3.50).

The price to pay for the extra delta functions is the new differentials $\mathrm{d}s_1$, $\mathrm{d}s_2$, $\mathrm{d}^3\mathbf{q}$ and $\mathrm{d}^3\mathbf{q}'$. The integrals over the momenta of the vector bosons are easy to perform, because the matrix element is independent of the decay angles in the Higgs decay, in the rest frame of the decay. This can be seen from the fact that the Higgs boson is a scalar particle, and has not got any preferred direction in space.

It is an advantage to keep the squared invariant masses of the vector bosons s_1 and s_2 fixed until the integrals over the other variables have been performed. In this way we can postpone integrating over the Breit-Wigner distributions in the vector boson propagators. These integrals can then be performed numerically at the end of the calculations.

3.3 Integrals Involving the Delta Functions

I will now exploit the three four-dimensional delta functions to perform the integrals over certain variables. The integrations themselves are trivial, but in addition we have to express all variables which have been integrated over, in terms of the remaining variables, according to the values they got from the delta functions. At the end of this section I will then express the momentum products in the matrix elements in terms of the remaining variables, which will be E_1, E_3, s_1, s_2 and ϕ.

Combining the expression for the phase space from the previous section, with the decay rates (3.26) and (3.49) from the first section, we can write the decay rate as:

$$\begin{aligned} \mathrm{d}\Gamma &= \frac{1}{(2\pi)^2}\,(2\pi)^4\,\delta^{(4)}(p-q-q')\,\frac{\mathrm{d}^3\mathbf{q}}{(2\pi)^3 2q^0}\,\frac{\mathrm{d}^3\mathbf{q}'}{(2\pi)^3 2q'^0} \\ &\quad\times (2\pi)^4\,\delta^{(4)}(q-q_1-q_2)\,\frac{\mathrm{d}^3\mathbf{q}_1}{(2\pi)^3 2E_1}\,\frac{\mathrm{d}^3\mathbf{q}_2}{(2\pi)^3 2E_2}\,\mathrm{d}s_1 \\ &\quad\times (2\pi)^4\,\delta^{(4)}(q'-q_3-q_4)\,\frac{\mathrm{d}^3\mathbf{q}_3}{(2\pi)^3 2E_3}\,\frac{\mathrm{d}^3\mathbf{q}_4}{(2\pi)^3 2E_4}\,\mathrm{d}s_2 \\ &\quad\times C_i\left(\prod_{j=1}^{2}\frac{g_j^2 N_j}{(s_j-m_V^2)^2+m_V^2\Gamma_V^2}\right) \\ &\quad\times \left[X_i+\sin(2\chi_1)\,\sin(2\chi_2)\,Y_i\right], \end{aligned} \tag{3.66}$$

where $i = h, A$. The constants C_i are equal to

$$C_h = \frac{\sqrt{2}G_F m_V^4}{m} \quad \text{and} \quad C_A = \frac{|\eta|^2}{4m}\,, \tag{3.67}$$

and the momentum products X_i and Y_i are given by:

$$X_h = (q_1\cdot q_3)(q_2\cdot q_4)+(q_1\cdot q_4)(q_2\cdot q_3)\,, \tag{3.68}$$

$$Y_h = (q_1\cdot q_3)(q_2\cdot q_4)-(q_1\cdot q_4)(q_2\cdot q_3)\,, \tag{3.69}$$

$$\begin{aligned} X_A &= -2[(q_1\cdot q_2)(q_3\cdot q_4)]^2 \\ &\quad -2[(q_1\cdot q_3)(q_2\cdot q_4)-(q_1\cdot q_4)(q_2\cdot q_3)]^2 \\ &\quad +(q_1\cdot q_2)(q_3\cdot q_4) \\ &\quad\times\{[(q_1\cdot q_3)+(q_2\cdot q_4)]^2+[(q_1\cdot q_4)+(q_2\cdot q_3)]^2\}\,, \end{aligned} \tag{3.70}$$

and

$$Y_A = (q_1\cdot q_2)(q_3\cdot q_4)\{[(q_1\cdot q_3)-(q_2\cdot q_4)]^2-[(q_1\cdot q_4)-(q_2\cdot q_3)]^2\}\,. \tag{3.71}$$

3.3.1 Performing the Integrals

We shall start by performing the integral over $\mathbf{q}'$. Here we use the three-momentum part of the following delta function, remembering that in the Higgs rest frame $p = (m, \mathbf{0})$:

$$\delta^{(4)}(p - q - q') = \delta(m - q^0 - q'^0)\, \delta^{(3)}(\mathbf{q} + \mathbf{q}')\,, \tag{3.72}$$

From the delta function in the integral,

$$\int \mathrm{d}^3\mathbf{q}'\, \delta^{(3)}(\mathbf{q} + \mathbf{q}') \sum_{\text{spin}} |\mathcal{M}|^2\,, \tag{3.73}$$

where $\sum_{\text{spin}} |\mathcal{M}|^2$ is the squared matrix element, we get the obvious relation

$$\mathbf{q}' = -\mathbf{q}\,. \tag{3.74}$$

Now I will use the remaining part of the delta function to perform the integral over $|\mathbf{q}|$. We write the differential $\mathrm{d}^3\mathbf{q}$ in polar coordinates:

$$\mathrm{d}^3\mathbf{q} = |\mathbf{q}|^2\, \mathrm{d}|\mathbf{q}|\, \mathrm{d}\Omega_q\,. \tag{3.75}$$

The integral we want to perform is

$$\int \frac{\mathrm{d}|\mathbf{q}|\, |\mathbf{q}|^2}{q^0 q'^0}\, \delta(m - q^0 - q'^0) \sum_{\text{spin}} |\mathcal{M}|^2\,. \tag{3.76}$$

In order to perform the integral we are going to need the following property of the delta function [19] (page 22):

$$\delta(f(x) - f(x_0)) = \frac{1}{|f'(x_0)|}\, \delta(x - x_0)\,. \tag{3.77}$$

We must in addition use the relations from (3.60) and (3.64) in the previous section:

$$q' = \sqrt{\mathbf{q}'^2 + s_2} = \sqrt{\mathbf{q}^2 + s_2}\,, \tag{3.78}$$

and

$$q^0 = \sqrt{\mathbf{q}^2 + s_1}\,. \tag{3.79}$$

From these equations we see that

$$\frac{\partial}{\partial|\mathbf{q}|}[m - q^0(|\mathbf{q}|) - q'^0(|\mathbf{q}|)] = -|\mathbf{q}|\, \frac{1}{q^0} - |\mathbf{q}|\, \frac{1}{q'^0} = -|\mathbf{q}|\, \frac{q^0 + q'^0}{q^0 q'^0}\,, \tag{3.80}$$

and this enables us to perform the integral:

$$\int \frac{\mathrm{d}|\mathbf{q}|\, |\mathbf{q}|^2}{q^0 q'^0}\, \delta(m - q^0 - q'^0) \sum_{\text{spin}} |\mathcal{M}|^2 = \frac{|\mathbf{q}|}{m} \sum_{\text{spin}} |\mathcal{M}|^2 \Big|_{q^0 + q'^0 = m}\,. \tag{3.81}$$

Having performed the integrals, $\mathbf{q}$, q^0 and q'^0 must be expressed in terms of the remaining variables. From the delta function $\delta(m - q^0 - q'^0)$ we get the equation

$$m - \sqrt{\mathbf{q}^2 + s_1} - \sqrt{\mathbf{q}^2 + s_1} = 0\,, \tag{3.82}$$

which can be solved to give

$$|\mathbf{q}| = \frac{\sqrt{\lambda(m^2, s_1, s_2)}}{2m}\,. \tag{3.83}$$

Here

$$\lambda(m^2, s_1, s_2) = m^4 + s_1^2 + s_2^2 - 2(m^2 s_1 + m^2 s_2 + s_1 s_2)\,, \tag{3.84}$$

is known as the Källen function. Having found the value of $|\mathbf{q}|$, we can use (3.78), (3.79) and (3.83) to find q^0 and q'^0:

$$\begin{aligned} q^0 &= \left(\frac{\lambda}{4m^2} + s_1\right)^{1/2} \\ &= \frac{1}{2m}[m^4 + s_1^2 + s_2^2 - 2(m^2 s_1 + m^2 s_2 + s_1 s_2) + 4m^2 s_1]^{1/2} \\ &= \frac{1}{2m}[m^4 + s_1^2 + s_2^2 + 2m^2 s_1 - 2m^2 s_2 - 2s_1 s_2]^{1/2} \\ &= \frac{1}{2m}[m^2 + s_1 - s_2]\,, \end{aligned} \tag{3.85}$$

and

$$\begin{aligned} q'^0 &= \left(\frac{\lambda}{4m^2} + s_2\right)^{1/2} \\ &= \frac{1}{2m}[m^4 + s_1^2 + s_2^2 - 2(m^2 s_1 + m^2 s_2 + s_1 s_2) + 4m^2 s_2]^{1/2} \\ &= \frac{1}{2m}[m^4 + s_1^2 + s_2^2 - 2m^2 s_1 + 2m^2 s_2 - 2s_1 s_2]^{1/2} \\ &= \frac{1}{2m}[m^2 - s_1 + s_2]\,. \end{aligned} \tag{3.86}$$

From (3.83), we see that the integral in (3.81) has the value

$$\int \frac{\mathrm{d}|\mathbf{q}|\,|\mathbf{q}|^2}{q^0 q'^0}\,\delta(m - q^0 - q'^0) \sum_{\text{spin}} |\mathcal{M}|^2 = \frac{\sqrt{\lambda(m^2, s_1, s_2)}}{2m^2} \sum_{\text{spin}} |\mathcal{M}|^2 \Big|_{q^0 + q'^0 = m}\,. \tag{3.87}$$

We have now performed the integrals over $|\mathbf{q}|$ and $\mathbf{q}'$. Some of the phase space has been integrated over, and the differential decay rate can be written in the form:

$$\mathrm{d}\Gamma = \frac{1}{(2\pi)^8\, 2^6}\,\frac{\sqrt{\lambda}}{2m^2}\,\mathrm{d}\Omega_q$$

$$\times \delta^{(4)}(q - q_1 - q_2)\,\frac{\mathrm{d}^3\mathbf{q}_1}{E_1}\,\frac{\mathrm{d}^3\mathbf{q}_2}{E_2}\,\mathrm{d}s_1$$
$$\times \delta^{(4)}(q' - q_3 - q_4)\,\frac{\mathrm{d}^3\mathbf{q}_3}{E_3}\,\frac{\mathrm{d}^3\mathbf{q}_4}{E_4}\,\mathrm{d}s_2$$
$$\times C_i \left(\prod_{j=1}^{2} \frac{g_j^2 N_j}{(s_j - m_V^2)^2 + m_V^2 \Gamma_V^2} \right)$$
$$\times \left[X_i + \sin(2\chi_1)\,\sin(2\chi_2)\,Y_i \right], \tag{3.88}$$

Next, we are going to perform the integral over $\mathbf{q}_2$:

$$\int \mathrm{d}^3\mathbf{q}_2\,\delta^{(3)}(\mathbf{q} - \mathbf{q}_1 - \mathbf{q}_2) \sum_{\text{spin}} |\mathcal{M}|^2 \,. \tag{3.89}$$

The delta function gives us the relation for conservation of momentum at the $V_1 f_1 \bar{f}_2$ vertex:

$$\mathbf{q}_2 = \mathbf{q} - \mathbf{q}_1 \,. \tag{3.90}$$

This, together with (3.83) shows us that

$$\begin{aligned} |\mathbf{q}_2|^2 &= |\mathbf{q}|^2 + |\mathbf{q}_1|^2 - 2|\mathbf{q}|\,|\mathbf{q}_1| \cos u \\ &= \frac{\lambda}{4m^2} + E_1^2 - \frac{\sqrt{\lambda}}{m} E_1 \cos u \,, \end{aligned} \tag{3.91}$$

in the massless fermion approximation where

$$E_1 = |\mathbf{q}_1|, \quad E_2 = |\mathbf{q}_2| \,. \tag{3.92}$$

Here u is the angle between $\mathbf{q}$ and $\mathbf{q}_1$, see figure 3.2.

The next thing I will do, is to integrate over $\cos u$. As can be seen in figure 3.2, I have chosen the direction of the axes in the Higgs rest frame so that the vector $\mathbf{q}$ points in the direction of the positive z-axis, and so that $\mathbf{q}_3$ and $\mathbf{q}_4$ lie in the xz-plane. We will later see that the decay rate is independent of the absolute direction in which $\mathbf{q}$ and $\mathbf{q}_3$ point, and only depends on the relative angle ϕ, see (3.2).

In order to perform the integral over $\cos u$ we write the $\mathbf{q}_1$ differential in polar coordinates:

$$\mathrm{d}^3\mathbf{q}_1 = |\mathbf{q}_1|^2\,\mathrm{d}|\mathbf{q}_1|\,\mathrm{d}(\cos u)\,\mathrm{d}v = E_1^2\,\mathrm{d}E_1\,\mathrm{d}(\cos u)\,\mathrm{d}v \,. \tag{3.93}$$

The angles u and v in the differential are defined in figure 3.2. For the following integral:

$$\int \mathrm{d}(\cos u)\,\delta(q^0 - E_1 - E_2) \sum_{\text{spin}} |\mathcal{M}|^2 \tag{3.94}$$

we must calculate

$$\frac{\partial}{\partial(\cos u)} \left[q^0 - E_1 - E_2 \right] = -\frac{\partial E_2}{\partial(\cos u)} \,, \tag{3.95}$$

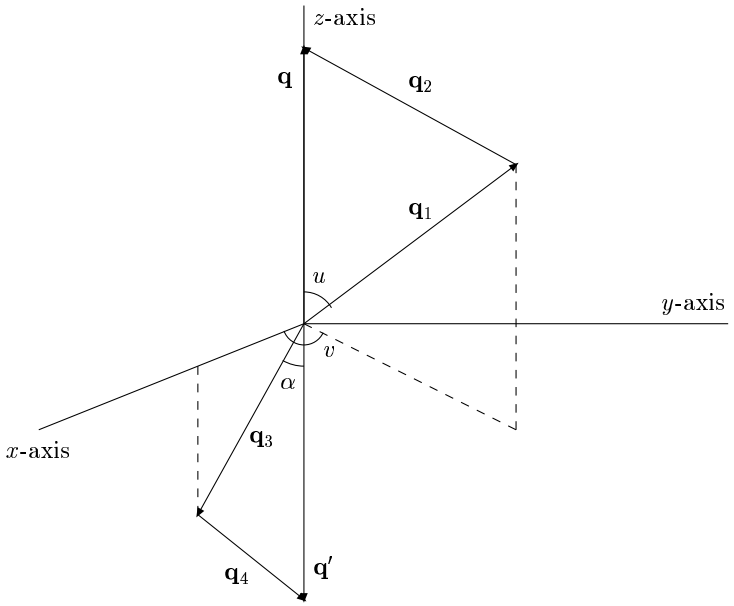

Figure 3.2: Definitions of the angles u, v and α. The momentum vector $\mathbf{q}'$ points in the negative z-direction. The vectors $\mathbf{q}_3$ and $\mathbf{q}_4$ lie in the xz-plane. The projection of $\mathbf{q}_1$ into the xy-plane is shown as a dashed line.

where we consider E_1 fixed. One can see from (3.91) and (3.92) that

$$\frac{\partial}{\partial(\cos u)} E_2^2 \;=\; -\frac{\sqrt{\lambda}}{m} E_1 \tag{3.96}$$

since λ and E_1 are fixed, and therefore

$$\begin{aligned} \frac{\partial E_2}{\partial(\cos u)} &= \frac{1}{2E_2} \frac{\partial}{\partial(\cos u)} E_2^2 \\ &= -\frac{\sqrt{\lambda}}{2m} \frac{E_1}{E_2} \,. \end{aligned} \tag{3.97}$$

We use the above equations and find that the integration over $\cos u$ gives:

$$\int \mathrm{d}(\cos u)\, \delta(q^0 - E_1 - E_2)\, \frac{E_1^2}{E_1\, E_2} \sum_{\text{spin}} |\mathcal{M}|^2 = \frac{2m}{\sqrt{\lambda}} \sum_{\text{spin}} |\mathcal{M}|^2 \Big|_{q^0 = E_1 + E_2} \,. \tag{3.98}$$

Having performed the integral over $\cos u$, we have to express the angle in terms of variables which remain to integrate over. From the delta function in the integral we get the relation

$$q^0 - E_1 - E_2 = 0 \,, \tag{3.99}$$

which leads to

$$E_2^2 = (q^0)^2 + E_1^2 - 2q^0 E_1 \,. \tag{3.100}$$

This equation, together with (3.85) and (3.91), leads to

$$\frac{\lambda}{4m^2} + E_1^2 - \frac{\sqrt{\lambda}}{m} E_1 \cos u = \frac{\lambda}{4m^2} + s_1 + E_1^2 - \frac{2E_1}{2m}(m^2 + s_1 - s_2) \,. \tag{3.101}$$

Solving the above equation, we find the expression for $\cos u$, which we wanted:

$$\cos u = \frac{1}{\sqrt{\lambda}\, E_1} \left[E_1(m^2 + s_1 - s_2) - m s_1 \right] . \tag{3.102}$$

We are now going to perform the integrals over $\mathbf{q}_4$ and $\cos\alpha$, where we will use the remaining delta function. These integrations are very similar to the integrations over $\mathbf{q}_2$ and $\cos u$, and I will therefore only state the results. The integral

$$\int \mathrm{d}^3\mathbf{q}_4 \, \delta^{(3)}(\mathbf{q}' - \mathbf{q}_3 - \mathbf{q}_4) \sum_{\text{spin}} |\mathcal{M}|^2 \,, \tag{3.103}$$

gives the relations

$$\mathbf{q}_4 = \mathbf{q}' - \mathbf{q}_3 \,, \tag{3.104}$$

and

$$\begin{aligned} |\mathbf{q}_4|^2 &= |\mathbf{q}'|^2 + |\mathbf{q}_3|^2 - 2|\mathbf{q}'|\,|\mathbf{q}_3| \cos\alpha \\ &= \frac{\lambda}{4m^2} + E_3^2 - \frac{\sqrt{\lambda}}{m} E_3 \cos\alpha \,, \end{aligned} \tag{3.105}$$

in the massless fermion approximation where

$$E_3 = |\mathbf{q}_3|, \quad E_4 = |\mathbf{q}_4| \,. \tag{3.106}$$

Here α is the angle between $\mathbf{q}'$ and $\mathbf{q}_3$. See figure 3.2.

The differential $\mathrm{d}^3\mathbf{q}_3$ must be written in polar coordinates

$$\mathrm{d}^3\mathbf{q}_3 = |\mathbf{q}_3|^2 \,\mathrm{d}|\mathbf{q}_3| \,\mathrm{d}(\cos\alpha)\,\mathrm{d}\beta = E_3^2 \,\mathrm{d}E_3 \,\mathrm{d}(\cos\alpha)\,\mathrm{d}\beta \,, \tag{3.107}$$

in order to perform the integral over $\cos\alpha$

$$\int \mathrm{d}(\cos\alpha)\, \delta(q'^0 - E_3 - E_4) \sum_{\text{spin}} |\mathcal{M}|^2 \,. \tag{3.108}$$

Integration over the angle β in the differential corresponds to rotating the coordinate system in figure 3.2 around the z-axis. If we compare (3.91) and (3.105) we can see that

$$\frac{\partial}{\partial(\cos\alpha)} \left[q'^0 - E_3 - E_4 \right] = -\frac{\partial E_4}{\partial(\cos\alpha)} = \frac{\sqrt{\lambda}}{2m} \frac{E_3}{E_4} \,, \tag{3.109}$$

and similar to the $\cos u$ integrations we find

$$\int \mathrm{d}(\cos\alpha)\,\delta(q'^0 - E_3 - E_4)\,\frac{E_3^2}{E_3\,E_4}\sum_{\text{spin}}|\mathcal{M}|^2 = \frac{2m}{\sqrt{\lambda}}\sum_{\text{spin}}|\mathcal{M}|^2\Big|_{q'^0=E_3+E_4}\,. \tag{3.110}$$

Again, similar to $\cos u$, $\cos\alpha$ must be expressed in terms of s_1, s_2 and E_3. From the relation

$$q'^0 - E_3 - E_4 = 0\,, \tag{3.111}$$

and from (3.86) and (3.105) we can find an expression for $\cos\alpha$:

$$\cos\alpha = \frac{1}{\sqrt{\lambda}\,E_3}[E_3(m^2 - s_1 + s_2) - ms_2]\,. \tag{3.112}$$

We have performed the integrals where we could use delta functions. The decay rate (3.88) can now be written in the form:

$$\begin{aligned}\mathrm{d}\Gamma &= \frac{1}{(2\pi)^8\,2^5\,\sqrt{\lambda}}\,\mathrm{d}E_1\,\mathrm{d}v\,\mathrm{d}E_3\,\mathrm{d}\beta\,\mathrm{d}\Omega_q\,\mathrm{d}s_1\,\mathrm{d}s_2 \\ &\quad\times C_i\left(\prod_{j=1}^{2}\frac{g_j^2 N_j}{(s_j - m_V^2)^2 + m_V^2\Gamma_V^2}\right) \\ &\quad\times[X_i + \sin(2\chi_1)\,\sin(2\chi_2)\,Y_i]\,,\end{aligned} \tag{3.113}$$

The next task will be to change integration variable from v into ϕ. The angle ϕ is defined in (3.2) as:

$$\cos\phi = \frac{(\mathbf{q}_1\times\mathbf{q}_2)\cdot(\mathbf{q}_3\times\mathbf{q}_4)}{|\mathbf{q}_1\times\mathbf{q}_2||\mathbf{q}_3\times\mathbf{q}_4|}\,. \tag{3.114}$$

From figure 3.2 and (3.114), we can see that the relation

$$v = \pi - \phi \tag{3.115}$$

holds, and therefore

$$\cos v = -\cos\phi\,. \tag{3.116}$$

I now want to change integration variables so that I integrate over the angle ϕ instead of the angle v. Using (3.115), we get

$$\begin{aligned}\int_0^{2\pi}\mathrm{d}v\,f(\cos\phi) &= \int_{\pi}^{-\pi}(-1)\,\mathrm{d}\phi\,f(\cos\phi) \\ &= \int_{-\pi}^{\pi}\mathrm{d}\phi\,f(\cos\phi)\end{aligned} \tag{3.117}$$

We see that $\mathrm{d}\phi$ can simply replace $\mathrm{d}v$ in the expression (3.113) for the decay rate. In this form for the decay rate we still have to express the momentum products X_i and Y_i in terms of the variables which remain to be integrated over, that is E_1, E_3, ϕ, s_1 and s_2.

3.3.2 Momentum Products

Now I will express the products of fermion momenta in terms of the variables s_1, s_2, E_1, E_3 and ϕ. Using $q_2 = q - q_1$, $q_4 = q' - q_3$ and $\mathbf{q}' = -\mathbf{q}$ we see that

$$\begin{aligned}
(q_1 \cdot q_3) &= E_1 E_3 - \mathbf{q}_1 \cdot \mathbf{q}_3 \,, \\
(q_2 \cdot q_4) &= (q^0 - E_1)(q'^0 - E_3) - (\mathbf{q} - \mathbf{q}_1) \cdot (-\mathbf{q} - \mathbf{q}_3) \\
&= q^0 q'^0 - q^0 E_3 - q'^0 E_1 + E_1 E_3 + \mathbf{q}^{\,2} + \mathbf{q} \cdot \mathbf{q}_3 - \mathbf{q} \cdot \mathbf{q}_1 - \mathbf{q}_1 \cdot \mathbf{q}_3 \,, \\
(q_1 \cdot q_4) &= E_1 (q'^0 - E_3) - \mathbf{q}_1 \cdot (-\mathbf{q} - \mathbf{q}_3) \\
&= q'^0 E_1 - E_1 E_3 + \mathbf{q} \cdot \mathbf{q}_1 + \mathbf{q}_1 \cdot \mathbf{q}_3 \,, \\
(q_2 \cdot q_3) &= (q^0 - E_1) E_3 - (\mathbf{q} - \mathbf{q}_1) \cdot \mathbf{q}_3 \\
&= q^0 E_3 - E_1 E_3 - \mathbf{q} \cdot \mathbf{q}_3 + \mathbf{q}_1 \cdot \mathbf{q}_3 \,. \qquad (3.118)
\end{aligned}$$

For massless fermions we also have:

$$(q_1 \cdot q_2) = \frac{1}{2}(q_1 + q_2)^2 = \frac{1}{2} s_1 \,, \qquad (3.119)$$

and

$$(q_3 \cdot q_4) = \frac{1}{2}(q_3 + q_4)^2 = \frac{1}{2} s_2 \,. \qquad (3.120)$$

We can find expressions for the three-momenta $\mathbf{q}$, $\mathbf{q}_1$ and $\mathbf{q}_3$ from figure 3.2 and from (3.83):

$$\begin{aligned}
\mathbf{q} &= \frac{\sqrt{\lambda}}{2m} (0, 0, 1) \,, \\
\mathbf{q}_1 &= E_1 (\sin u \, \cos v, \sin u \, \sin v, \cos u) \,, \\
\mathbf{q}_3 &= E_3 (\sin \alpha, 0, -\cos \alpha) \,. \qquad (3.121)
\end{aligned}$$

Here, the angles u and α are given by (3.102) and (3.112):

$$\cos u = \frac{1}{\sqrt{\lambda} E_1} [E_1 (m^2 + s_1 - s_2) - m s_1] \,, \qquad (3.122)$$

and

$$\cos \alpha = \frac{1}{\sqrt{\lambda} E_3} [E_3 (m^2 - s_1 + s_2) - m s_2] \,. \qquad (3.123)$$

These expressions allow us to find the products of the three-momenta. At the same time we can use (3.116), $\cos v = -\cos \phi$, to replace v by ϕ:

$$\mathbf{q}_1 \cdot \mathbf{q}_3 = -E_1 E_3 (\sin u \sin \alpha \cos \phi + \cos u \cos \alpha) \,, \qquad (3.124)$$

$$\begin{aligned}
\mathbf{q} \cdot \mathbf{q}_3 &= -\frac{\sqrt{\lambda}}{2m} E_3 \cos \alpha \\
&= \frac{-E_3}{2m} (m^2 - s_1 + s_2) + \frac{1}{2} s_2 \,, \qquad (3.125)
\end{aligned}$$

$$\begin{aligned}\mathbf{q}\cdot\mathbf{q}_1 &= \frac{\sqrt{\lambda}}{2m}E_1\cos u \\ &= \frac{E_1}{2m}(m^2+s_1-s_2)-\frac{1}{2}s_1\,,\end{aligned} \tag{3.126}$$

and

$$\mathbf{q}^{\,2} = \frac{\lambda}{4m^2}\,. \tag{3.127}$$

We also have to express the products $\sin u\sin\alpha$ and $\cos u\cos\alpha$ in terms of the variables s_1, s_2, E_1 and E_3. From (3.122) and (3.123), and the fact that

$$\sin u\sin\alpha = \sqrt{(1-\cos u^2)(1-\cos\alpha^2)} \tag{3.128}$$

one can see that:

$$\sin u\sin\alpha = \frac{m}{\lambda E_1 E_3}\sqrt{R}\,, \tag{3.129}$$

where

$$\begin{aligned}R &= 16m^2 s_1 s_2 E_1^2 E_3^2 \\ &\quad - 8ms_1s_2(m^2-s_1+s_2)E_1^2E_3 - 8ms_1s_2(m^2+s_1-s_2)E_1E_3^2 \\ &\quad + 4m^2s_1s_2^2E_1^2 + 4m^2s_1^2s_2E_3^2 \\ &\quad + 4s_1s_2[m^4-(s_1-s_2)^2]E_1E_3 \\ &\quad - 2ms_1s_2^2(m^2+s_1-s_2)E_1 - 2ms_1^2s_2(m^2-s_1+s_2)E_3 \\ &\quad + m^2s_1^2s_2^2\,,\end{aligned} \tag{3.130}$$

and that

$$\begin{aligned}\cos u\cos\alpha &= \frac{1}{\lambda E_1E_3}[(m^4-(s_1-s_2)^2)E_1E_3 \\ &\quad - ms_2(m^2+s_1-s_2)E_1 - ms_1(m^2-s_1+s_2)E_3 \\ &\quad + m^2s_1s_2]\,.\end{aligned} \tag{3.131}$$

The expressions we found for q^0 and $q^{'0}$, (3.85) and (3.86), were

$$q^0 = \frac{1}{2m}(m^2+s_1-s_2)\,, \tag{3.132}$$

and

$$q'^0 = \frac{1}{2m}(m^2-s_1+s_2)\,. \tag{3.133}$$

These equations can be combined to give

$$q^0q'^0 = \frac{1}{4m^2}(m^4-s_1^2-s_2^2+2s_1s_2)\,. \tag{3.134}$$

From (3.118) and the following results, we can now write down the momentum products:

$$\begin{aligned}
(q_1\cdot q_3) &= E_1E_3(1+\sin u\sin\alpha\cos\phi+\cos u\cos\alpha)\,,\\
(q_2\cdot q_4) &= E_1E_3(1+\sin u\sin\alpha\cos\phi+\cos u\cos\alpha)-E_1m-E_3m+\frac{1}{2}m^2\,,\\
(q_1\cdot q_4) &= E_1m-\frac{1}{2}s_1-E_1E_3(1+\sin u\sin\alpha\cos\phi+\cos u\cos\alpha)\,,\\
(q_2\cdot q_3) &= E_3m-\frac{1}{2}s_2-E_1E_3(1+\sin u\sin\alpha\cos\phi+\cos u\cos\alpha)\,. \qquad (3.135)
\end{aligned}$$

Here I have not expressed $\cos u\cos\alpha$ and $\sin u\sin\alpha$ in terms of other variables, because this would make the expressions very long and difficult to read.

The CP-even case: X_h and Y_h

In order to get the momentum products X_h and Y_h, we must multiply out the products in (3.135). X_h and Y_h can be written as

$$X_h = X_a + X_b\,, \quad Y_h = X_a - X_b\,, \qquad (3.136)$$

where

$$X_a = (q_1\cdot q_3)(q_2\cdot q_4) \qquad (3.137)$$

and

$$X_b = (q_1\cdot q_4)(q_2\cdot q_3)\,. \qquad (3.138)$$

From (3.135) we see that

$$\begin{aligned}
X_a &= E_1^2E_3^2(1+\sin u\sin\alpha\cos\phi+\cos u\cos\alpha)^2\\
&\quad + E_1E_3m\left(\frac{1}{2}m-E_1-E_3\right)\\
&\quad \times(1+\sin u\sin\alpha\cos\phi+\cos u\cos\alpha) \qquad (3.139)
\end{aligned}$$

and

$$\begin{aligned}
X_b &= E_1^2E_3^2(1+\sin u\sin\alpha\cos\phi+\cos u\cos\alpha)^2\\
&\quad + E_1E_3\left[\frac{1}{2}(s_1+s_2)-m(E_1+E_3)\right]\\
&\quad \times(1+\sin u\sin\alpha\cos\phi+\cos u\cos\alpha)\\
&\quad + E_1E_3m^2-\frac{1}{2}E_1ms_2-\frac{1}{2}E_3ms_1+\frac{1}{4}s_1s_2\,. \qquad (3.140)
\end{aligned}$$

We are now ready to write down the final expressions for the products X_h and Y_h in terms of the variables E_1, E_3, s_1, s_2 and ϕ:

$$\begin{aligned} X_h &= 2E_1^2E_3^2(1+\sin u\sin\alpha\cos\phi+\cos u\cos\alpha)^2 \\ &\quad + E_1E_3\left[\frac{1}{2}(m^2+s_1+s_2)-2m(E_1+E_3)\right] \\ &\quad \times(1+\sin u\sin\alpha\cos\phi+\cos u\cos\alpha) \\ &\quad + E_1E_3m^2-\frac{1}{2}E_1ms_2-\frac{1}{2}E_3ms_1+\frac{1}{4}s_1s_2\,, \end{aligned} \tag{3.141}$$

and

$$\begin{aligned} Y_h &= \frac{1}{2}(m^2-s_1-s_2)E_1E_3(1+\sin u\sin\alpha\cos\phi+\cos u\cos\alpha) \\ &\quad - E_1E_3m^2+\frac{1}{2}E_1ms_2+\frac{1}{2}E_3ms_1-\frac{1}{4}s_1s_2\,. \end{aligned} \tag{3.142}$$

Remember that $\cos u\cos\alpha$ and $\sin u\sin\alpha$ here are functions of the variables E_1, E_3, s_1 and s_2, see (3.122) and (3.123).

The CP-odd case: X_A and Y_A

The products X_A and Y_A in the matrix element for decay of a CP-odd Higgs boson can be calculated from the expressions (3.70) and (3.71). We need the momentum products (3.119), (3.120) and (3.135). I have used REDUCE [22] to perform these calculations:

$$\begin{aligned} X_A &= E_1E_3(\cos u\cos\alpha+\sin u\sin\alpha\cos\phi) \\ &\quad \times\{E_1E_3[m^4-(s_1-s_2)^2]-E_1ms_2[m^2+s_1-s_2] \\ &\quad - E_3ms_1[m^2-s_1+s_2]+m^2s_1s_2\} \\ &\quad - \frac{1}{2}\lambda E_1^2E_3^2(\cos u\cos\alpha+\sin u\sin\alpha\cos\phi)^2 \\ &\quad + \frac{1}{16}\{-8E_1^2E_3^2[\lambda+4m^2(s_1+s_2)] \\ &\quad + 4E_1ms_1(4E_3^2-s_2)(m^2+s_1-s_2)+4E_3ms_2(4E_1^2-s_1)(m^2-s_1+s_2) \\ &\quad + 8E_1^2m^2s_2(s_1-s_2)+8E_3^2m^2s_1(s_2-s_1) \\ &\quad + s_1s_2[m^4+(s_1-s_2)^2]\}\,, \end{aligned} \tag{3.143}$$

and

$$\begin{aligned} Y_A &= \frac{1}{16}s_1s_2[16E_1E_3m^2-4E_1m(m^2-s_1+s_2) \\ &\quad - 4E_3m(m^2+s_1-s_2)+m^4-(s_1-s_2)^2]\,. \end{aligned} \tag{3.144}$$

3.4 Integrals over Energy and Angle Variables

We start this section with an expression for the decay rate after the integrals over the delta functions have been performed:

$$\begin{aligned} \mathrm{d}\Gamma &= C_i \left(\prod_{j=1}^{2} \frac{g_j^2 N_j}{(s_j - m_V^2)^2 + m_V^2 \Gamma_V^2} \right) [X_i + \sin(2\chi_1)\, \sin(2\chi_2)\, Y_i] \\ &\quad \times \frac{1}{(2\pi)^8 2^5 \sqrt{\lambda}}\, \mathrm{d}E_1\, \mathrm{d}E_3\, \mathrm{d}\beta\, \mathrm{d}\Omega_q\, \mathrm{d}s_1\, \mathrm{d}s_2\, \mathrm{d}\phi\,, \quad i = h, A\,, \end{aligned} \tag{3.145}$$

where

$$C_h = \frac{\sqrt{2} G_F m_V^4}{m}\,, \qquad C_A = \frac{|\eta|^2}{4m}\,, \tag{3.146}$$

and X_h, Y_h, X_A and Y_A are given by (3.141), (3.142), (3.143) and (3.144) in the previous section.

From these expressions, one can see that the decay rate is independent of all angular integration variables, except ϕ. We can therefore perform the integrations over β and Ω_q quite easily:

$$\int \mathrm{d}\beta\, \mathrm{d}\Omega_q f(E_1, E_3, s_1, s_2, \phi) = 8\pi^2 f(E_1, E_3, s_1, s_2, \phi)\,. \tag{3.147}$$

These integrations result in a factor $8\pi^2$ in the decay rate.

The next task of this section is to integrate the expression (3.145) over E_1 and E_3. But before we start with this I will find expressions for the limits of integration, which should depend only on the variables s_1, s_2 and ϕ. From (3.122) and (3.123) we see that $\cos u$ and $\cos\alpha$ are functions of E_1 and E_3, respectively. The integration limits of E_1 and E_3 must be given by $\cos u = \pm 1$ and $\cos\alpha = \pm 1$. The value $\cos u = 1$ is equivalent to the situation where the first fermion f_1 decays in the direction of the Z boson from which it came. This is the direction of the positive z-axis in figure 3.2. It can be shown that this decay configuration is consistent with conservation of momentum and energy, for massless fermions. So are the other three limits for $\cos u$ and $\cos\alpha$.

Solving the equations $\cos u = \pm 1$ and $\cos\alpha = \pm 1$ for E_1 and E_3 gives the maximum and minimum values for each variable:

$$\begin{aligned} E_{1\,\max} &= \frac{m^2 + s_1 - s_2 + \sqrt{\lambda}}{4m} \\ E_{1\,\min} &= \frac{m^2 + s_1 - s_2 - \sqrt{\lambda}}{4m} \\ E_{3\,\max} &= \frac{m^2 - s_1 + s_2 + \sqrt{\lambda}}{4m} \\ E_{3\,\min} &= \frac{m^2 - s_1 + s_2 - \sqrt{\lambda}}{4m}\,. \end{aligned} \tag{3.148}$$

Remember that m is the value of the Higgs boson mass.

For the integrals over E_1 and E_3, the following simplifications will be useful:

$$\begin{aligned}
\frac{1}{a-b}-\frac{1}{a+b} &= \frac{2b}{a^2-b^2}\\
\frac{1}{(a-b)^2}-\frac{1}{(a+b)^2} &= \frac{4ab}{(a^2-b^2)^2}\\
\frac{1}{(a-b)^3}-\frac{1}{(a+b)^3} &= \frac{6a^2b+2b^3}{(a^2-b^2)^3}\\
(m^2+s_1-s_2)^2-\lambda &= 4m^2s_1\\
(m^2-s_1+s_2)^2-\lambda &= 4m^2s_2\,.
\end{aligned} \tag{3.149}$$

Below, I have listed the integrals of the different powers in E_1 and E_3:

$$\begin{aligned}
\int_{E_{1\,\min}}^{E_{1\,\max}} \mathrm{d}E_1 &= \frac{\sqrt{\lambda}}{2m}\\
\int_{E_{3\,\min}}^{E_{3\,\max}} \mathrm{d}E_3 &= \frac{\sqrt{\lambda}}{2m}\\
\int_{E_{1\,\min}}^{E_{1\,\max}} \mathrm{d}E_1\,E_1 &= \frac{1}{8m^2}\sqrt{\lambda}(m^2+s_1-s_2)\\
\int_{E_{3\,\min}}^{E_{3\,\max}} \mathrm{d}E_3\,E_3 &= \frac{1}{8m^2}\sqrt{\lambda}(m^2-s_1+s_2)\\
\int_{E_{1\,\min}}^{E_{1\,\max}} \mathrm{d}E_1\,E_1^2 &= \frac{\sqrt{\lambda}(\lambda+3m^2s_1)}{24m^3}\\
\int_{E_{3\,\min}}^{E_{3\,\max}} \mathrm{d}E_3\,E_3^2 &= \frac{\sqrt{\lambda}(\lambda+3m^2s_2)}{24m^3}\,.
\end{aligned} \tag{3.150}$$

We are also going to need the following integration formulae [24]: For

$$R=a+bx+cx^2\,,\qquad \Delta=4ac-b^2\,, \tag{3.151}$$

we have

$$\begin{aligned}
\int \sqrt{R}\,\mathrm{d}x &= \frac{(2cx+b)\,\sqrt{R}}{4c}+\frac{\Delta}{8c}\int\frac{\mathrm{d}x}{\sqrt{R}}\\
\int x\sqrt{R}\,\mathrm{d}x &= \frac{\sqrt{R^3}}{3c}-\frac{(2cx+b)b}{8c^2}\sqrt{R}-\frac{b\Delta}{16c^2}\int\frac{\mathrm{d}x}{\sqrt{R}}\\
\int \frac{x\,\mathrm{d}x}{\sqrt{R}} &= \frac{\sqrt{R}}{c}-\frac{b}{2c}\int\frac{\mathrm{d}x}{\sqrt{R}}\\
\int \frac{x^2\,\mathrm{d}x}{\sqrt{R}} &= \left(\frac{x}{2c}-\frac{3b}{4c^2}\right)\sqrt{R}+\left(\frac{3b^2}{8c^2}-\frac{a}{2c}\right)\int\frac{\mathrm{d}x}{\sqrt{R}}\,.
\end{aligned} \tag{3.152}$$

In addition, for $c<0$ and $\Delta<0$ we also have [24]:

$$\int\frac{\mathrm{d}x}{\sqrt{R}}=\frac{-1}{\sqrt{-c}}\arcsin\frac{2cx+b}{\sqrt{-\Delta}}\,. \tag{3.153}$$

I have used REDUCE [22] to perform the integrals over E_1 and E_3, and for parts of the other long calculations in this section. The features of REDUCE which have been most useful to me, are solving of equations up to fourth order, finding the coefficients of polynomials and simplification of expressions.

3.4.1 Integrating the CP-even Matrix Element

We are now going to integrate the decay rate in (3.145) over E_1 and E_3 for the case of a CP-even Higgs boson. For fixed values of s_1 and s_2, X_h and Y_h are the only parts of the integrand that depend on E_1 and E_3. Using (3.129), (3.131), (3.141) and (3.142) we can find the full dependence of X_h and Y_h on E_1 and E_3. This shows us that X_h and Y_h both consist of two terms, where one is a polynomial in E_1 and E_3, and the other is the square root of a second-degree polynomial in E_1 and E_3 multiplied by a polynomial in E_1 and E_3. We have

$$\begin{aligned} X_h &= X_1 + X_2 \\ Y_h &= Y_1 + Y_2 \,, \end{aligned} \tag{3.154}$$

where X_2 and Y_2 are the pure polynomial parts, and X_1 and Y_1 contain square roots.

From the formulae (3.150) we find that the integrals of X_2 and Y_2 result in:

$$\begin{aligned} \int_{E_{1\,\min}}^{E_{1\,\max}} \mathrm{d}E_1 \int_{E_{3\,\min}}^{E_{3\,\max}} \mathrm{d}E_3 \, X_2 &= \frac{\lambda}{288\, m^2} \left(\lambda + 12 s_1 s_2 + 2 s_1 s_2 \cos 2\phi\right) \\ \int_{E_{1\,\min}}^{E_{1\,\max}} \mathrm{d}E_1 \int_{E_{3\,\min}}^{E_{3\,\max}} \mathrm{d}E_3 \, Y_2 &= 0 \,. \end{aligned} \tag{3.155}$$

The remaining integrals of X_1 and Y_1 are a bit more complicated, because the integrands contain square roots. Let us first write down the expressions for X_1 and Y_1:

$$\begin{aligned} X_1 &= P_X \sqrt{R_1} \\ Y_1 &= C_Y \sqrt{R_1} \,, \end{aligned} \tag{3.156}$$

where $R_1 = R$, as given by (3.130), and

$$\begin{aligned} P_X = \frac{m \cos\phi}{2\lambda^2} \{ & 16 E_1 E_3 m^2 (m^2 - s_1 - s_2) \\ & - 4 E_1 m (m^4 - 2 m^2 s_1 + s_1^2 - s_2^2) \\ & - 4 E_3 m (m^4 - 2 m^2 s_2 - s_1^2 + s_2^2) \\ & + m^2 [m^4 - m^2 (s_1 + s_2) - (s_1 - s_2)^2] \\ & + (s_1 + s_2)(s_1 - s_2)^2 \} \end{aligned} \tag{3.157}$$

and

$$C_Y = \frac{m \, \cos\phi}{2\,\lambda} \left[m^2 - s_1 - s_2\right] . \tag{3.158}$$

As can be seen, P_X is a first-degree polynomial in E_1 and E_3, and C_Y is a constant in the energy integration variables. To perform the integrals we will need the value of R_1 as a function of E_1 for $E_1 = E_{1\,\max}$ and for $E_1 = E_{1\,\min}$. The result is:

$$R_1(E_{1\,\min}) = R_1(E_{1\,\max}) = 0\,. \tag{3.159}$$

This makes the integration a bit simpler. Using (3.152) we find:

$$\begin{aligned}
\int_{E_{1\,\min}}^{E_{1\,\max}} \mathrm{d}E_1 X_1 &= 0 \\
\int_{E_{1\,\min}}^{E_{1\,\max}} \mathrm{d}E_1 Y_1 &= \frac{s_1 s_2 \cos\phi}{16} \int_{E_{1\,\min}}^{E_{1\,\max}} \frac{\mathrm{d}E_1}{\sqrt{R_1}} \\
&\quad \times [-4E_3^2 m(m^2 - s_1 - s_2) \\
&\quad + 2E_3(m^4 - 2m^2 s_1 + s_1^2 - s_2^2) \\
&\quad - m s_2(m^2 - s_1 - s_2)]\,.
\end{aligned} \tag{3.160}$$

We can see from (3.153) that we must know the signs of c and Δ in order to perform the integral

$$\int_{E_{1\,\min}}^{E_{1\,\max}} \frac{\mathrm{d}E_1}{\sqrt{R_1}}\,. \tag{3.161}$$

Here the quantities c and Δ are defined by

$$R_1 = a + bE_1 + cE_1^2\,, \tag{3.162}$$

see (3.151). The coefficients a, b and c have the following values:

$$\begin{aligned}
a &= m s_1^2 s_2[4mE_3^2 - 2E_3(m^2 - s_1 + s_2) + m s_2] \\
b &= 2 s_1 s_2\{-4E_3^2 m(m^2 + s_1 - s_2) \\
&\quad + 2E_3[m^4 - (s_1 - s_2)^2] \\
&\quad - m s_2(m^2 + s_1 - s_2)\} \\
c &= 4m s_1 s_2[4E_3^2 m - 2E_3 m^2 + 2E_3 s_1 - 2E_3 s_2 + m s_2]\,.
\end{aligned} \tag{3.163}$$

Notice that a, b and c depend on E_3, but not on E_1.

To find the sign of c I solve the second-degree equation $c(E_3) = 0$. The roots of this equation are:

$$E_3 = \left\{ \frac{m^2 - s_1 + s_2 + \sqrt{\lambda}}{4m}\,,\ \frac{m^2 - s_1 + s_2 - \sqrt{\lambda}}{4m} \right\}\,. \tag{3.164}$$

Actually, these solutions are equal to $E_{3\,\max}$ and $E_{3\,\min}$, respectively. Because the coefficient of E_3^2 in c, $16m^2 s_1 s_2$, is positive, the second-degree polynomial c (as a function of E_3) must be negative between its zeros. That is, c is negative between $E_{3\,\min}$ and $E_{3\,\max}$. Next, I study the sign of Δ between $E_{3\,\min}$ and $E_{3\,\max}$. From (3.151) and (3.163), one can see that Δ must be a fourth-degree polynomial in E_3. I solve the equation $\Delta(E_3) = 0$. It has got

the same roots as $c(E_3) = 0$, and both of the roots have multiplicity two. This shows that Δ must contain a factor c^2. And indeed we find that

$$\Delta = \frac{-\lambda c^2}{4m}\,, \tag{3.165}$$

independent of the value of E_3.

From (3.83) one can see that a negative λ would lead to imaginary momentum for the vector bosons. We therefore know that λ must be positive, and thus that Δ must be negative for all E_3. Having found that both c and Δ are negative between $E_{3\,\mathrm{min}}$ and $E_{3\,\mathrm{max}}$, which is the region of interest, we are now ready to perform the integral, using (3.153):

$$\int_{E_{1\,\mathrm{min}}}^{E_{1\,\mathrm{max}}} \frac{\mathrm{d}E_1}{\sqrt{R_1}} = \frac{-\arcsin\{\mathrm{sign}[4E_3^2 m - 2E_3(m^2 - s_1 + s_2) + m s_2]\}}{\sqrt{R_3}}\,, \tag{3.166}$$

where

$$R_3 = -m s_1 s_2 [4E_3^2 m - 2E_3(m^2 - s_1 + s_2) + m s_2]\,. \tag{3.167}$$

Here, sign() is the function which returns the sign of its argument. We solve the equation

$$4E_3^2 m - 2E_3(m^2 - s_1 + s_2) + m s_2 = 0\,, \tag{3.168}$$

and find that also this equation has got the roots in (3.164). This means that the expression (3.168) must be negative between $E_{3\,\mathrm{min}}$ and $E_{3\,\mathrm{max}}$, because the coefficient of E_3^2 in this expression is positive. We now see that

$$\int_{E_{1\,\mathrm{min}}}^{E_{1\,\mathrm{max}}} \frac{\mathrm{d}E_1}{\sqrt{R_1}} = \frac{\pi}{2\sqrt{R_3}}\,. \tag{3.169}$$

When we use the result from (3.169) in (3.160) we finally get:

$$\begin{aligned}\int_{E_{1\,\mathrm{min}}}^{E_{1\,\mathrm{max}}} \mathrm{d}E_1\, Y_1 \;&=\; \frac{\pi s_1 s_2 \cos\phi}{32\sqrt{R_3}}[-4E_3^2 m(m^2 - s_1 - s_2) \\ &\quad + 2E_3(m^4 - 2m^2 s_1 + s_1^2 - s_2^2) - m s_2(m^2 - s_1 - s_2)]\,.\end{aligned} \tag{3.170}$$

What now remains of this section contains the integration of this expression over E_3. We use the integration formulae in (3.152) and find:

$$\int_{E_{3\,\mathrm{min}}}^{E_{3\,\mathrm{max}}} \mathrm{d}E_3 \int_{E_{1\,\mathrm{min}}}^{E_{1\,\mathrm{max}}} \mathrm{d}E_1\, Y_1 \;=\; \frac{\lambda\pi s_1 s_2}{256m}(m^2 - s_1 - s_2)\cos\phi \int_{E_{3\,\mathrm{min}}}^{E_{3\,\mathrm{max}}} \frac{\mathrm{d}E_3}{\sqrt{R_3}}\,, \tag{3.171}$$

Here I have also used the fact that

$$R_3(E_{3\,\mathrm{min}}) = R_3(E_{3\,\mathrm{max}}) = 0\,. \tag{3.172}$$

As for the E_3 integration, we must determine the signs of c and Δ, see (3.151), in order to perform the integral

$$\int_{E_{3\,\mathrm{min}}}^{E_{3\,\mathrm{max}}} \frac{\mathrm{d}E_3}{\sqrt{R_3}}\,. \tag{3.173}$$

Here a, b and c are the coefficients of E_3 in R_3. From (3.167) we can see that c is negative. We also find that

$$\Delta = -4m^2 s_1^2 s_2^2 \lambda\,, \tag{3.174}$$

and this shows that Δ is negative. The integral can now be performed. It has the value:

$$\int_{E_{3\,\min}}^{E_{3\,\max}} \frac{\mathrm{d}E_3}{\sqrt{R_3}} = \frac{\pi}{2\sqrt{s_1 s_2}\, m}\,. \tag{3.175}$$

The final expression for the integral of Y_1 becomes:

$$\int_{E_{3\,\min}}^{E_{3\,\max}} \mathrm{d}E_3 \int_{E_{1\,\min}}^{E_{1\,\max}} \mathrm{d}E_1\, Y_1 = \frac{\lambda}{288m^2}\left(\frac{3}{4}\,\pi\right)^2 \sqrt{s_1 s_2}\,(m^2 - s_1 - s_2)\cos\phi\,. \tag{3.176}$$

To conclude this part, we write down the decay rate for a CP-even Higgs boson from (3.145), (3.155), (3.160) and (3.176):

$$\begin{aligned}\frac{\mathrm{d}\Gamma}{\mathrm{d}\phi\,\mathrm{d}s_1\,\mathrm{d}s_2} &= \frac{8}{9}\sqrt{2}\,G_F m_V^4 \prod_{j=1}^{2}\left(\frac{g_j^2}{(s_j - m_V^2)^2 + m_V^2\Gamma_V^2} N_j\right)\frac{\sqrt{\lambda(m^2, s_1, s_2)}}{(8\pi)^6 m^3} \\ &\quad \times [\lambda(m^2, s_1, s_2) + 12 s_1 s_2 \\ &\quad + \left(\frac{3}{4}\,\pi\right)^2 \sqrt{s_1 s_2}\,(m^2 - s_1 - s_2)\sin 2\chi_1\,\sin 2\chi_2\,\cos\phi \\ &\quad + 2 s_1 s_2 \cos 2\phi]\,.\end{aligned} \tag{3.177}$$

We thus confirm the differential decay rate given in [10].

3.4.2 Integrating the CP-odd Matrix Element

We are now going to perform the integrals of X_A and Y_A over E_1 and E_3, see (3.143) and (3.144). As was the case for the CP-even matrix element, X_A and Y_A consist of polynomials in E_1 and E_3, but unlike the CP-even case the factor $\sin u \sin\alpha$ which contains the square root (3.130) turns out to have zero coefficient, so that X_A and Y_A are pure polynomials. I have used REDUCE [22] and the formulae (3.150) to show that:

$$\int_{E_{1\,\min}}^{E_{1\,\max}} Y_A\,\mathrm{d}E_1 = 0\,, \tag{3.178}$$

$$\begin{aligned}\int_{E_{1\,\min}}^{E_{1\,\max}} X_A\,\mathrm{d}E_1 &= \frac{s_1 s_2\sqrt{\lambda}}{48m}\{m\cos 2\phi[4E_3^2 m - 2E_3(m^2 - s_1 + s_2) + m s_2] \\ &\quad + \lambda + 8E_3^2 m^2 - 4E_3 m(m^2 - s_1 + s_2) + 2m^2 s_2\}\,,\end{aligned} \tag{3.179}$$

and

$$\int_{E_{1\,\min}}^{E_{1\,\max}} \int_{E_{3\,\min}}^{E_{3\,\max}} X_A\,\mathrm{d}E_1\,\mathrm{d}E_3 = \frac{\lambda^2 s_1 s_2}{576m^2}(4 - \cos 2\phi)\,. \tag{3.180}$$

Using the expression (3.145) for the decay rate, we can write down the differential decay rate for a CP-odd Higgs boson as a function of s_1, s_2 and ϕ:

$$\begin{aligned}\frac{\mathrm{d}\Gamma}{\mathrm{d}\phi\,\mathrm{d}s_1\,\mathrm{d}s_2} &= \frac{|\eta|^2}{9(8\pi)^6 m^3}\left(\prod_{j=1}^{2}\frac{g_j^2 N_j}{(s_j-m_V^2)^2+m_V^2\Gamma_V^2}\right)\\ &\quad\times[\lambda(m^2,s_1,s_2)]^{3/2}s_1 s_2(4-\cos 2\phi)\,. \end{aligned} \tag{3.181}$$

This confirms the result in [10].

3.5 Numerical Integration and Distributions

In this section I will perform the integrals over s_1 and s_2 numerically, and plot and discuss the resulting distributions $\mathrm{d}\Gamma/\mathrm{d}\phi$.

Let us first study the integration limits of s_1 and s_2. From conservation of momentum and energy at the HV_1V_2-vertex, we see that

$$\sqrt{s_1}+\sqrt{s_2}\le m \Rightarrow s_2 \le (m-\sqrt{s_1})^2\,, \tag{3.182}$$

where m is the Higgs mass, as usual. We now get

$$\frac{\mathrm{d}\Gamma}{\mathrm{d}\phi} = \int_0^{m^2}\mathrm{d}s_1\int_0^{(m-\sqrt{s_1})^2}\mathrm{d}s_2\,\frac{\mathrm{d}\Gamma}{\mathrm{d}\phi\,\mathrm{d}s_1\mathrm{d}s_2}\,. \tag{3.183}$$

Since we are not interested in the normalisation of the distributions $\mathrm{d}\Gamma/\mathrm{d}\phi$, but only in their shape, we calculate the normalised distributions:

$$\begin{aligned}\left(\frac{2\pi}{\Gamma_h}\right)\frac{\mathrm{d}\Gamma_h}{\mathrm{d}\phi} &= 1+\alpha(m)\sin 2\chi_1\sin 2\chi_2\cos\phi\\ &\quad+\beta(m)\cos 2\phi\,,\end{aligned} \tag{3.184}$$

and

$$\left(\frac{2\pi}{\Gamma_A}\right)\frac{\mathrm{d}\Gamma_A}{\mathrm{d}\phi} = 1-\frac{1}{4}\cos 2\phi\,, \tag{3.185}$$

Here the coefficients $\alpha(m)$ and $\beta(m)$ are the ratios of integrals:

$$\alpha(m) = \left(\frac{3}{4}\pi\right)^2\frac{A(m)}{F(m)} \tag{3.186}$$

and

$$\beta(m) = \frac{2B(m)}{F(m)} \tag{3.187}$$

with the integrals $F(m)$, $A(m)$ and $B(m)$ defined by

$$\begin{aligned} F(m) &= \int_0^1 \frac{\mathrm{d}x_1}{(x_1-\mu)^2+\mu\gamma} \\ &\quad \times \int_0^{(1-\sqrt{x_1})^2} \mathrm{d}x_2 \, \frac{\sqrt{\lambda(1,x_1,x_2)}}{(x_2-\mu)^2+\mu\gamma} \\ &\quad \times \left[\lambda(1,x_1,x_2) + 12x_1x_2\right], \end{aligned} \tag{3.188}$$

$$\begin{aligned} A(m) &= \int_0^1 \frac{\mathrm{d}x_1\sqrt{x_1}}{(x_1-\mu)^2+\mu\gamma} \\ &\quad \times \int_0^{(1-\sqrt{x_1})^2} \mathrm{d}x_2 \, \frac{\sqrt{x_2}\sqrt{\lambda(1,x_1,x_2)}}{(x_2-\mu)^2+\mu\gamma} \\ &\quad \times (1-x_1-x_2) \end{aligned} \tag{3.189}$$

and

$$\begin{aligned} B(m) &= \int_0^1 \frac{\mathrm{d}x_1\, x_1}{(x_1-\mu)^2+\mu\gamma} \\ &\quad \times \int_0^{(1-\sqrt{x_1})^2} \mathrm{d}x_2 \, \frac{x_2\sqrt{\lambda(1,x_1,x_2)}}{(x_2-\mu)^2+\mu\gamma}\,. \end{aligned} \tag{3.190}$$

Here μ and γ are defined by

$$\mu = \left(\frac{m_V}{m}\right)^2, \qquad \gamma = \left(\frac{\Gamma_V}{m}\right)^2, \tag{3.191}$$

and we have changed integration variables to $x_1 = s_1/m^2$ and $x_2 = s_2/m^2$.

The coefficients $\alpha(m)$ and $\beta(m)$ can be seen in figures 3.3 and 3.4, both for Higgs decay to WW and for decay to ZZ. These plots confirm the shapes of $\alpha(m)$ and $\beta(m)$ from [10].

The normalised distributions $(2\pi/\Gamma_h)(\mathrm{d}\Gamma_h/\mathrm{d}\phi)$ are shown in figure 3.5. Also these confirm the results in [10].

Notice that the CP-odd distribution is independent of the Higgs mass, whereas the CP-even distribution is most strongly correlated for large values of $\alpha(m)$. From figure 3.3, we see that $\alpha(m)$ reaches its maximum value for $m \approx 200$ GeV.

Notice also that the distribution is more correlated in the case of Higgs decay to a pair of W bosons, than for decay to a pair of Z bosons. This is due to the fact that the factor $\sin 2\chi_1 \sin 2\chi_2$ is equal to unity for the case of a W-pair, but is smaller than unity for the case of a Z-pair, see table 3.1. The smallest value for $\sin 2\chi_1 \sin 2\chi_2$ is reached when both Z bosons decay to charged leptons.

For large Higgs masses, both $\alpha(m)$ and $\beta(m)$ get very small, and therefore the distributions for a CP-even Higgs become uncorrelated in this limit.

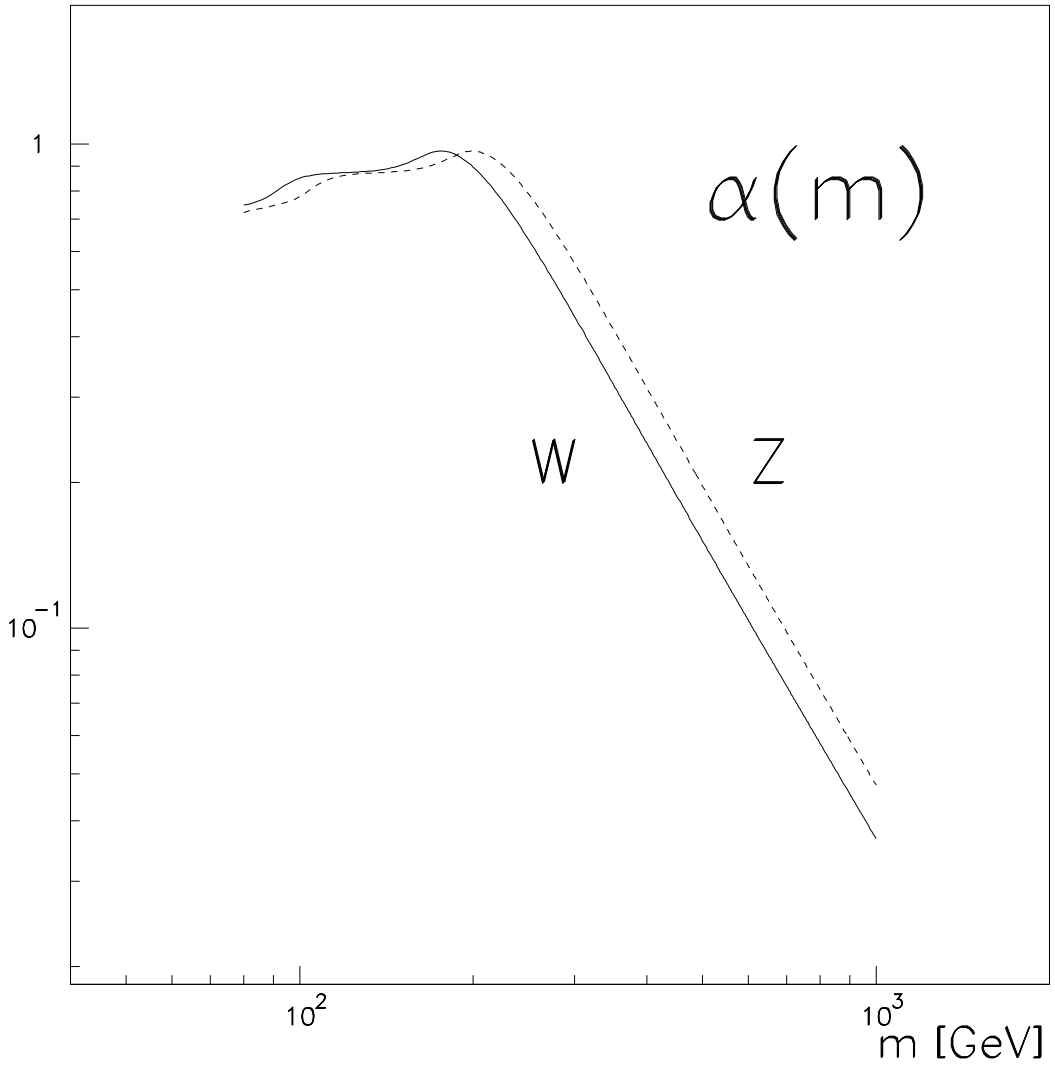

Figure 3.3: The ratio $\alpha(m)$ between the integrals $A(m)$ and $F(m)$. Decay to WW and to ZZ. See also (3.184).

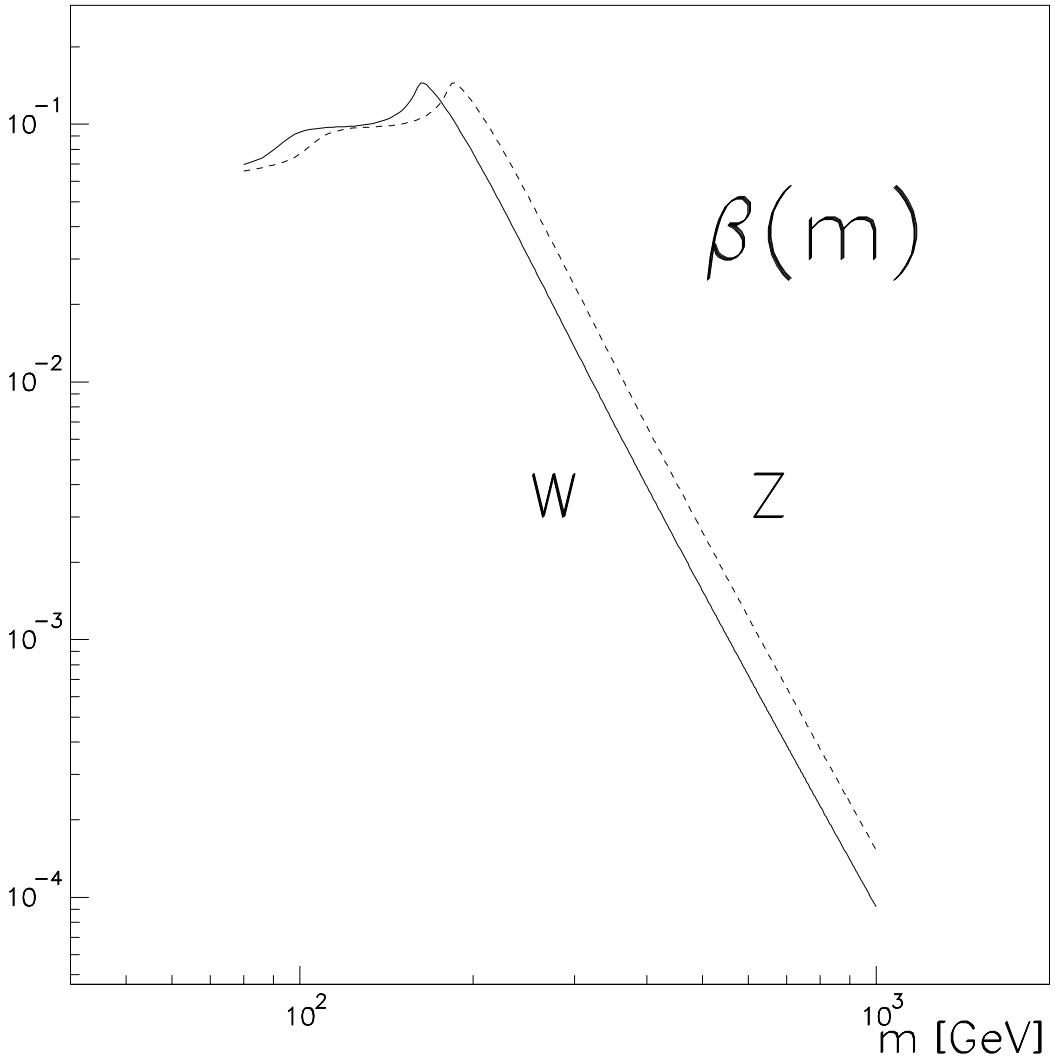

Figure 3.4: The ratio $\beta(m)$ between the integrals $B(m)$ and $F(m)$. Decay to WW and to ZZ. See also (3.184).

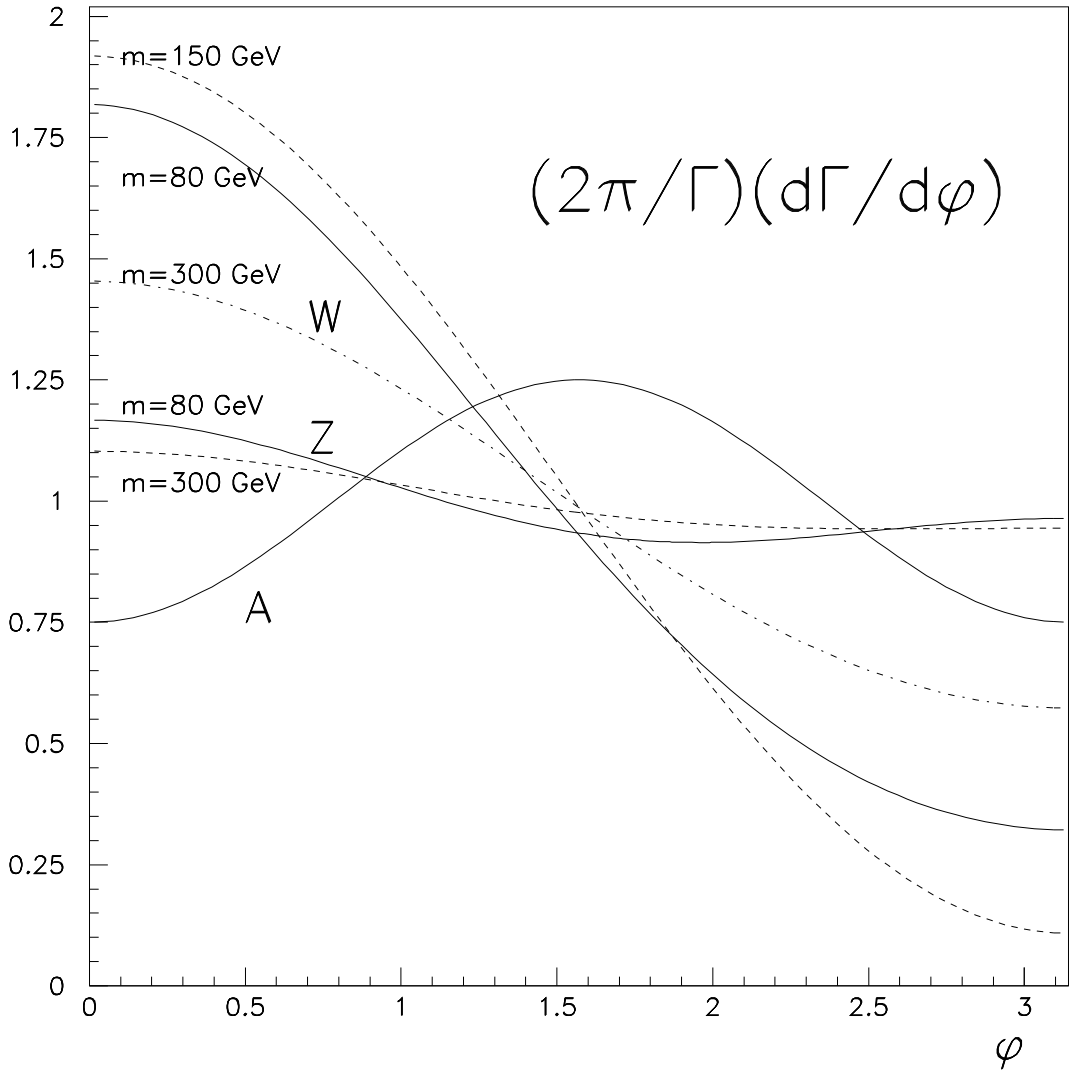

Figure 3.5: The distribution $(2\pi/\Gamma)\mathrm{d}\Gamma/\mathrm{d}\phi$ for CP-even or CP-odd Higgs. In the CP-even case, decay to WW or ZZ, for different values of the Higgs mass m. The ZZ pair decays to $l^+l^-b\bar{b}$. See similar plot in [10].

Chapter 4

Monte Carlo Studies

The main purpose of this chapter will be to assess the integrated luminosity required in order to measure the CP-property of a Higgs boson at the LHC, through angular distributions like $\mathrm{d}\Gamma/\mathrm{d}\phi$, see (3.184) and (3.185), and distributions of other angular variables in the decay

$$H \to V_1 V_2 \to f_1 \bar{f}_2 f_3 \bar{f}_4 \,. \tag{4.1}$$

Here V_1V_2 are either the vector bosons W^+W^- or ZZ. The Monte Carlo program PYTHIA [26, 27] has been modified in order to allow the Higgs boson to decay as a CP-odd particle, or as a CP-even particle, in the decay channel (4.1).

I am assuming a simple model, where there are several Higgs bosons, at least one of which is CP-odd, hereafter denoted A, and one CP-even, denoted h, and where the coupling of the CP-odd Higgs boson to the vector bosons W^+W^- and ZZ is of the same order of magnitude as the coupling of the CP-even Higgs boson to the same vector bosons. The Higgs particles are assumed to be eigenstates of CP-parity. The general Higgs boson, either CP-even or CP-odd, is denoted by H.

This is not, of course, a realistic physical model, because in a renormalisable quantum field theory which conserves CP in the Higgs sector, the AV_1V_2 coupling is only induced at the one-loop level, and must therefore be smaller than the hV_1V_2 coupling which exists at tree-level.

On the other hand, in a model with CP-violation, it is possible to have Higgs bosons which are not eigenstates under CP [6], but are strongly mixed states of CP-even and CP-odd states.

The following Monte Carlo analyses for the simple CP-conserving model described above can be seen as a first approach to Monte Carlo analyses for a CP-violating theory with mixing of the states.

To simplify the Monte Carlo simulations, I will take the Standard Model as a starting point, and assume that both h and A have the production and decay rates of the Standard Model Higgs boson. The only deviation from the Minimal Standard Model is therefore that there exists a CP-odd Higgs boson which has a significant decay rate for the channel $A \to V_1V_2$, and that it in this channel decays according to the matrix element for a CP-odd scalar (3.46), but with the rate of the Standard Model Higgs.

This is of course unrealistic, as there is only one Higgs boson in the Minimal Standard Model, and this is a CP-even scalar. But it is still a starting point for background analyses, and might give some rough idea of the possibility of measuring the CP-property of a Higgs boson in a more complicated, and more realistic model.

I want to estimate whether the distributions of the observable ϕ defined by (3.2) in the previous chapter, and other angular observables to be defined in the following, can be used to determine the CP-properties of a Higgs boson at the LHC. In order to avoid an ambiguous definition of the angular observables, we must be able to distinguish between the fermion and the antifermion in the decay of the vector bosons:

$$V_i \to f_j \bar{f}_k \,. \tag{4.2}$$

Here $(i, j, k) = (1, 1, 2)$ or $(2, 3, 4)$.

The relevant decay channels where the Standard Model Higgs boson will be searched for in the ATLAS experiment [29] (page 675), are

- $H \to ZZ^* \to 4l$
- $H \to ZZ \to 4l$
- $H \to ZZ \to lljj$
- $H \to WW \to l\nu jj$.

Here l stands for either an electron or a positron e, or a muon μ. The particle ν is a neutrino of either type, and j is a jet of hadrons. The notation ZZ^* means that one Z boson has an invariant mass lower than the nominal Z boson mass (is off the mass shell).

With charged leptons it is easy to separate the fermion from the antifermion, but with quarks this is not so trivial, because of the hadronisation. The exception is the b-quark, where it is possible to determine (with some efficiency) whether a jet comes from a b-quark or a b-antiquark through the method called b-tagging [28].

Of the channels listed above I have chosen to study the second one:

$$H \to ZZ \to 4l \,, \tag{4.3}$$

also called "The Gold-Plated Channel". This is a very clean channel at the LHC. The background is actually smaller than the signal, after a cut on the invariant mass of the Higgs boson [29]. Of the the channels mentioned above it is the one best suited for my purposes.

The most important background-channel for this decay at LHC is continuum ZZ production through quark-antiquark fusion [29, 30, 31]:

$$q\bar{q} \to ZZ \to 4l \,. \tag{4.4}$$

In addition, continuum ZZ production through gluon-gluon fusion:

$$gg \to ZZ \to 4l \,, \tag{4.5}$$

contributes significantly to the background. The matrix element of this channel is not included in PYTHIA though, and I have therefore not been able to simulate it.

I have studied the distribution of several angular observables in the decay (4.3). In the simulation of the background distributions I have only used the channel (4.4), and the question is how much the channel (4.5) would change the distributions, if included in the simulations. The angular distributions of the leptons in the decay (4.3) is determined by the spin polarisations of the two Z bosons.For quark-antiquark fusion with massless quarks the Z bosons will be produced with complete transverse polarisations, while they for the gluon-gluon fusion will be mainly transversely polarised[1] [30, 31]. There is therefore reason to believe that the angular distributions of the leptons are similar in the two cases, as long as the fraction of longitudinally polarised Z boson is small for the gluon-gluon fusion.

The cross section of (4.5) has been calculated, and compared to the cross section of (4.4) [30]. I have used these results when estimating the total background cross section.

4.1 Monte Carlo Event Generation

For the Monte Carlo analyses I have used the PYTHIA event generator [26, 27] version 6.204. In this section I am going to give an introduction to Monte Carlo event generation based on the PYTHIA program.

With the development of quantum mechanics in the beginning of the previous century came the introduction of randomness and probability in physical processes. Monte Carlo simulation is useful because it allows us to estimate the probabilities of many processes that it would take much longer, or indeed be impossible, to find by analytical calculations. All Monte Carlo simulation builds on the principle of a random number generator, that is a piece of program code which returns numbers between 0 and 1, in an almost completely random way. Random numbers can be used to select a value of a random variable according to a probability distribution.

In high energy physics, Monte Carlo event generators simulate the interactions which take part in collisions between and decay of particles. All properties of an event are chosen according to the corresponding probability distributions.

We have good theoretical descriptions for parts of these interactions, the so-called hard processes. The hard process is the part of the interaction which takes place at high energy, and decides the main characteristics of the interaction. The cross sections for the hard processes, which are a measure of the probability that the process will take place, can be calculated in perturbative quantum field theories.

On the other hand, there are parts of the interactions, among these the hadronisation of quarks and gluons, for which we do not have any fundamental theoretical understanding or description.

A good high energy physics event generator must nevertheless include all parts of the interaction between particles. The generation of an event can be divided into several stages:

[1] E. W. N. Glover was friendly to answer a question concerning the polarisation of the Z bosons in continuum production through gluon-gluon and quark-antiquark fusion

- **Incoming particles.** The beam particles, for instance two protons, are described by their parton-distribution functions (pdf's), which contain information about the flavour content of the beam particles, and how the partons share the total momentum of the beam particle. For a proton, the partons are mainly quarks and gluons. The total cross section σ for a process $ij \to k$ can thus be expressed as:

$$\sigma(ij \to k) = \int \mathrm{d}x_1 \int \mathrm{d}x_2 \, f_i^1(x_1) \, f_j^2(x_2) \, \hat{\sigma}(ij \to k) \tag{4.6}$$

  Here $\hat{\sigma}$ is the cross section for the hard process, and the $f_i^a(x)$ are the pdf's, describing the probability of finding a parton i inside the beam particle a, with momentum fraction x of the total beam particle momentum.

- **Initial and Final State Showers.** Radiation of gluons and/or photons from the initial and final state particles of the hard process constitutes an important part of the interactions. There are two ways of modelling this radiation. Either the full matrix elements can be calculated to each order, or one might use the model of parton showers. The disadvantage with the matrix element method is that the expressions soon become very complicated, sometimes already for one-loop corrections. The parton shower model on the other hand uses approximations of the full matrix elements. In this model a combination of branchings where one parton splits into two, produces the radiation. The parton shower model has no limit on the number of emitted gluons or photons, but is unfortunately not so exact, and can not be used for all kinds of analyses. Depending on the area of application, one of these models, or a combination of both can be used. In PYTHIA the parton shower model is default, and the matrix element method is only available for the $e^+e^- \to q\bar{q}$ process.

- **The Hard Process.** This is the part of the process which can be calculated from first principles in quantum field theory. The differential cross section of the hard process is used as a probability distribution. The events are generated in different parts of the phase space according to the differential cross section. In PYTHIA the hard process also includes decays of resonances, like the heavy vector bosons Z and W, and the Higgs boson, in the mass range where its width is not too large.

- **Hadronisation of Quarks and Gluons.** Particles with colour charge are confined. At low energies they can not exist as free particles, but will always be bound together in colour neutral hadrons. Fragmentation, or hadronisation of particles with colour charge takes place when the kinetic energy of the particles gets so low that the perturbative expansion of QCD breaks down. In this part of the interaction quarks and gluons get bound together in colour neutral composite particles, hadrons. Because the perturbative treatment breaks down in this energy range, fragmentation can not be calculated from first principles in QCD. Phenomenological models have been developed though. There are three main schools, called string fragmentation, independent fragmentation and cluster fragmentation, respectively. String fragmentation is the default in PYTHIA. In this model it is assumed that the potential energy in

the colour field between two objects with opposite colour charge grows linearly with distance. This colour field can be pictured as a string, which will break and produce a new quark-antiquark pair when the potential energy is large enough. Thus a single quark-antiquark pair might produce several hadrons, depending on their kinetic energy before the fragmentation starts. As a part of the hadronisation process unstable hadrons, when produced, decay into stable particles. Unstable leptons also decay.

4.2 PYTHIA: Modifications and Settings

In this section I describe the modifications I have done to PYTHIA in order to allow the Higgs boson to decay as a CP-odd scalar particle in the decay

$$H \to V_1 V_2 \to f_1 \bar{f}_2 f_3 \bar{f}_4 \,. \tag{4.7}$$

I also give the values I have used for the PYTHIA parameters and switches in my analysis.

The change I have made in PYTHIA, is to include the (squared) matrix element (3.46) for the decay (4.8) of the CP-odd Higgs boson A, in the angular weight for this decay channel:

$$A \to V_1 V_2 \to f_1 \bar{f}_2 f_3 \bar{f}_4 \,. \tag{4.8}$$

Here $V_1 V_2$ are two heavy vector bosons, either W^+W^- or ZZ.

In a Two-Higgs-Doublet Model (2HDM) which conserves CP-parity in the Higgs sector, there are five physical Higgs bosons, three of which are neutral. Of the neutral Higgs bosons, two are CP-even, and one is CP-odd. The CP-odd Higgs boson is often denoted by A. In a renormalisable model, the coupling AV_1V_2 is only induced at the one loop level, and in fact the decay rate of the channel

$$A \to V_1 V_2 \tag{4.9}$$

is set to zero in PYTHIA.

As part of the modifications, a new switch was introduced in PYTHIA. A switch is some variable that can take on integer values, and which determines the choice between different scenarios in the event generation. This new switch has the name `MSTP(25)`. It is used to determine the decay scheme of the Higgs bosons in the decay (4.7), either according to the matrix element for a CP-even Higgs boson, or according to the matrix element for a CP-odd Higgs boson. `MSTP(25)` can have the following values:

- `MSTP(25)=0`: This is the default value. Both CP-even and CP-odd Higgs bosons would decay according to the correct matrix elements, but the CP-odd decay (4.8) does not take place, because its decay rate is equal to zero by default in PYTHIA.

- `MSTP(25)=1`: All neutral Higgs bosons in a 2HDM and in the Standard Model decay according to the CP-even matrix element.

- `MSTP(25)=2`: All neutral Higgs bosons in a 2HDM and in the Standard Model decay according to the CP-odd matrix element.

Below I have included the piece of code that gives the angular weight in the decay (4.7). First I have listed the original version of the code. In this version all Higgs bosons decay according to the CP-even matrix element:

```
      ELSEIF(IREF(IP,7).EQ.25.OR.IREF(IP,7).EQ.35.OR.
     &  IREF(IP,7).EQ.36) THEN
C...Angular weight for h0 -> Z0 + Z0 or W+ + W- -> 4 quarks/leptons.
        IF(IP.EQ.1) WTMAX=SH**2
        IF(IP.GE.2) WTMAX=P(IREF(IP,8),5)**4
        KFA=IABS(K(IREF(IP,1),2))
        IF(KFA.EQ.23) THEN
          KFLF1A=IABS(KFL1(1))
          EF1=KCHG(KFLF1A,1)/3D0
          AF1=SIGN(1D0,EF1+0.1D0)
          VF1=AF1-4D0*EF1*XWV
          KFLF2A=IABS(KFL1(2))
          EF2=KCHG(KFLF2A,1)/3D0
          AF2=SIGN(1D0,EF2+0.1D0)
          VF2=AF2-4D0*EF2*XWV
          VA12AS=4D0*VF1*AF1*VF2*AF2/((VF1**2+AF1**2)*(VF2**2+AF2**2))
          WT=8D0*(1D0+VA12AS)*PKK(3,5)*PKK(4,6)+
     &    8D0*(1D0-VA12AS)*PKK(3,6)*PKK(4,5)
        ELSEIF(KFA.EQ.24) THEN
          WT=16D0*PKK(3,5)*PKK(4,6)
        ELSE
          WT=WTMAX
        ENDIF
```

Next follows my modified version, where the value of the switch `MSTP(25)` determines which angular weights are chosen:

```
      ELSEIF(IREF(IP,7).EQ.25.OR.IREF(IP,7).EQ.35.OR.
     &  IREF(IP,7).EQ.36) THEN
C...Angular weight for h0/A0 -> Z0 + Z0 or W+ + W- -> 4 quarks/leptons.
        IF(IP.EQ.1) WTMAX=SH**2
        IF(IP.GE.2) WTMAX=P(IREF(IP,8),5)**4
        KFA=IABS(K(IREF(IP,1),2))
        IF(KFA.EQ.23) THEN
          KFLF1A=IABS(KFL1(1))
          EF1=KCHG(KFLF1A,1)/3D0
          AF1=SIGN(1D0,EF1+0.1D0)
```

```
          VF1=AF1-4D0*EF1*XWV
          KFLF2A=IABS(KFL1(2))
          EF2=KCHG(KFLF2A,1)/3D0
          AF2=SIGN(1D0,EF2+0.1D0)
          VF2=AF2-4D0*EF2*XWV
          VA12AS=4D0*VF1*AF1*VF2*AF2/((VF1**2+AF1**2)
     &      *(VF2**2+AF2**2))
          IF((MSTP(25).EQ.0.AND.IREF(IP,7).NE.36).OR.MSTP(25).EQ.1)
     &      THEN
C...CP-even decay
            WT=8D0*(1D0+VA12AS)*PKK(3,5)*PKK(4,6)+
     &        8D0*(1D0-VA12AS)*PKK(3,6)*PKK(4,5)
          ELSE
C...CP-odd decay
            WT=((PKK(3,5)+PKK(4,6))**2 +(PKK(3,6)+PKK(4,5))**2
     &        -2*PKK(3,4)*PKK(5,6)
     &        -2*(PKK(3,5)*PKK(4,6)-PKK(3,6)*PKK(4,5))**2/
     &        (PKK(3,4)*PKK(5,6))
     &        +VA12AS*(PKK(3,5)+PKK(3,6)-PKK(4,5)-PKK(4,6))*
     &        (PKK(3,5)+PKK(4,5)-PKK(3,6)-PKK(4,6)))/(1+VA12AS)
          ENDIF
        ELSEIF(KFA.EQ.24) THEN
          IF((MSTP(25).EQ.0.AND.IREF(IP,7).NE.36).OR.MSTP(25).EQ.1)
     &      THEN
C...CP-even decay
            WT=16D0*PKK(3,5)*PKK(4,6)
          ELSE
C...CP-odd decay
            WT=0.5D0*((PKK(3,5)+PKK(4,6))**2 +(PKK(3,6)+PKK(4,5))**2
     &        -2*PKK(3,4)*PKK(5,6)
     &        -2*(PKK(3,5)*PKK(4,6)-PKK(3,6)*PKK(4,5))**2/
     &        (PKK(3,4)*PKK(5,6))
     &        +(PKK(3,5)+PKK(3,6)-PKK(4,5)-PKK(4,6))*
     &        (PKK(3,5)+PKK(4,5)-PKK(3,6)-PKK(4,6)))
          ENDIF
        ELSE
            WT=WTMAX
        ENDIF
```

Some explanations are needed now. First, this part of the code is taken from the subroutine PYRESD, which simulates the decay of resonances. The part which I have quoted is only a small part of this subroutine. It gives the angular weight specifically for the decay (4.7) with the Higgs boson either the Standard Model Higgs boson or one of the three

neutral Higgs bosons in a 2HDM. The angular weight simply gives the correct shape of the probability distribution for the momenta of the four fermions. The normalisation of this angular weight, or probability distribution, is not important, because the normalisation to the correct decay rate is performed in some other part of the program.

I will explain the most relevant of the variables used. `IREF(IP,7)` gives the `KF` particle code of the mother of the two resonances in the decay. That is, this variable gives the particle code of the Higgs boson in the decay (4.7). `IREF(IP,1)` gives the `KF` particle code for the first of the two vector bosons in the decay (4.7), that is it tells if the Higgs bosons decayed into two Z bosons or into two W bosons.

The `KF` particle code is the Particle Data Group [21] particle code, with some local PYTHIA extensions. For each distinct particle (either discovered in an experiment or theoretically predicted), there exists a corresponding distinct signed integer number. Particle-antiparticle pairs have `KF` code with the same absolute value but opposite signs. The relevant `KF` codes for the above pieces of code are:

- `KF` $= 23$: The Z boson
- `KF` $= 24$: The W^+ boson. The W^- boson has `KF` $= -24$.
- `KF` $= 25$: The Standard-Model Higgs boson, or the lightest of the two neutral, CP-even Higgs bosons in a 2HDM.
- `KF` $= 35$: The heavy neutral, CP-even Higgs boson in a 2HDM.
- `KF` $= 36$: The neutral, CP-odd Higgs boson in a 2HDM.

The variables `AFi` and `VFi` are the vector or axial parts respectively of the coupling $V_i f_j \bar{f}_k$, where $(i, j, k) = (1, 1, 2), (2, 3, 4)$. The expression

```
4D0*VF1*AF1*VF2*AF2/((VF1**2+AF1**2)*(VF2**2+AF2**2))
```

therefore corresponds to $(\sin 2\chi_1 \sin 2\chi_2)$ in the theoretical calculation of the matrix elements in the previous chapter of this thesis.

The arrays `PKK(i,j)` are vector products between the four-momenta of particle i and particle j, with an extra factor 2:

$$\texttt{PKK(i,j)} = 2(p_i \cdot p_j)\,. \tag{4.10}$$

The particle numbering here, i and j, needs explanation. In `PYRESD` there is an internal numbering of the particles in the decay (4.7). The two vector bosons are numbered 1 and 2. The four fermions and anti-fermions are numbered from 3 to 6. Thus `PKK(3,5)` is equal to the four-product of the momenta of fermions 1 and 3 in (4.7), and so on.

This concludes the description of the changes I have made to PYTHIA. The last part of this section concerns the PYTHIA settings I used in the event simulations. Except when explicitly otherwise stated I have used the default settings of PYTHIA, version 6.204, with

the modification I have explained above. For more details about the default settings and the parameters and switches I describe, see [26].

I wanted to simulate Higgs boson production at LHC, and therefore I initialised PYTHIA for a p on p collider at 14 GeV CoM energy. I have set `MSEL` $= 0$, which allows me to choose the hard process(es) to be simulated freely. For the simulation of signal events, I have set `MSUB(102)` $= 1$. This switches on the hard process Higgs production via gluon-gluon fusion, which is the dominant channel for Higgs production in the relevant mass range for the channel

$$H \to ZZ \to 4l\,, \tag{4.11}$$

from $m_H = 2m_Z$ to $m_H \approx 700$ GeV ($m_Z = 91.2$ GeV) [29, 32]. The mass of the Higgs boson is set with the parameter `PMAS(25,1)`. The Higgs particle which is produced and subsequently decay is a Standard-Model Higgs boson. I set `MSTP(25)` $= 1$ or `MSTP(25)` $= 2$, to let the Higgs boson decay as a CP-even or a CP-odd scalar, respectively. Notice that it is the Standard-Model Higgs, with the Standard-Model decay rate that decays as a CP-odd scalar in the channel (4.7). I repeat that I do not intend to simulate a realistic physical model, but a simple unrealistic model. Still I will get some idea of how the angular distributions depend on the CP of the Higgs boson, also in a model with mixing of CP-states.

To simulate the total cross section times branching ration for the channel (4.11), I have switched on all the following Higgs boson production channels [32]:

- `ISUB` $= 24$ and `ISUB` $= 26$ are Higgs production through the Higgs-strahlung process, or Bjorken process, with the W or Z boson, respectively.
- `ISUB` $= 102$: Higgs production through gluon fusion.
- `ISUB` $= 121$: Higgs production through heavy quark fusion.
- `ISUB` $= 123$ and `ISUB` $= 124$ are Higgs production through ZZ-fusion or W^+W^--fusion, respectively.

The most important of these are Higgs production through gluon fusion and Higgs production through vector boson fusion.

For the background events I have set `MSUB(22)` $= 1$, which switches on the hard process continuum ZZ production through quark-antiquark fusion. This is the dominant background channel for the process (4.11) at the LHC, but there is also another important background channel, continuum ZZ production through gluon-gluon fusion. The matrix element for this last channel is not included in PYTHIA, so it has not been possible to simulate the distributions of the observables for it.

I have used only the quark-antiquark fusion background channel to simulate the total cross section times branching ratio of the background. There exist calculations of the relative size of the cross section for the gluon-gluon fusion channel compared to that for the quark-antiquark fusion channel [30], and I have used these results in order to get a realistic estimate of the background cross section times branching ratio.

It is possible to switch on and off the different decay channels of a particle in PYTHIA. I have used this option to restrict the possible decay channels of the Higgs boson, so that it only decays into two Z bosons. I have also switched off all decay channels of the Z boson except the decay into an e^+e^- or $\mu^+\mu^-$ pair. This is the most efficient way of simulating the events I am interested in. Decay channels can be switched on or off through the switch `MDME(IDC,1)`. IDC is the number of the decay channel. Setting `MDME(IDC,1)` equal to zero corresponds to switching off the channel IDC. For more details about `MDME(IDC,1)`, see [26].

Final-state radiation and hadronisation have been switched off for the event simulation, whereas initial-state radiation has been switched on (default). This is performed through the switches `MSTP(61)` for initial state radiation, `MSTP(71)` for final state radiation, and `MSTP(81)`, `MSTP(91)`, `MSTP(111)`, `MSTJ(1)` and `MSTJ(21)` for different parts of the hadronisation machinery.

I expect the simulations to give fairly realistic results even though final state radiation and hadronisation have been switched off. Hadronisation would not change the results much, since I have been working with a channel with only leptons in the final state. I do not expect leptons that come from decay of hadrons or heavy quarks to contribute much to the background. The final state radiation on the other hand would have some effect on the measured momenta of the leptons. If a lepton radiates a photon before it is detected, this photon is likely to have a momentum with a direction almost parallel to the electron momentum. The electromagnetic calorimeter might therefore detect the photon energy as part of the electron energy, and the measured momentum will have the same value as if no radiation had taken place [28] (pages 197-200). This is the reason why I expect the simulation to be fairly accurate even without final state radiation.

In order to increase the efficiency of background events surviving the kinematic cuts, I have used the parameters `CKIN(1)` and `CKIN(2)`, which set lower and upper limits on the invariant mass of the Z boson pair produced in the background process. Because I am only interested in background events with Z boson invariant mass near the nominal Higgs mass, this might increase the efficiency of background events surviving the kinematic cuts strongly. I will describe the values of these parameters and the kinematic cuts I have used in the next section. I have also set the parameters `CKIN(41)` and `CKIN(43)`, which set lower limits on the invariant mass of the first and second Z boson produced, to the values `CKIN(41)` $= 20$ and `CKIN(43)` $= 20$. This corresponds to a lower limit of 20 GeV on the invariant mass of simulated Z bosons. The `CKIN()` parameters have been set to default values in the simulation where I have estimated the total cross section times branching ratio for signal and background.

The last switch to describe is `MSTP(128)`. I have set it equal to 1, in order to make the search for the mothers of decay products easier in the event analysis.

I have now described all PYTHIA settings I have used which depart from the defaults. An overview of the described variables can be found in table 4.1.

Variable	Comment
CKIN(1)	lower limit on Z pair (background)
CKIN(2)	upper limit on Z pair (background)
CKIN(41)	$= 20$, lower cut on mass of first Z
CKIN(43)	$= 20$, lower cut on mass of second Z
MDME(IDC,1)	switch on/off decay channel IDC
MSEL	$= 0$, to select hard processes freely
MSTJ(1)	$= 0$, hadronisation off
MSTJ(21)	$= 0$, hadronisation off
MSTP(25)	CP-even or CP-odd decay of Higgs
MSTP(61)	$= 1$, initial state radiation on (default)
MSTP(71)	$= 0$, final state radiation off
MSTP(81)	$= 0$, hadronisation off
MSTP(91)	$= 0$, hadronisation off
MSTP(111)	$= 0$, hadronisation off
MSTP(128)	$= 1$, easier search
MSUB(ISUB)	switch on/off hard process ISUB
PMAS(25,1)	the Higgs boson mass

Table 4.1: Overview of PYTHIA settings that depart from the default values.

4.3 Observables and Kinematic Cuts

This section contains a description of the different observables I have studied and used in the statistical analysis. I also give plots which show the distributions in the different observables for decays of CP-even and CP-odd Higgs bosons, and background events.

In addition, I describe the kinematic cuts I have used. The cuts are similar to the cuts described for this channel in the ATLAS TDR [29].

I conclude the section with tables which summarise the cross sections, cut percentages and expected number of events after reconstruction and kinematic cuts for different values of Higgs mass and integrated luminosity.

Let us start with definitions of rapidity, pseudorapidity and transverse momentum [21]. These are very useful notions when analysing events. A direction for the z-axis has to be chosen. Usually the z-axis is defined to be along the beam axis. For a given z-axis the transverse momentum $p_\perp$ of a particle, or a system with total momentum $p = (E, p_x, p_y, p_z)$ is

$$p_\perp \equiv \sqrt{p_x^2 + p_y^2}\,. \tag{4.12}$$

The rapidity y is defined as

$$y \equiv \frac{1}{2} \ln \left(\frac{E + p_z}{E - p_z} \right) = \tanh^{-1} \left(\frac{p_z}{E} \right) , \tag{4.13}$$

whereas the pseudorapidity η is equal to

$$\eta \equiv - \ln[\tan(\theta/2)] . \tag{4.14}$$

Here θ is the polar angle of the three-momentum $\mathbf{p}$, relative to the chosen z-axis. For $\theta = 0$ the pseudorapidity has the value $\eta = \infty$, for $\theta = \pi/2$ we have $\eta = 0$ and for $\theta = \pi$ we have $\eta = -\infty$. It can be shown that for $|\mathbf{p}| \gg m$, and for $\theta \gg 1/\gamma$, where m is the invariant mass of the particle, the pseudorapidity η is approximately equal to the rapidity y. For massless particles the relations below hold identically, but for relativistic particles with mass, they are only approximations:

$$\cos\theta \approx \frac{p_z}{E} , \text{ and } \tan \left(\frac{\theta}{2} \right) \approx \left(\frac{E - p_z}{E + p_z} \right)^{1/2} \tag{4.15}$$

This implies

$$\eta \approx \frac{1}{2} \ln \left(\frac{E + p_z}{E - p_z} \right) = y . \tag{4.16}$$

4.3.1 Kinematic Cuts

Now I am ready to list the kinematic cuts I have used. The particles we are interested in are electrons and/or muons, but for simplicity I will call them leptons below. The pseudorapidity and transverse momenta are calculated in the laboratory frame, which is the same as the CoM frame of the two incoming protons, with the z-axis defined as the beam axis. In order to survive the kinematic cuts, an event has to fulfil the following criteria:

- 4 leptons (electrons or muons) with $|\eta| < 2.5$
- of these, 2 leptons with $p_\perp > 7$ GeV and 2 leptons with $p_\perp > 20$ GeV
- 2 lepton-antilepton pairs with invariant masses $m(2l)$ such that $|m(2l) - m_Z| < 6$ GeV, where m_Z is the mass of the Z boson.
- the invariant mass $m(4l)$ of the four leptons should satisfy $|m(4l) - m_H| < 1.64\,\sigma_m$, where $\sigma_m = [(\Gamma_H/2.36)^2 + (0.02 m_H)^2]^{1/2}$, see [29]. Here Γ_H is the width of the Higgs boson, and m_H is its mass.

The cuts on pseudorapidity and transverse momentum select events with outgoing leptons that are not too close to the beam axis direction. It is more probable that an interesting interaction has taken place for this kind of events, because the large angle relative to

the beam axis indicates that these leptons come from a hard process, and that they are not simply decay products of the beam remnant. (The beam remnant comes from the quarks and gluons in the protons that do not take part in the hard interaction.) In addition, detectors for colliding beam experiments are mostly built as a "barrel" around the beam tube. Therefore the experimental resolution is much better for angles close to the perpendicular direction. For directions too close to the beam axis it might be impossible to measure the momentum of a particle.

I have used the same values for the cuts as described in the ATLAS TDR for this channel [29] (pages 694 and 714).

In PYTHIA I obtained the value of Γ_H from the parameter `PMAS(25,2)` which contains the total width of the Standard Model Higgs boson for the given value of the Higgs mass. For comparison, I have calculated the value of Γ_H from the following formula [4] (page 23):

$$\Gamma(H \to VV) = 2(1)\frac{\sqrt{2}G_F m_H^3}{32\pi}\sqrt{1-x_V}\left(1 - x_V + \frac{3}{4}x_V^2\right), \tag{4.17}$$

for $V = W(Z)$, and with $x_V = 4m_V^2/m_H^2$, by noting that the decay channels $H \to WW$ and $H \to ZZ$ are the dominant ones in the relevant mass range [13, 33]. Then we get for the total width:

$$\Gamma_H(\text{tot}) \approx \Gamma(H \to WW) + \Gamma(H \to ZZ)\,. \tag{4.18}$$

Table 4.2 shows a comparison of the values obtained with the two methods. The formula (4.17) is only a tree-level result, so I do not expect it to be as accurate as the value obtained from PYTHIA.

m_H [GeV]	Γ_H [GeV] from PYTHIA	Γ_H [GeV] from (4.18)
200	1.36	1.41
250	3.99	4.00
300	8.36	8.37

Table 4.2: The total width Γ_H, of the Standard Model Higgs boson, for three different Higgs masses. Values obtained from PYTHIA, PMAS(25,2), and from the formula (4.18).

See table 4.3 for an overview of the values of `CKIN(1)` and `CKIN(2)` used in the simulation. These values are chosen to maximise the efficiency of generation of background events that survive kinematic cuts, at the same time as none of the events we are interested in should be cut away. The distribution of the invariant mass of the two Z bosons is not changed by the initial state radiation, because of the way the initial state radiation is generated. Final state radiation on the other hand, would shift the invariant mass of the two Z bosons toward lower energies.

m_H [GeV]	$1.64\,\sigma_m$ [GeV] from PYTHIA	CKIN(1)	CKIN(2)
200	6.63	190	210
250	8.66	235	265
300	11.43	280	320

Table 4.3: The values of CKIN(1) and CKIN(2) used in the simulation, compared to the value of the cut on the Higgs mass, $1.64\,\sigma_m$.

4.3.2 Observables

Next, I am going to describe the observables I have studied. I have looked at in total seven different observables including one that is similar but not identical to ϕ as it is defined in (3.2).

As I mentioned in the introduction of this chapter, the CP-state of the Higgs boson in the decay (4.1) determines the polarisation of the vector bosons, and this polarisation in turn determines the distributions of the decay angles in the decays of the vector bosons.

The decays of the two Z bosons can be defined by the polar and azimuthal decay angles in the respective rest frame of each Z boson. It is natural to study each decay in its own CoM frame, because the phase space factor of the decay rate is isotropic here, and any deviations from flat distributions must come from the matrix element. One of the azimuthal angles should be trivial. This can be seen by noting that the decay rate must be invariant under rotations around the axis of the Z momenta in the Higgs boson rest frame, see figure 3.2.

We are left with two polar angles, and one azimuthal angle describing the decays of the Z bosons [8–14]. I have denoted these angles by $\cos\theta_1^*$, $\cos\theta_3^*$ and ϕ_{13}^*. They are defined as follows:

First, the momenta of the four leptons are boosted to the rest frame of the Higgs boson they are assumed to come from. For background events this is equivalent to boosting them to the CoM frame of the four leptons. Next, the system is rotated so that the reconstructed momentum of the first of the two Z bosons lies in the xz-plane. The choice of which Z boson is first is arbitrary. Then the system is rotated one more time, so that *the momentum of the first Z boson points along the positive z-axis.* The momentum of the other Z boson now points along the negative z-axis, because we are in the CoM frame of the two Z bosons, see figure 3.2.

The momenta of the decay products of the first Z boson, l_1 and $\bar{l}_2$ are now boosted to the rest frame of the first Z boson, and correspondingly the decay products of the second Z boson, l_3 and $\bar{l}_4$ are boosted to the rest frame of the second Z boson. The angle $\cos\theta_1^*$ is defined as the polar angle of l_1, in the rest frame of the first Z boson. Similarly $\cos\theta_3^*$

is the polar angle of l_3, in the rest frame of the second Z boson. Notice that both $\cos\theta_1^*$ and $\cos\theta_3^*$ are defined relative to the *positive* z-axis, and not relative to the direction of the corresponding Z boson momentum. For a definition of the angles $\cos\theta_1^*$ and $\cos\theta_3^*$, see figure 4.1.

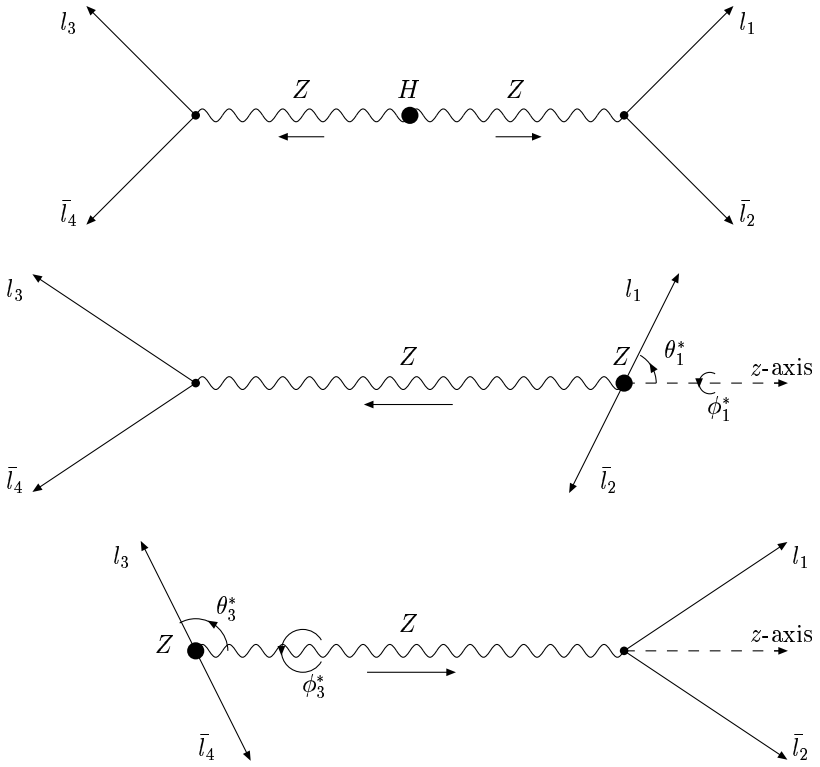

Figure 4.1: Definition of the decay angles in the decays of the Z bosons. The black dots show which particle is at rest in the given frame. Higgs rest frame (top), rest frame of first Z boson (middle), rest frame of second Z boson (bottom). I got the idea to this figure from [8].

The angle ϕ_{13}^* is defined as

$$\phi_{13}^* = |\phi_1^* - \phi_3^* + 2\pi n| \,, \tag{4.19}$$

where n is an integer, chosen so that $(\phi_1^* - \phi_3^* + 2\pi n)$ lies between $-\pi$ and π. The angles ϕ_1^* and ϕ_3^* are the azimuthal angles of l_1 and l_3 in the rest frames of the corresponding Z bosons, see figure 4.1.

I also define a third observable $\cos\theta_{13}^*$, which can be considered as a combination of the information in the three observables I have already mentioned.[2] The observable $\cos\theta_{13}^*$ is defined as the angle between the momentum of l_1, $\mathbf{p}_1$, and the momentum of l_3, $\mathbf{p}_3$, where

[2]The observable $\cos\theta_{13}^*$ was suggested by T. Sjöstrand.

$\mathbf{p}_1$ is measured in the rest frame of the first Z boson and $\mathbf{p}_3$ is measured in the rest frame of the second Z boson. This makes $\cos\theta^*_{13}$ the angle between two momentum vectors which are defined in two different frames of reference. Thus it is no physical decay angle, but a function of the four angles θ^*_1, θ^*_3, ϕ^*_1 and ϕ^*_3:

$$\cos\theta^*_{13} = \cos\theta^*_1 \cos\theta^*_3[1 - \cos(\phi^*_1 - \phi^*_3)] + \cos(\theta^*_1 - \theta^*_3)\cos(\phi^*_1 - \phi^*_3) \tag{4.20}$$

Notice that ϕ^*_{13} is also a difference between angles measured in two different frames, but because we boost along the z-axis in order to get from the Higgs rest frame to the respective Z boson rest frames, the azimuthal angles ϕ^*_1 and ϕ^*_3 are invariant under these two boosts. Therefore we would get the same value of ϕ_{13} if ϕ_1 and ϕ_3 were measured in the Higgs rest frame.

One can now easily show that the relation between the angle ϕ (3.2), defined in the previous chapter, and the angle ϕ^*_{13} is given by:

$$\phi^*_{13} = \pi - \phi\,. \tag{4.21}$$

There are three more observable angles which I have studied. They are chosen to distinguish between background and signal events. The first two are different definitions of the polar angle in the decay of the Higgs boson. These angles are expected to be completely isotropically distributed for the signal events, because the Standard Model Higgs boson is a scalar particle. The angle $\cos\theta^*_{ZH}$ is defined as the polar decay angle of the first Z boson in the Higgs rest frame, relative to the direction of the Higgs momentum. The second angle, $\cos\theta^*_{ZZ}$, is defined as the polar decay angle of the first Z boson in the Higgs rest frame, relative to the z-axis (the beam axis). See figure 4.2 for the angle $\cos\theta^*_{ZH}$.

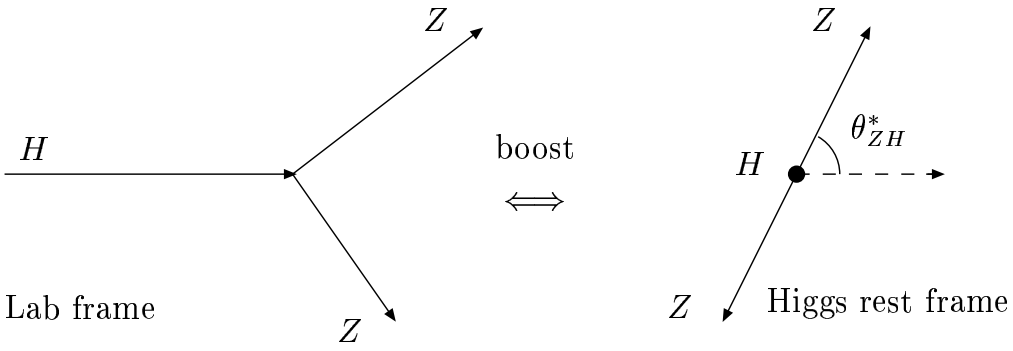

Figure 4.2: The angle $\cos\theta^*_{ZH}$, defined in the Higgs rest frame.

The last observable I have studied is the angle ϕ^*_{sum}, defined as

$$\phi^*_{\text{sum}} = |\phi^*_1 + \phi^*_3 + 2\pi n|\,, \tag{4.22}$$

where n is again chosen so that $(\phi_1^*+\phi_3^*+2\pi n)$ lies between $-\pi$ and π. This is the azimuthal angle in the Z boson decays which we expect to be isotropic, because of invariance under rotations of the system. Thus it serves as a check.

At the end of this section I have included plots of five of the seven observables mentioned above. The two observables which are not shown are $\cos\theta_{ZZ}^*$ and ϕ_{sum}^*. The reason to exclude $\cos\theta_{ZZ}^*$ is that it is very similar to $\cos\theta_{ZH}^*$, so there is no need to show both distributions. I have excluded ϕ_{sum}^* because it is indeed completely isotropic, both in the two types of signal as well as in the background.

I show distributions of each observable, before and after selecting events with the kinematic cuts described in this section for $m_H = 200$ GeV. See figures 4.3–4.7. In addition each observable is shown for decay of a CP-even Higgs boson, a CP-odd Higgs, and the quark-antiquark fusion background channel. The normalisation is arbitrary, because my intention is to show the shapes of the distributions. The ratio of events before and after cuts is correct shown though, except in the case of the background events, where I have multiplied the distribution after cuts by 20, so that the shape should be clearly visible compared to the distribution before cuts (the ratio of background events surviving cuts is a few percent). The cross section times branching ratios and the ratio of events surviving cuts are summarised in tables in the next section.

In appendix A I have shown the same plots for the Higgs masses $m_H = 250$ GeV and $m_H = 300$ GeV. See figures A.1–A.10.

The information in these distributions can be summarised as follows: Let us start with the two observables $\cos\theta_1^*$ and $\cos\theta_3^*$, which by symmetry must be identical. The difference between the distributions for the CP-even and CP-odd case is not ruined by the kinematic cuts for either of the values of m_h. We see that the background distributions are similar in shape to the CP-odd distribution before cuts. The cuts ruin some of this similarity though, and makes the background distribution after cuts more isotropic.

It is interesting to note that the value of the Higgs mass does not have any effect on the distribution for the CP-odd case. For the CP-even case we see that values of $\cos\theta_1^*$ and $\cos\theta_3^*$ around zero become more and more probable as the Higgs mass increases, the distributions become more peaked around zero.

Next I discuss the observable ϕ_{13}^*. Again we notice that the CP-odd distributions do not vary with the Higgs mass. The CP-even distributions become more and more isotropic as the Higgs mass increases. We see some correlation for $m_h = 200$ GeV, and the correlation is just visible for $m_h = 250$ GeV, but for $m_h = 300$ GeV, the correlation can be ignored. The shape of neither signal distribution is changed by the kinematic cuts. The background is uncorrelated for all values of the Higgs mass, and this is also unchanged by the kinematic cuts, except in the case of $m_h = 200$ GeV, where we see a small correlation similar to the CP-even case after cuts.

For the observable $\cos\theta_{13}^*$, the CP-odd distribution is again independent of the value of the Higgs mass. The CP-even distribution is peaked in the forward and backward directions, opposite to the CP-odd which is peaked for the normal direction. We see a tendency here too, that the CP-even distribution becomes more uncorrelated with increasing Higgs mass, but the effect is much weaker than for the observable ϕ_{13}^*. The signal distributions

are not much changed by the kinematic cuts, if at all. The background is also here flat and unchanged by the cuts, except for $m_h = 200$ GeV, where we see a small correlation after cuts.

When it comes to the observable $\cos\theta^*_{ZH}$, we see that it is completely isotropic for the two types of signal, but that the cuts change the distributions slightly so that angles close to the normal direction become a bit more probable compared to the forward and backward directions. The deviation from an isotropic distribution increases slightly with the Higgs mass, both for the CP-even and the CP-odd case. Among the observables I have studied, this is the one where the CP-even and CP-odd distributions are most similar.

The background on the other hand is strongly peaked in the forward and backward directions for this observable. After cuts most of these peaks disappear for the background. The distribution for $m_h = 200$ GeV is almost flat after cuts, whereas the distribution for $m_h = 300$ GeV has kept some of the peaks in the forward and backward directions.

The fact that the distribution in ϕ^*_{13} becomes isotropic when the Higgs mass increases in the CP-even case, and that it is independent of the Higgs mass in the CP-odd case, is consistent with the expressions for the decay rates $\mathrm{d}\Gamma/\mathrm{d}\phi$ in (3.184) and (3.185) in the previous chapter. The shape of the ϕ^*_{13} distributions is also as we expected from these expressions, see figure 3.5.

4.3.3 Cross Sections and Expected Number of Events after Cuts

The tables 4.4–4.7 summarise the cross section times branching ratios $\sigma \times BR$, the percent of events which survive kinematic cuts (cut%), and the expected number of events after reconstruction and kinematic cuts, n, for three different Higgs boson masses and for two values of the integrated luminosity $\int \mathcal{L}\,\mathrm{d}t$. I have used the following formula to calculate the expected number of events that survive reconstruction and kinematic cuts:

$$n = \sigma \times BR \int \mathcal{L}\,\mathrm{d}t\,(\text{cut}\%)\,(0.9)^4\,. \tag{4.23}$$

Here the factor $(0.9)^4$ comes from an expected reconstruction efficiency of 90% for electrons and muons at ATLAS [29] (page 714).

I have obtained the background cross section times branching ratio by using the formula:

$$\sigma_{\text{tot}} \times BR = 1.35\,\sigma(q\bar{q} \to ZZ) \times BR\,. \tag{4.24}$$

The factor 1.35 I have found by noting that the cross section for the channel $gg \to ZZ$ is expected to be 35–45% of the $q\bar{q} \to ZZ$ cross section for a CoM energy of 16 GeV [30]. The CoM energy at the LHC is now expected to be 14 GeV, and therefore I use the lower limit 35% (the gluon distribution functions for the proton are largest for small values of the momentum fraction x, and decreases when x increases.)

I have compared the values obtained for cross section times branching ratios and expected number of events with the values found in the ATLAS internal note in ref. [32] for the same Higgs masses and with the same kinematic cuts. In this note the quoted

signal cross section times branching ratios is approximately 10–20% higher than the values I have found from default PYTHIA settings. This might be due to the fact that different parton distribution functions have been used. The quoted expected number of signal and background events, with kinematic cuts similar to the ones I have used, is also higher than the values I have found. This might not be so difficult to explain, knowing that simulation of the ATLAS detector has been used to find the reconstruction efficiencies and the background rejections in the note, whereas I have used a simpler analysis model to find the fraction surviving cuts. This fact together with the effect of different parton distribution functions might be enough to explain the differences in the results.

m_H [GeV]	$\sigma \times BR$ [fb] signal	$\sigma \times BR$ [fb] background
200	11.1	95.2
250	8.97	95.2
300	7.19	95.2

Table 4.4: The cross section times branching ratio (BR) for signal events, and for background events for three different Higgs masses

m_H [GeV]	Surviving cuts (%) signal	Surviving cuts (%) background
200	50.5	3.24
250	46.5	2.13
300	43.3	1.37

Table 4.5: The fraction of events surviving kinematic cuts

m_H [GeV]	Number of signal events	Number of background events
200	368	202
250	274	133
300	204	86

Table 4.6: Expected number of events for an integrated luminosity of 100 fb^{-1}

m_H [GeV]	Number of signal events	Number of background events
200	110	61
250	82	40
300	62	26

Table 4.7: Expected number of events for an integrated luminosity of 30 fb^{-1}

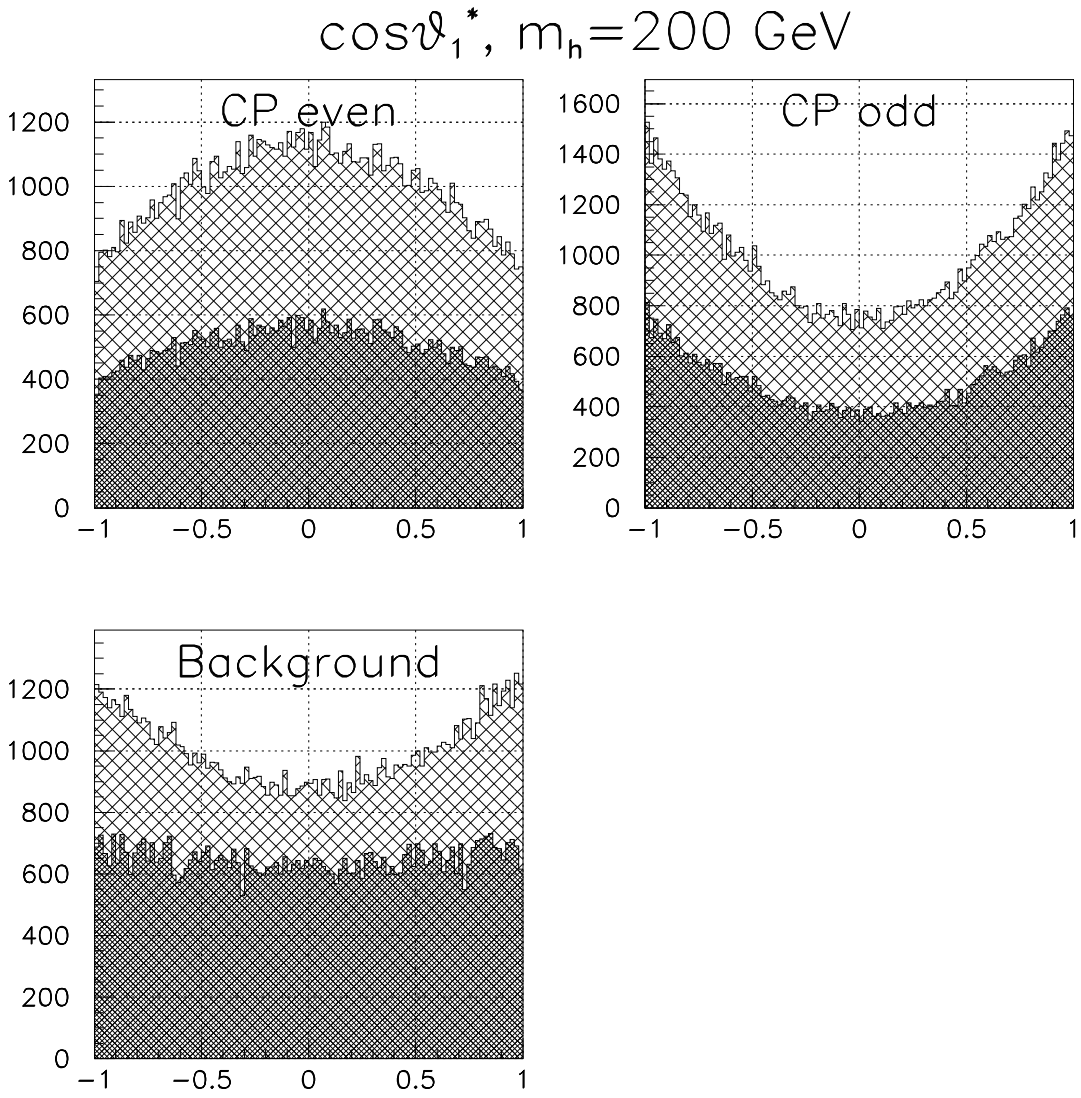

Figure 4.3: Higgs mass $m_h = 200$ GeV. The distribution of $\cos\theta_1^*$, for a CP-even and a CP-odd Higgs, and for background events ($q\bar{q} \to ZZ \to 4l$), before (light) and after (dark) kinematic cuts. For the background the distribution after cuts is multiplied by a factor 20, compared to the distribution before cuts.

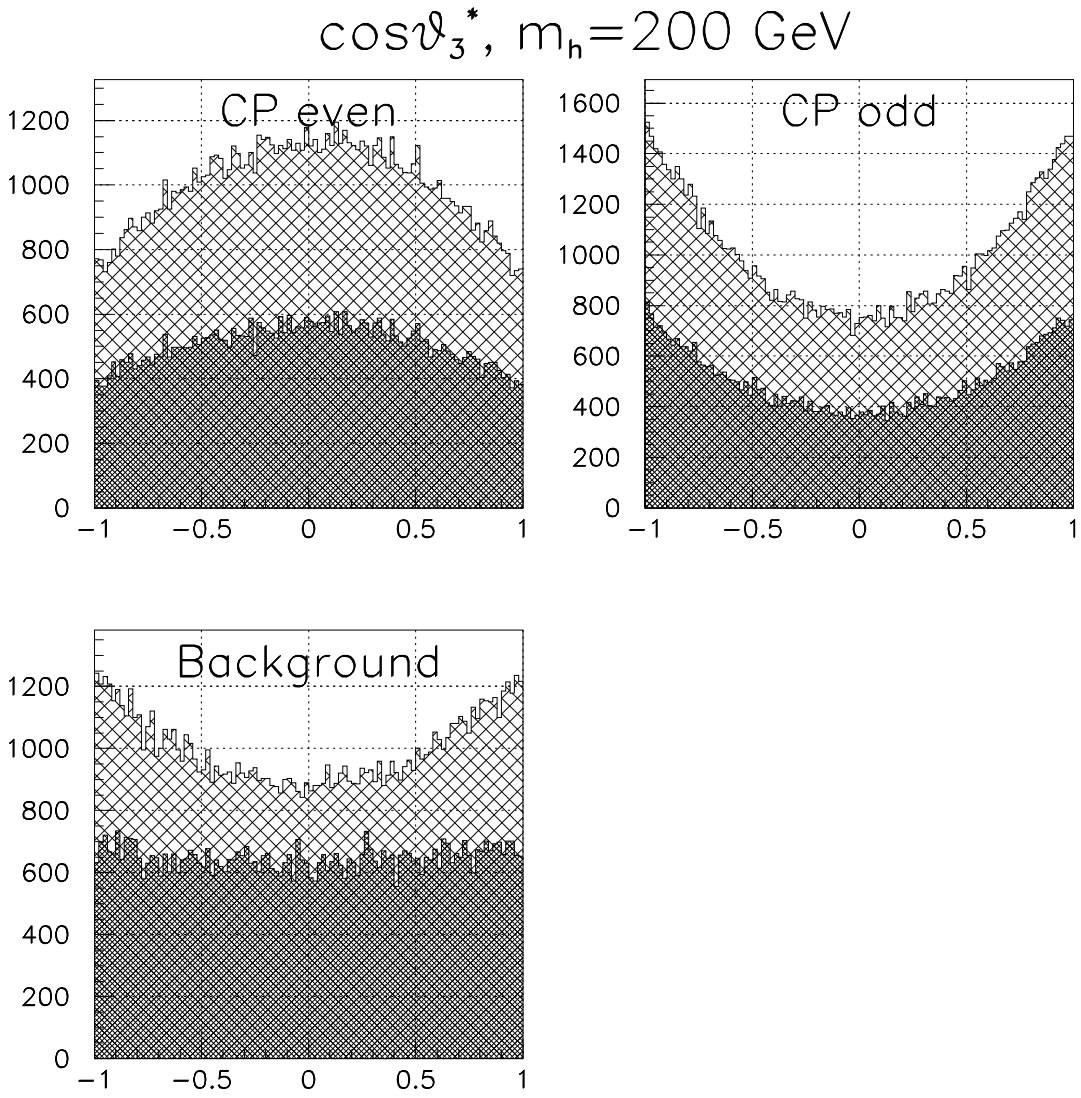

Figure 4.4: Higgs mass $m_h = 200$ GeV. The distribution of $\cos\theta_3^*$, for a CP-even and a CP-odd Higgs, and for background events ($q\bar{q} \to ZZ \to 4l$), before (light) and after (dark) kinematic cuts. For the background the distribution after cuts is multiplied by a factor 20, compared to the distribution before cuts.

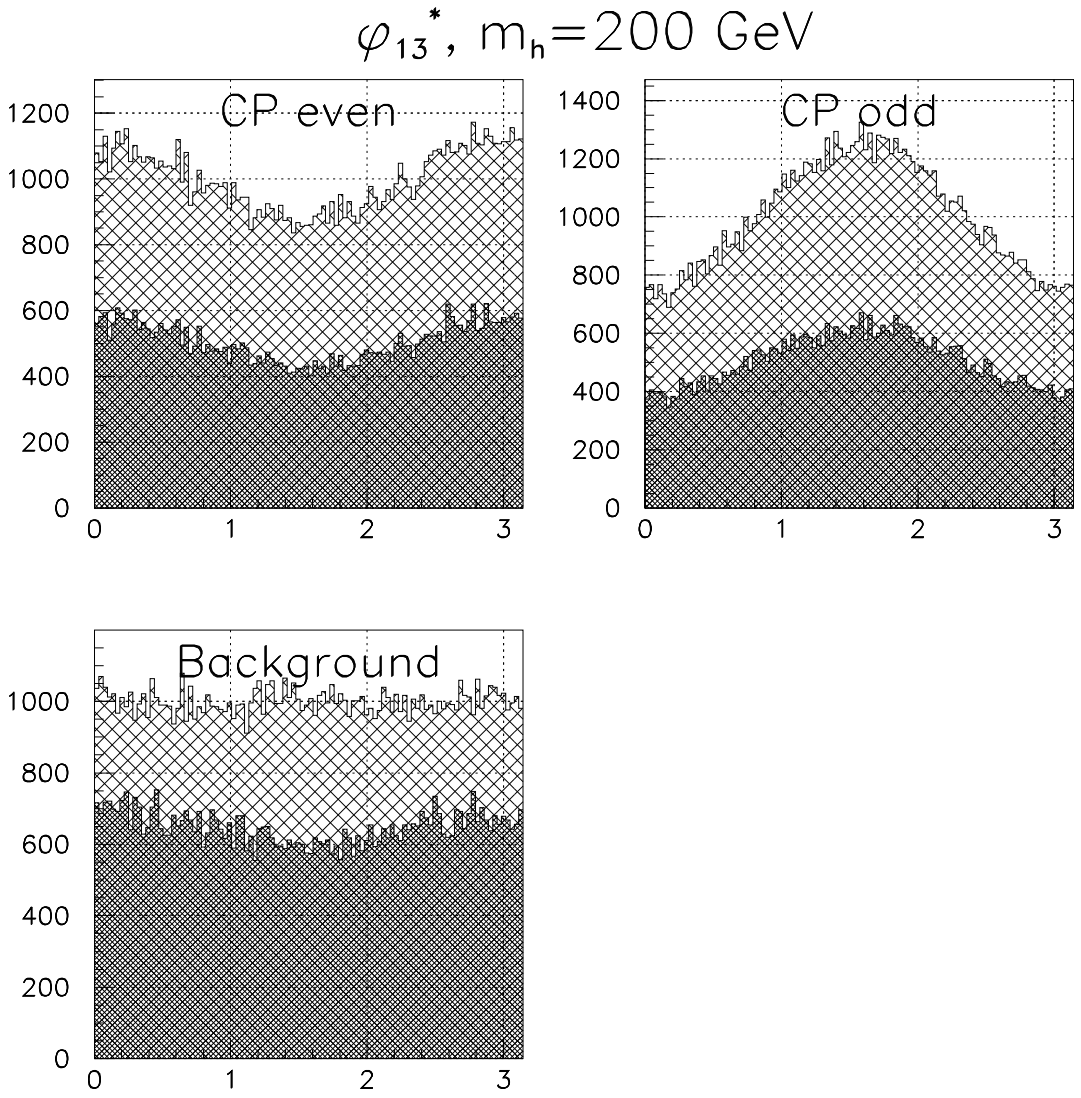

Figure 4.5: Higgs mass $m_h = 200$ GeV. The distribution of ϕ_{13}^*, for a CP-even and a CP-odd Higgs, and for background events ($q\bar{q} \to ZZ \to 4l$), before (light) and after (dark) kinematic cuts. For the background the distribution after cuts is multiplied by a factor 20, compared to the distribution before cuts.

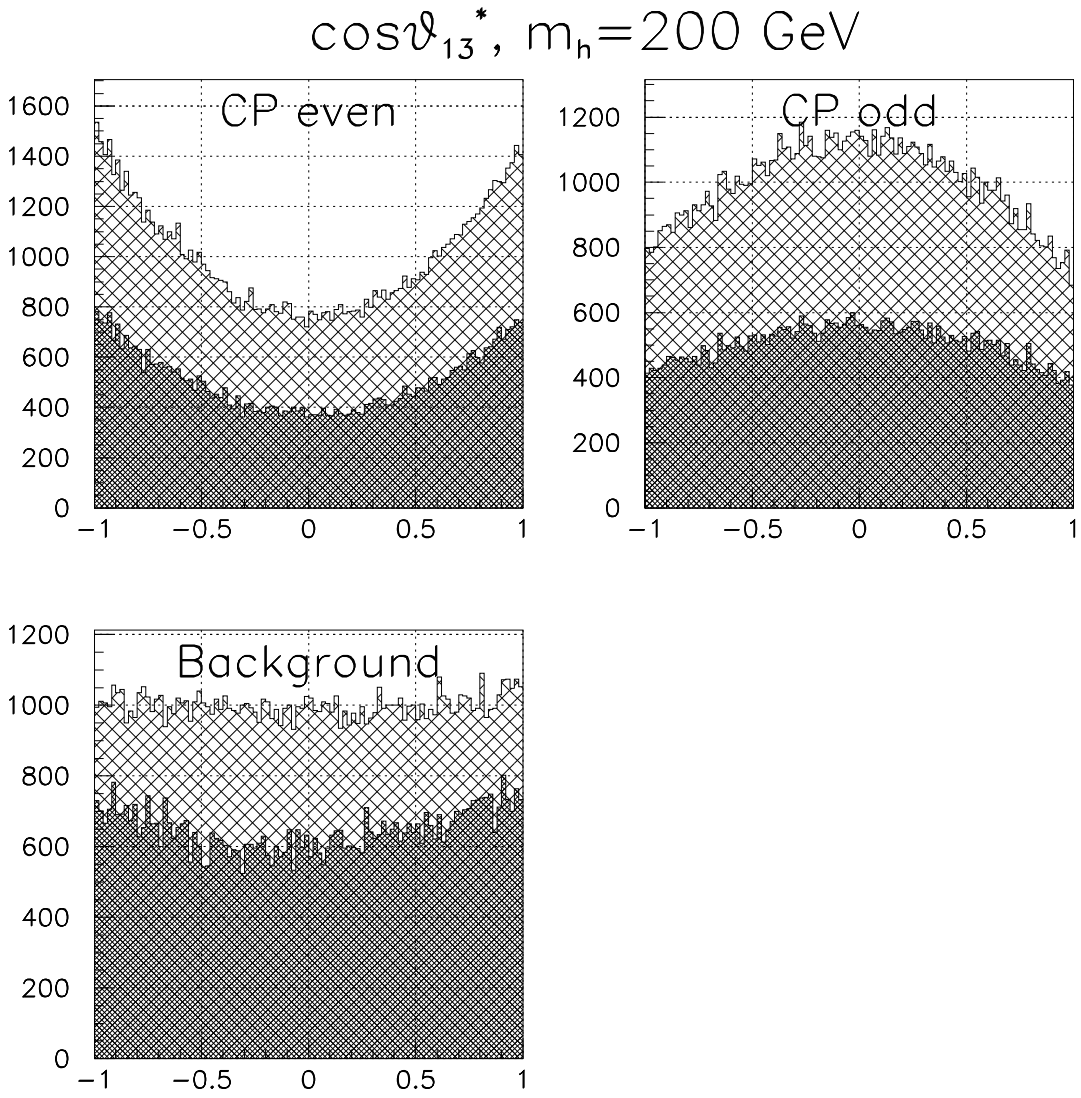

Figure 4.6: Higgs mass $m_h = 200$ GeV. The distribution of $\cos\theta^*_{13}$, for a CP-even and a CP-odd Higgs, and for background events ($q\bar{q} \to ZZ \to 4l$), before (light) and after (dark) kinematic cuts. For the background the distribution after cuts is multiplied by a factor 20, compared to the distribution before cuts.

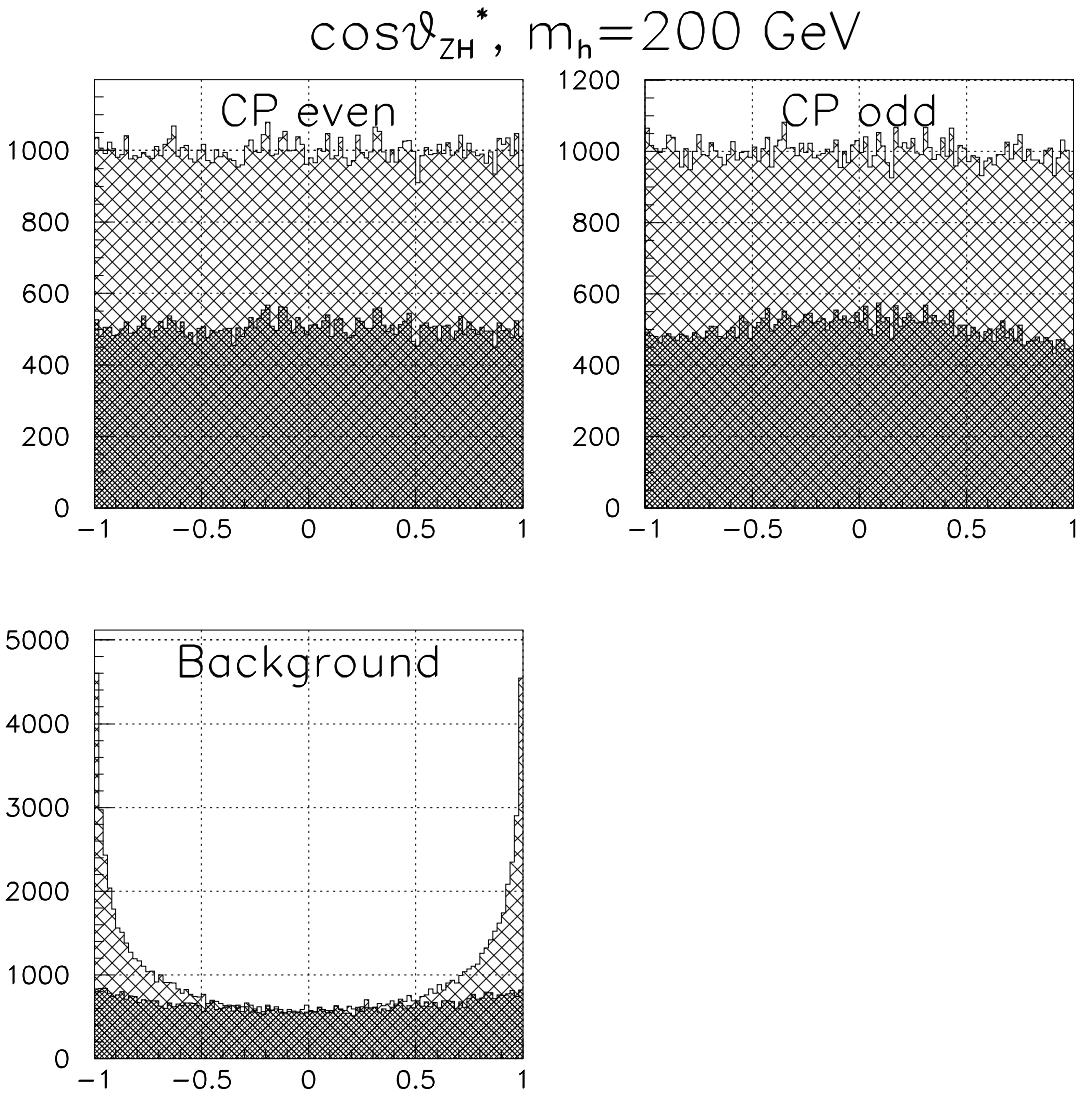

Figure 4.7: Higgs mass $m_h = 200$ GeV. The distribution of $\cos\theta^*_{ZH}$, for a CP-even and a CP-odd Higgs, and for background events ($q\bar{q} \to ZZ \to 4l$), before (light) and after (dark) kinematic cuts. For the background the distribution after cuts is multiplied by a factor 20, compared to the distribution before cuts.

4.4 Statistical Method

In this section I will describe the statistical method I am going to use. I want to make use of the observables described in the previous section, to test the two hypotheses "CP-even Higgs boson" and "CP-odd Higgs boson" against simulated experiments. My goal is to assess the amount of integrated luminosity necessary in order to draw a conclusion about the CP-property of a discovered Higgs boson from these observables.

My starting point is the least squares method. I use the modified minimum chi-square method [34] (page 171):

$$Q^2 = \sum_{i=1}^{N} \frac{[Y_i - f_i(\bar{\theta})]^2}{Y_i} \tag{4.25}$$

Here Y_i are the number of events in histogram bins, and $f_i(\bar{\theta})$ are the expectation values of Y_i, according to some model. The vector $\bar{\theta}$ contains the parameters of the model.

In its usual form the minimum chi-square method has got the variance σ_i^2 in the denominator (instead of Y_i). The *modified* minimum chi-square method uses Y_i instead of σ_i^2. Asymptotically for a large number of bins and a large number of events per bin, the two methods give the same result. This can be seen from the fact that $f_i(\bar{\theta})$ is the expectation value of Y_i, and that we have $\sigma_i^2 \approx f_i(\bar{\theta})$ when the number of bins is large.

In the limit of a large number of events Y_i becomes approximately normal. When $\bar{\theta}$ is known, when there are many events in each bin, and for large N, then Q^2 is asymptotically distributed as $\chi^2(N)$. The distributions $\chi^2(N)$ for some selected values of N can be seen in figure 4.8.

I expect Q^2 to be generally larger for the "wrong" model than for the "correct" one. We know, of course, which hypothesis is correct for a given simulated experiment. I will determine how often Q^2 has the smallest value for the correct hypothesis. By demanding that this must be the case in 95 out of 100 experiments, I can estimate the necessary integrated luminosity in order to decide the CP-property of a discovered Higgs boson.

I am going to use the following notation for Q^2:

$$(Q^2)_x^a = \sum_{i=1}^{N} \frac{[h_i - (w f_i^a + (1-w) g_i)]^2}{h_i} \quad a = h, A\,. \tag{4.26}$$

Here f_i^a, g_i and h_i are histograms of distributions in some observable x, and N is the number of bins in the histograms. The distributions f_i^a and g_i are the theoretically expected distributions for signal events and background events, respectively. The signal can be either of type $a = h$, CP-even Higgs boson, or $a = A$, CP-odd Higgs boson. The histogram h_i represents the experimentally measured distribution in x. In the simulated experiment, the Higgs boson must be chosen to be either CP-even or CP-odd. The expression $(w f_i^a + (1 - w) g_i)$ is the theoretically expected value of h_i for a given hypothesis $a = h$ or $a = A$. Here w equals the signal fraction of events in the experiment and $(1 - w)$ equals the background fraction.

The theoretical predictions f_i^a and g_i are determined by Monte Carlo simulation of a large number of events. The experiments are simulated with the expected number of signal

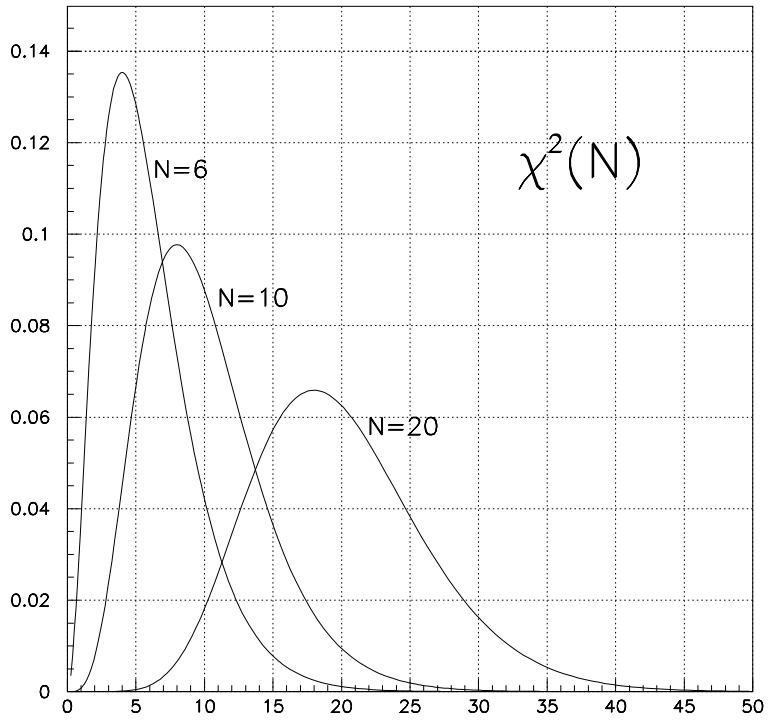

Figure 4.8: The distributions $\chi^2(N)$ for N equal to 6, 10 and 20.

and background events for a given integrated luminosity, after kinematic cuts. The effect of kinematic cuts on the distributions f_i^a and g_i is also taken into account. The value of the parameter w can be obtained by minimising $(Q^2)_x^a$ with respect to w for some observable x.

In the previous section several angular observables which can be used to separate the two signals $a = h$ and $a = A$ from each other, and from the background, were introduced. The observable $\cos\theta^*_{ZH}$ will be used to determine the value of w, because its distribution for the two signal hypotheses $a = h$ and $a = A$ is similar, and different from its distribution for background events.

I also tried to determine w by taking the average of the value obtained from all observables. This resulted in negative values for w when testing the CP-odd hypothesis against CP-even Higgs bosons in the experiment, but positive values of w for the CP-even hypothesis. I concluded that it was better to choose a method for determining w which would give a value close to the actual fraction of signal events (which is known for Monte Carlo simulated experiments) for the "wrong" hypothesis as well as for the "correct" one.

I will use the value of w determined from $\cos\theta^*_{ZH}$ when calculating $(Q^2)_x^a$ for the five observables $\cos\theta^*_1$, $\cos\theta^*_3$, ϕ^*_{13}, $\cos\theta^*_{13}$ and $\cos\theta^*_{ZH}$. Then I will take the sum of $(Q^2)_x^a$ over

the four first of these observables for a given hypothesis:

$$(Q^2)^a = \sum_{x=1}^{4} (Q^2)_x^a \tag{4.27}$$

This sum $(Q^2)^a$ will then be used as the value of Q^2 for either hypothesis, $a = h$ or $a = A$. The reason why $\cos\theta^*_{ZH}$ is not included when calculating $(Q^2)^a$, is that it gives approximately the same value of Q^2 for the two hypotheses. This is just as we would expect because the distribution of $\cos\theta^*_{ZH}$ is so similar for the two hypotheses.

The statistical method now can be described as follows:

- Choose a value of the Higgs mass, m_H, and a value of the integrated luminosity. Select the Higgs boson to be either CP-even or CP-odd.
- Determine the form of the distributions f_i^a and g_i for each observable x for the given Higgs mass.
- Calculate the expected number of signal and background events to survive the kinematic cuts.
- Simulate 100 different experiments, where
  - the actual number of simulated signal events surviving the cuts, n_{sign} and the actual number of background events surviving the cuts, n_{back}, are chosen according to a Poisson distribution around the expected values,
  - the values of Q^2 for the two different hypotheses CP-even Higgs boson, $a = h$, and CP-odd Higgs boson, $a = A$, are calculated.
- How often is Q^2 for the "correct" hypothesis smaller than Q^2 for the "wrong" hypothesis? We know, of course, whether the generated Higgs bosons in the experiments were CP-even or CP-odd.
- If Q^2 for the "correct" hypothesis is smallest in 95 out of 100 experiments, then we can expect to be able to determine the CP-state of the Higgs boson of our simple model, for the given integrated luminosity. If this is not the case, try with a higher integrated luminosity.
- Repeat the above procedure for the other CP-state of the Higgs boson, and for several values of the Higgs boson mass.

The expected number of signal and background events varies with the value of the integrated luminosity and of the Higgs mass. Therefore also the number of bins N has to be varied in order to avoid that the number of events per bin gets too small. The number of bins should always be as large as possible to get as much information from the simulated data as possible.

4.5 Results of the Statistical Analysis

This section contains the results of the statistical analysis. I will give the results in the form of tables and plots. Most of the plots are in appendix B. I will discuss all results of the Monte Carlo analysis in this section though.

First I give an overview of the number of bins I have used in the histograms in the statistical analysis. As I discussed in the previous section, the number of bins should be as large as possible, both because the simulated data then is better exploited, and because the asymptotic properties of the modified minimum chi-squared method, discussed in the previous section, depend on a large number of bins.

When the number of events in one of the bins of the experimental distribution Y_i equals zero, though, the method either has to be changed, or the data has to be rebinned for a smaller number of bins.

I have chosen to rebin the data (to run the simulation again for a smaller number of bins). The alternative would be to throw away the bin with zero events in the Y_i distribution, or to combine the bin with zero events with the bin before or after.

I must admit that the choice of method is somewhat arbitrary, due to the fact that my statistical analysis is not so accurate from the start. For the small number of events available it would probably have been better to work with the maximum likelihood method [34] (page 171).

On the other hand, I am not trying to make a highly specialised statistical analysis of the simulated data, but only to get some estimate of the amount of information in the observables I have studied. The theoretical model I have used as a basis for the simulations, is also only an approximation. The advantage from these approximations is naturally that the results could be obtained in a shorter time than what would otherwise have been the case.

In table 4.8 below I have shown the number of bins used for different settings in the simulations. Here also I have to admit that this is probably not the perfect binning for the data. I started with 20 bins, and reduced the number of bins in the cases where I had problems with empty bins in Y_i. It is my opinion that this method can be justified from the same arguments as above.

At the end of this section and in appendix B, I have shown all the plots which are the results of the statistical analysis. In figures 4.9–4.20 in this section I show histograms for the sum $(Q^2)^a = \sum_{x=1}^{4} (Q^2)_x^a$, where the sum goes over the four observables $\cos\theta_1^*$, $\cos\theta_3^*$, ϕ_{13}^* and $\cos\theta_{13}^*$.

I show histograms for the hypotheses of a CP-even, $a = h$, and a CP-odd, $a = A$, Higgs boson, as well as the difference $(Q^2)^h - (Q^2)^A$. See the previous section for more details on the statistical method. The histograms are shown for three different values of the Higgs mass, for either a CP-even or a CP-odd Higgs boson in the simulated experiments, and for two different values of the integrated luminosity, $\int \mathcal{L} dt = 100$ fb^{-1} and $\int \mathcal{L} dt = 30$ fb^{-1}. The values of the integrated luminosity correspond to the values quoted in the ATLAS TDR [29]. The histograms show the results of 100 simulated experiments.

In appendix B I show the corresponding histograms of $(Q^2)_x^a$ for each of the four ob-

m_h [GeV]	200	250	300
$\int \mathcal{L} dt = 100$ fb^{-1} CP-even	20 bins	10 bins	20 bins
$\int \mathcal{L} dt = 100$ fb^{-1} CP-odd	20 bins	10 bins	20 bins
$\int \mathcal{L} dt = 30$ fb^{-1} CP-even	10 bins	10 bins	6 bins
$\int \mathcal{L} dt = 30$ fb^{-1} CP-odd	10 bins	10 bins	6 bins

Table 4.8: Number of bins N used in the histograms in the statistical analysis, for different values of the integrated luminosity $\int \mathcal{L} dt$, the CP-state of the Higgs boson in the simulated experiments, and for the Higgs mass.

servables $\cos\theta_1^*$, $\cos\theta_3^*$, ϕ_{13}^* and $\cos\theta_{13}^*$. In addition I have shown the distributions in w, for the CP-even and CP-odd hypotheses. Remember that w is the value which is used in the statistical analysis, for the fraction of signal events in the experiments, and that w is determined from the observable $\cos\theta_{ZH}^*$. In addition to w, the same histograms as for the other four observables, is shown for $\cos\theta_{ZH}^*$. See figures B.1–B.36 in the appendix.

How can the information in all these histograms be summarised? Let us start with a table which shows how often the correct hypothesis would be chosen, using the statistical method in the previous section, see table 4.9.

m_h [GeV]	200	250	300
$\int \mathcal{L} dt = 100$ fb^{-1} CP-even	98%	100%	100%
$\int \mathcal{L} dt = 100$ fb^{-1} CP-odd	99%	100%	100%
$\int \mathcal{L} dt = 30$ fb^{-1} CP-even	84%	98%	99%
$\int \mathcal{L} dt = 30$ fb^{-1} CP-odd	87%	99%	98%

Table 4.9: In how many out of 100 experiments is the value of Q^2 for the "correct" hypothesis smaller than the value of Q^2 for the "wrong" hypothesis? The results are shown for different values of the Higgs mass, for the two CP-states of the Higgs boson in the simulated experiments, and for two values of the integrated luminosity.

From table 4.9, we see that an integrated luminosity of $\int \mathcal{L} dt = 30$ fb^{-1} probably would be sufficient to draw a conclusion about the CP-state of a Higgs boson with mass $m_h = 250$ GeV or $m_h = 300$ GeV, at the LHC, assuming the simple CP-conserving model

I have used (see the introduction to this chapter for an explanation of the model).

For a Higgs mass of $m_h = 200$ GeV an integrated luminosity of $\int \mathcal{L}dt = 100$ fb^{-1} would probably be necessary in order to measure the CP-state.

In table 4.10 I have shown the mean values and the root-mean-square values for the histograms of $(Q^2)^h - (Q^2)^A$ in figures 4.9–4.20. Notice that the mean values are negative

m_h [GeV]	200	250	300
$\int \mathcal{L}dt = 100$ fb^{-1} CP-even	-79.00 RMS 48.50	-151.7 RMS 46.40	-175.3 RMS 65.89
$\int \mathcal{L}dt = 100$ fb^{-1} CP-odd	113.8 RMS 54.39	129.9 RMS 43.30	129.6 RMS 47.82
$\int \mathcal{L}dt = 30$ fb^{-1} CP-even	-26.45 RMS 31.39	-42.90 RMS 26.92	-39.00 24.30
$\int \mathcal{L}dt = 30$ fb^{-1} CP-odd	33.10 RMS 35.02	46.70 RMS 29.81	34.95 RMS 21.90

Table 4.10: An overview of the mean and root-mean-square (RMS) values for the histograms of $(Q^2)^h - (Q^2)^A$.

for a CP-even Higgs boson simulated in the experiments, and positive for a CP-odd Higgs boson. This is consistent with the fact that $(Q^2)^h - (Q^2)^A$ will have a negative value when $(Q^2)^h$ is the smallest one, and a positive value when $(Q^2)^A$ is the smallest.

The RMS values are smaller for the lower value of the integrated luminosity. Clearly, the RMS values and the absolute values of the means, depend both on the number of bins used, and on the statistical significance of the simulated experiments. The number of bins used in the statistical method, determines the expectation value of the $\chi^2(N)$ distribution, and therefore the expected value of $(Q^2)^a_x$ in the case of a correct hypothesis and high statistics. The expected value of $(Q^2)^a_x$ is therefore smaller for a smaller number of bins, see figure 4.8 for the distribution $\chi^2(N)$ for different values of N. The sum $(Q^2)^a$ will also depend on the number of bins used in the chi-squared method.

As for the statistical significance of the experiments, a higher number of events will give a larger difference between the value $(Q^2)^a_x$ for the correct and for the wrong hypothesis. This will lead to larger values for the RMS of the difference $(Q^2)^h - (Q^2)^A$. Both these effects are consistent with the mean and RMS values in table 4.10.

How do the different observables contribute to the information about the CP-state of

the Higgs boson?

The histograms of $(Q^2)_x^h - (Q^2)_x^A$ can give some impression about how much information the different observables x contain about the CP-state of a Higgs boson, assuming the simple CP-conserving model described earlier. If the value of $(Q^2)_x$ for the "correct" hypothesis often is smaller than the value of $(Q^2)_x$ for the "wrong" hypothesis, then the observable contains more information than if this happens more seldom.

By comparing the histograms of $(Q^2)_x^h - (Q^2)_x^A$ for the two polar angles $\cos\theta_1^*$ and $\cos\theta_3^*$ for different values of the Higgs mass, we can see that these two observables contain more information about the CP-state of a Higgs boson for higher values of the Higgs mass.

For the angle ϕ_{13}^* it is the other way around. It contains less information for higher values of the Higgs mass.

This can be explained from the fact that the distributions $\cos\theta_1^*$ and $\cos\theta_3^*$, become more correlated when the Higgs mass increases for the CP-even Higgs, whereas the distribution of ϕ_{13}^* becomes almost uncorrelated for the CP-even Higgs, for increasing Higgs masses. For the CP-odd Higgs the distributions in all observables change little or not at all with the Higgs mass. See the discussion of the distributions of the observables in the subsection 4.3.2.

I conclude that for all three values of the Higgs mass, all four observables contain information about the CP-state of a Higgs boson. For the Higgs mass $m_h = 200$ GeV the four observables contain about the same amount of information, whereas for the Higgs mass $m_h = 300$ GeV, the two polar angles $\cos\theta_1^*$ and $\cos\theta_3^*$ are clearly more significant than the other two observables.

Concerning the fraction of signal events w, and the observable $\cos\theta_{ZH}^*$, notice that the distributions of w are very similar for the two hypotheses CP-even and CP-odd, and that $(Q^2)_x$ have almost identical values for the two hypotheses, for the observable $\cos\theta_{ZH}^*$. This shows that the distributions of $\cos\theta_{ZH}^*$ are very similar for the CP-even and the CP-odd Higgs bosons, as we would expect.

It is interesting to compare the distributions $(Q^2)_x^a$ with $\chi^2(N)$, where N is the number of bins used in the histograms in the statistical analysis, 6, 10 and 20 respectively. See figure 4.8 for plots of the $\chi^2(N)$ distributions for these values of N. From the histograms in figures B.1–B.36 one can see that the distributions in $(Q^2)_x^a$ are quite similar to the corresponding $\chi^2(N)$ distributions for the correct hypotheses, whereas $(Q^2)_x^a$ tend to have larger values for the wrong hypotheses.

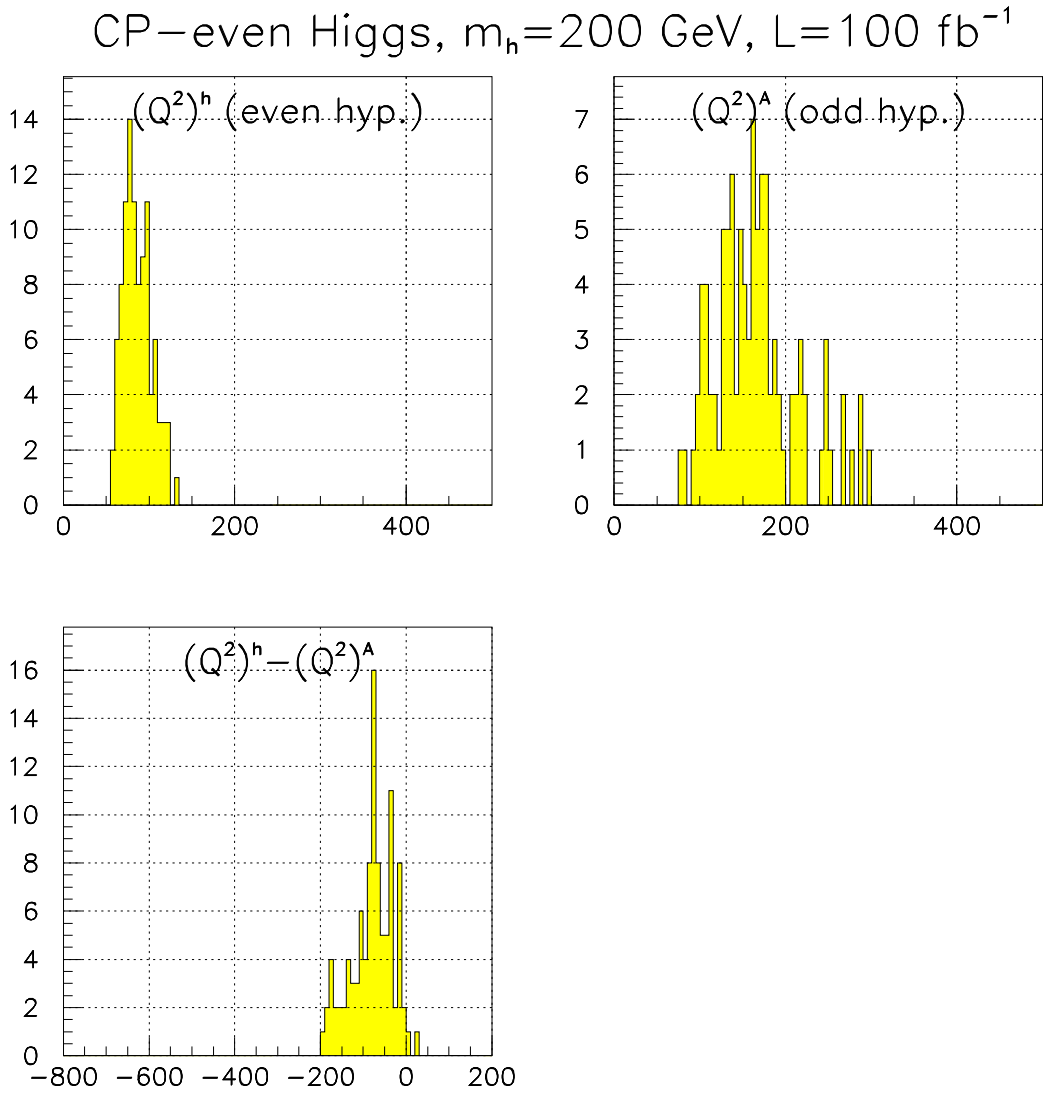

Figure 4.9: CP-even Higgs boson with mass $m_h = 200$ GeV, integrated luminosity $\int \mathcal{L} dt = 100$ fb^{-1}. The sum $(Q^2)^a = \sum_{x=1}^{4} (Q^2)^a_x$ is shown for the CP-even hypothesis $a = h$ and for the CP-odd hypothesis $a = A$. The difference between the value of $(Q^2)^a$ for the two hypotheses, $(Q^2)^h - (Q^2)^A$, is also shown.

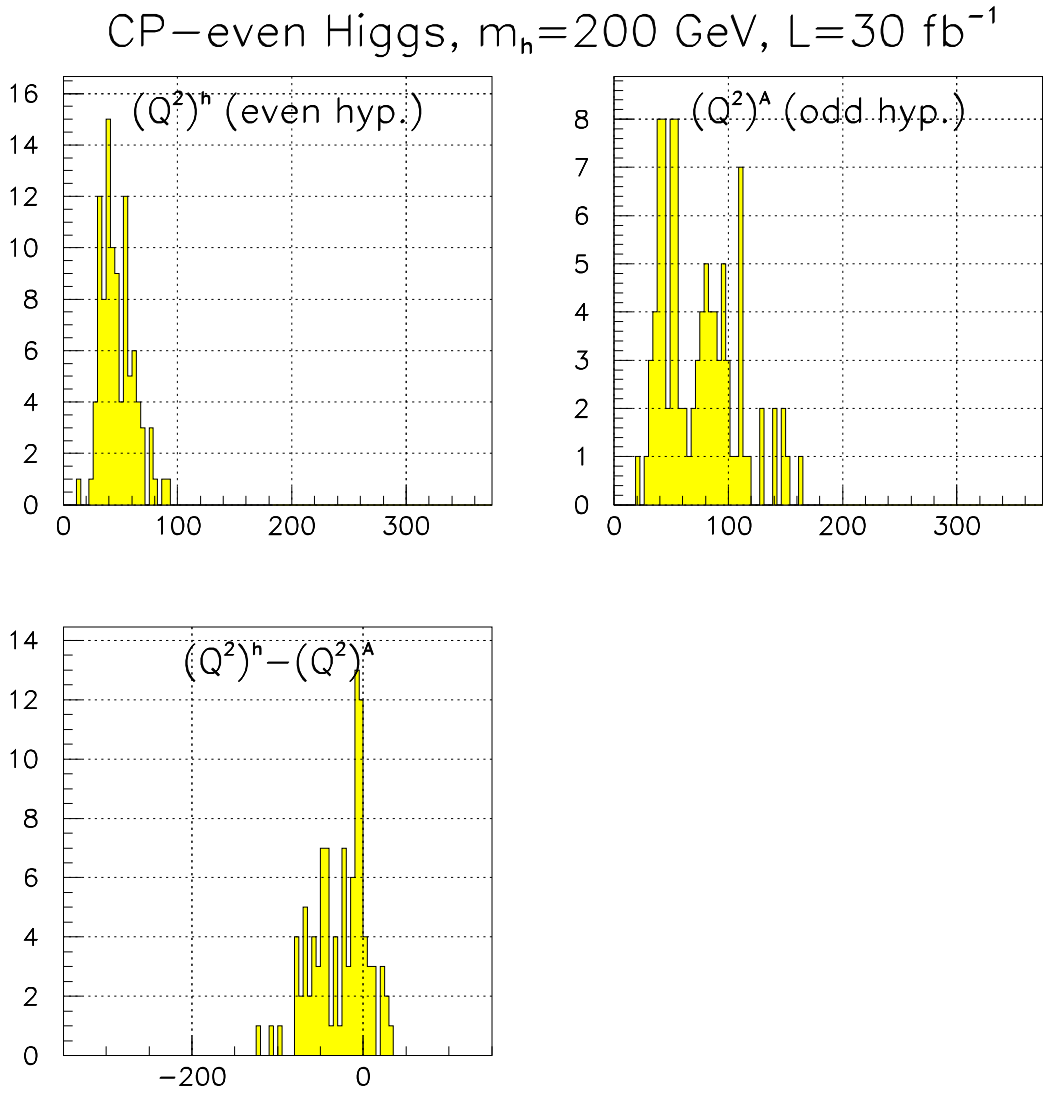

Figure 4.10: As figure 4.9, but with lower integrated luminosity, 30 fb^{-1}.

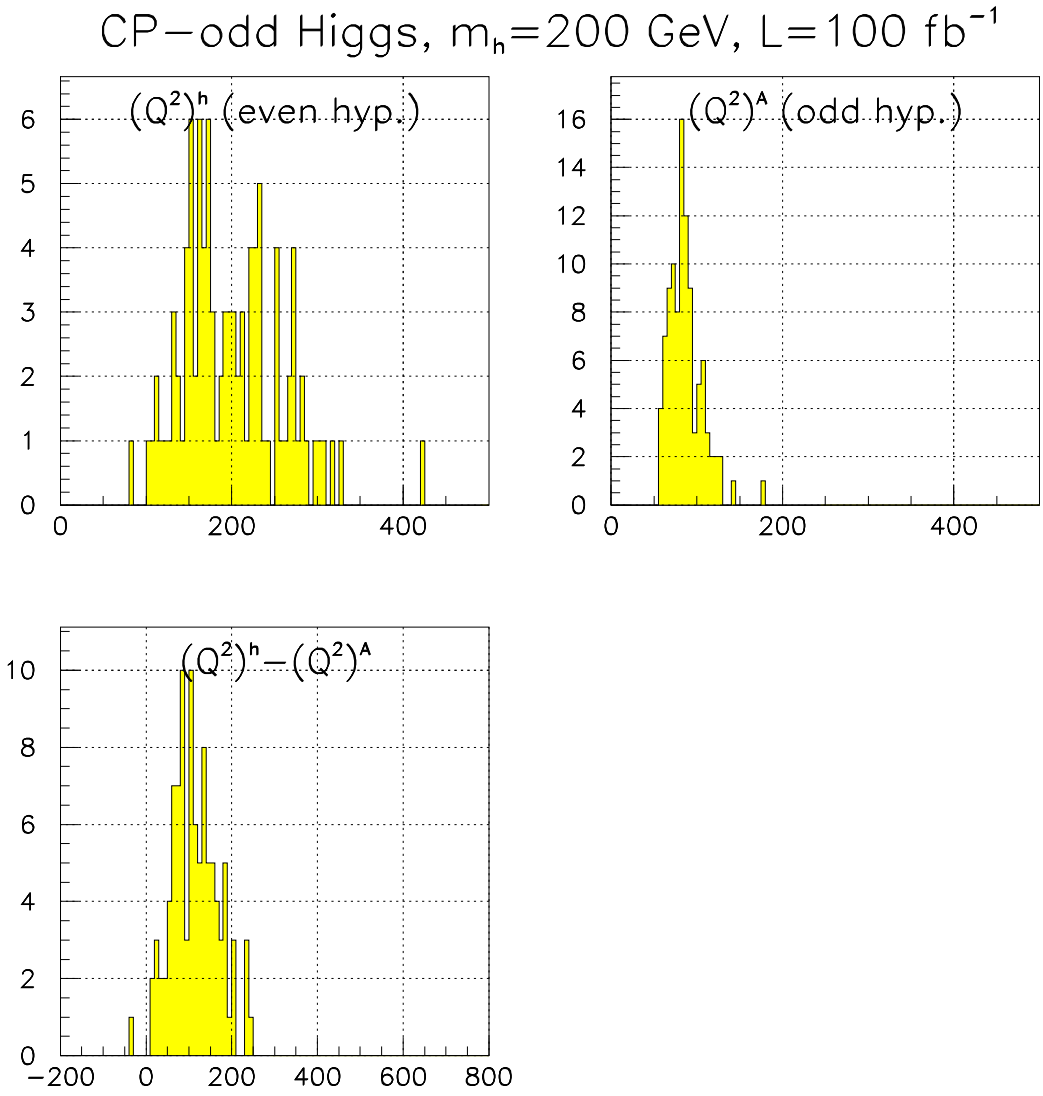

Figure 4.11: CP-odd Higgs boson with mass $m_h = 200$ GeV, integrated luminosity $\int \mathcal{L} dt = 100$ fb^{-1}. The sum $(Q^2)^a = \sum_{x=1}^{4} (Q^2)^a_x$ is shown for the CP-even hypothesis $a = h$ and for the CP-odd hypothesis $a = A$. The difference between the value of $(Q^2)^a$ for the two hypotheses, $(Q^2)^h - (Q^2)^A$, is also shown.

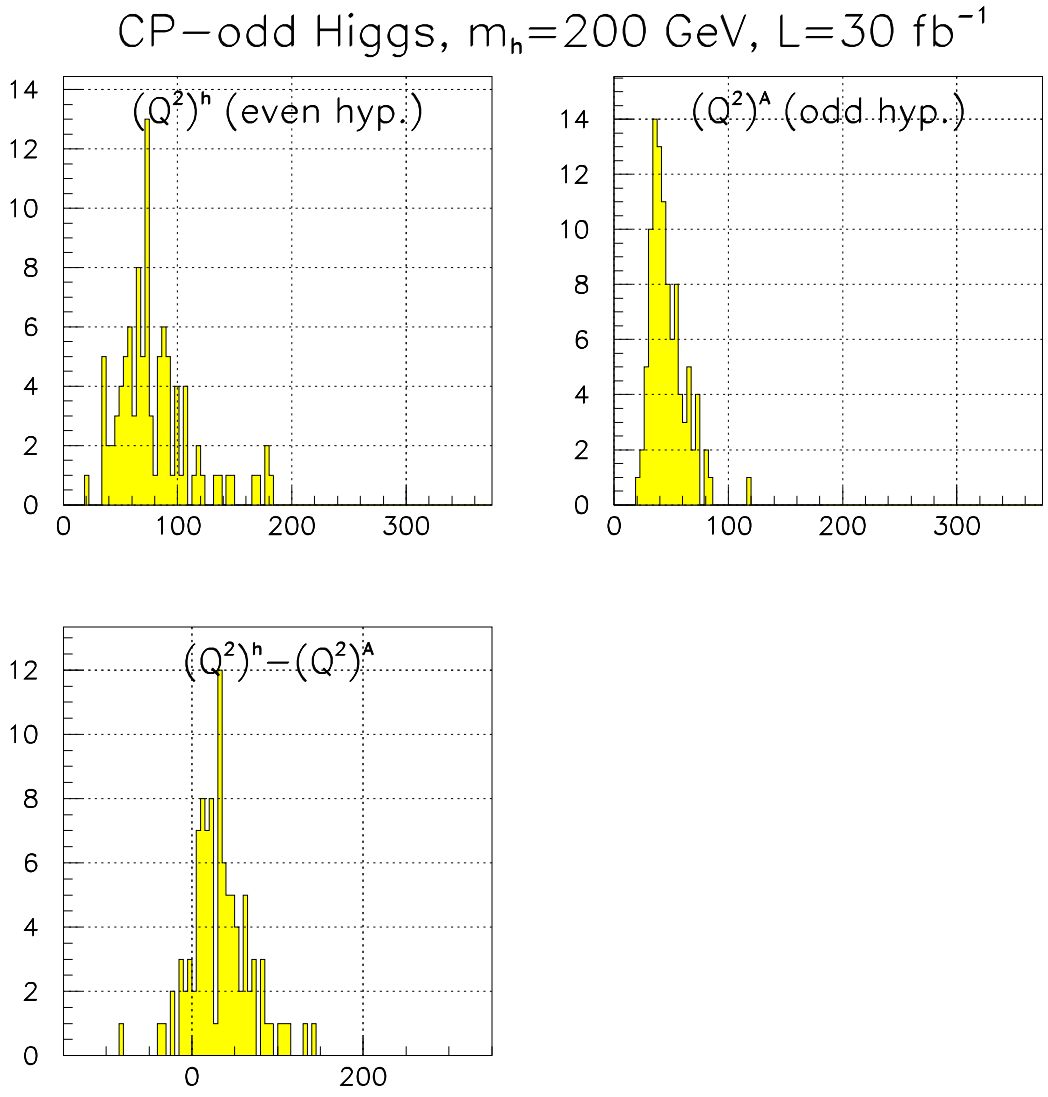

Figure 4.12: As figure 4.11, but with lower integrated luminosity, 30 fb^{-1}.

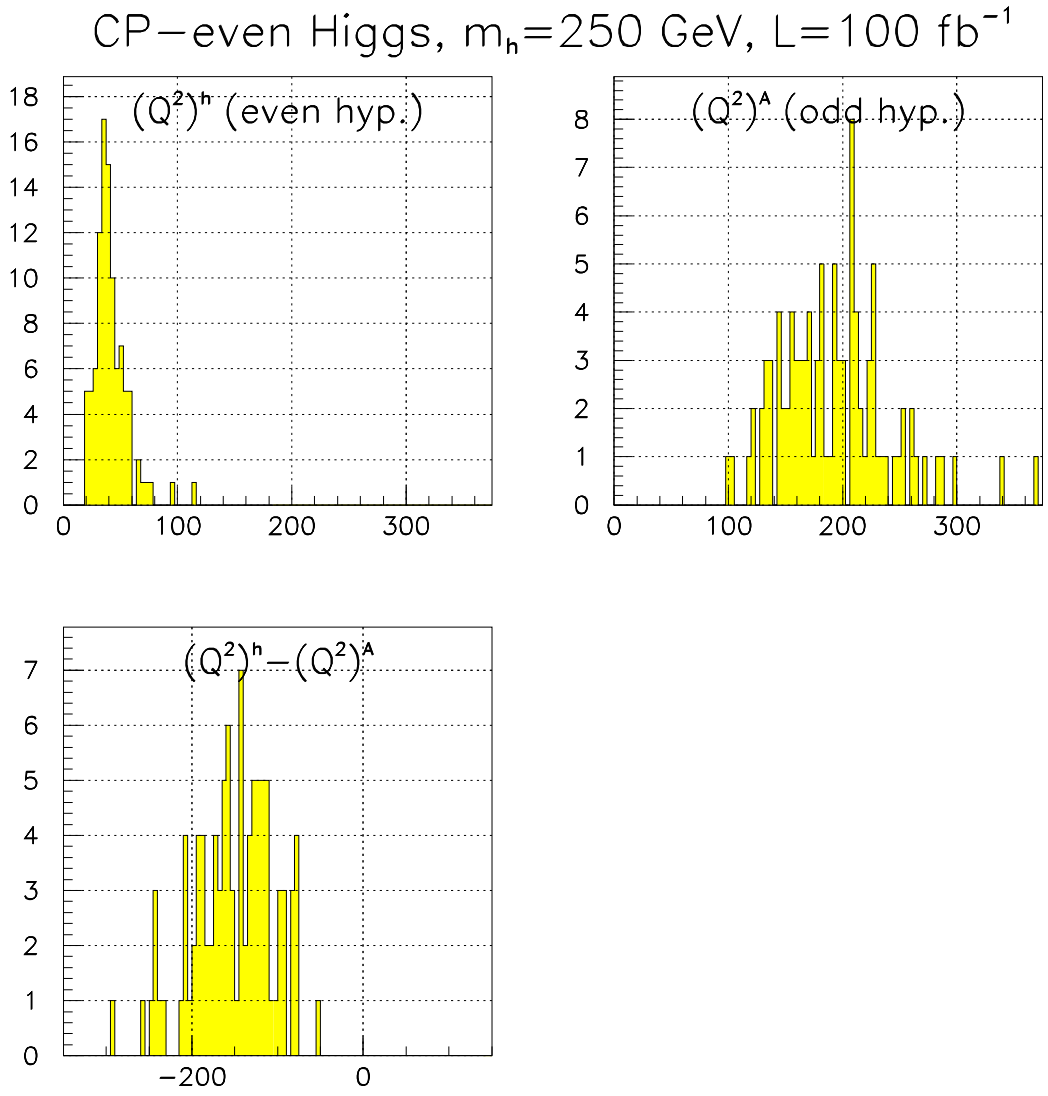

Figure 4.13: CP-even Higgs boson with mass $m_h = 250$ GeV, integrated luminosity $\int \mathcal{L} dt = 100$ fb^{-1}. The sum $(Q^2)^a = \sum_{x=1}^{4} (Q^2)^a_x$ is shown for the CP-even hypothesis $a = h$ and for the CP-odd hypothesis $a = A$. The difference between the value of $(Q^2)^a$ for the two hypotheses, $(Q^2)^h - (Q^2)^A$, is also shown.

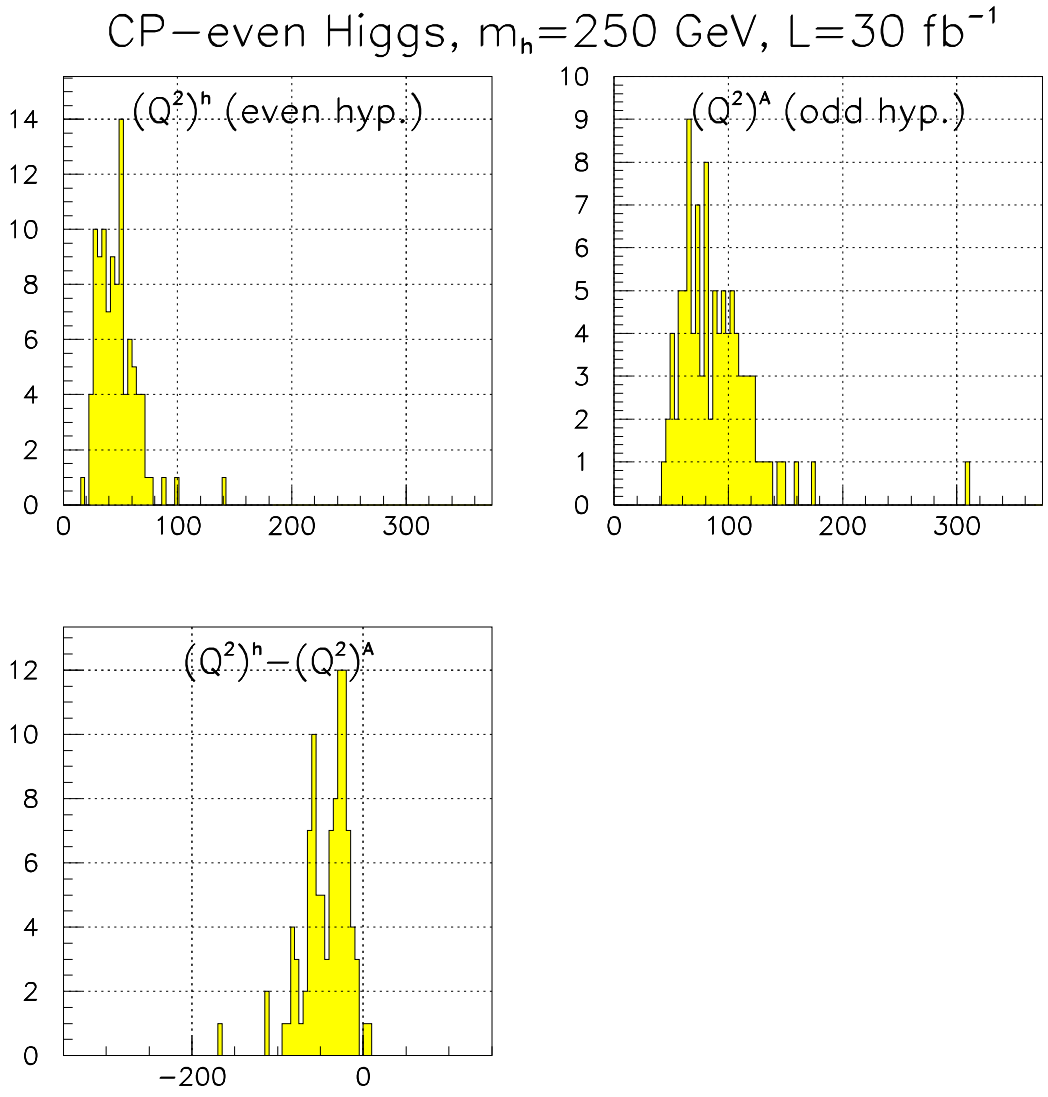

Figure 4.14: As figure 4.13, but with lower integrated luminosity, 30 fb^{-1}.

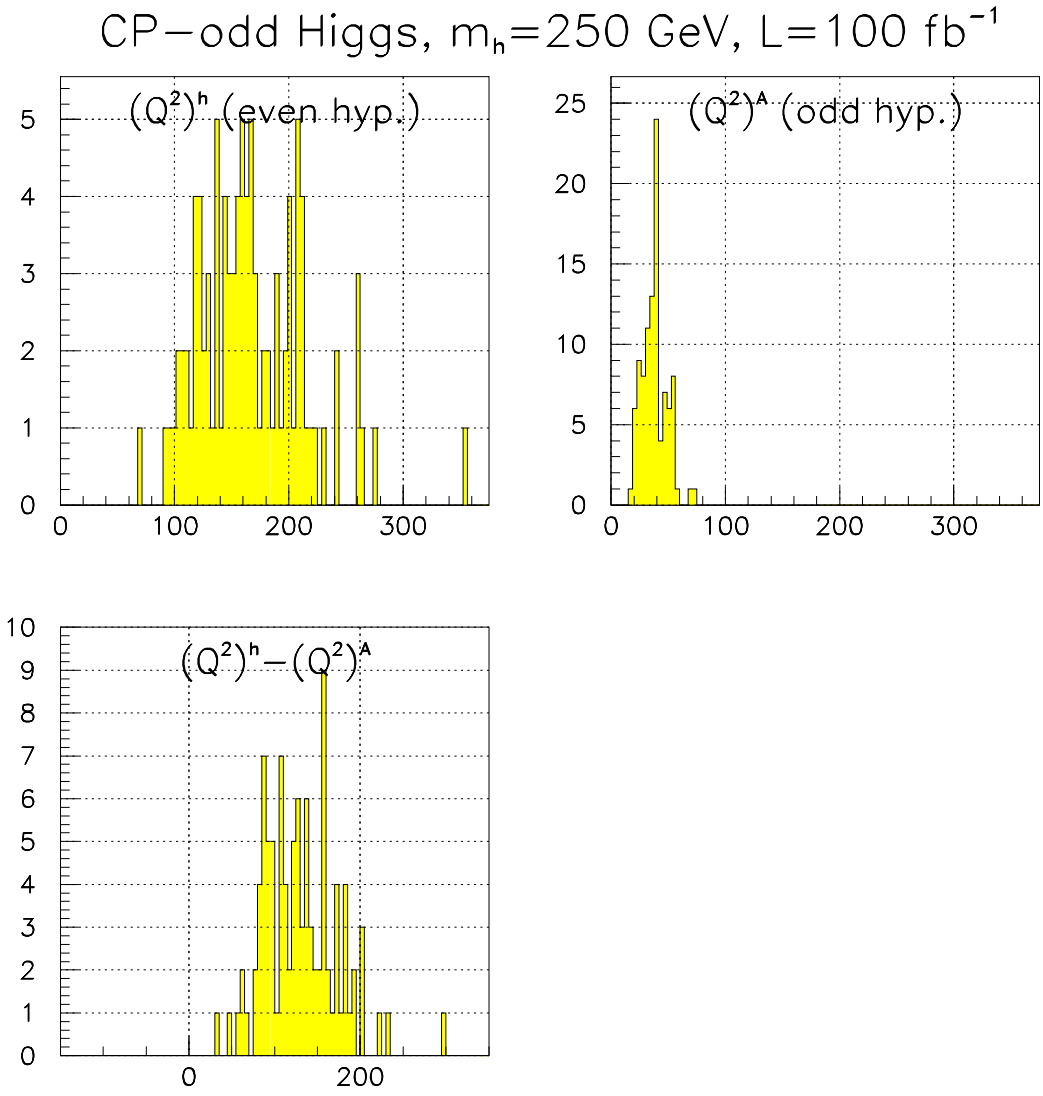

Figure 4.15: CP-odd Higgs boson with mass $m_h = 250$ GeV, integrated luminosity $\int \mathcal{L} dt = 100$ fb^{-1}. The sum $(Q^2)^a = \sum_{x=1}^{4} (Q^2)^a_x$ is shown for the CP-even hypothesis $a = h$ and for the CP-odd hypothesis $a = A$. The difference between the value of $(Q^2)^a$ for the two hypotheses, $(Q^2)^h - (Q^2)^A$, is also shown.

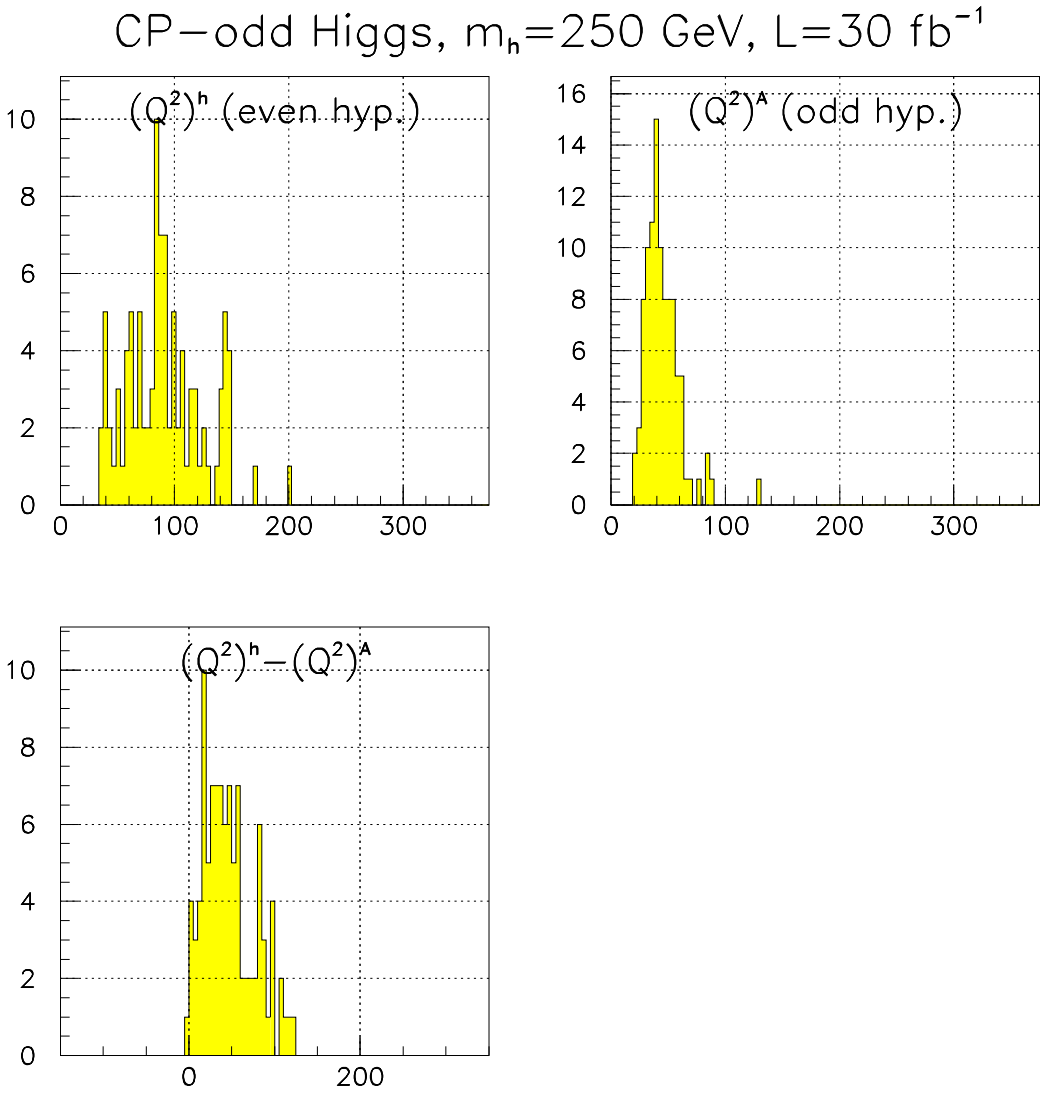

Figure 4.16: As figure 4.15, but with lower integrated luminosity, 30 fb^{-1}.

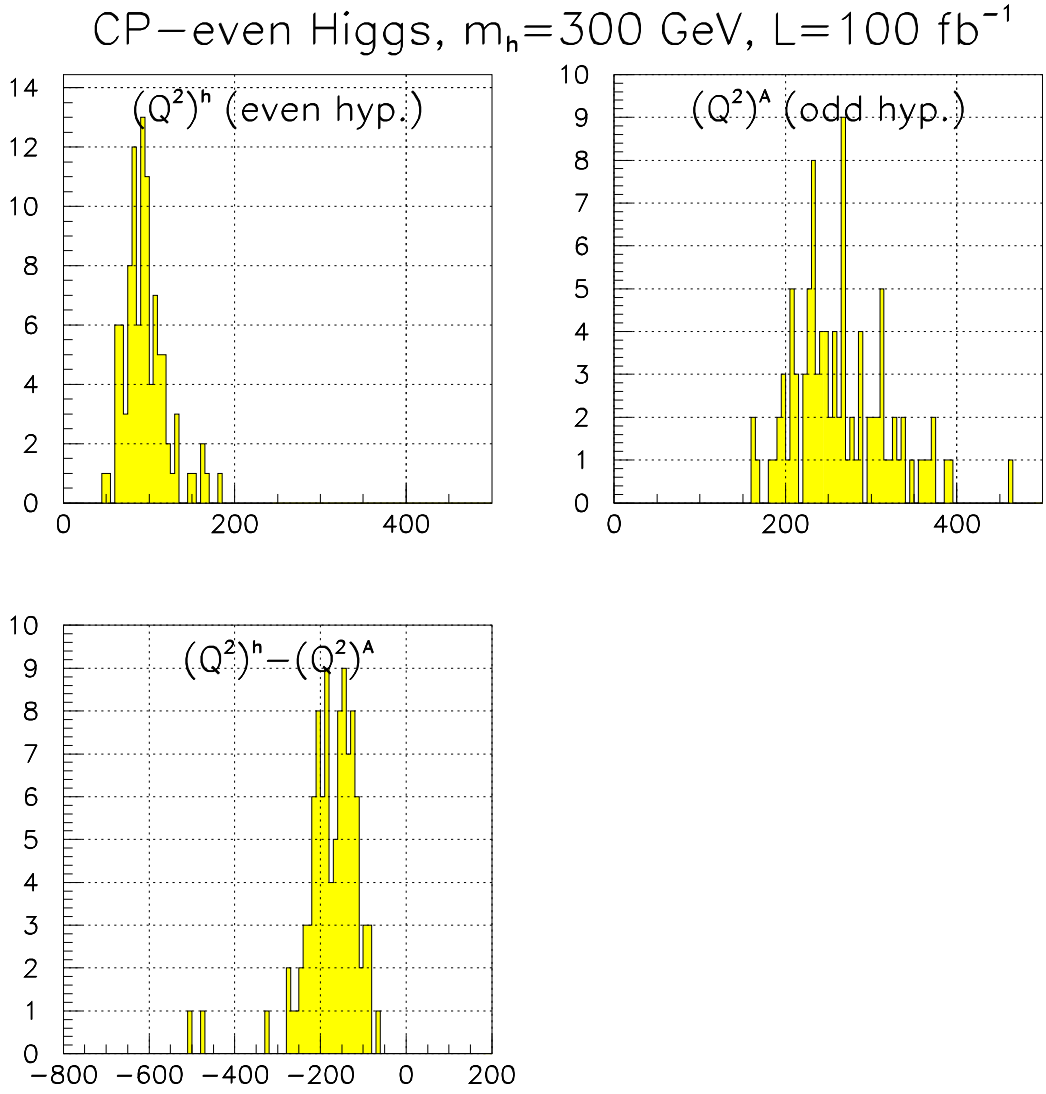

Figure 4.17: CP-even Higgs boson with mass $m_h = 300$ GeV, integrated luminosity $\int \mathcal{L} dt = 100$ fb^{-1}. The sum $(Q^2)^a = \sum_{x=1}^{4} (Q^2)^a_x$ is shown for the CP-even hypothesis $a = h$ and for the CP-odd hypothesis $a = A$. The difference between the value of $(Q^2)^a$ for the two hypotheses, $(Q^2)^h - (Q^2)^A$, is also shown.

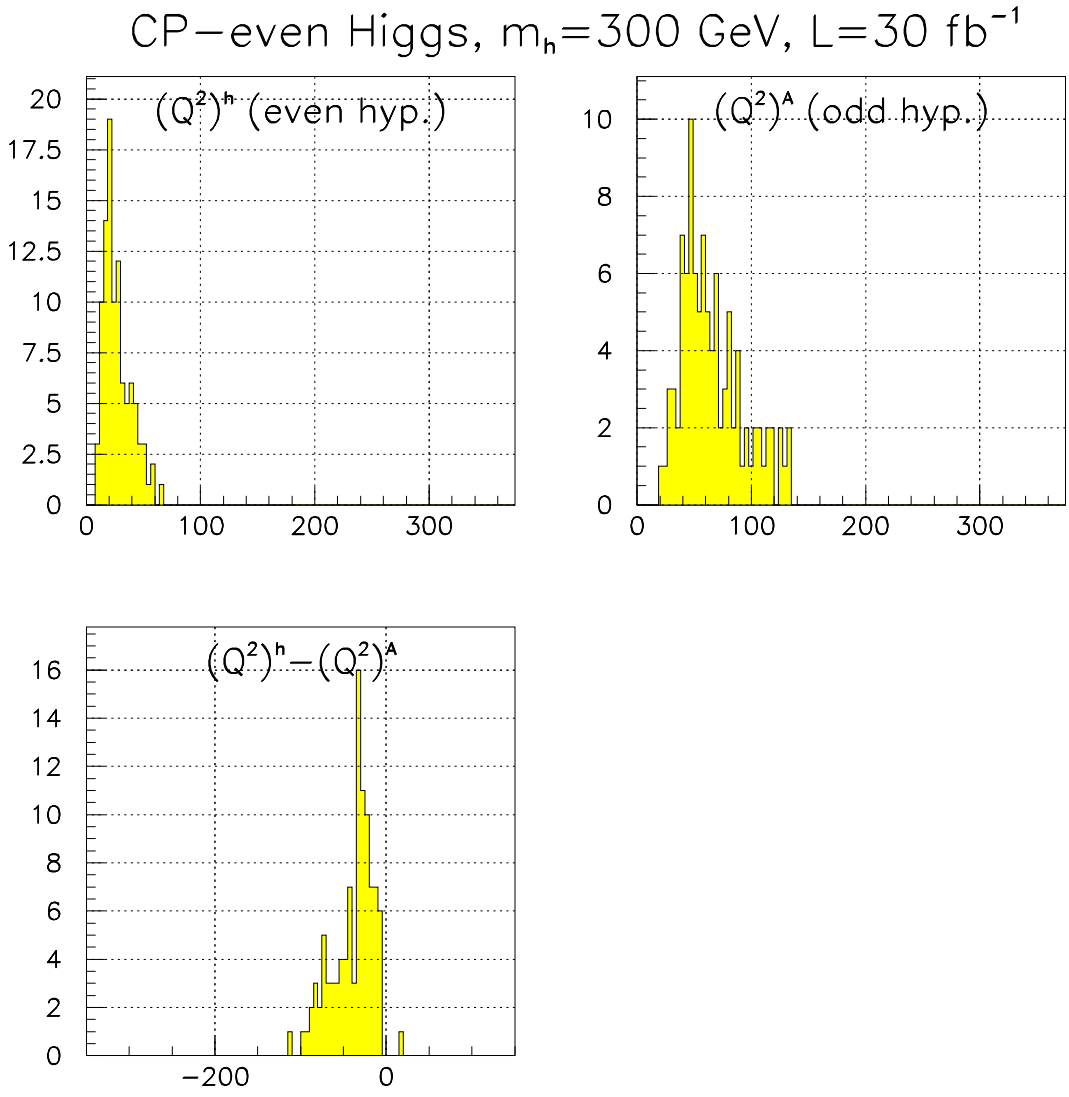

Figure 4.18: As figure 4.17, but with lower integrated luminosity, 30 fb^{-1}.

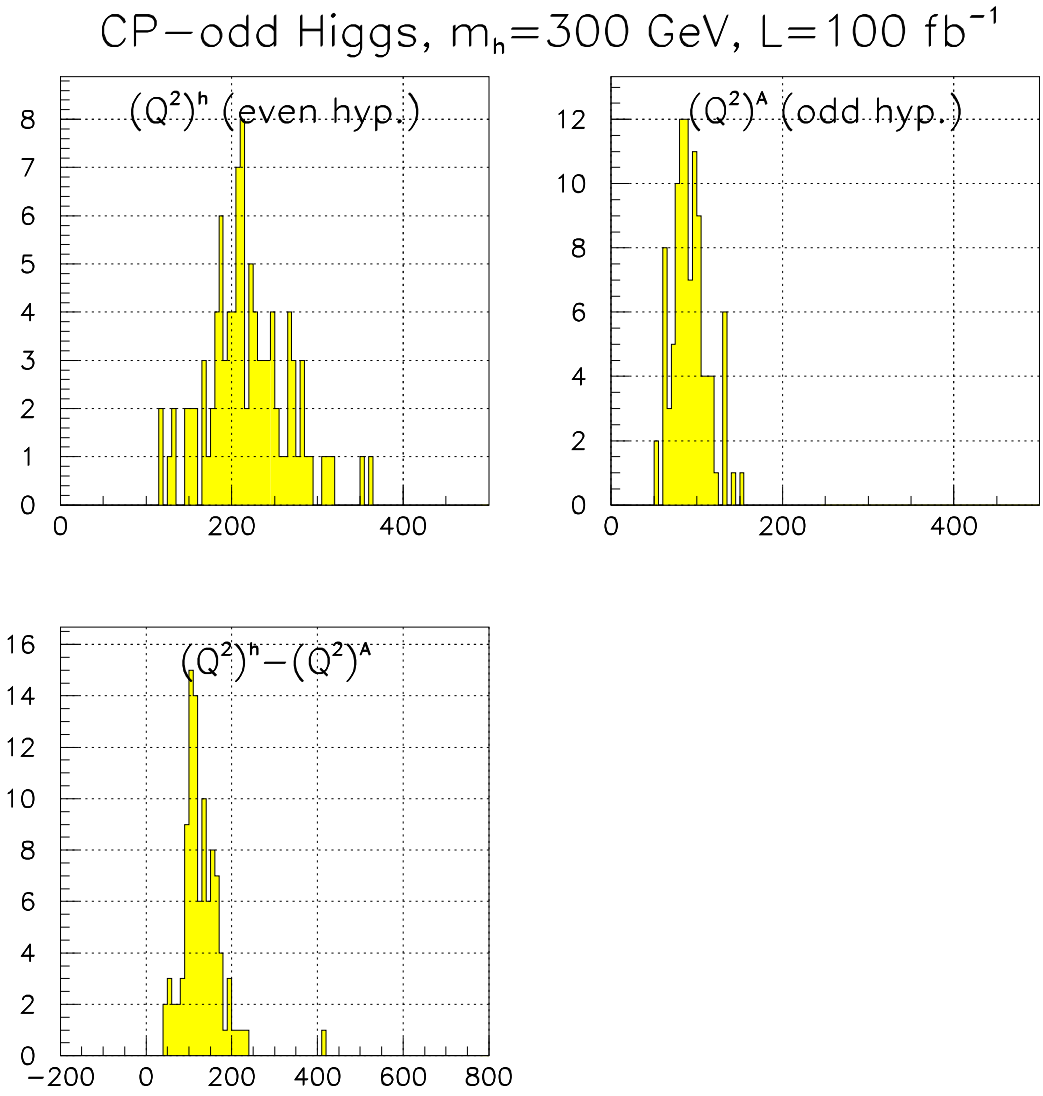

Figure 4.19: CP-odd Higgs boson with mass $m_h = 300$ GeV, integrated luminosity $\int \mathcal{L} dt = 100$ fb^{-1}. The sum $(Q^2)^a = \sum_{x=1}^{4} (Q^2)^a_x$ is shown for the CP-even hypothesis $a = h$ and for the CP-odd hypothesis $a = A$. The difference between the value of $(Q^2)^a$ for the two hypotheses, $(Q^2)^h - (Q^2)^A$, is also shown.

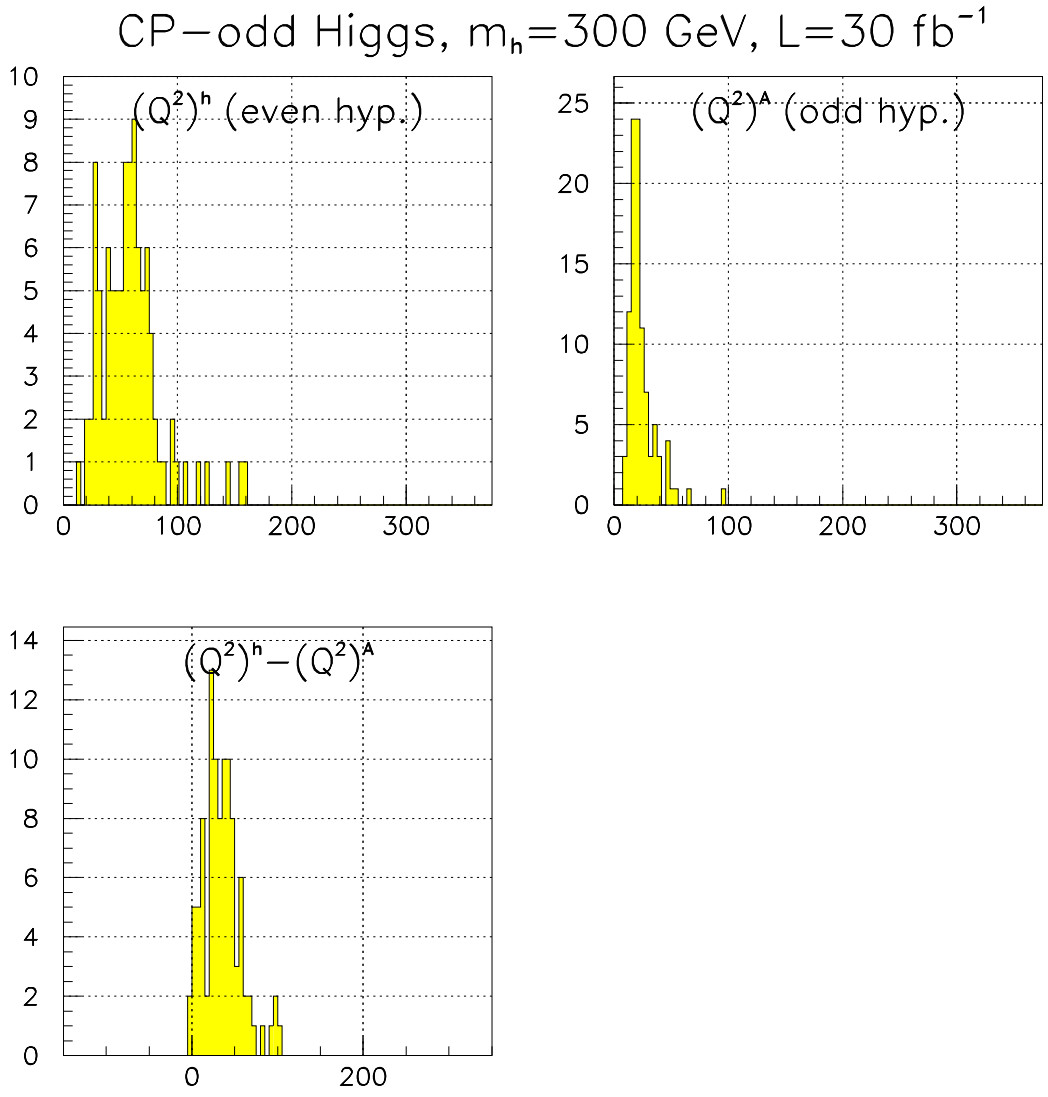

Figure 4.20: As figure 4.19, but with lower integrated luminosity, 30 fb^{-1}.

Chapter 5

Conclusions

In this thesis I have studied several angular correlations in the decay

$$H \to V_1 V_2 \to 4f\,, \tag{5.1}$$

which are sensitive to the CP-property of the Higgs boson H.

In chapter 3 the decay rate $\mathrm{d}\Gamma/\mathrm{d}\phi$ was calculated for the case of a CP-even and a CP-odd Higgs boson. These calculations have been performed before, and I confirmed the earlier obtained results [10]. We saw that the decay rate $\mathrm{d}\Gamma/\mathrm{d}\phi$ is independent of the Higgs mass for the CP-odd Higgs boson, and that it depends on the value of the Higgs mass for the CP-even Higgs boson. In the limit of a heavy Higgs boson, the correlation in ϕ disappears for the decay of the CP-even Higgs.

The distribution of $\mathrm{d}\Gamma/\mathrm{d}\phi$ also depends on whether the vector bosons V_1V_2 are W^+W^- or ZZ, and in the case of a ZZ pair, on the flavour of the two fermion-antifermion pairs.

We saw that the correlation was strongest for decay to a W^+W^- pair, and that the angle ϕ was almost uncorrelated for the decay

$$h \to ZZ \to 4l\,, \tag{5.2}$$

where $4l$ denotes two pairs of electrons (electron-positron) and/or muons.

In chapter 4, a Monte Carlo analysis of the sensitivity for several observables, to the CP-states of a Higgs boson at the LHC was performed, using the program PYTHIA. The analysis was performed for a simple model with at least two Higgs bosons, one CP-even and one CP-odd, which both have the same production rate as the SM Higgs boson. The decay rate for the Higgs bosons, in the channel (5.2), was also assumed to be identical to the standard model rate.

The dominant background channel for this decay mode is continuum ZZ production through quark-antiquark fusion. Unfortunately there is another important background channel which could not be simulated with PYTHIA. This channel is continuum ZZ production through gluon-gluon fusion. In the analysis I have assumed that the decay distributions are similar for the two background channels. This I conclude from the fact that the polarisations of the Z pairs produced via the two channels are similar.

The decay distributions I studied, have been suggested earlier as sensitive to the CP-property of the Higgs boson [9–14]. I studied the polar decay angles in the decays of the Z bosons, in the rest frames of the Z bosons, and the relative azimuthal angle between the decay planes of the two decays $Z \to l^+l^-$. This last angle is uniquely related to the angle ϕ defined in chapter 3.

In addition I defined an observable which combines the information in the three other angles. This is the angle between the momenta of the two negatively charged leptons, where the momenta are defined in the rest frames of the corresponding Z boson.[1]

I found that the CP-state of a pure CP-even or CP-odd Higgs boson can be measured at the LHC, provided that the production and decay rates are at least as large as the rates of the SM Higgs boson, and that the Higgs mass is above the threshold for decay into two real Z bosons. For a Higgs boson with mass $m_h = 200$ GeV, which seems to be the most probable of the three values I have studied, an integrated luminosity of 100 fb^{-1} would be necessary. This corresponds to a few years of running with high luminosity at the LHC.

For a Higgs mass of $m_h = 250$ GeV or larger, the CP-state can be measured already for an integrated luminosity of 30 fb^{-1}, which probably will be reached after the first few years of running with medium luminosity at the LHC.

These are the results for a Higgs boson which is purely CP-even or CP-odd, and which has a fairly large decay rate to weak vector bosons.

What are the possibilities to measure the CP-property of a Higgs boson for a more general model? Provided that the mixing between Higgs bosons of different CP-states is large, so that it is easy to measure, that the mixing does not reduce the decay rate of the lightest Higgs boson to weak vector bosons too much, and that the coupling constant η for the CP-odd decay to vector bosons by some mechanism is not too small, the CP-even and CP-odd components of a mixed Higgs boson can probably be measured in this channel. It is also necessary, of course, that the Higgs boson is sufficiently heavy to decay into two real Z bosons.

The experimental data at present makes a Higgs boson lighter than 200 GeV most probable. Still, a Higgs boson with mass $m_h \geq 180$ GeV is not experimentally excluded, and until this is the case, it it would be wise to explore how to study the properties of a Higgs boson also in this mass range.

It would be interesting to perform Monte Carlo analyses for the decay mode (5.2), given a more realistic CP-violating model, like MSSM with explicit CP-violation [6]. There might also be other observables for this decay than the ones I have studied, which are worth examining, for instance the energy weighted decay rate introduced in [10]. In order to get a better estimate of the background distributions, it would be necessary to study the distributions of decay angles for ZZ continuum production through gluon-gluon fusion. The effect of CP-violation and mixing of states on the effective coupling constant η for a CP-odd decay of a (mixed) Higgs boson into a pair of weak vector bosons, would also have to be calculated.

It is important to identify and study observables which are sensitive to the CP-properties

[1] This observable was suggested by T. Sjöstrand.

of a Higgs boson with mass above $2m_Z$, at the LHC. If such a Higgs boson is discovered, it will not be enough to confirm that it is mainly CP-even or CP-odd. We should also try to determine how large a possible mixing is. This might be examined through decay correlations such as the ones studied in this thesis.

We do not know what coming experiments will reveal about the sector of electroweak symmetry breaking, but it is likely to change our view of the fundamental interactions in nature, and to give rise to new puzzles which will be for the next generation of physicists to unravel. This has always been the way physics has developed, and it will most certainly be so also for the future.

Appendix A

Angular Correlations

This appendix contains plots similar to figures 4.3–4.7, but for the Higgs masses $m_h = 250\,\text{GeV}$ and $m_h = 300\,\text{GeV}$. The plots show distributions of the observables $\cos\theta_1^*$, $\cos\theta_3^*$, ϕ_{13}^*, $\cos\theta_{13}^*$ and $\cos\theta_{ZH}^*$, before and after kinematic cuts. For a discussion of the observables and the distributions, see subsection 4.3.2.

A.1 Higgs boson with mass 250 GeV

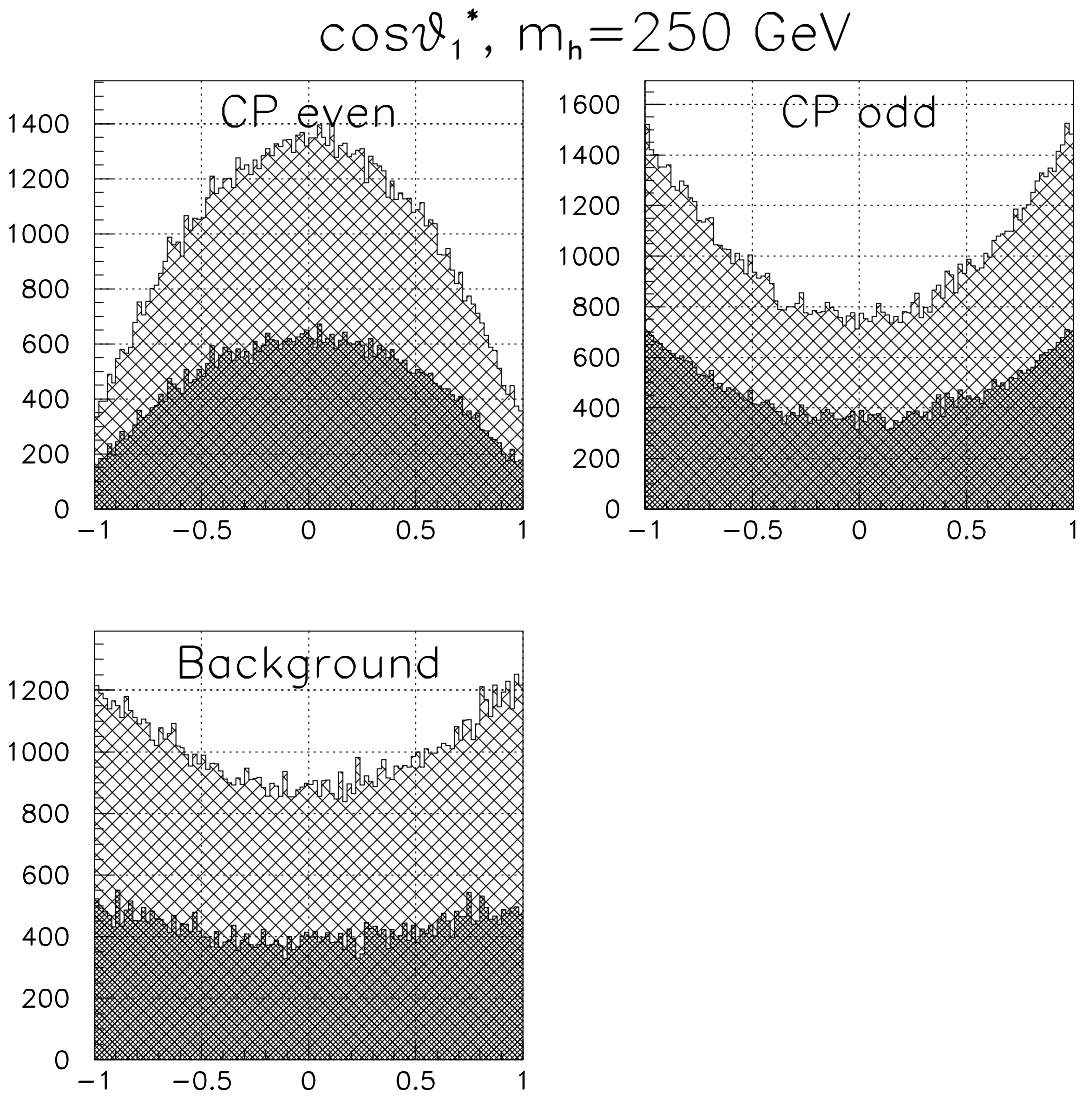

Figure A.1: Higgs mass $m_h = 250$ GeV. The distribution of $\cos\theta_1^*$, for a CP-even and a CP-odd Higgs, and for background events ($q\bar{q} \to ZZ \to 4l$), before (light) and after (dark) kinematic cuts. For the background the distribution after cuts is multiplied by a factor 20, compared to the distribution before cuts.

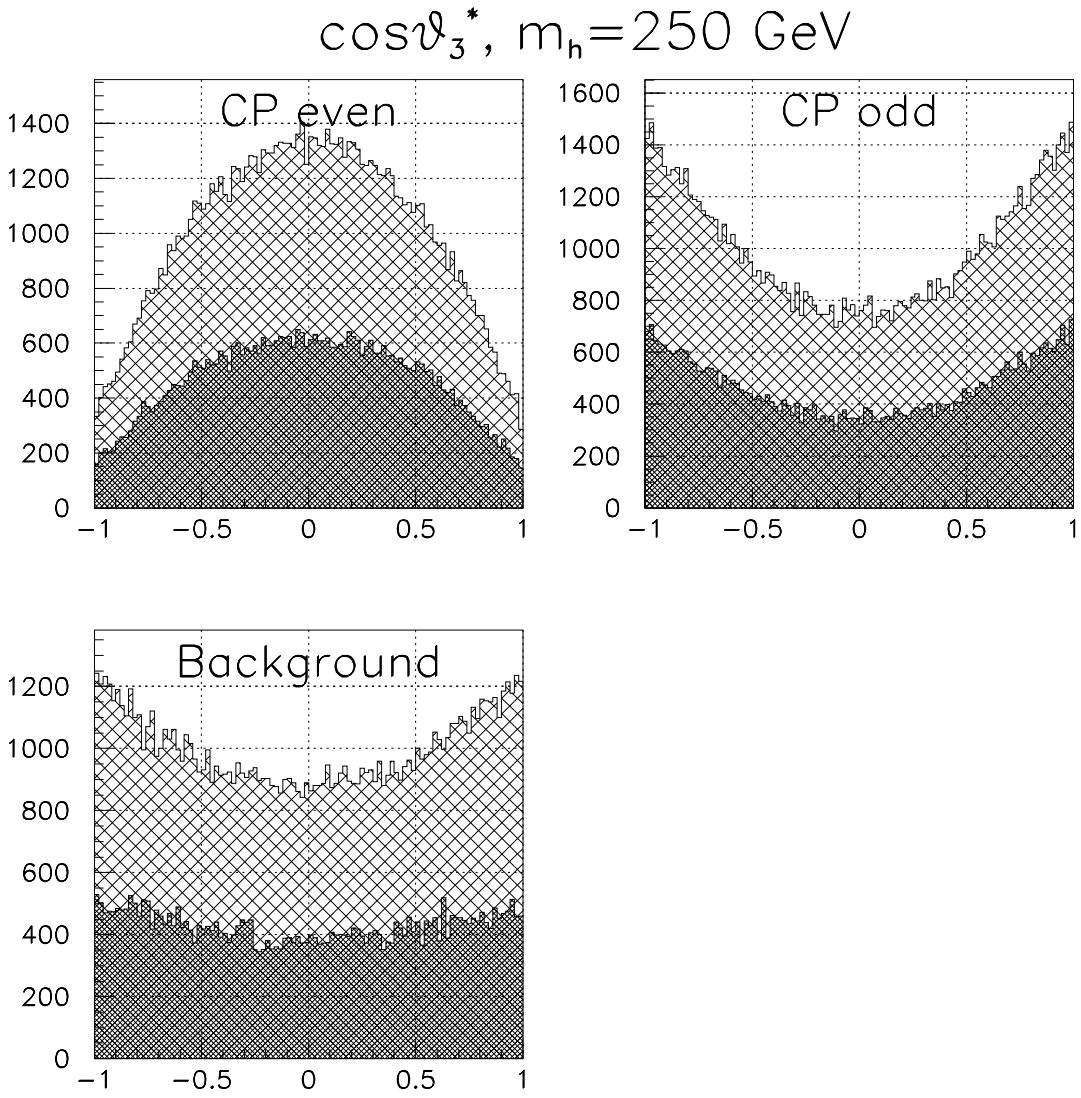

Figure A.2: Higgs mass $m_h = 250$ GeV. The distribution of $\cos\theta_3^*$, for a CP-even and a CP-odd Higgs, and for background events ($q\bar{q} \to ZZ \to 4l$), before (light) and after (dark) kinematic cuts. For the background the distribution after cuts is multiplied by a factor 20, compared to the distribution before cuts.

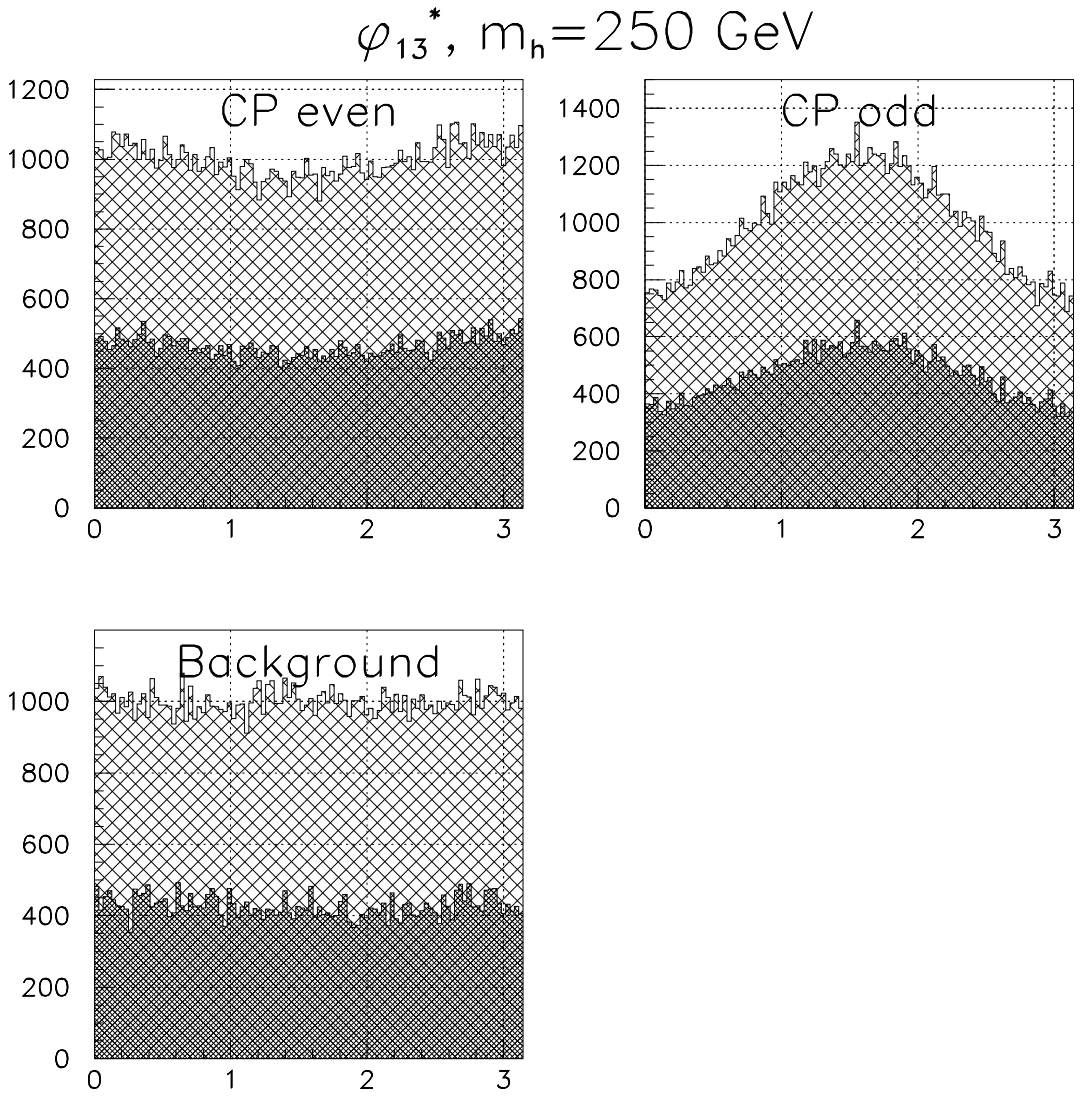

Figure A.3: Higgs mass $m_h = 250$ GeV. The distribution of ϕ^*_{13}, for a CP-even and a CP-odd Higgs, and for background events ($q\bar{q} \to ZZ \to 4l$), before (light) and after (dark) kinematic cuts. For the background the distribution after cuts is multiplied by a factor 20, compared to the distribution before cuts.

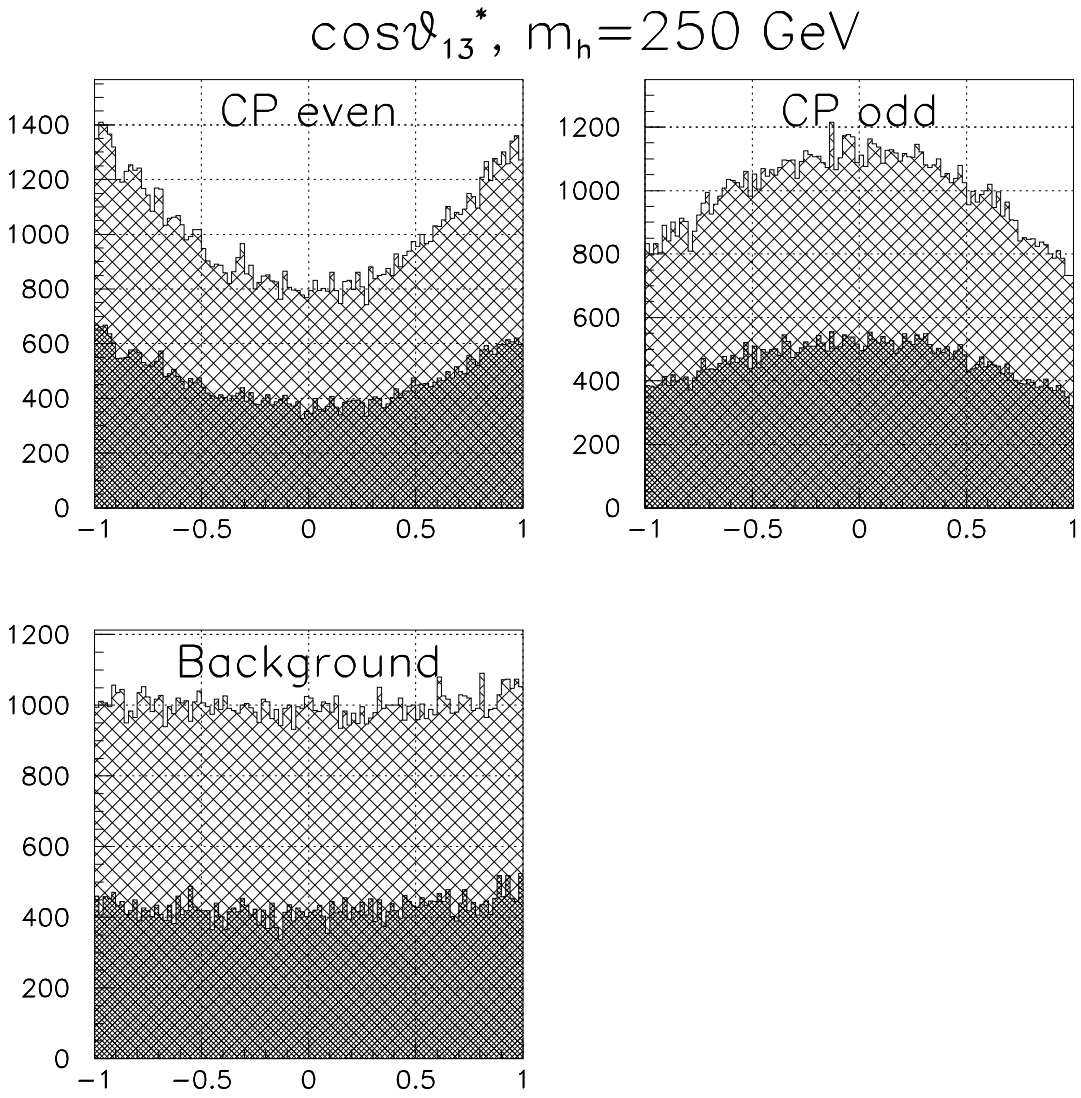

Figure A.4: Higgs mass $m_h = 250$ GeV. The distribution of $\cos\theta^*_{13}$, for a CP-even and a CP-odd Higgs, and for background events ($q\bar{q} \to ZZ \to 4l$), before (light) and after (dark) kinematic cuts. For the background the distribution after cuts is multiplied by a factor 20, compared to the distribution before cuts.

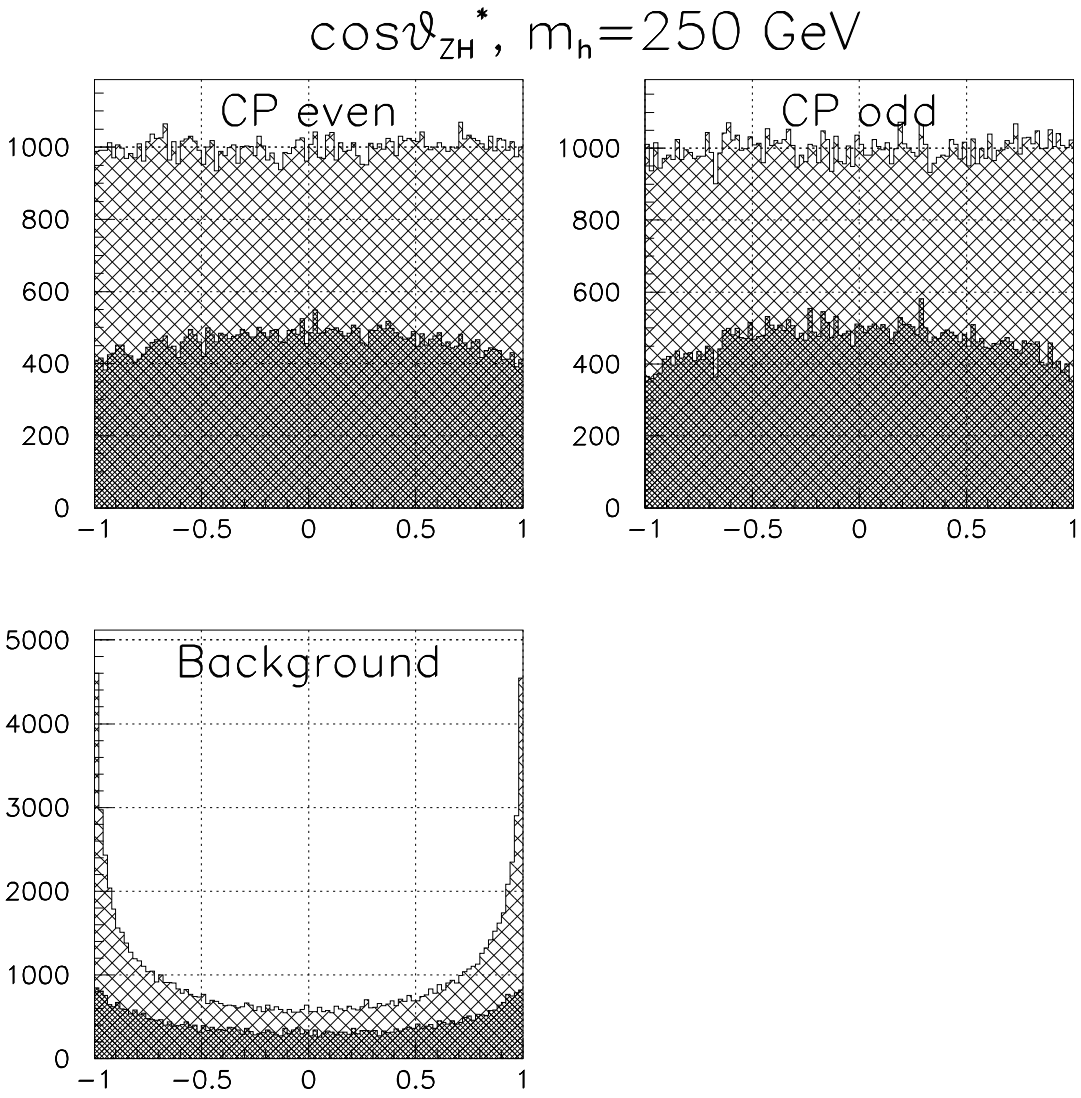

Figure A.5: Higgs mass $m_h = 250$ GeV. The distribution of $\cos\theta^*_{ZH}$, for a CP-even and a CP-odd Higgs, and for background events ($q\bar{q} \to ZZ \to 4l$), before (light) and after (dark) kinematic cuts. For the background the distribution after cuts is multiplied by a factor 20, compared to the distribution before cuts.

A.2 Higgs boson with mass 300 GeV

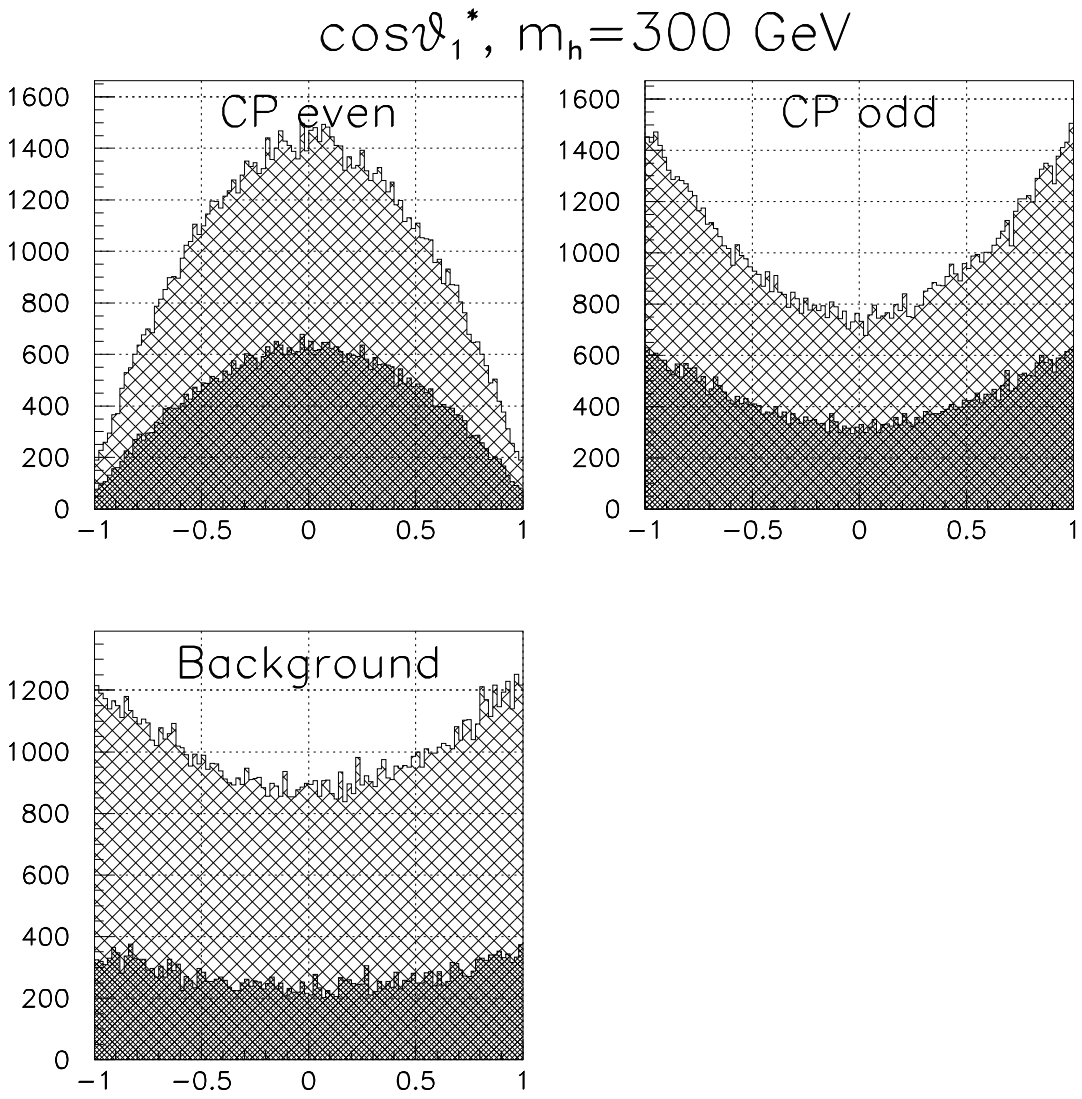

Figure A.6: Higgs mass $m_h = 300$ GeV. The distribution of $\cos\theta_1^*$, for a CP-even and a CP-odd Higgs, and for background events ($q\bar{q} \to ZZ \to 4l$), before (light) and after (dark) kinematic cuts. For the background the distribution after cuts is multiplied by a factor 20, compared to the distribution before cuts.

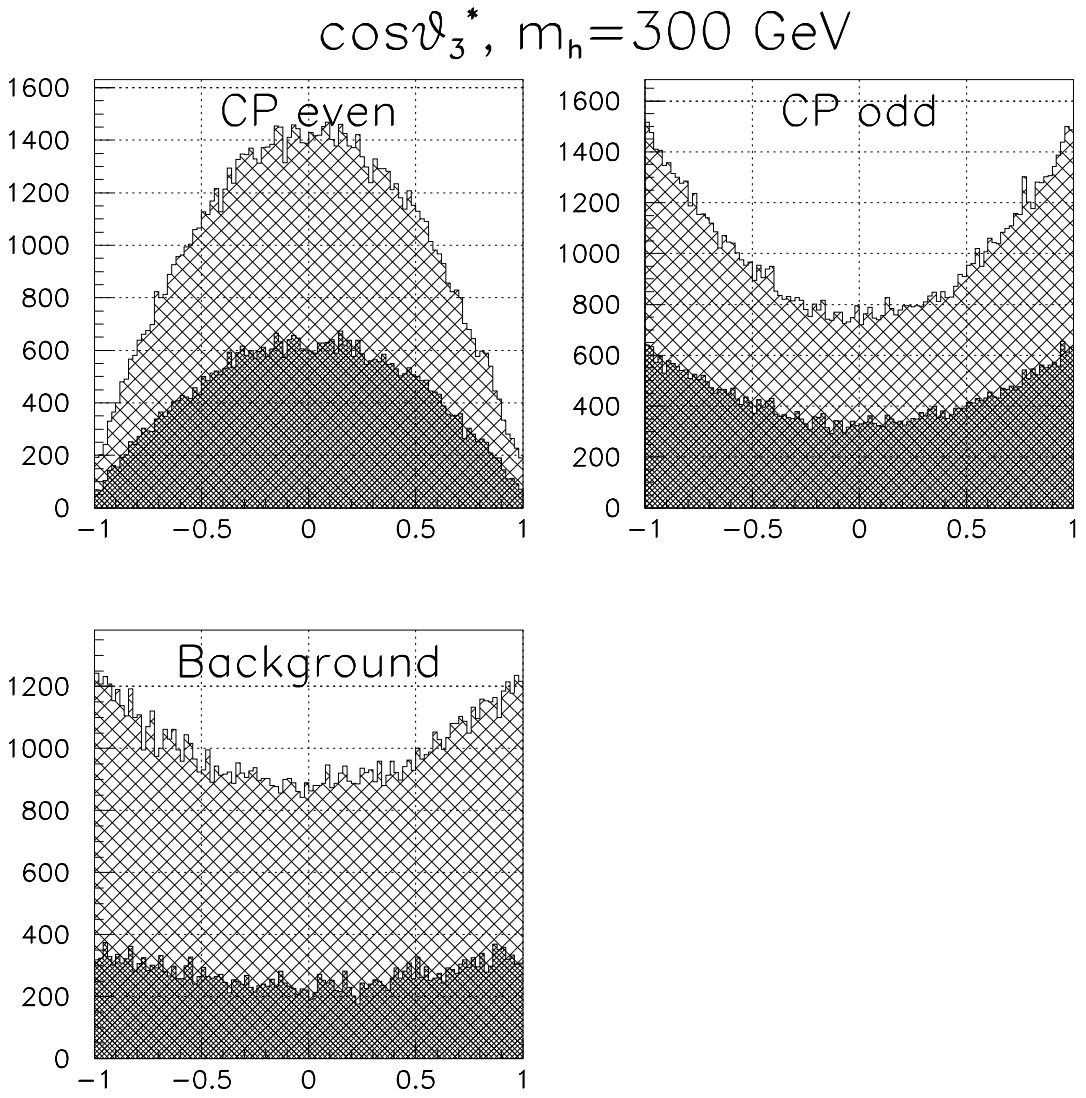

Figure A.7: Higgs mass $m_h = 300$ GeV. The distribution of $\cos\theta_3^*$, for a CP-even and a CP-odd Higgs, and for background events ($q\bar{q} \to ZZ \to 4l$), before (light) and after (dark) kinematic cuts. For the background the distribution after cuts is multiplied by a factor 20, compared to the distribution before cuts.

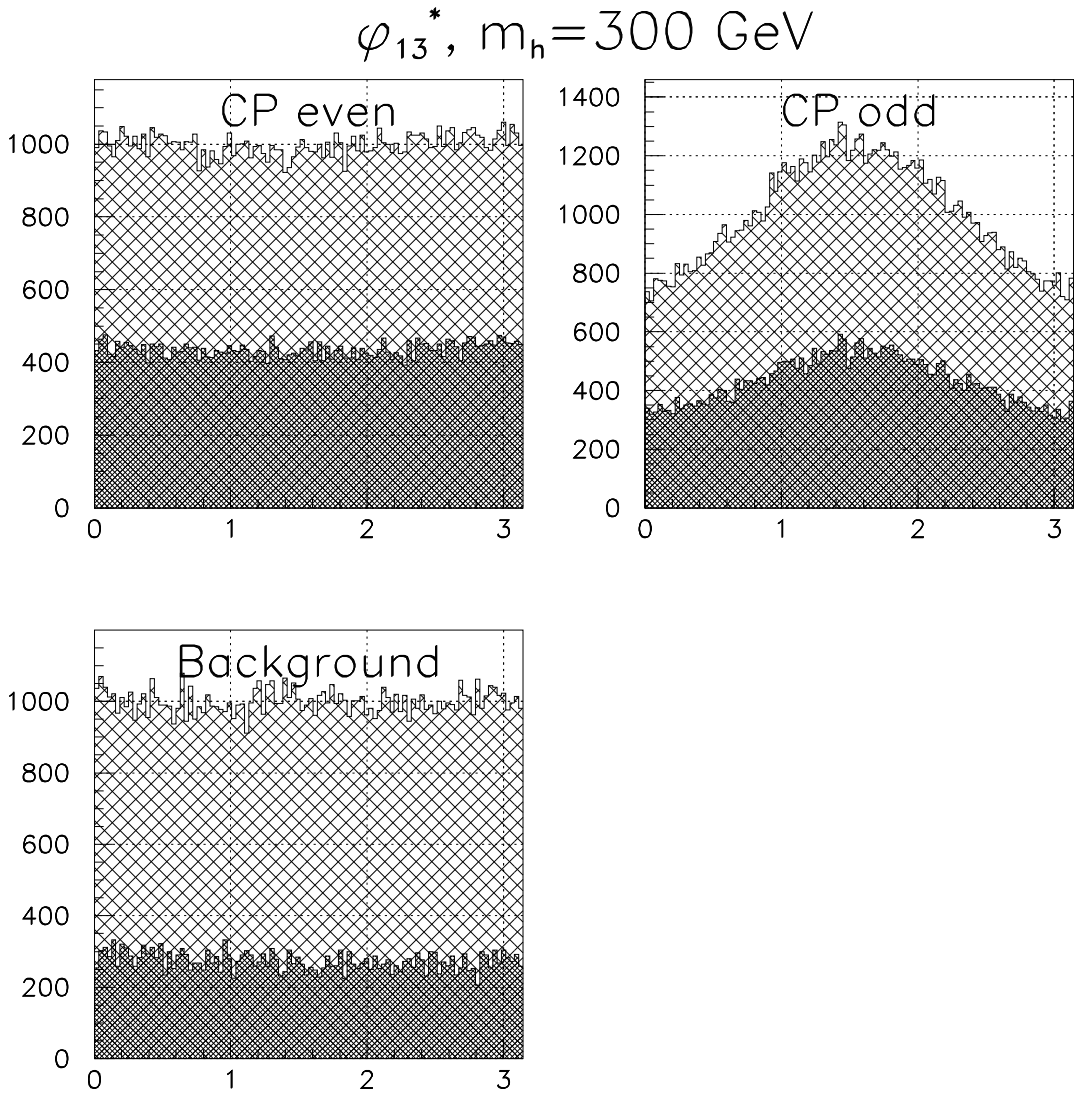

Figure A.8: Higgs mass $m_h = 300$ GeV. The distribution of ϕ_{13}^*, for a CP-even and a CP-odd Higgs, and for background events ($q\bar{q} \to ZZ \to 4l$), before (light) and after (dark) kinematic cuts. For the background the distribution after cuts is multiplied by a factor 20, compared to the distribution before cuts.

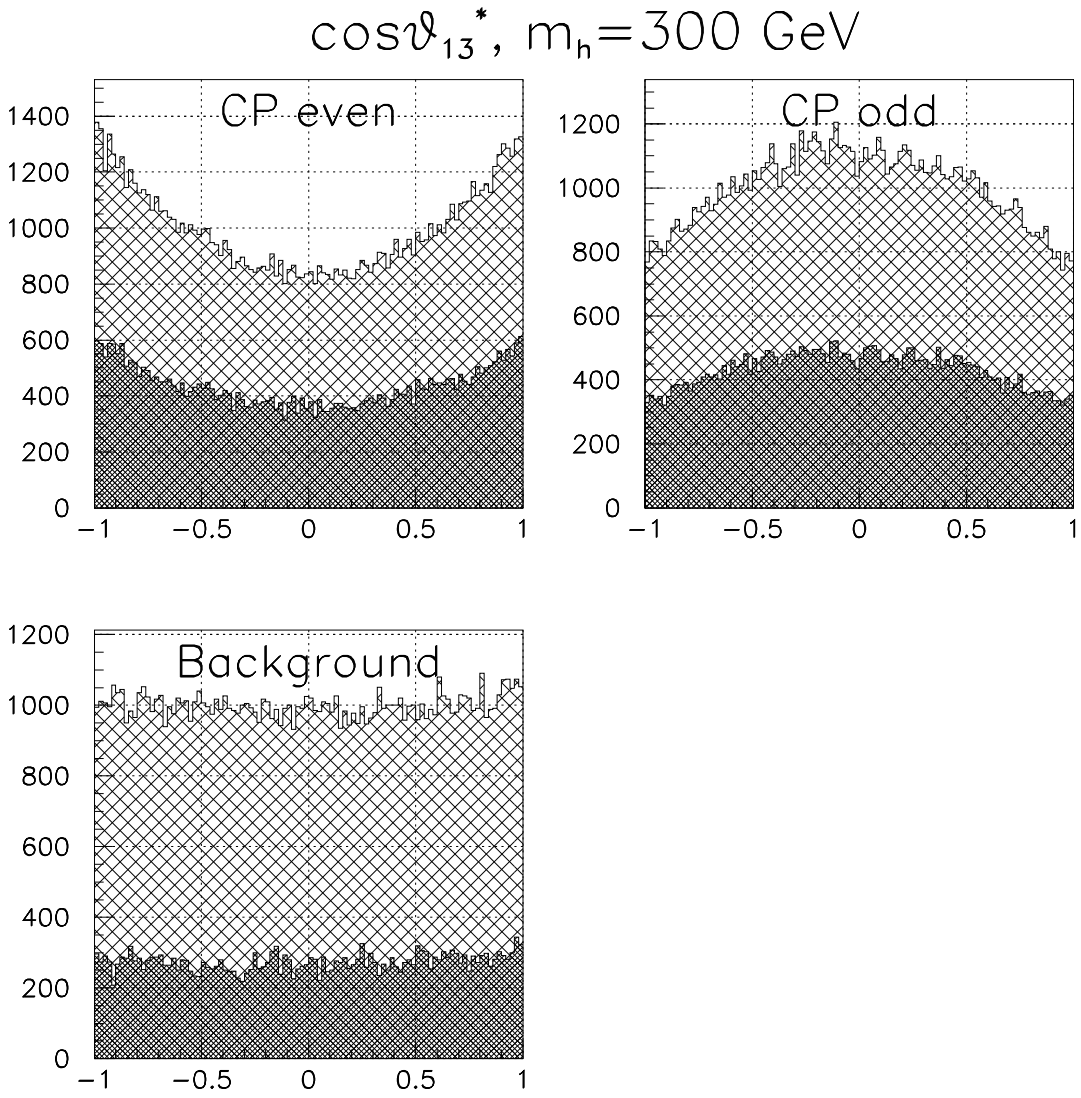

Figure A.9: Higgs mass $m_h = 300$ GeV. The distribution of $\cos\theta^*_{13}$, for a CP-even and a CP-odd Higgs, and for background events ($q\bar{q} \to ZZ \to 4l$), before (light) and after (dark) kinematic cuts. For the background the distribution after cuts is multiplied by a factor 20, compared to the distribution before cuts.

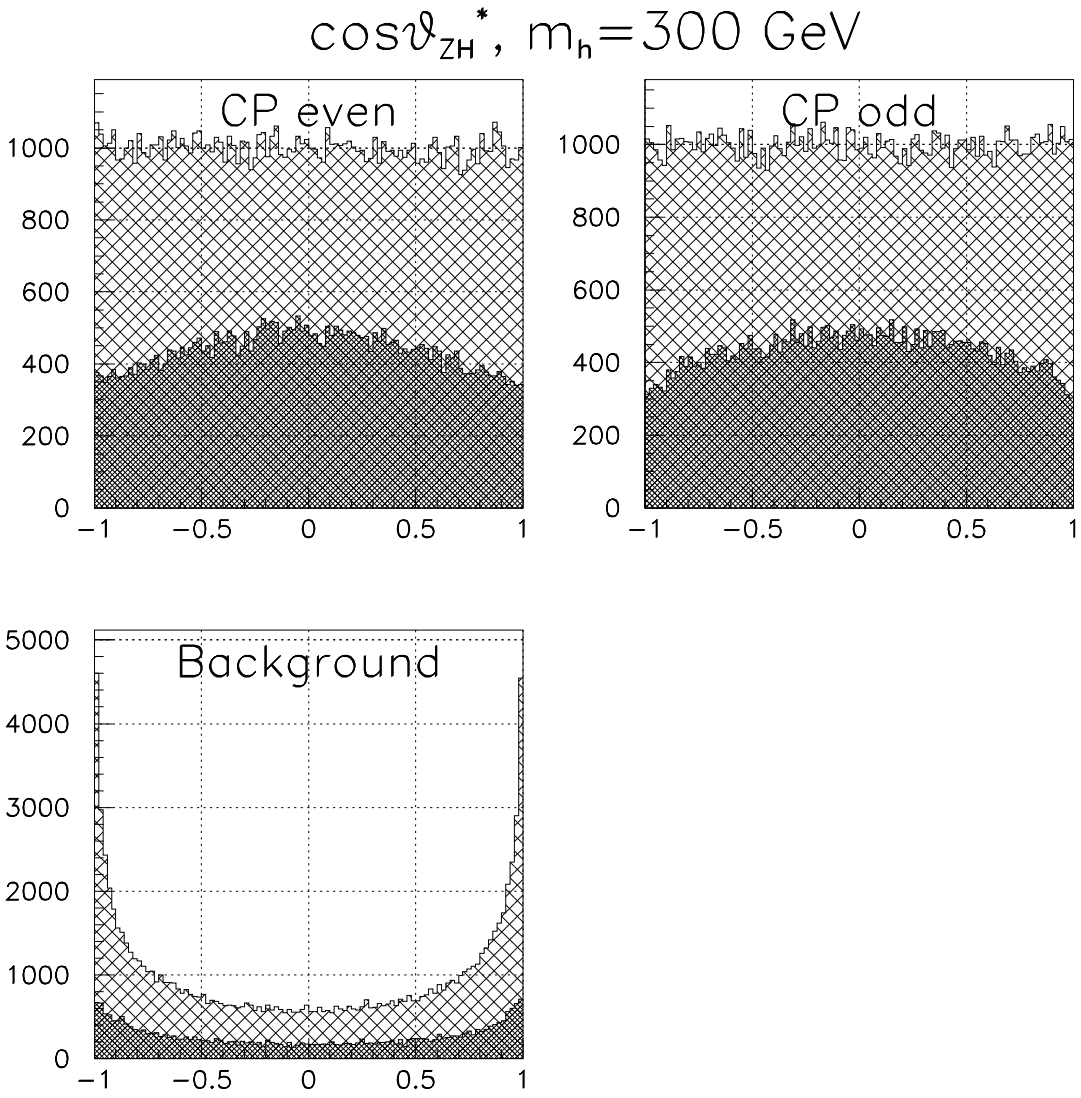

Figure A.10: Higgs mass $m_h = 300$ GeV. The distribution of $\cos\theta^*_{ZH}$, for a CP-even and a CP-odd Higgs, and for background events ($q\bar{q} \to ZZ \to 4l$), before (light) and after (dark) kinematic cuts. For the background the distribution after cuts is multiplied by a factor 20, compared to the distribution before cuts.

Appendix B

Statistical Results

This appendix contains most of the plots from the statistical analysis in chapter 4. For a discussion of the results, see section 4.5. The appendix is divided into three sections, one for each value of the Higgs mass, $m_h = 200$ GeV, $m_h = 250$ GeV and $m_h = 300$ GeV.

The plots show the distributions of $(Q^2)^a_x$, given by (4.26) on page 78, for several observables x and for the two different hypotheses CP-even Higgs, $a = h$, and CP-odd Higgs, $a = A$.

For each value of the Higgs mass, the results are given for two different values of the integrated luminosity, and for either CP-even or CP-odd Higgs bosons simulated in the experiments.

From the following figures, one can see that the amount of information in the simulated experiments depends on the luminosity in an obvious way: when the luminosity decreases, the amount of information also decreases.

The dependence on the Higgs mass of the different observables is as follows: for the lowest Higgs mass considered, 200 GeV, the four observables $\cos\theta_1^*$, $\cos\theta_3^*$, ϕ_{13}^* and $\cos\theta_{13}^*$ have about the same sensitivity to the CP of the Higgs. For higher values of the Higgs mass, 250 and 300 GeV, the sensitivity of $\cos\theta_1^*$ and $\cos\theta_3^*$ increases, whereas the sensitivity of ϕ_{13}^* and $\cos\theta_{13}^*$ decreases.

B.1 Higgs boson with mass 200 GeV

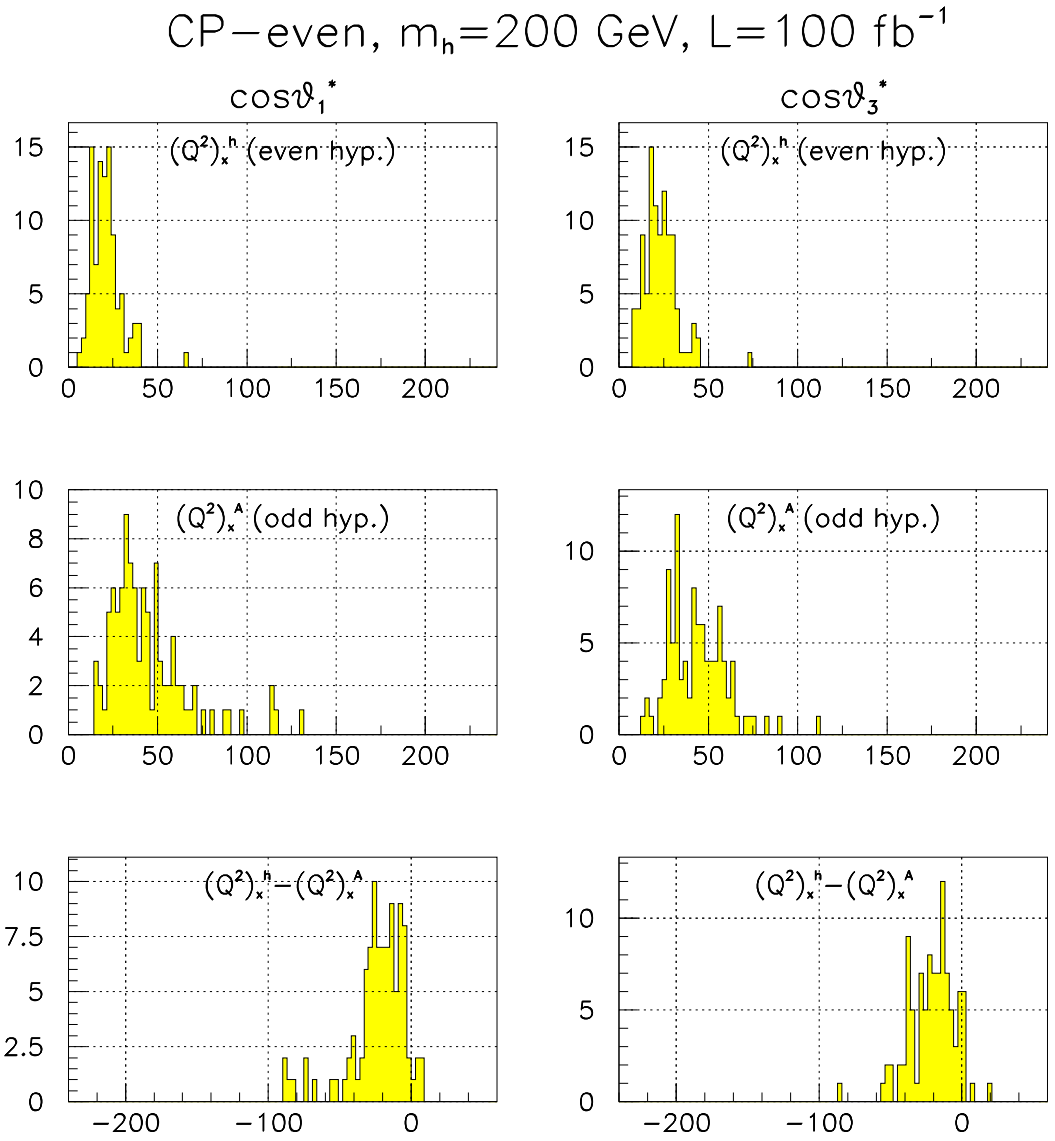

Figure B.1: The observables $\cos\theta_1^*$ and $\cos\theta_3^*$. CP-even Higgs boson with mass $m_h = 200$ GeV, integrated luminosity $\int \mathcal{L} dt = 100$ fb^{-1}. The histogram of $(Q^2)_x^a$ is shown for the CP-even hypothesis $a = h$ and for the CP-odd hypothesis $a = A$. The difference between the values of $(Q^2)_x^a$ for the two hypotheses, $(Q^2)_x^h - (Q^2)_x^A$, is also shown. Here x refers to the observable $\cos\theta_1^*$ or $\cos\theta_3^*$.

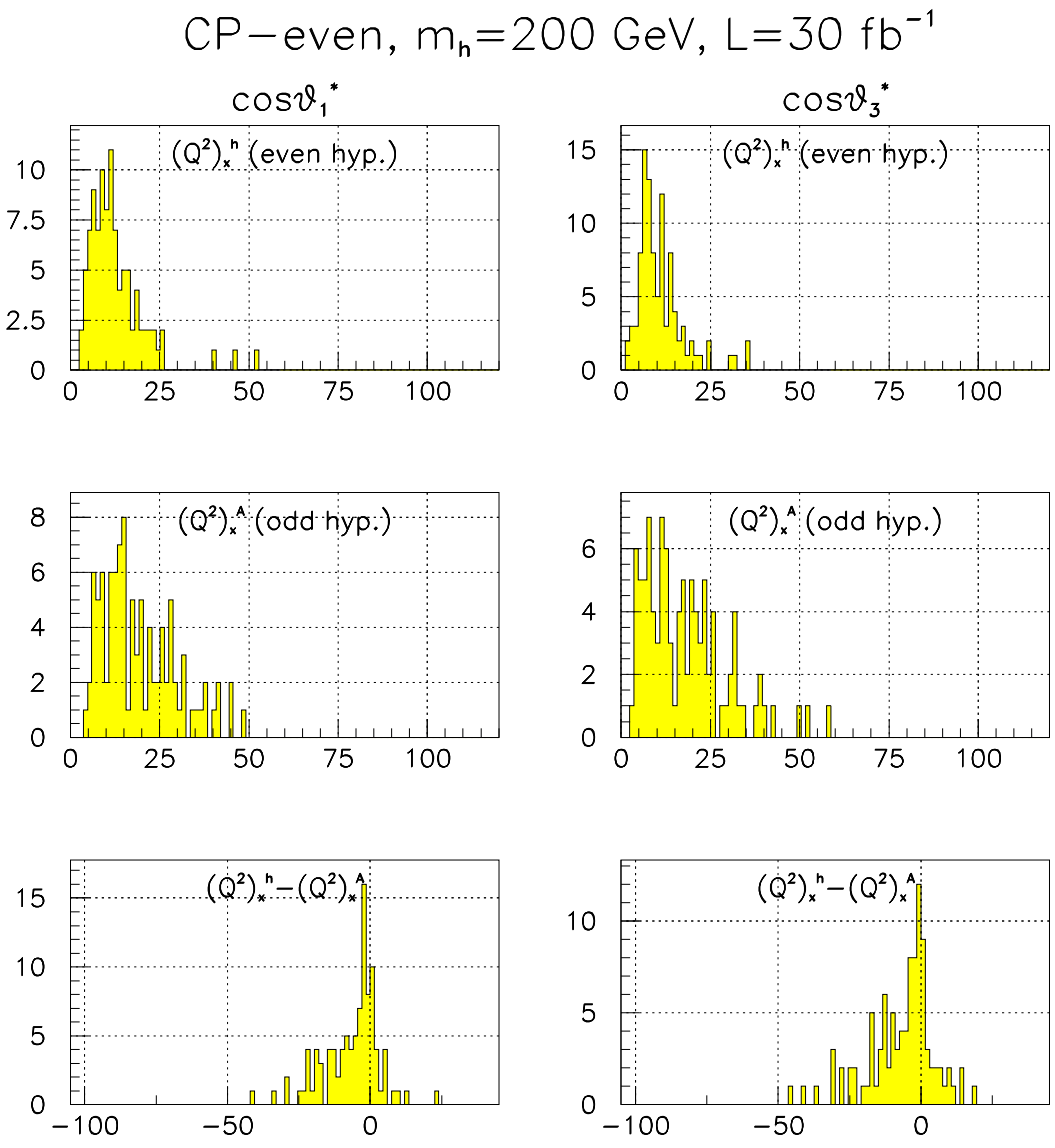

Figure B.2: Same as figure B.1, but for a lower integrated luminosity, 30 fb^{-1}.

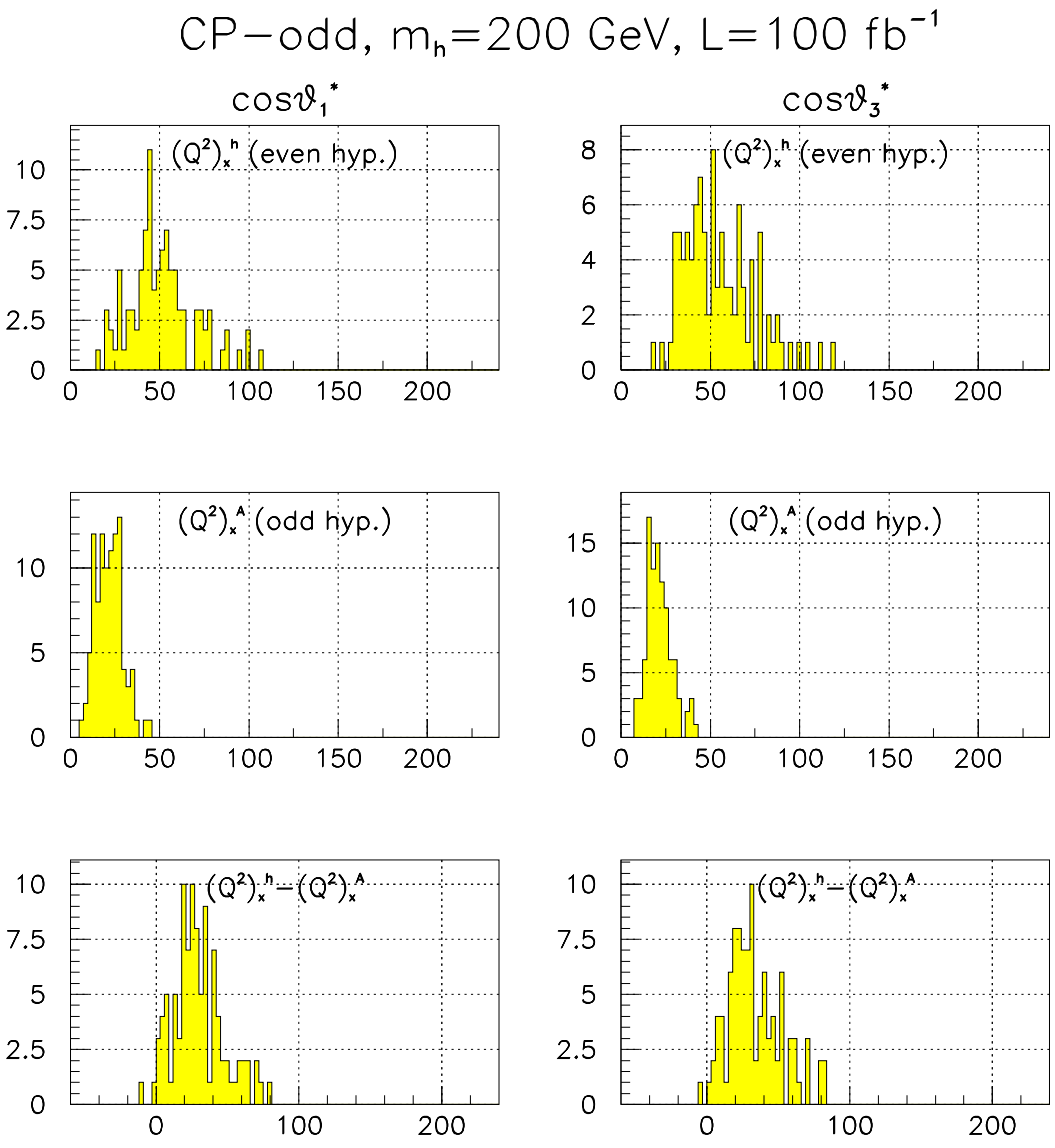

Figure B.3: The observables $\cos\theta_1^*$ and $\cos\theta_3^*$. CP-odd Higgs boson with mass $m_h = 200$ GeV, integrated luminosity $\int \mathcal{L} dt = 100$ fb^{-1}. The histogram of $(Q^2)_x^a$ is shown for the CP-even hypothesis $a = h$ and for the CP-odd hypothesis $a = A$. The difference between the values of $(Q^2)_x^a$ for the two hypotheses, $(Q^2)_x^h - (Q^2)_x^A$, is also shown. Here x refers to the observable $\cos\theta_1^*$ or $\cos\theta_3^*$.

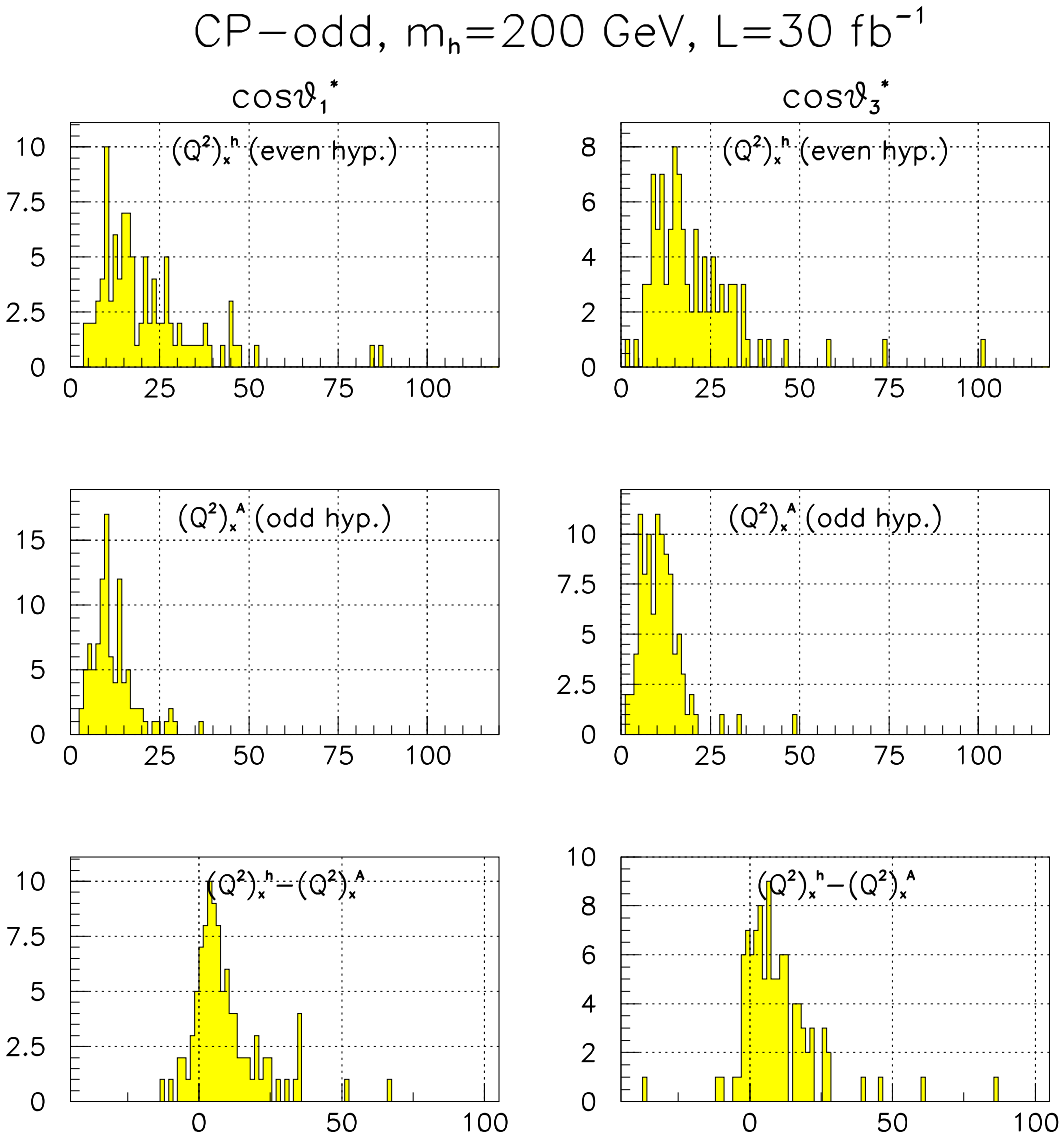

Figure B.4: Same as figure B.3, but for a lower integrated luminosity, 30 fb^{-1}.

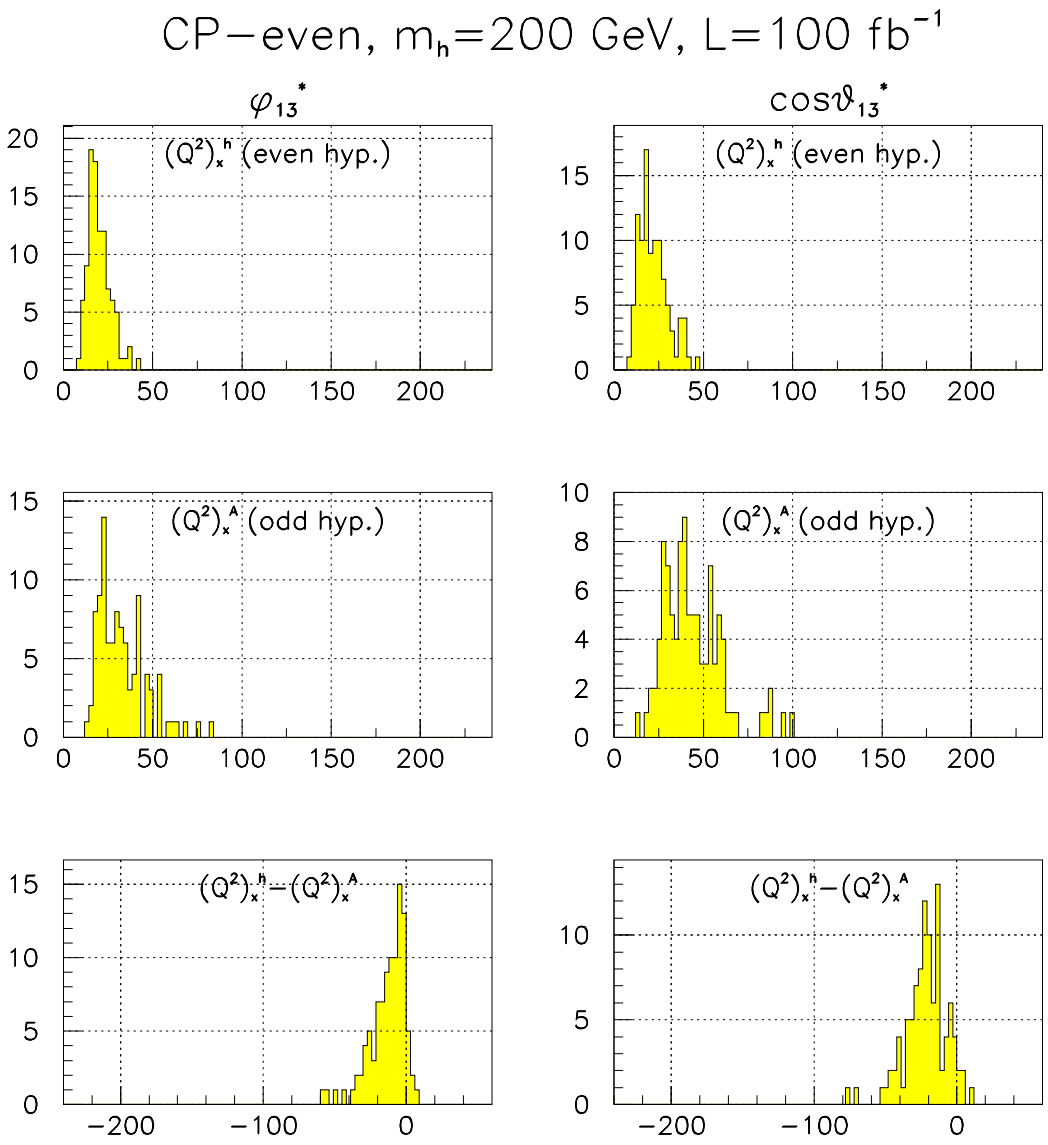

Figure B.5: The observables ϕ^*_{13} and $\cos\theta^*_{13}$. CP-even Higgs boson with mass $m_h = 200$ GeV, integrated luminosity $\int \mathcal{L} dt = 100$ fb^{-1}. The histogram of $(Q^2)^a_x$ is shown for the CP-even hypothesis $a = h$ and for the CP-odd hypothesis $a = A$. The difference between the values of $(Q^2)^a_x$ for the two hypotheses, $(Q^2)^h_x - (Q^2)^A_x$, is also shown. Here x refers to the observable ϕ^*_{13} or $\cos\theta^*_{13}$.

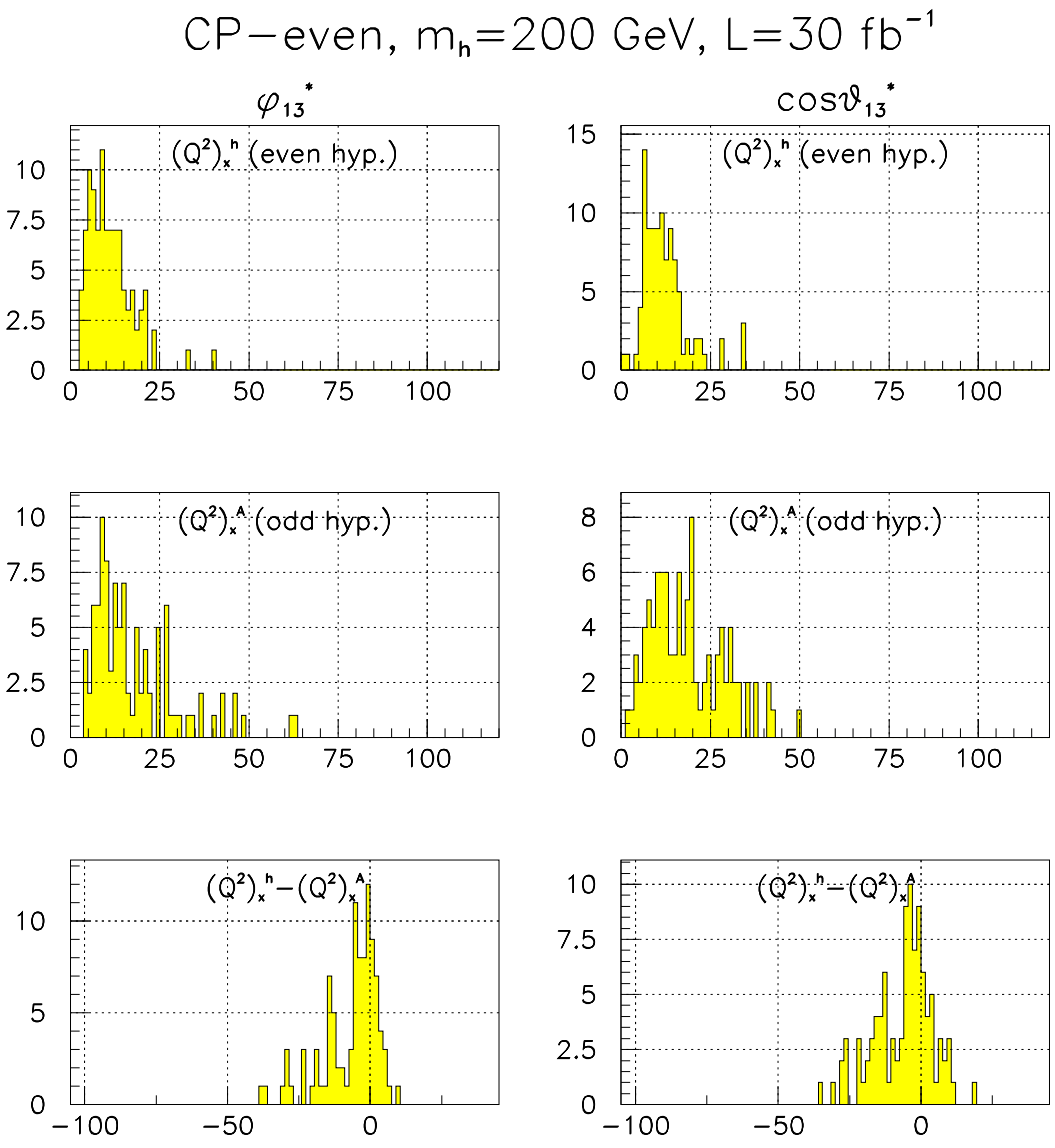

Figure B.6: Same as figure B.5, but for a lower integrated luminosity, 30 fb^{-1}.

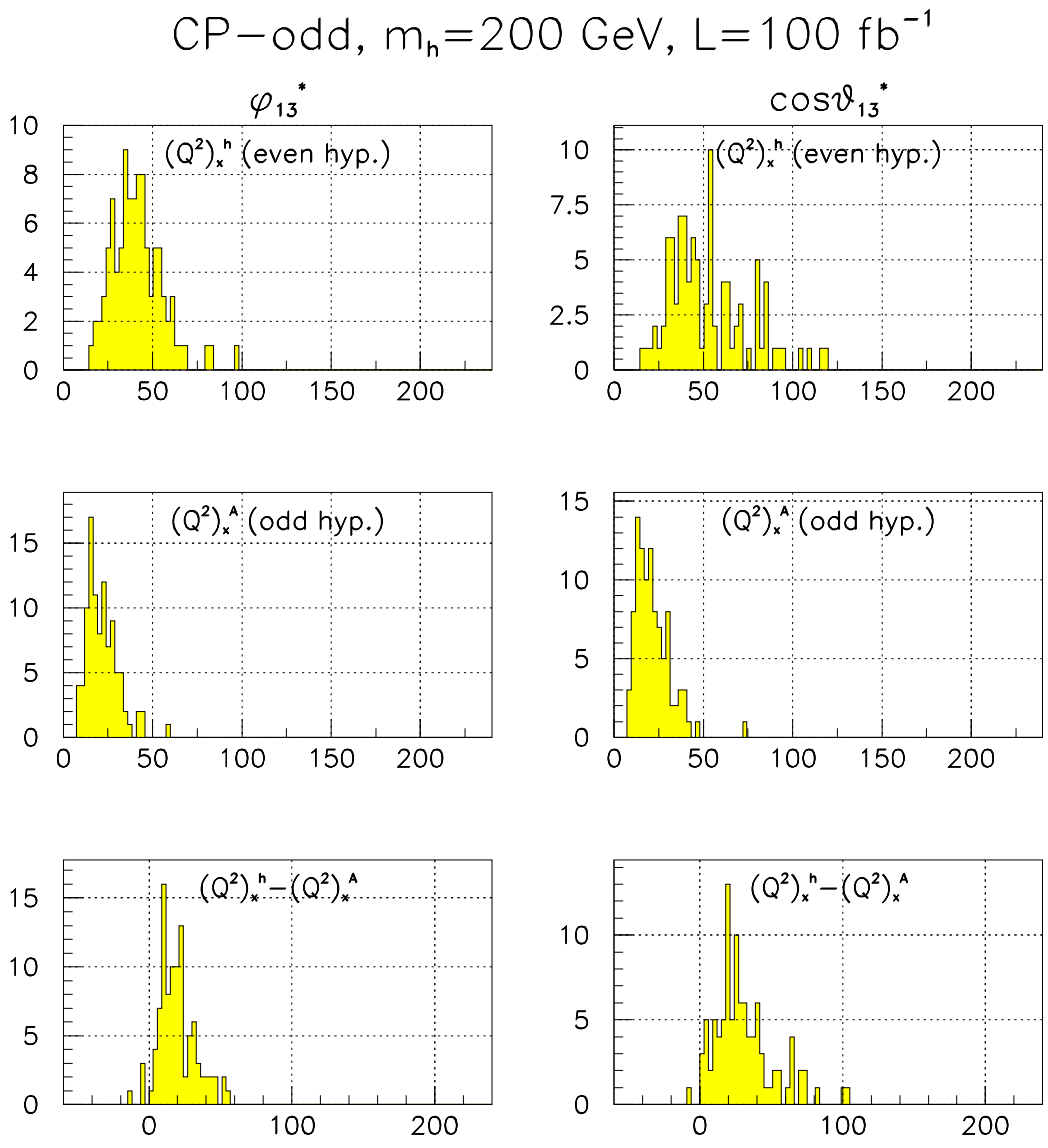

Figure B.7: The observables ϕ^*_{13} and $\cos\theta^*_{13}$. CP-odd Higgs boson with mass $m_h = 200$ GeV, integrated luminosity $\int \mathcal{L} dt = 100$ fb^{-1}. The histogram of $(Q^2)^a_x$ is shown for the CP-even hypothesis $a = h$ and for the CP-odd hypothesis $a = A$. The difference between the values of $(Q^2)^a_x$ for the two hypotheses, $(Q^2)^h_x - (Q^2)^A_x$, is also shown. Here x refers to the observable ϕ^*_{13} or $\cos\theta^*_{13}$.

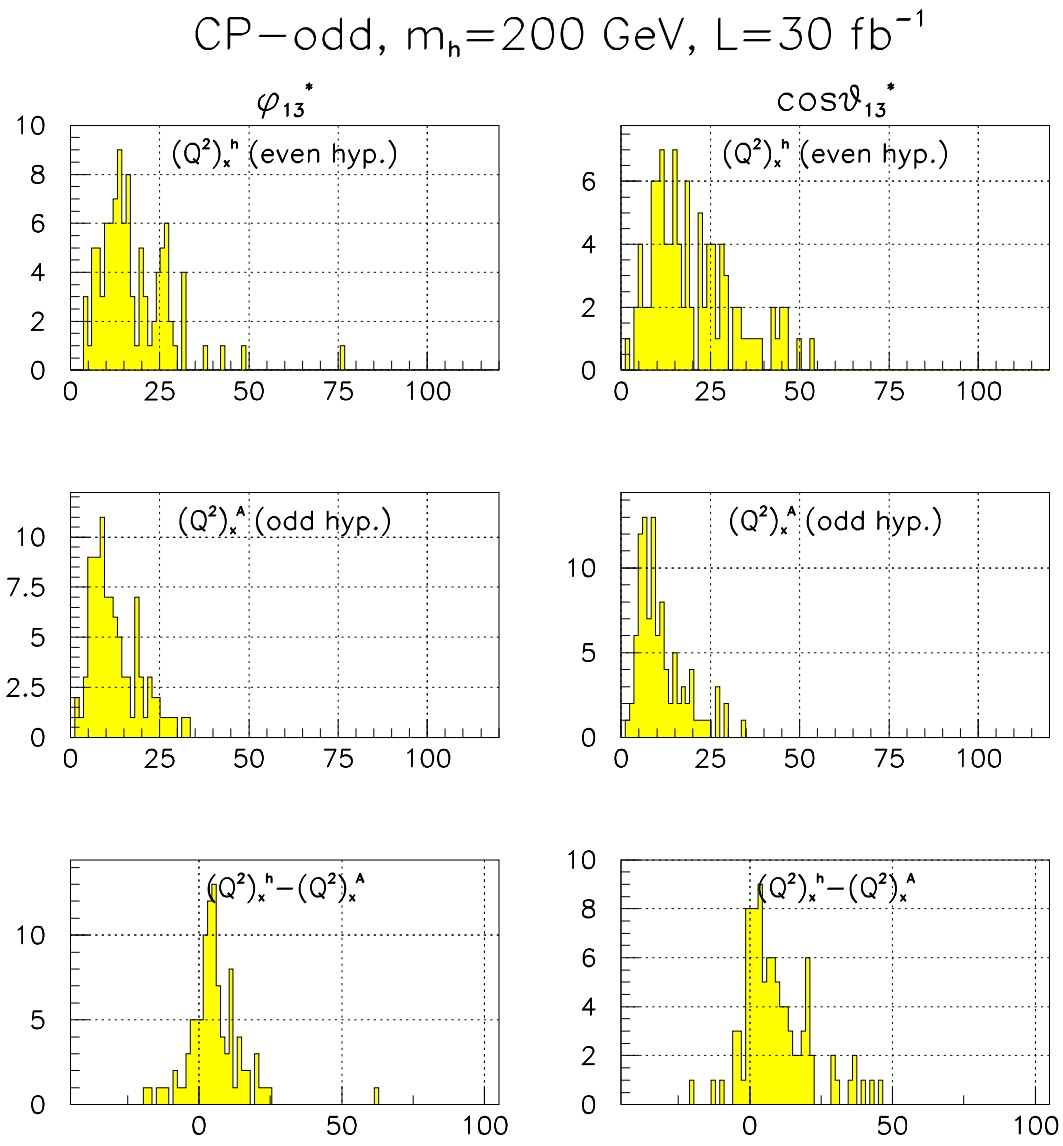

Figure B.8: Same as figure B.7, but for a lower integrated luminosity, 30 fb^{-1}.

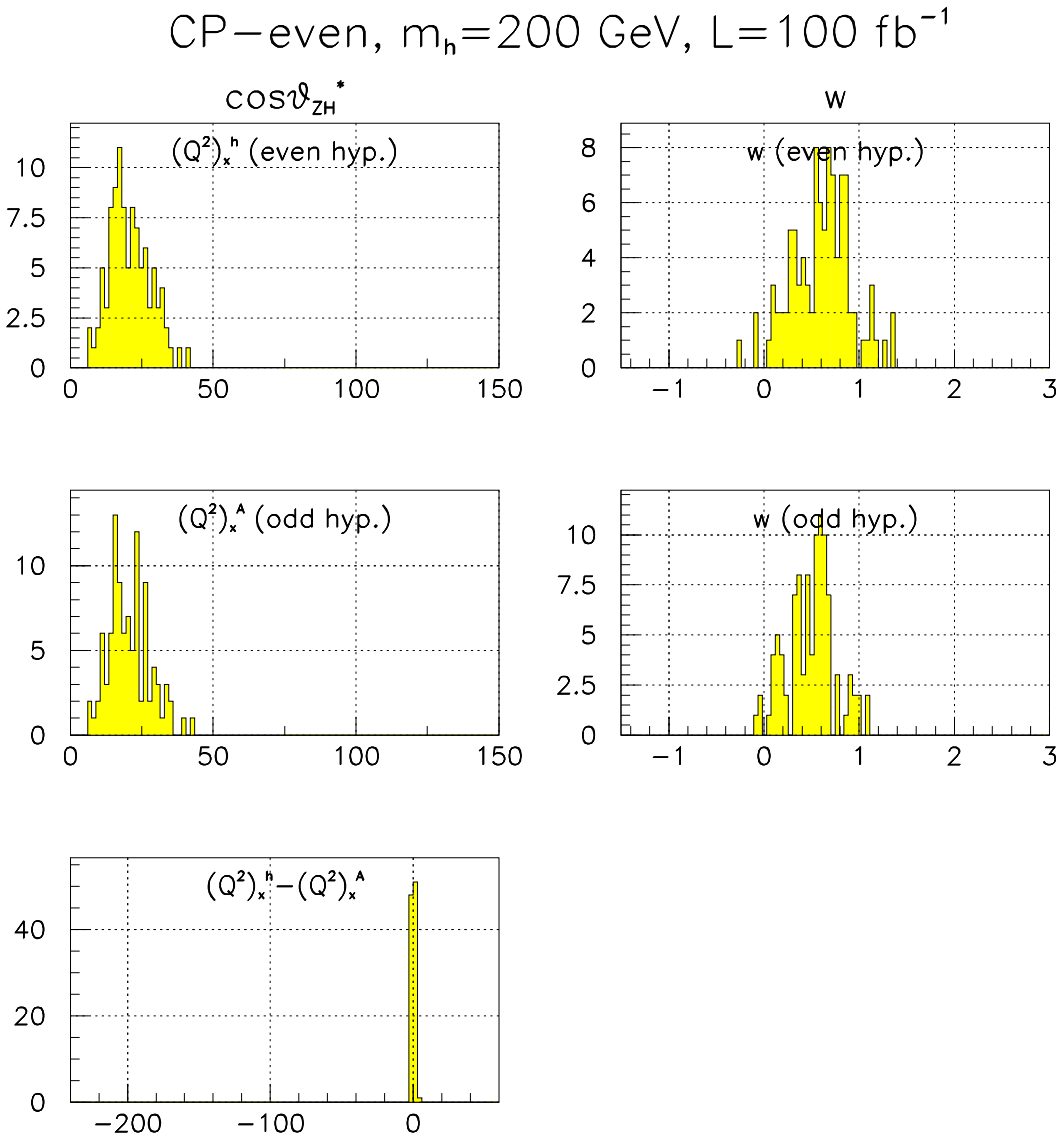

Figure B.9: The fraction of signal events in the experiments, w, and the observable $\cos\theta^*_{ZH}$. CP-even Higgs boson with mass $m_h = 200$ GeV, integrated luminosity $\int \mathcal{L} \mathrm{d}t = 100$ fb^{-1}. The fraction w is shown for the CP-even and the CP-odd hypothesis. The histogram of $(Q^2)^a_x$ is shown for the CP-even hypothesis $a = h$ and for the CP-odd hypothesis $a = A$. The difference between the values of $(Q^2)^a_x$ for the two hypotheses, $(Q^2)^h_x - (Q^2)^A_x$, is also shown. Here x stands for the observable $\cos\theta^*_{ZH}$.

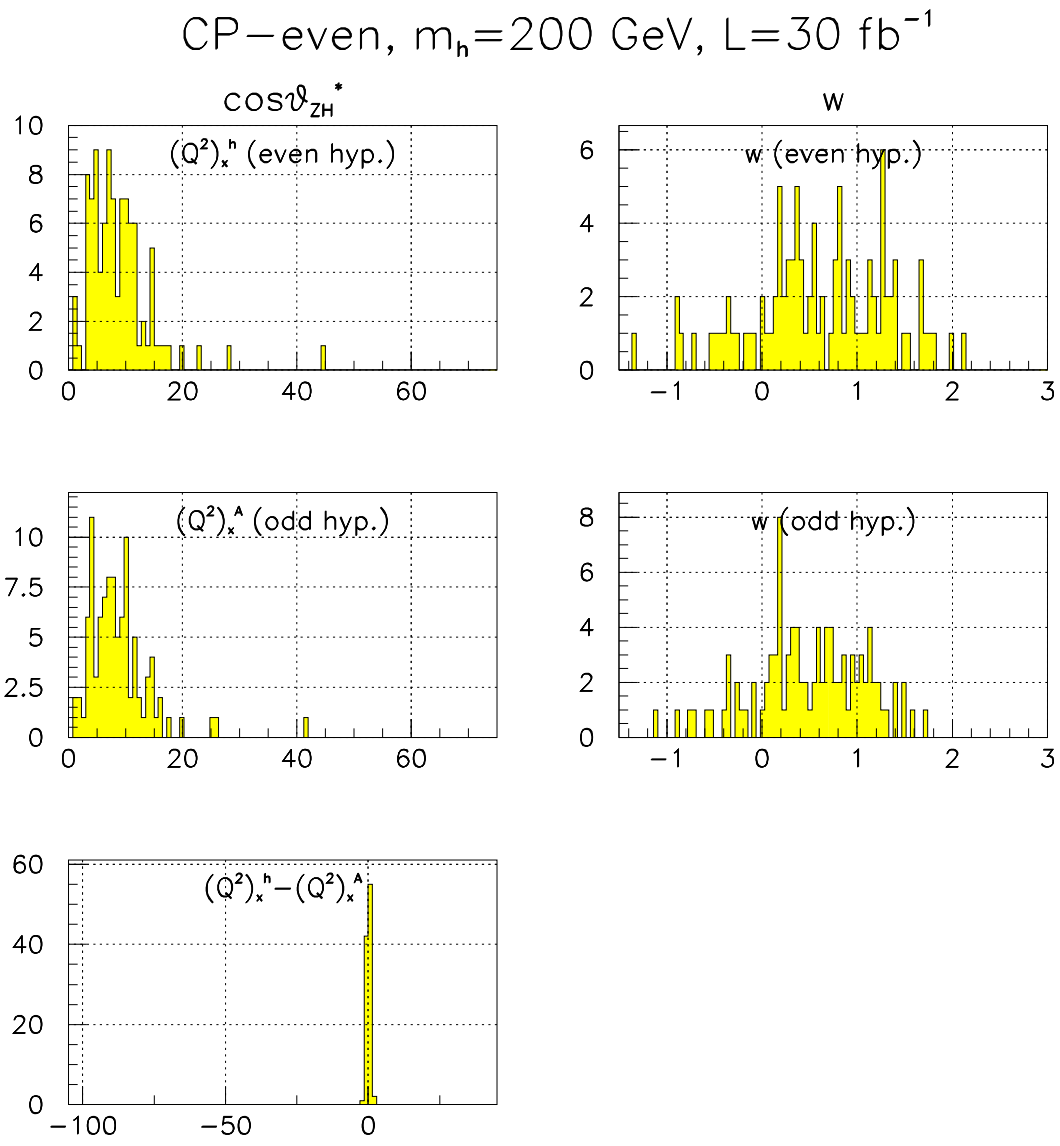

Figure B.10: Same as figure B.9, but for a lower integrated luminosity, 30 fb^{-1}.

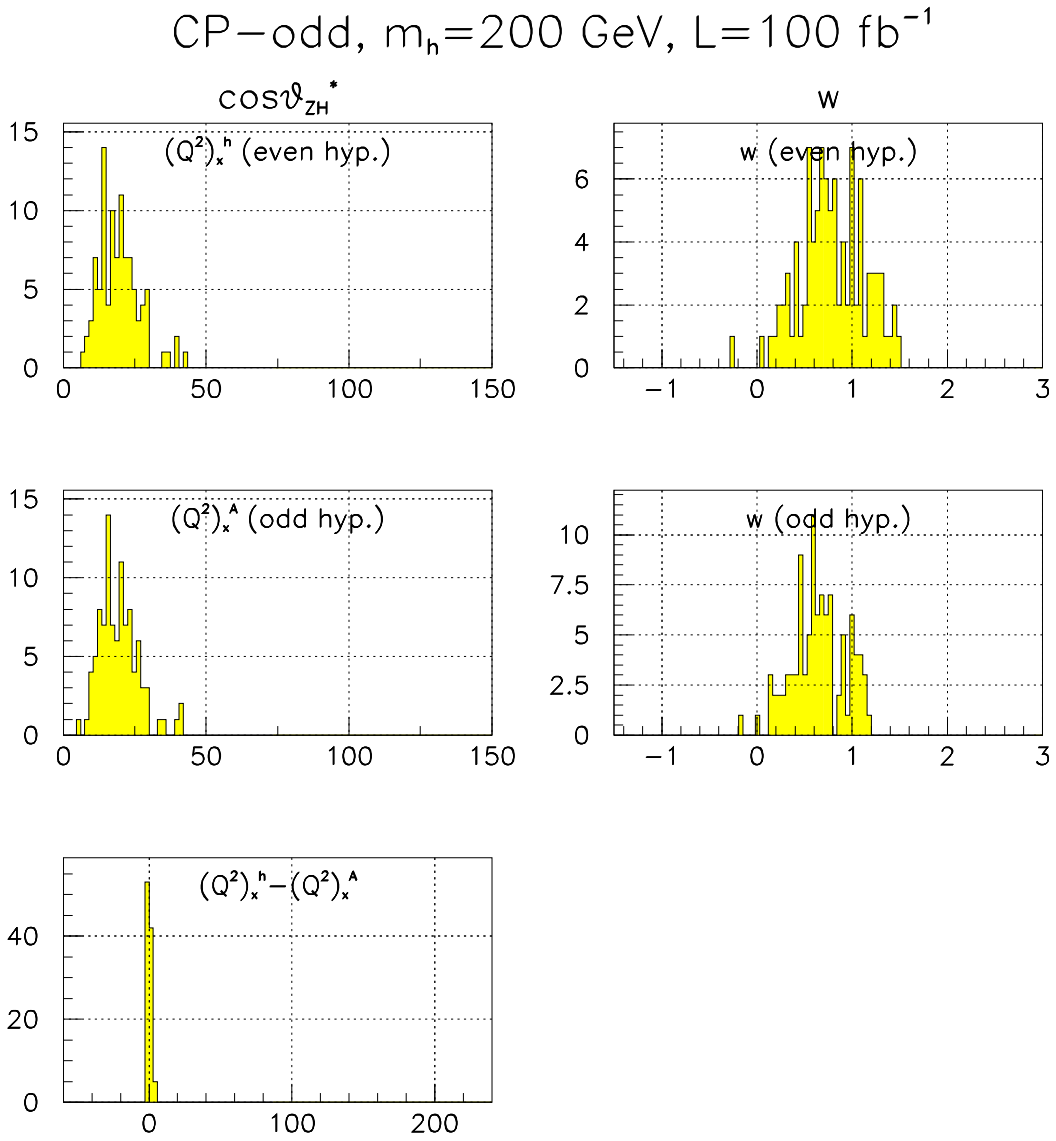

Figure B.11: The fraction of signal events in the experiments, w, and the observable $\cos\theta^*_{ZH}$. CP-odd Higgs boson with mass $m_h = 200$ GeV, integrated luminosity $\int \mathcal{L} dt = 100\ \text{fb}^{-1}$. The fraction w is shown for the CP-even and the CP-odd hypothesis. The histogram of $(Q^2)^a_x$ is shown for the CP-even hypothesis $a = h$ and for the CP-odd hypothesis $a = A$. The difference between the values of $(Q^2)^a_x$ for the two hypotheses, $(Q^2)^h_x - (Q^2)^A_x$, is also shown. Here x stands for the observable $\cos\theta^*_{ZH}$.

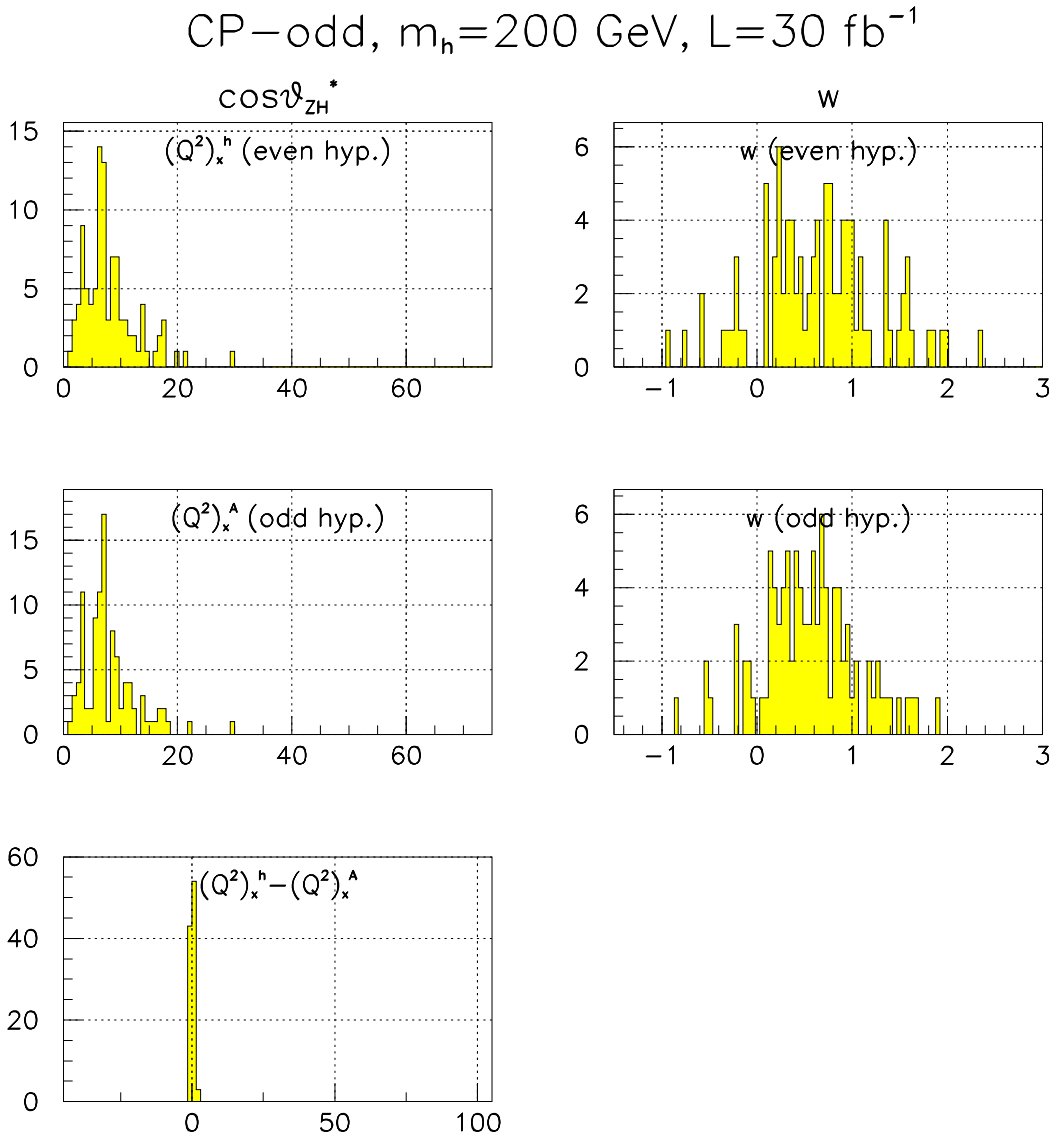

Figure B.12: Same as figure B.11, but for a lower integrated luminosity, 30 fb^{-1}.

B.2 Higgs boson with mass 250 GeV

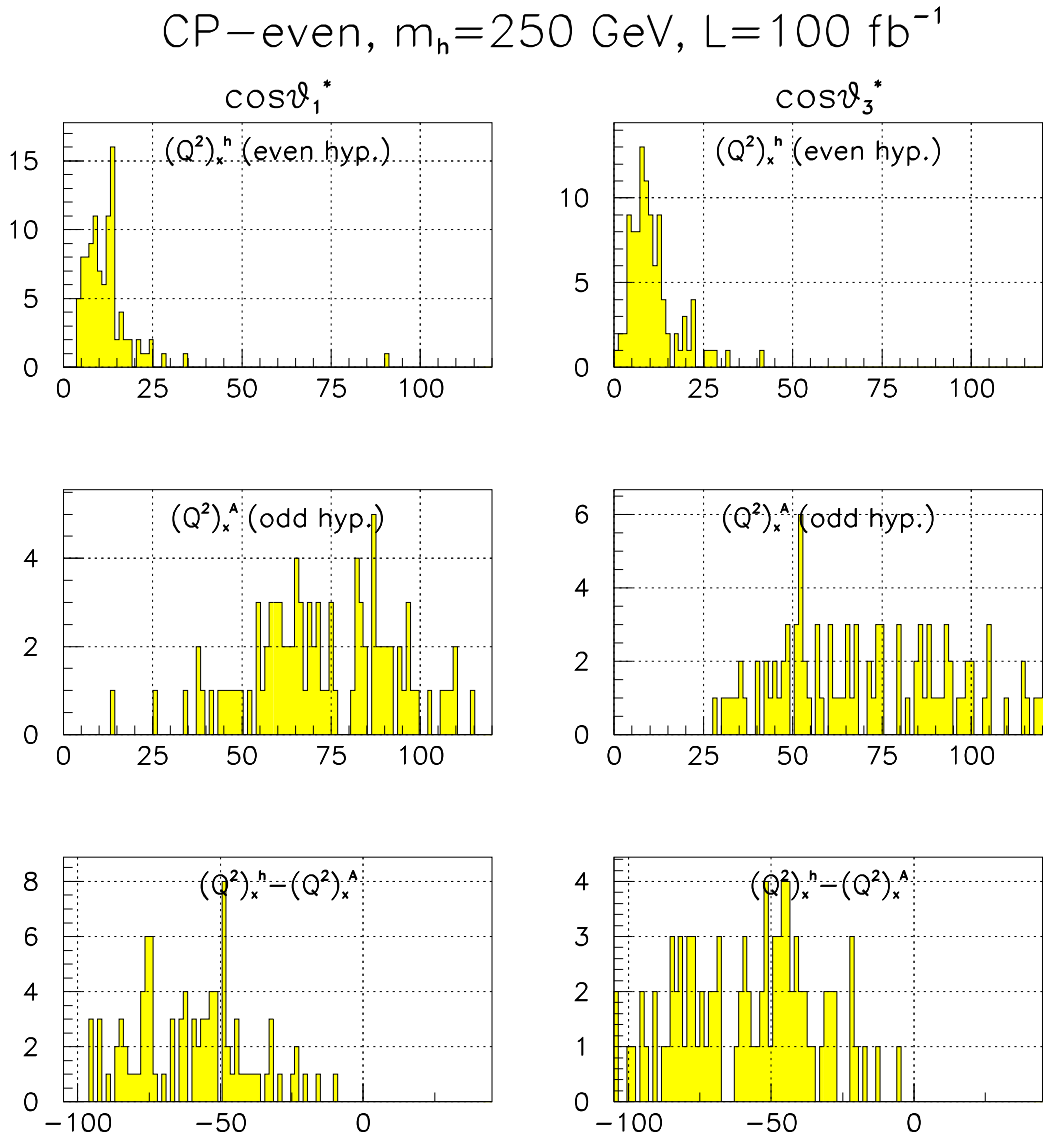

Figure B.13: The observables $\cos\theta_1^*$ and $\cos\theta_3^*$. CP-even Higgs boson with mass $m_h = 250$ GeV, integrated luminosity $\int \mathcal{L} dt = 100$ fb^{-1}. The histogram of $(Q^2)_x^a$ is shown for the CP-even hypothesis $a = h$ and for the CP-odd hypothesis $a = A$. The difference between the values of $(Q^2)_x^a$ for the two hypotheses, $(Q^2)_x^h - (Q^2)_x^A$, is also shown. Here x refers to the observable $\cos\theta_1^*$ or $\cos\theta_3^*$.

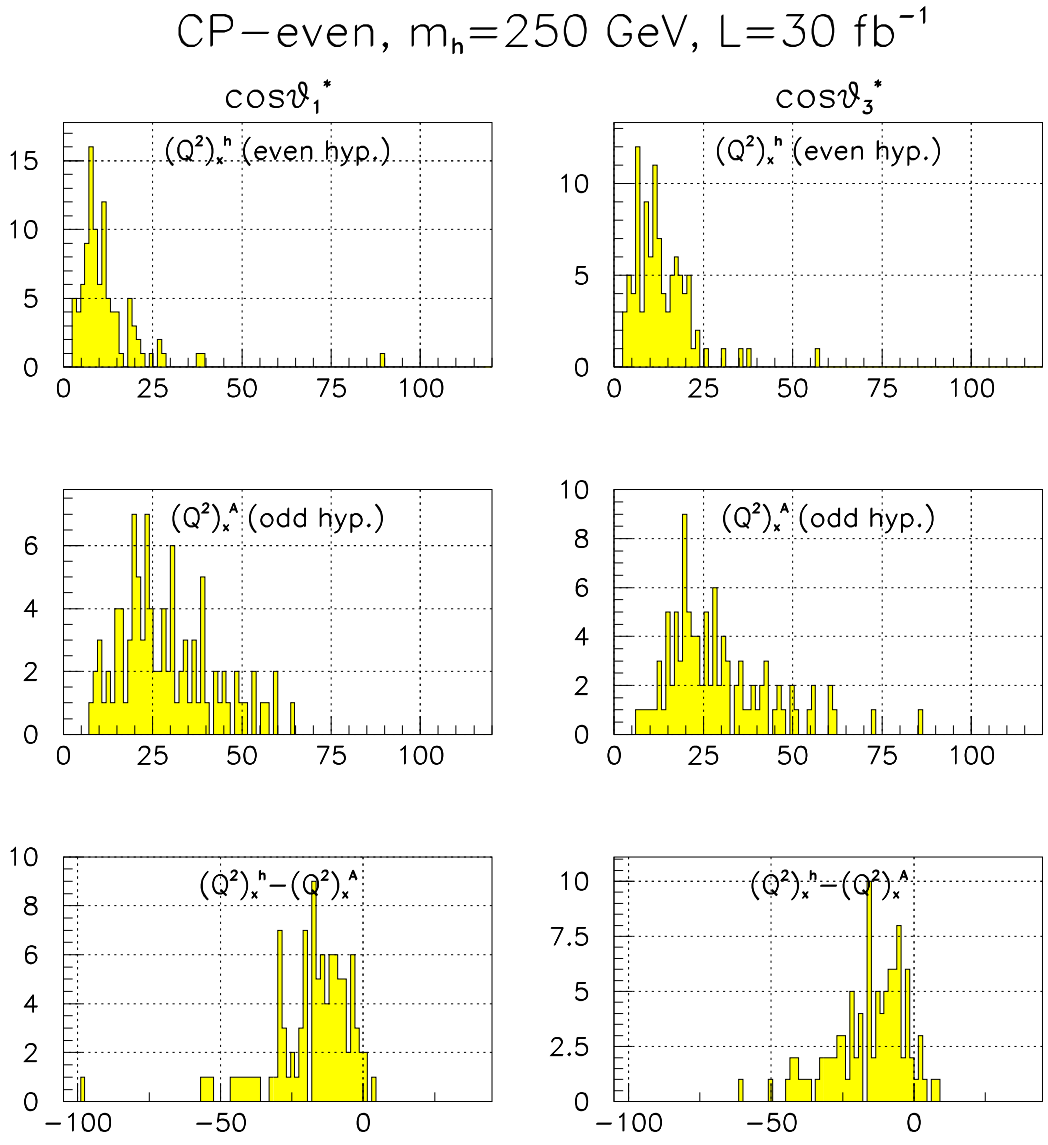

Figure B.14: Same as figure B.13, but for a lower integrated luminosity, 30 fb^{-1}.

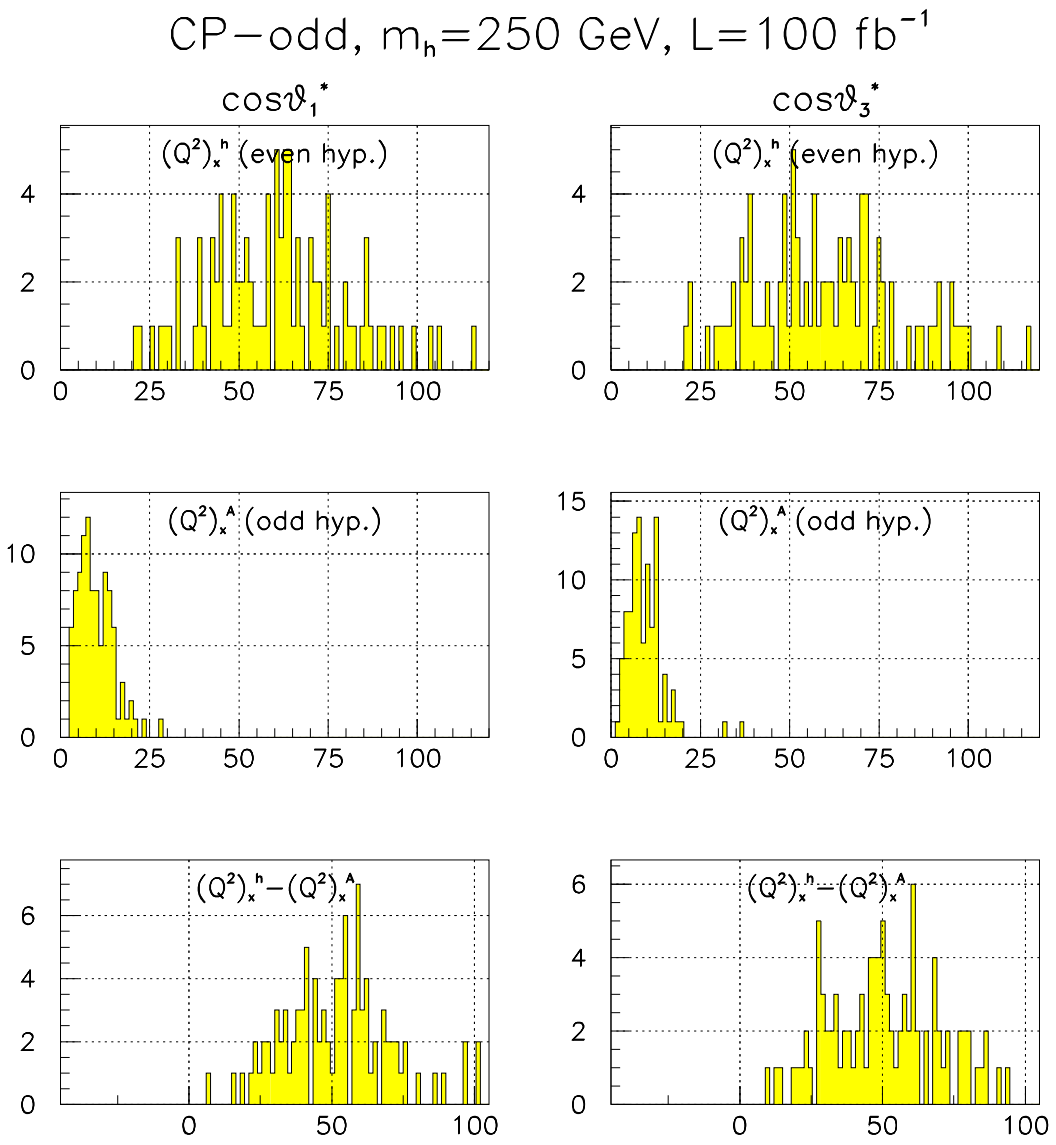

Figure B.15: The observables $\cos\theta_1^*$ and $\cos\theta_3^*$. CP-odd Higgs boson with mass $m_h = 250$ GeV, integrated luminosity $\int \mathcal{L} dt = 100$ fb^{-1}. The histogram of $(Q^2)_x^a$ is shown for the CP-even hypothesis $a = h$ and for the CP-odd hypothesis $a = A$. The difference between the values of $(Q^2)_x^a$ for the two hypotheses, $(Q^2)_x^h - (Q^2)_x^A$, is also shown. Here x refers to the observable $\cos\theta_1^*$ or $\cos\theta_3^*$.

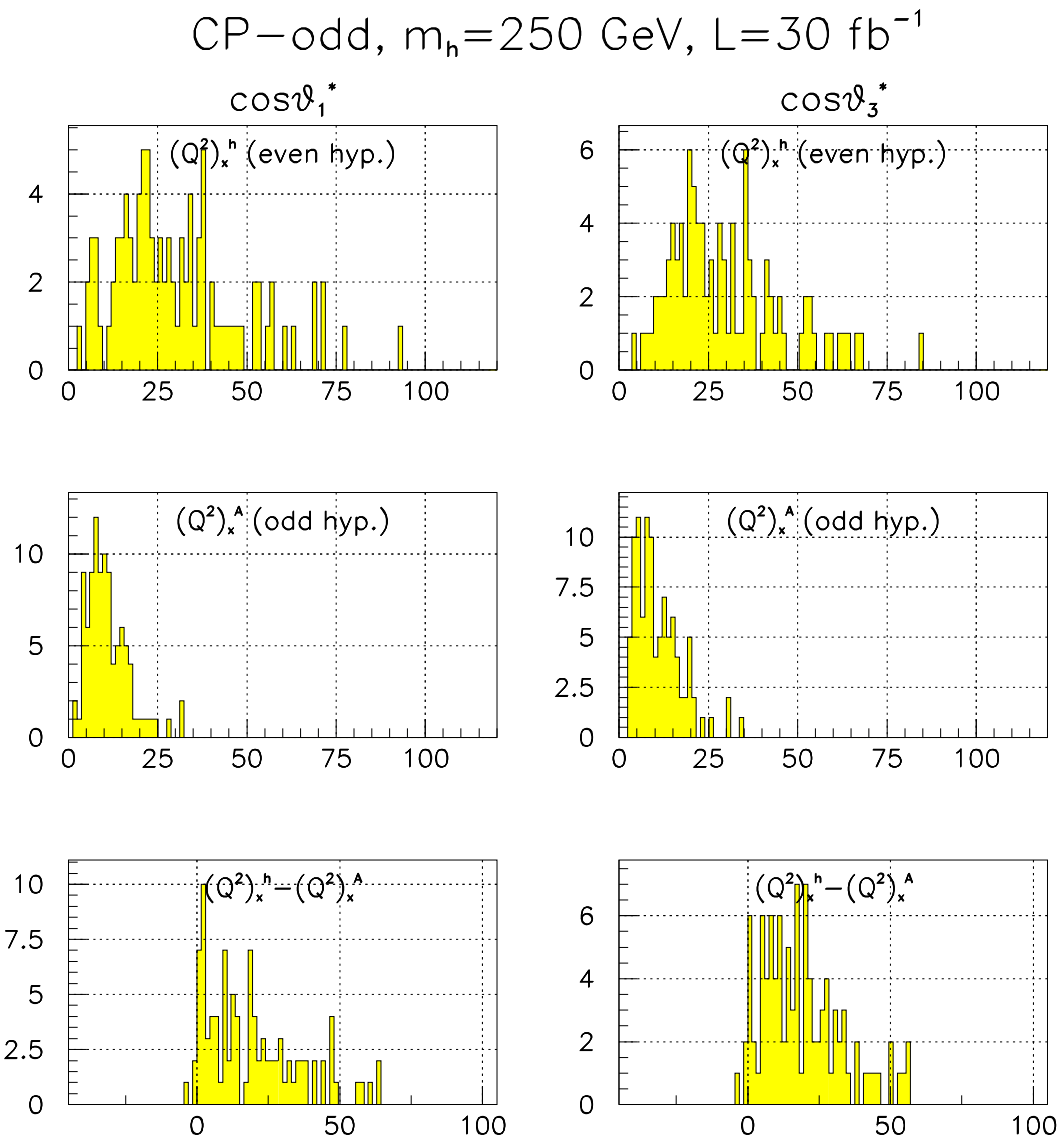

Figure B.16: Same as figure B.15, but for a lower integrated luminosity, 30 fb^{-1}.

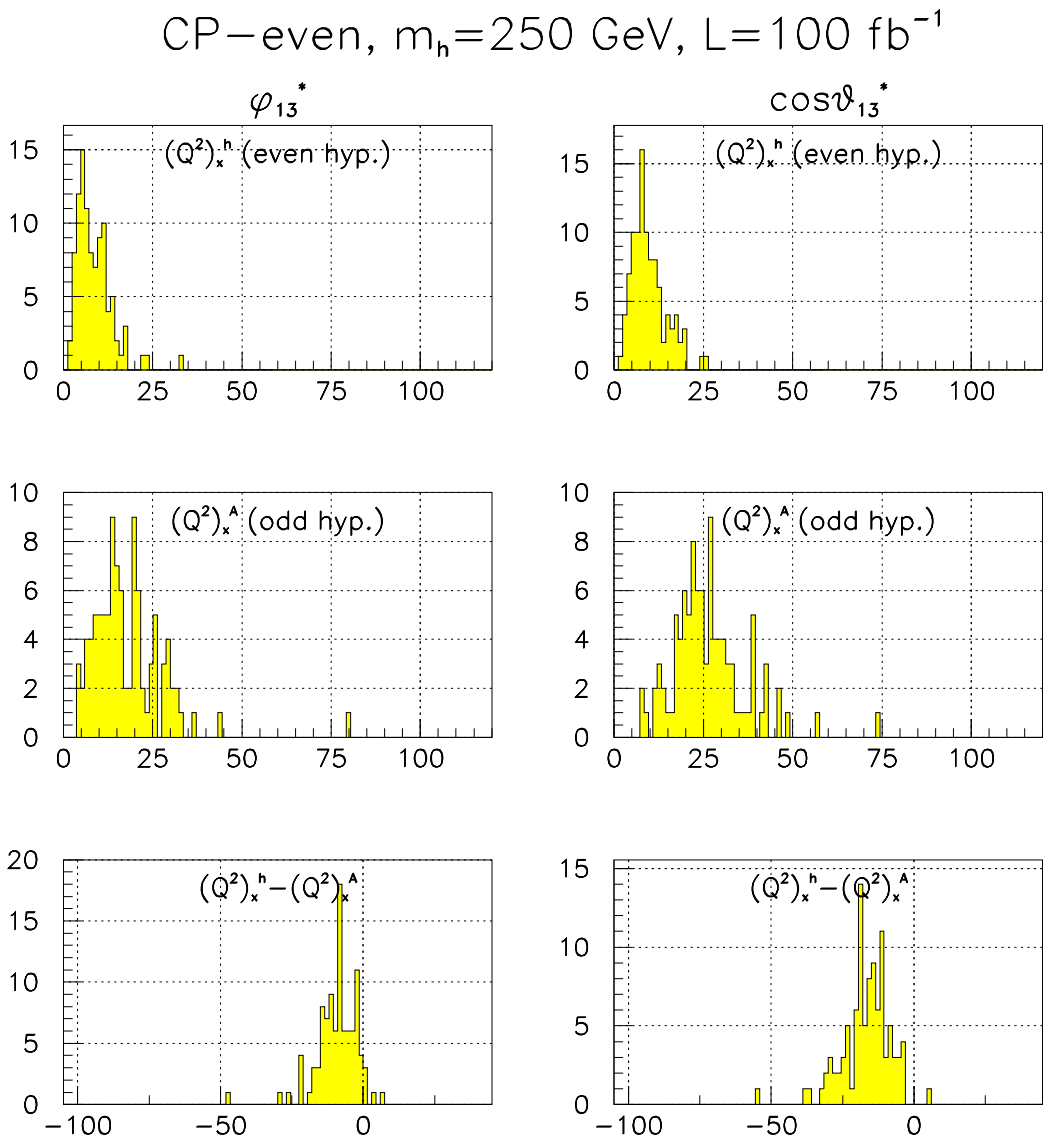

Figure B.17: The observables ϕ^*_{13} and $\cos\theta^*_{13}$. CP-even Higgs boson with mass $m_h = 250$ GeV, integrated luminosity $\int \mathcal{L} dt = 100$ fb^{-1}. The histogram of $(Q^2)^a_x$ is shown for the CP-even hypothesis $a = h$ and for the CP-odd hypothesis $a = A$. The difference between the values of $(Q^2)^a_x$ for the two hypotheses, $(Q^2)^h_x - (Q^2)^A_x$, is also shown. Here x refers to the observable ϕ^*_{13} or $\cos\theta^*_{13}$.

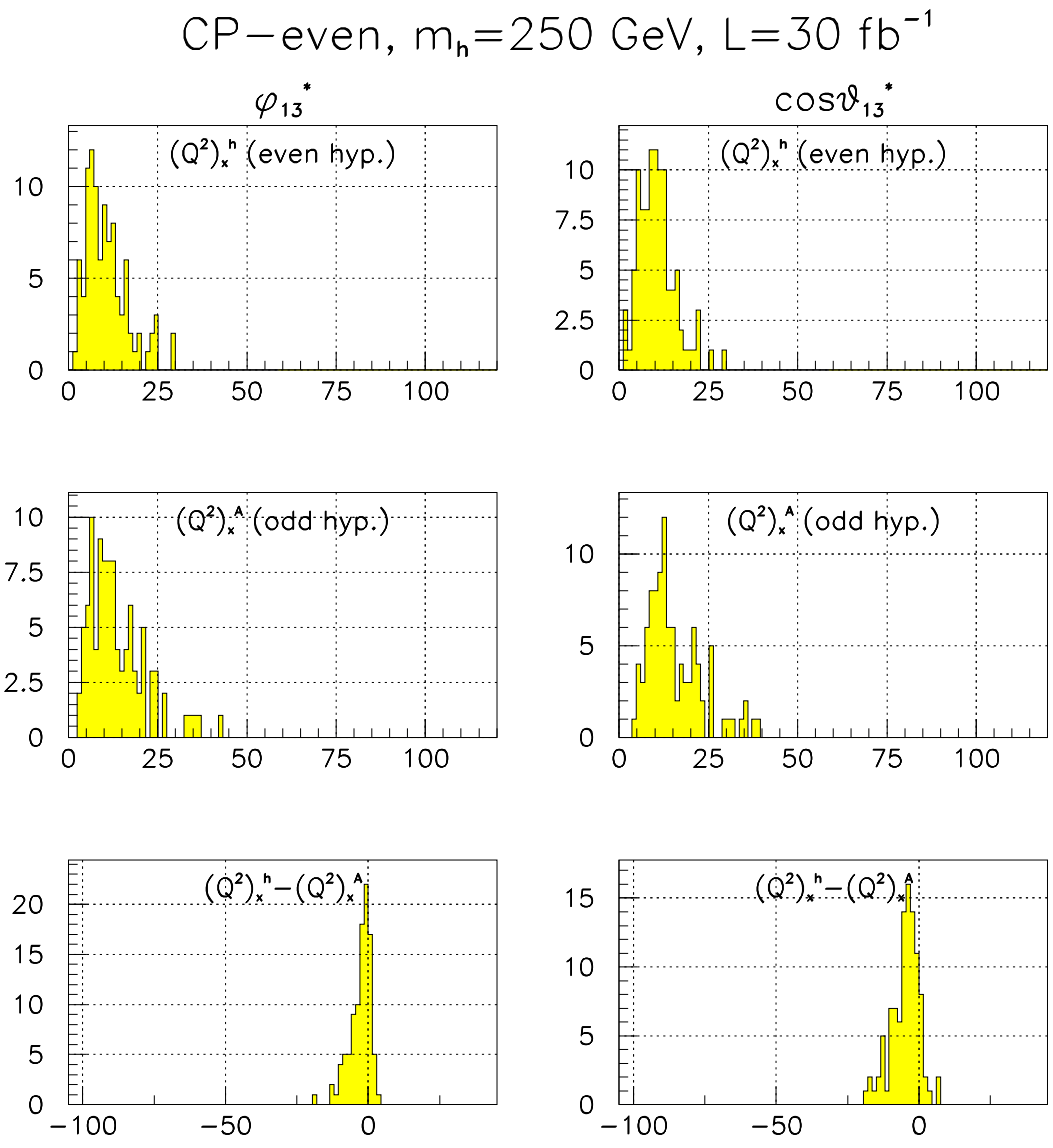

Figure B.18: Same as figure B.17, but for a lower integrated luminosity, 30 fb^{-1}.

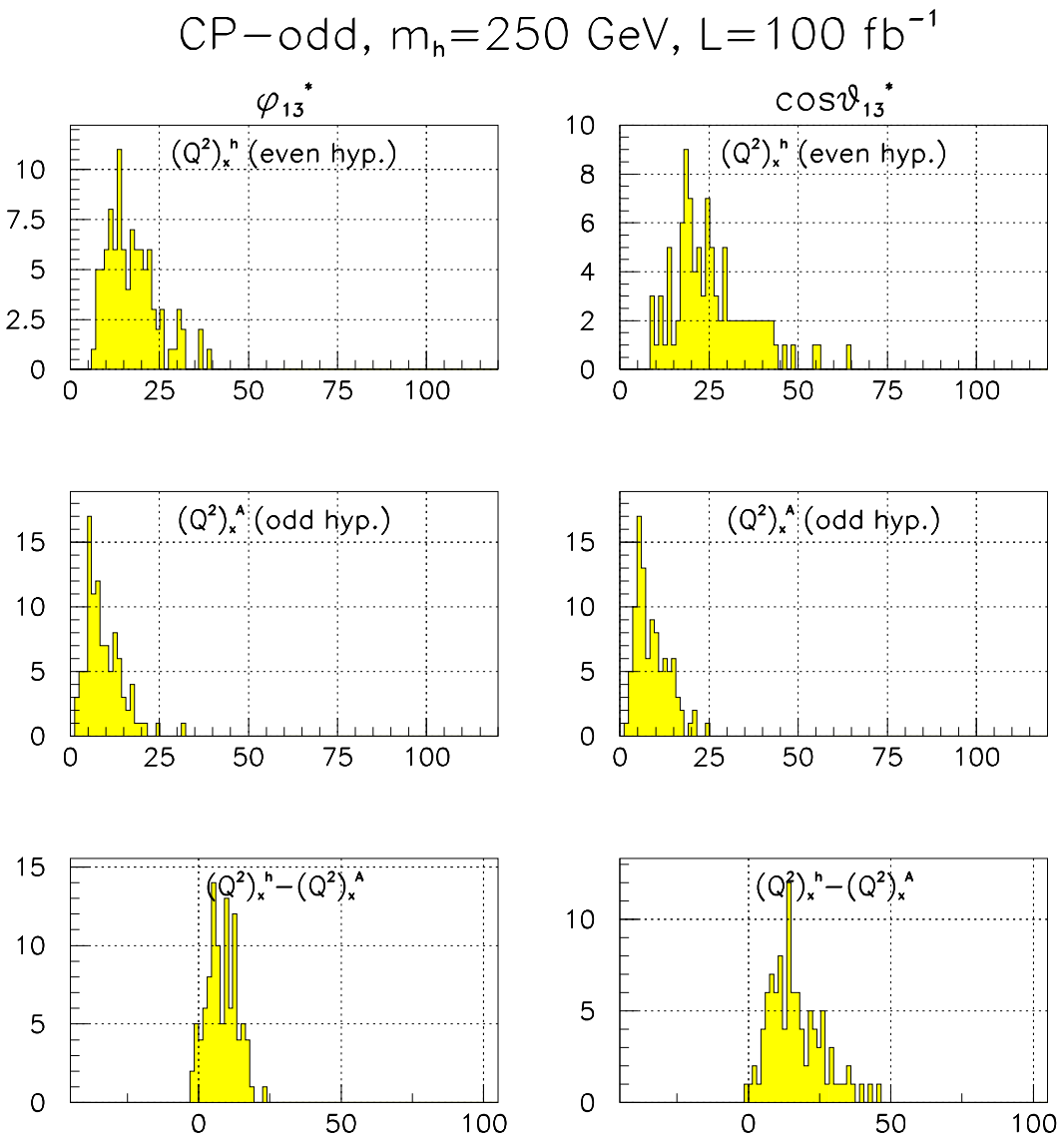

Figure B.19: The observables ϕ^*_{13} and $\cos\theta^*_{13}$. CP-odd Higgs boson with mass $m_h = 250$ GeV, integrated luminosity $\int \mathcal{L} dt = 100$ fb^{-1}. The histogram of $(Q^2)^a_x$ is shown for the CP-even hypothesis $a = h$ and for the CP-odd hypothesis $a = A$. The difference between the values of $(Q^2)^a_x$ for the two hypotheses, $(Q^2)^h_x - (Q^2)^A_x$, is also shown. Here x refers to the observable ϕ^*_{13} or $\cos\theta^*_{13}$.

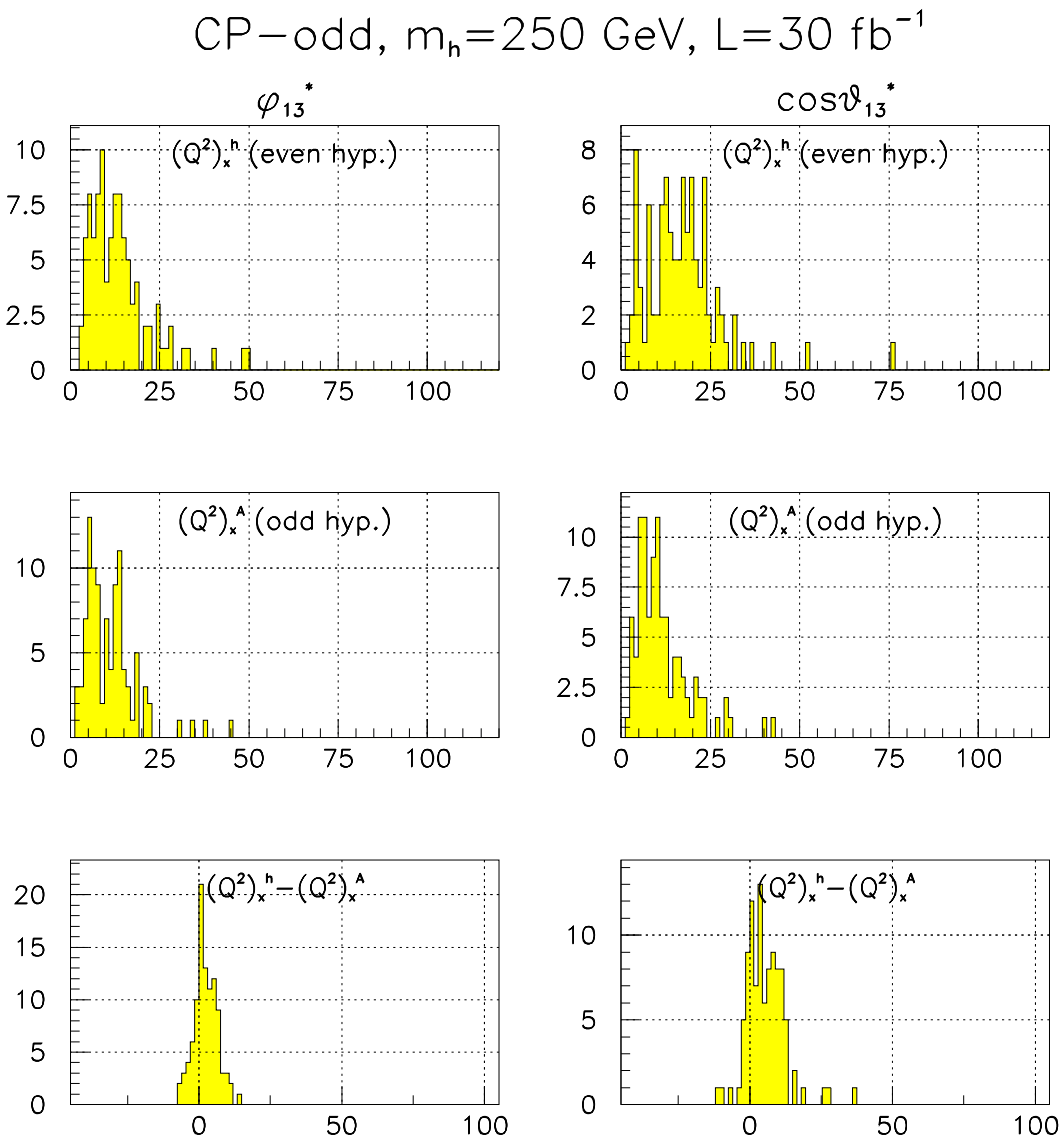

Figure B.20: Same as figure B.19, but for a lower integrated luminosity, 30 fb^{-1}.

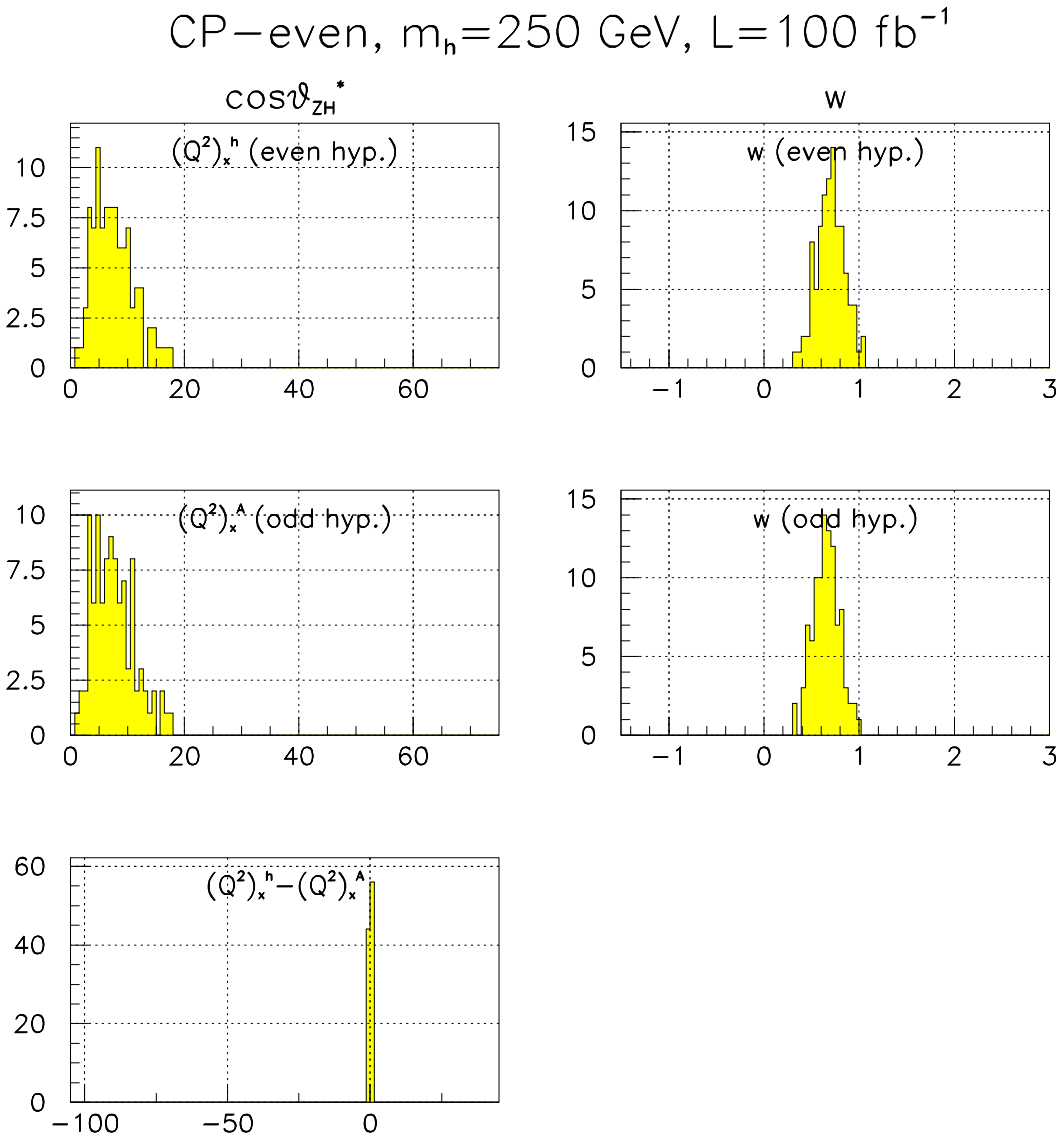

Figure B.21: The fraction of signal events in the experiments, w, and the observable $\cos\theta^*_{ZH}$. CP-even Higgs boson with mass $m_h = 250$ GeV, integrated luminosity $\int \mathcal{L} dt = 100$ fb^{-1}. The fraction w is shown for the CP-even and the CP-odd hypothesis. The histogram of $(Q^2)^a_x$ is shown for the CP-even hypothesis $a = h$ and for the CP-odd hypothesis $a = A$. The difference between the values of $(Q^2)^a_x$ for the two hypotheses, $(Q^2)^h_x - (Q^2)^A_x$, is also shown. Here x stands for the observable $\cos\theta^*_{ZH}$.

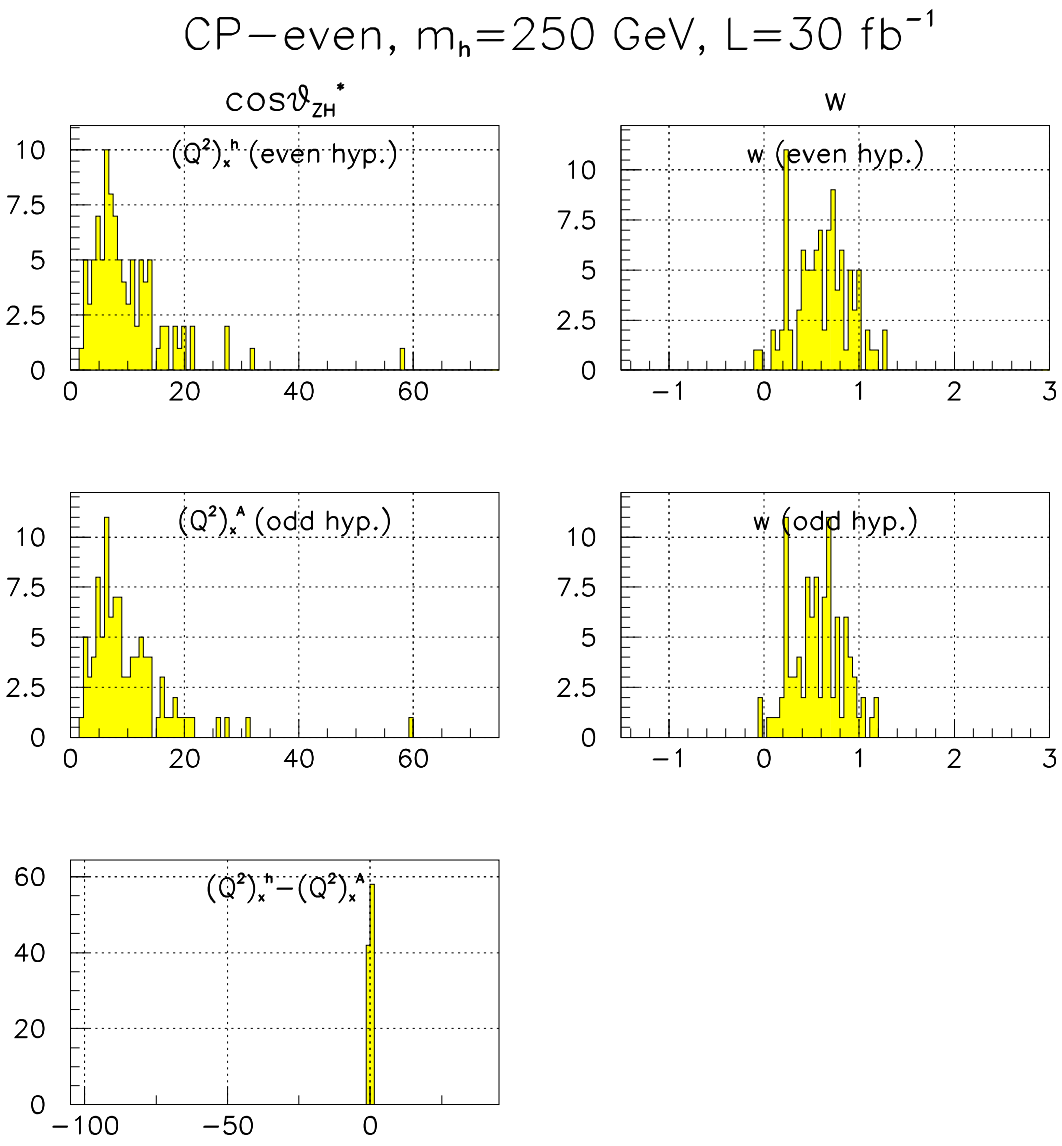

Figure B.22: Same as figure B.21, but for a lower integrated luminosity, 30 fb^{-1}.

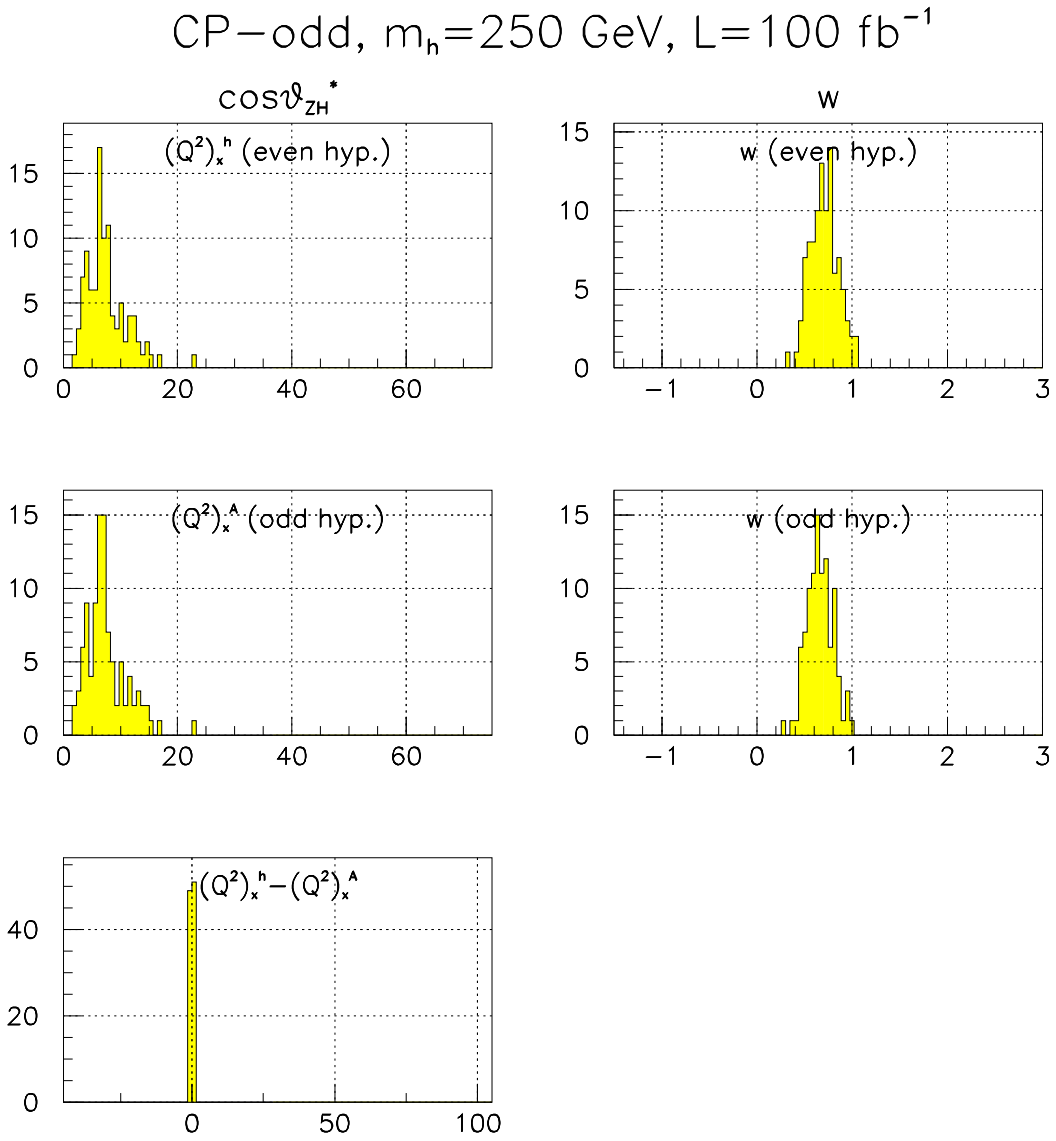

Figure B.23: The fraction of signal events in the experiments, w, and the observable $\cos\theta^*_{ZH}$. CP-odd Higgs boson with mass $m_h = 250$ GeV, integrated luminosity $\int \mathcal{L} dt = 100$ fb^{-1}. The fraction w is shown for the CP-even and the CP-odd hypothesis. The histogram of $(Q^2)^a_x$ is shown for the CP-even hypothesis $a = h$ and for the CP-odd hypothesis $a = A$. The difference between the values of $(Q^2)^a_x$ for the two hypotheses, $(Q^2)^h_x - (Q^2)^A_x$, is also shown. Here x stands for the observable $\cos\theta^*_{ZH}$.

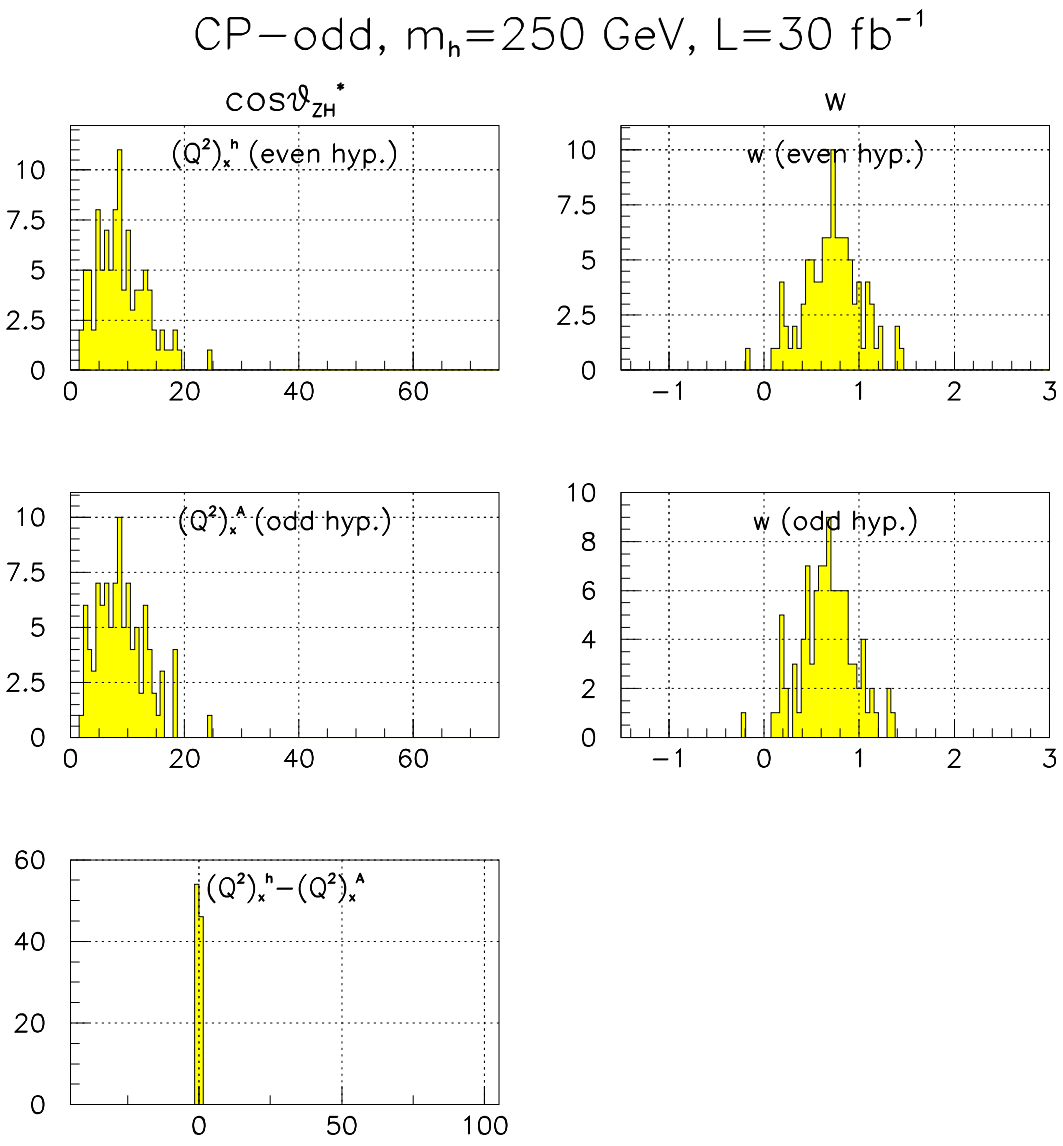

Figure B.24: Same as figure B.23, but for a lower integrated luminosity, 30 fb^{-1}.

B.3 Higgs boson with mass 300 GeV

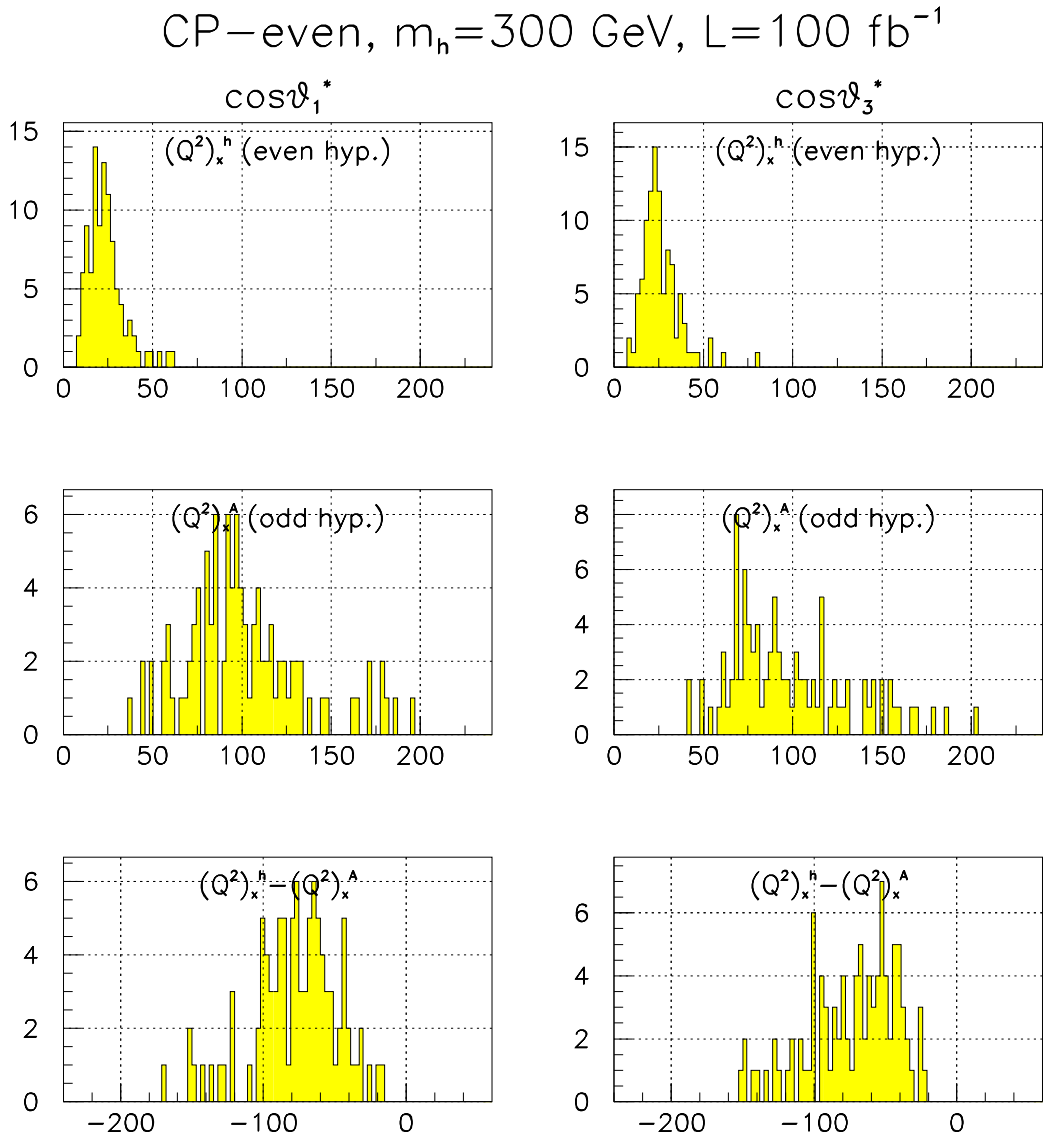

Figure B.25: The observables $\cos\theta_1^*$ and $\cos\theta_3^*$. CP-even Higgs boson with mass $m_h = 300$ GeV, integrated luminosity $\int \mathcal{L} dt = 100$ fb^{-1}. The histogram of $(Q^2)_x^a$ is shown for the CP-even hypothesis $a = h$ and for the CP-odd hypothesis $a = A$. The difference between the values of $(Q^2)_x^a$ for the two hypotheses, $(Q^2)_x^h - (Q^2)_x^A$, is also shown. Here x refers to the observable $\cos\theta_1^*$ or $\cos\theta_3^*$.

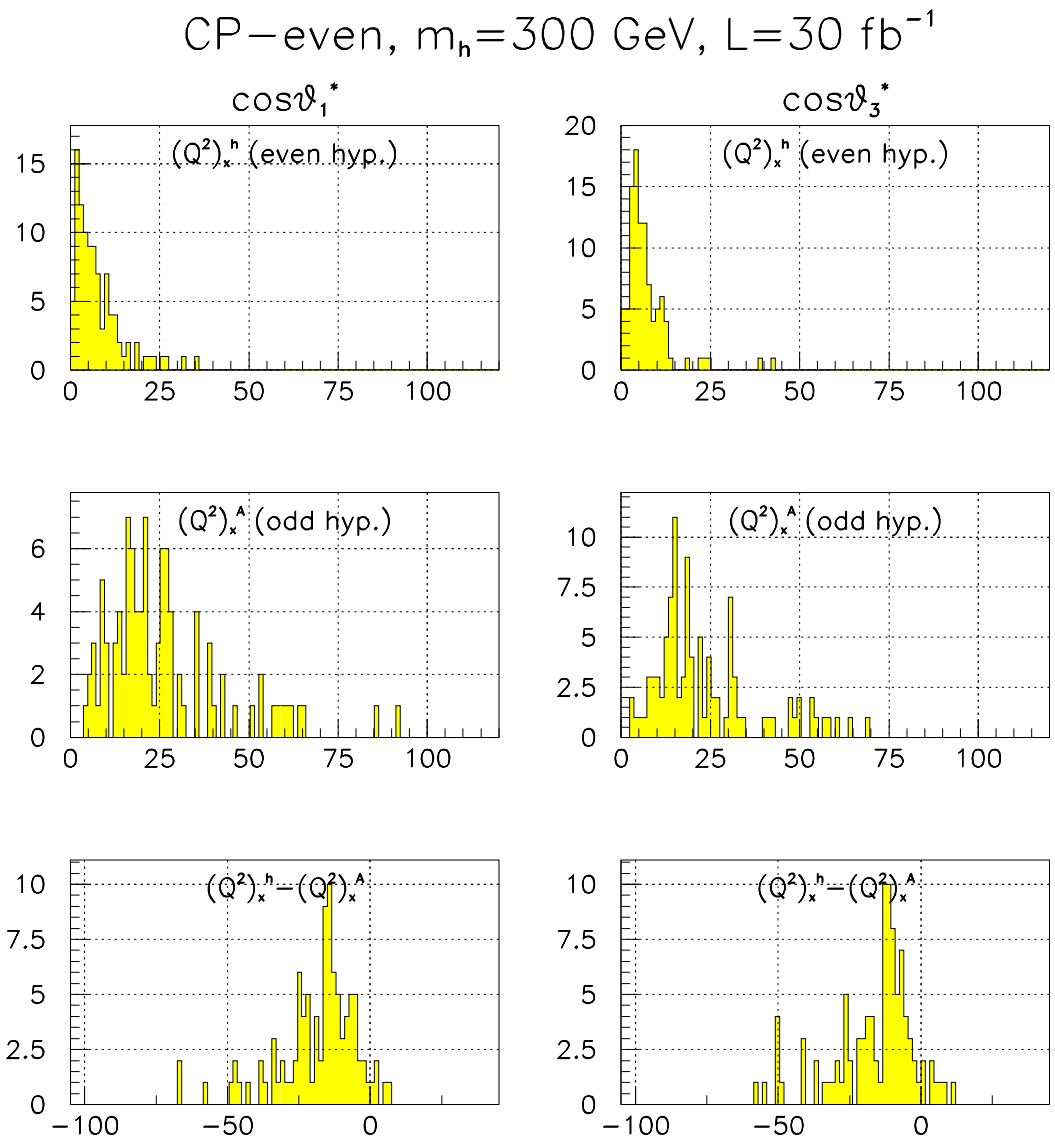

Figure B.26: Same as figure B.25, but for a lower integrated luminosity, 30 fb^{-1}.

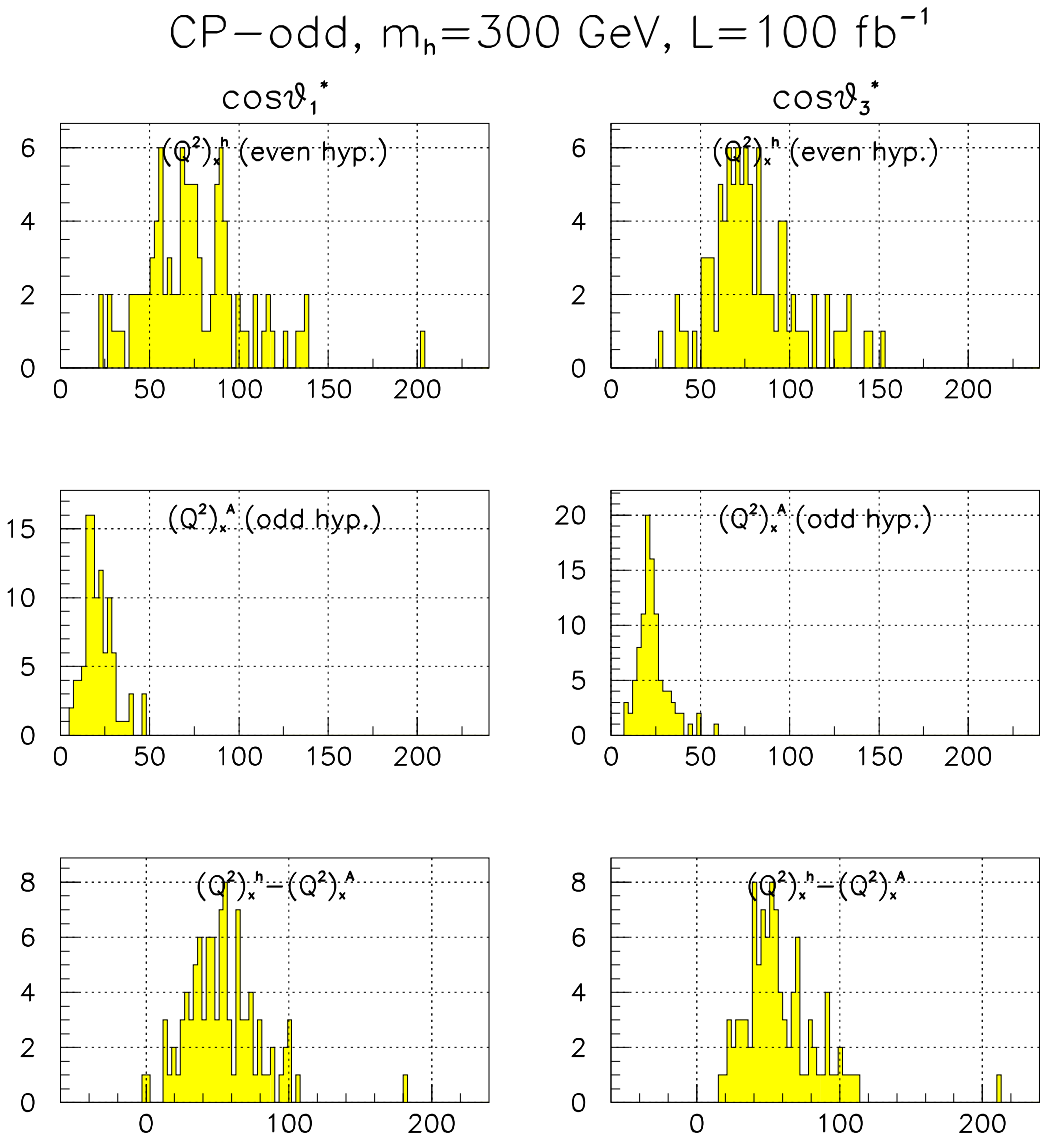

Figure B.27: The observables $\cos\theta_1^*$ and $\cos\theta_3^*$. CP-odd Higgs boson with mass $m_h = 300$ GeV, integrated luminosity $\int \mathcal{L} dt = 100$ fb^{-1}. The histogram of $(Q^2)_x^a$ is shown for the CP-even hypothesis $a = h$ and for the CP-odd hypothesis $a = A$. The difference between the values of $(Q^2)_x^a$ for the two hypotheses, $(Q^2)_x^h - (Q^2)_x^A$, is also shown. Here x refers to the observable $\cos\theta_1^*$ or $\cos\theta_3^*$.

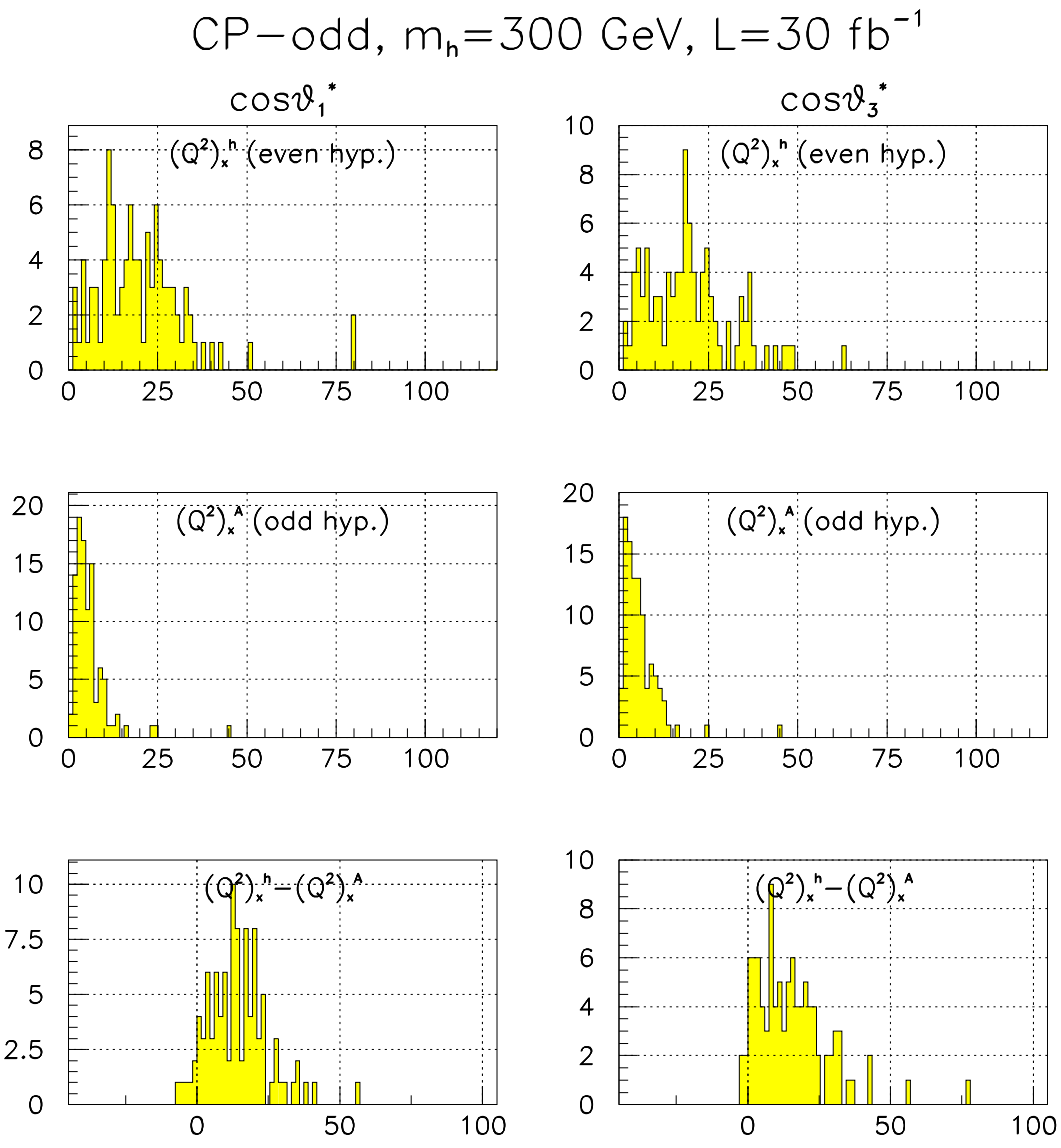

Figure B.28: Same as figure B.27, but for a lower integrated luminosity, 30 fb^{-1}.

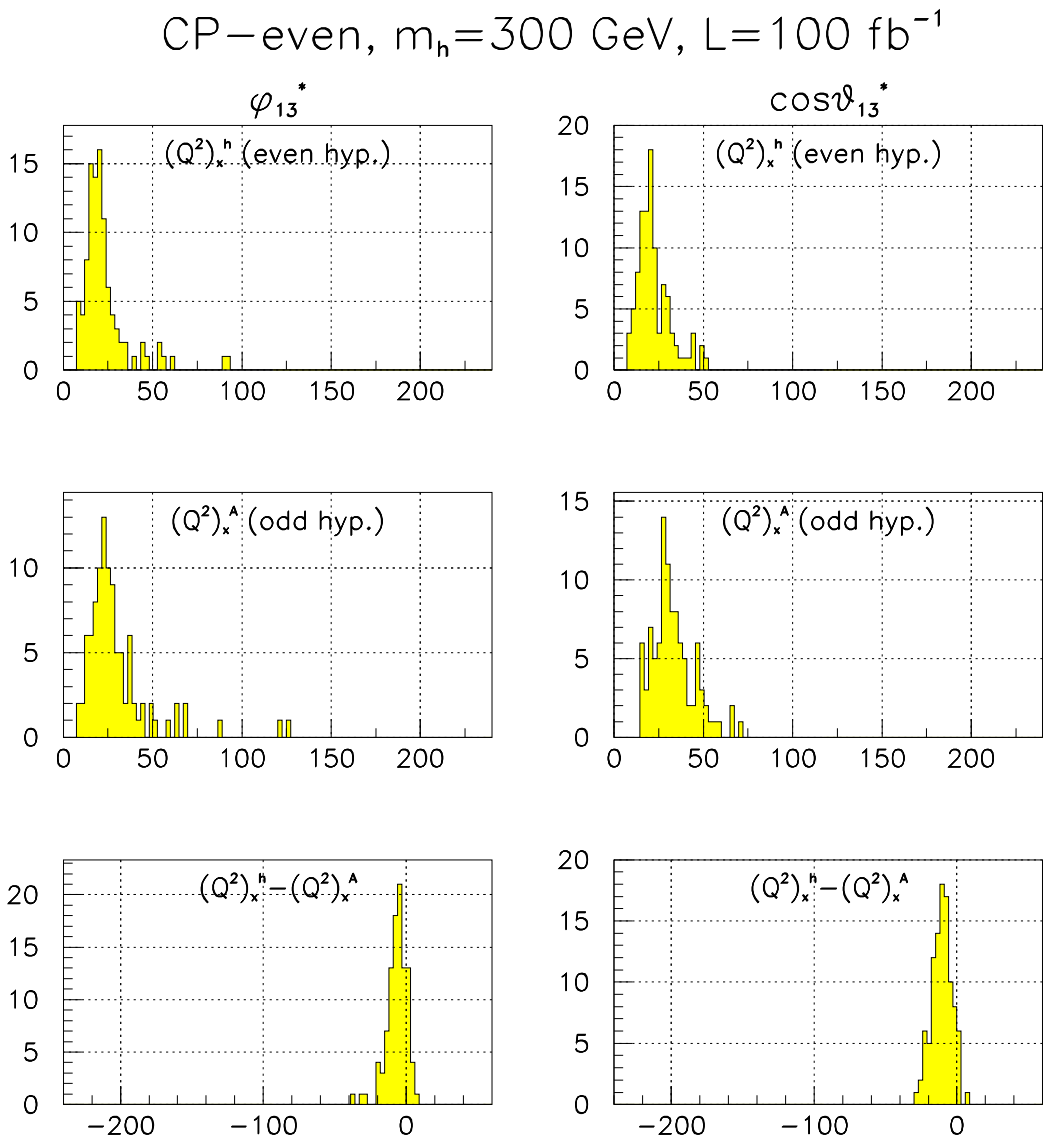

Figure B.29: The observables ϕ^*_{13} and $\cos\theta^*_{13}$. CP-even Higgs boson with mass $m_h = 300$ GeV, integrated luminosity $\int \mathcal{L} dt = 100$ fb^{-1}. The histogram of $(Q^2)^a_x$ is shown for the CP-even hypothesis $a = h$ and for the CP-odd hypothesis $a = A$. The difference between the values of $(Q^2)^a_x$ for the two hypotheses, $(Q^2)^h_x - (Q^2)^A_x$, is also shown. Here x refers to the observable ϕ^*_{13} or $\cos\theta^*_{13}$.

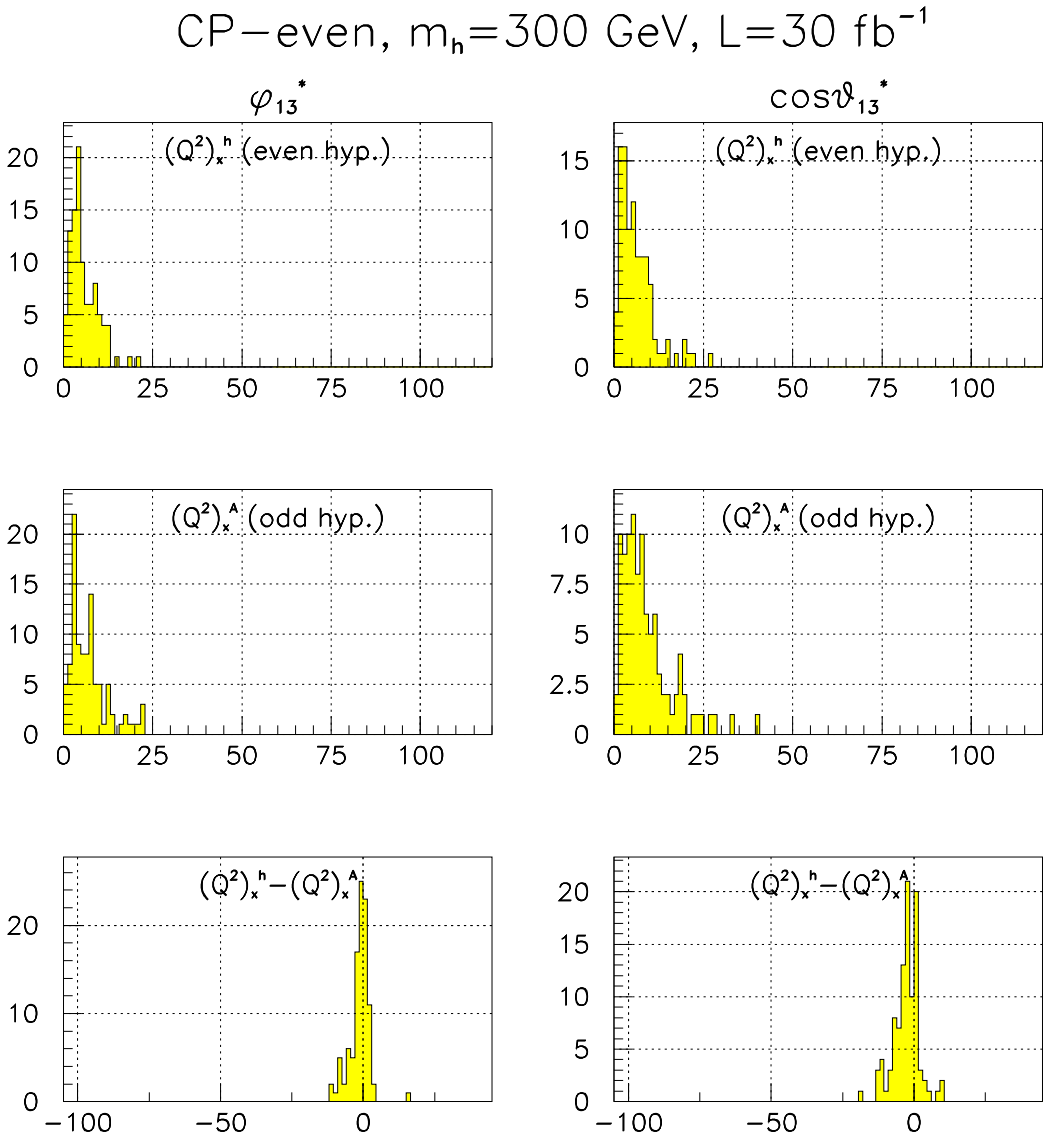

Figure B.30: Same as figure B.29, but for a lower integrated luminosity, 30 fb^{-1}.

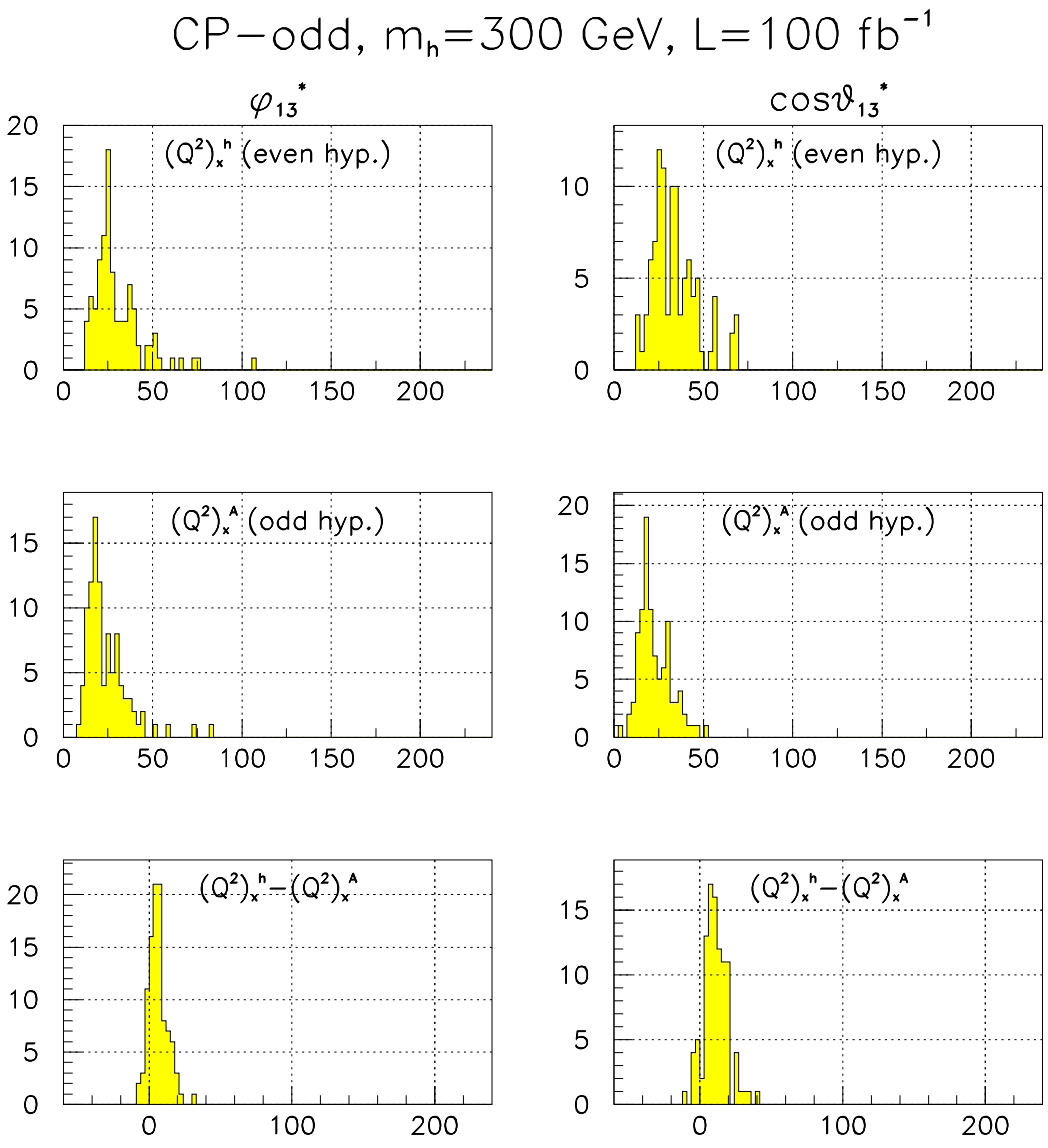

Figure B.31: The observables ϕ^*_{13} and $\cos\theta^*_{13}$. CP-odd Higgs boson with mass $m_h = 300$ GeV, integrated luminosity $\int \mathcal{L} dt = 100$ fb^{-1}. The histogram of $(Q^2)^a_x$ is shown for the CP-even hypothesis $a = h$ and for the CP-odd hypothesis $a = A$. The difference between the values of $(Q^2)^a_x$ for the two hypotheses, $(Q^2)^h_x - (Q^2)^A_x$, is also shown. Here x refers to the observable ϕ^*_{13} or $\cos\theta^*_{13}$.

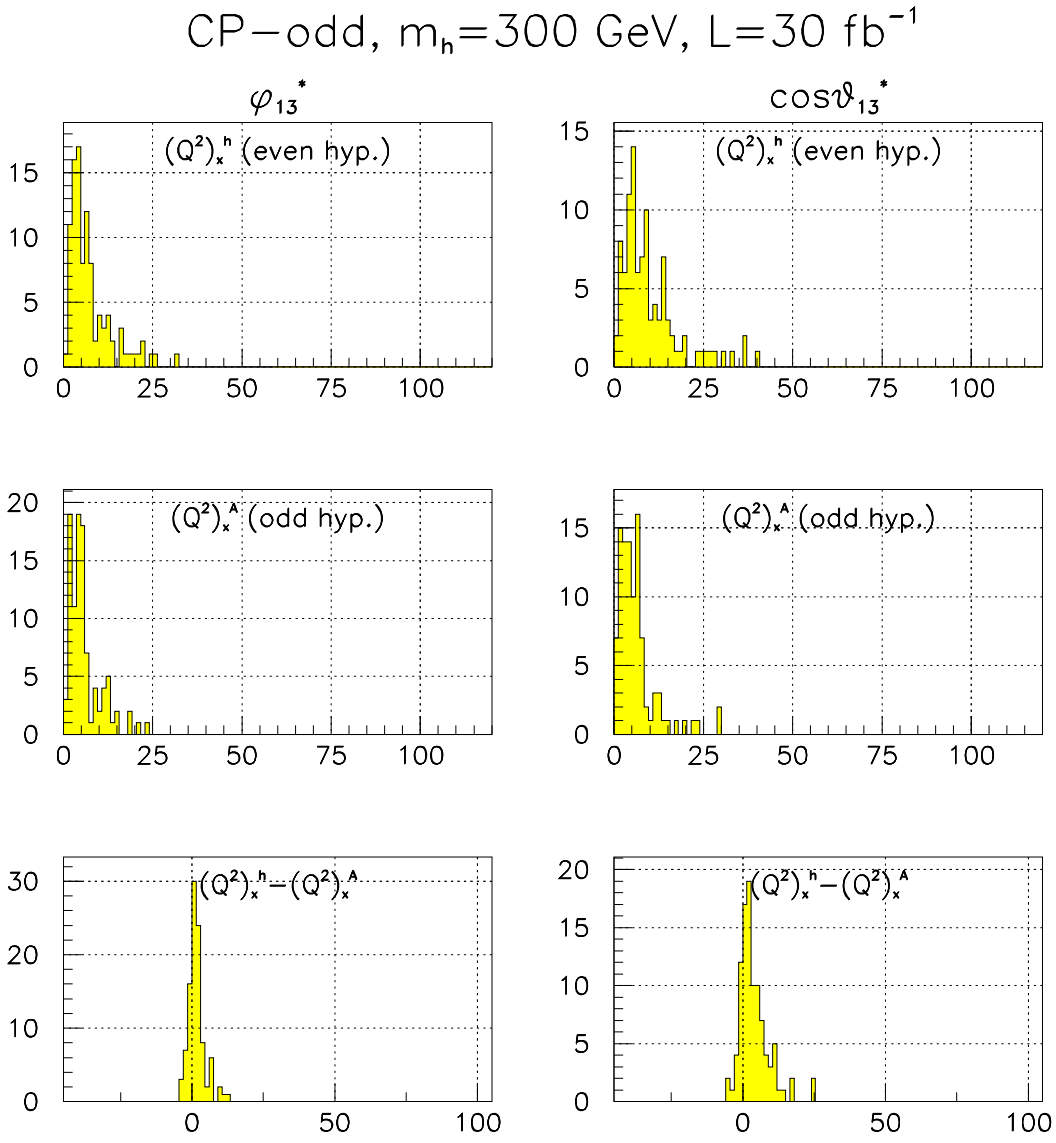

Figure B.32: Same as figure B.31, but for a lower integrated luminosity, 30 fb^{-1}.

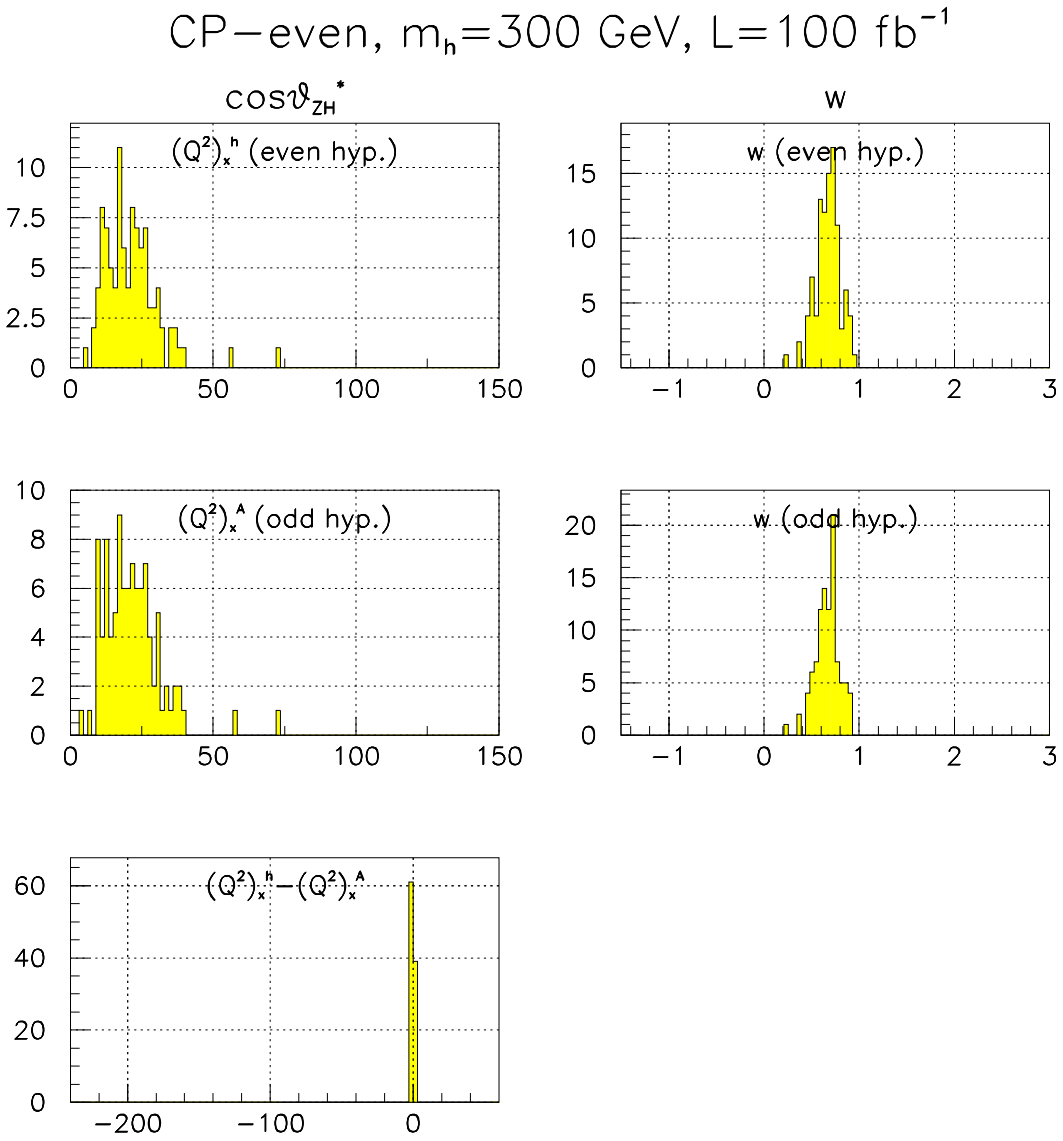

Figure B.33: The fraction of signal events in the experiments, w, and the observable $\cos\theta^*_{ZH}$. CP-even Higgs boson with mass $m_h = 300$ GeV, integrated luminosity $\int \mathcal{L} dt = 100$ fb^{-1}. The fraction w is shown for the CP-even and the CP-odd hypothesis. The histogram of $(Q^2)^a_x$ is shown for the CP-even hypothesis $a = h$ and for the CP-odd hypothesis $a = A$. The difference between the values of $(Q^2)^a_x$ for the two hypotheses, $(Q^2)^h_x - (Q^2)^A_x$, is also shown. Here x stands for the observable $\cos\theta^*_{ZH}$.

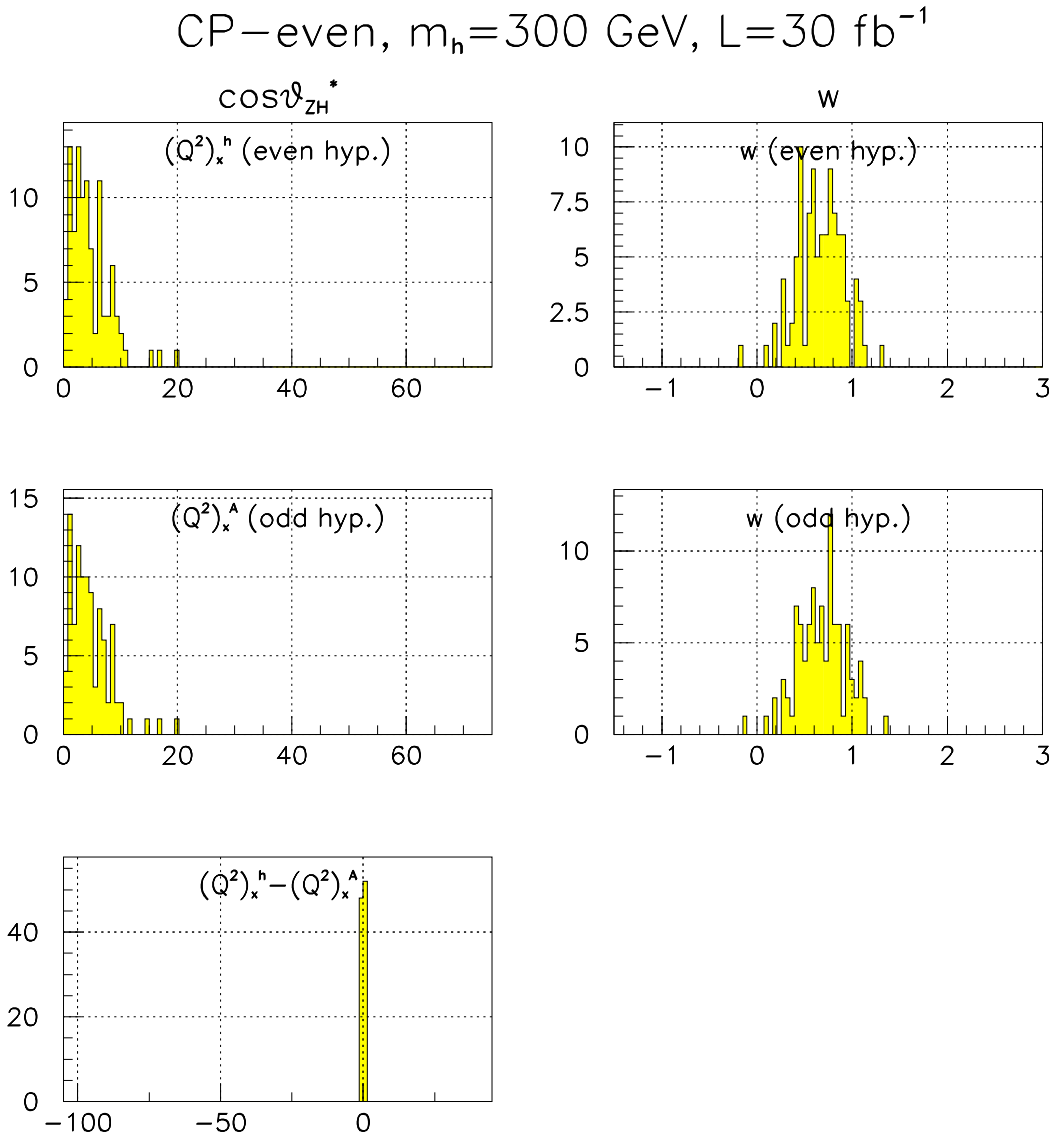

Figure B.34: Same as figure B.33, but for a lower integrated luminosity, 30 fb^{-1}.

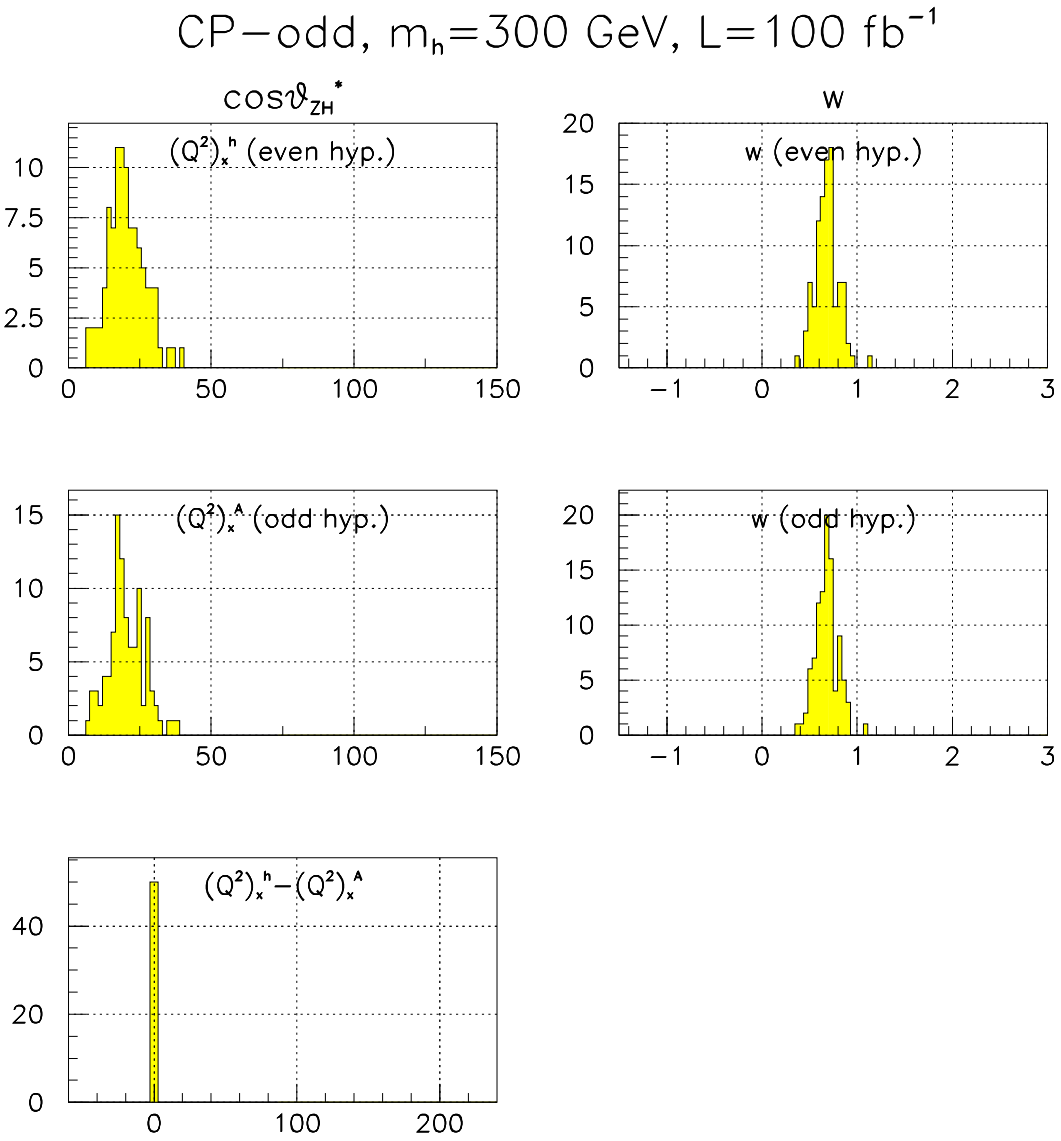

Figure B.35: The fraction of signal events in the experiments, w, and the observable $\cos\theta^*_{ZH}$. CP-odd Higgs boson with mass $m_h = 300$ GeV, integrated luminosity $\int \mathcal{L} dt = 100\ \text{fb}^{-1}$. The fraction w is shown for the CP-even and the CP-odd hypothesis. The histogram of $(Q^2)^a_x$ is shown for the CP-even hypothesis $a = h$ and for the CP-odd hypothesis $a = A$. The difference between the values of $(Q^2)^a_x$ for the two hypotheses, $(Q^2)^h_x - (Q^2)^A_x$, is also shown. Here x stands for the observable $\cos\theta^*_{ZH}$.

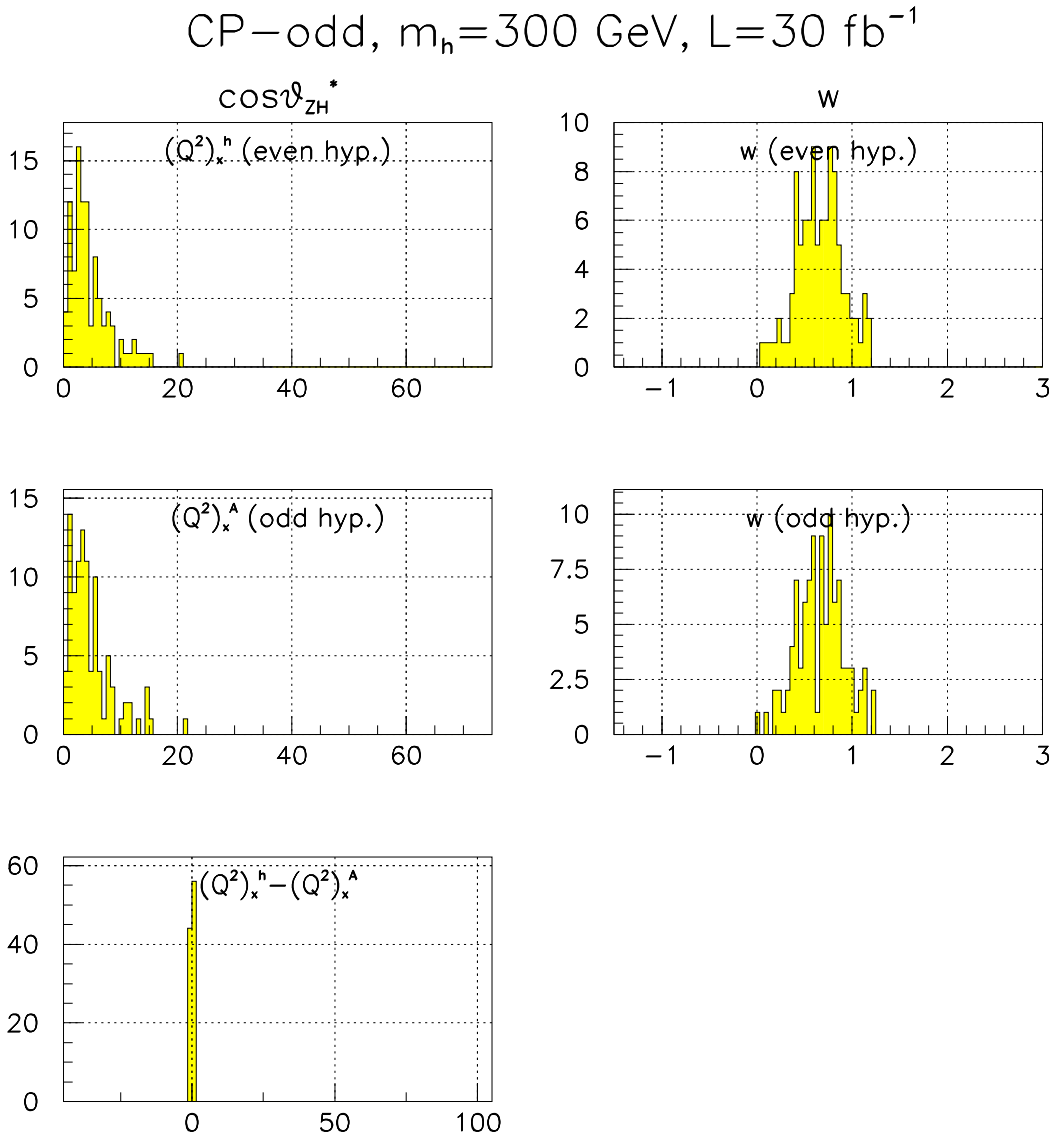

Figure B.36: Same as figure B.35, but for a lower integrated luminosity, 30 fb^{-1}.

Appendix C

Fortran Code

This appendix contains the source code of a fortran program I have used for the simulation of experiments and for the statistical analysis.

In order to compile the program, it has to be linked with PYTHIA (the modifications described in section 4.2 are included in the version 6.206 of PYTHIA), and with CERNLIB. Use the following commands (in Linux or UNIX):

```
> f77 -c pythia6206.f
```

This produces the file `pythia6206.o`, which can be linked with other fortran programs, without being compiled again (saves a lot of time).

```
> f77 -o stat stat.f pythia6206.o -L/cern/pro/lib -lpdflib
 -lpacklib -lmathlib -lkernlib -lphtools -lnsl -lcrypt -ldl
```

This command compiles the file `stat.f` and links it with `pythia6206.o` and CERNLIB (CERNLIB might be placed somewhere else on a different server). The CERNLIB library is needed for the HBOOK routines in the program. The executable file produced gets the name `stat`.

Here follows the source code of the fortran program `STAT`:

```
      PROGRAM STAT

C...Simulating NEXP "experiments" with number of signal and background
C...events chosen around the expectation values after a Poisson
C...distribution. For each "experiment", calculate chi^2 for the
C...hypothesis H=S and H=PS. Histogram distributions in chi^2.

C...All real arithmetic in double precision.
      IMPLICIT DOUBLE PRECISION(A-H, O-Z)
C...Three Pythia functions return integers, so need declaring.
      INTEGER PYK,PYCHGE,PYCOMP
C...Parameter statement to help give large particle numbers
```

```
C...(left- and right-handed SUSY, Technicolour, excited fermions,
C...extra dimensions).
      PARAMETER (KSUSY1=1000000,KSUSY2=2000000,KTECHN=3000000,
     &KEXCIT=4000000,KDIMEN=5000000)

      integer nwpawc
      parameter (nwpawc=1000000)
      integer ipaw
      common /pawc/ ipaw(nwpawc)

C...EXTERNAL statement links PYDATA on most machines.
      EXTERNAL PYDATA

C...Commonblocks.
C...The event record.
      COMMON/PYJETS/N,NPAD,K(4000,5),P(4000,5),V(4000,5)
C...Parameters.
      COMMON/PYDAT1/MSTU(200),PARU(200),MSTJ(200),PARJ(200)
C...Particle properties + some flavour parameters.
      COMMON/PYDAT2/KCHG(500,4),PMAS(500,4),PARF(2000),VCKM(4,4)
C...Decay information.
      COMMON/PYDAT3/MDCY(500,3),MDME(8000,2),BRAT(8000),KFDP(8000,5)
C...Selection of hard scattering subprocesses.
      COMMON/PYSUBS/MSEL,MSELPD,MSUB(500),KFIN(2,-40:40),CKIN(200)
C...Parameters.
      COMMON/PYPARS/MSTP(200),PARP(200),MSTI(200),PARI(200)
C...Supersymmetry parameters.
      COMMON/PYMSSM/IMSS(0:99),RMSS(0:99)

C...Vectors and type definitions
      CHARACTER *13 NAME
      REAL CTHE1, CTHE3, PHI13, CTHE13, CTHEWH, CTHEWZ
      REAL PI
      REAL FSCS, FPSS, GS, HS, WSCD(5), WSCN(5), WSC(5)
      REAL WPSD(5), WPSN(5), WPS(5), WSCA, WPSA
      REAL CH2SC(5), CH2PS(5), CH2SCA, CH2PSA
      DIMENSION IFM(4)
      DIMENSION ILEPT(10), IPAIR(4,2)
      REAL FSCHI1(20), FPSHI1(20), GHIST1(20), HHIST1(20)
      REAL FSCHI2(20), FPSHI2(20), GHIST2(20), HHIST2(20)
      REAL FSCHI3(20), FPSHI3(20), GHIST3(20), HHIST3(20)
      REAL FSCHI4(20), FPSHI4(20), GHIST4(20), HHIST4(20)
      REAL FSCHI5(20), FPSHI5(20), GHIST5(20), HHIST5(20)
```

```
      REAL AMUS, AMUB

C...Invariant mass function
      XM2(I,J)=SQRT((P(I,4)+P(J,4))**2-(P(I,1)+P(J,1))**2-
     &         (P(I,2)+P(J,2))**2-(P(I,3)+P(J,3))**2)

C...Set the length of array IPAW(NWPAWC)
      CALL HLIMIT(nwpawc)

C...Number of experiments, number of events per experiment.
C...Type of signal: (1) scalar or (2) pseudoscalar.
C...Name of ouput file (.hbook).
      NEXP=100
      ISIG=1
      AMUS=203.
      AMUB=87.
      NAME='stathl/chi2__'
C...Initial and final state radiation on (1) or off (2)
C...Also hadronisation, fragmentation and decays on (1) or off (2)
      MRADI=1
      MRADF=2
      MHADR=2

C...Kinematic cuts on events before simulating (internal PYTHIA).
      CKIN(1)=280D0
      CKIN(2)=320D0
      CKIN(41)=20D0
      CKIN(43)=20D0

C...Pick Higgs mass and decay mode, h0 -> ZZ
      PMAS(25,1)=300D0
      KZ=23
      IWZ=KZ

C...Only allow H decay to selected channel.
      DO 100 IDC=MDCY(25,2),MDCY(25,2)+MDCY(25,3)-1
        IF(IABS(KFDP(IDC,1)).NE.IWZ.OR.IABS(KFDP(IDC,2)).NE.IWZ)
     &  MDME(IDC,1)=MIN(0,MDME(IDC,1))
 100  CONTINUE

C...Only allow W/Z decays to leptons.
      DO 110 IDC=MDCY(24,2),MDCY(24,2)+MDCY(24,3)-1
        IF(IABS(KFDP(IDC,1)).LE.10.OR.IABS(KFDP(IDC,1)).GE.20)
```

```
     &  MDME(IDC,1)=MIN(0,MDME(IDC,1))
 110  CONTINUE
      DO 120 IDC=MDCY(23,2),MDCY(23,2)+MDCY(23,3)-1
        IF(IABS(KFDP(IDC,1)).NE.11.AND.IABS(KFDP(IDC,1)).NE.13)
     &  MDME(IDC,1)=MIN(0,MDME(IDC,1))
 120  CONTINUE

C...Switch off showers and hadronization for quick and dirty simulation.
C...Initial and final state radiation.
      IF(MRADI.EQ.2) MSTP(61)=0
      IF(MRADF.EQ.2) MSTP(71)=0
      IF(MHADR.EQ.2) THEN
         MSTP(81)=0
         MSTP(91)=0
         MSTP(111)=0
         MSTJ(1)=0
         MSTJ(21)=0
      ENDIF

C...Set history option for simpler search.
      MSTP(128)=1

C...Book histograms for distributions of W and chi^2.
      PI=PARU(1)
      CALL HBOOK1(11,'CTEH1, Weight W, Scalar hyp.',
     &     100, -1.5, 3., 0.0)
      CALL HBOOK1(12,'CTEH1, Weight W, Pseudosc hyp.',
     &     100, -1.5, 3., 0.0)
      CALL HBOOK1(13,'CTEH1, Chi2, Scalar hyp.', 100, 0., 150., 0.0)
      CALL HBOOK1(14,'CTEH1, Chi2, Pseudo hyp.', 100, 0., 240., 0.0)
      CALL HBOOK1(15,'CTEH1, (Chi2)sc - (Chi2)ps',
     &     100, -140., 60., 0.0)
      CALL HBOOK1(21,'CTEH3, Weight W, Scalar hyp.',
     &     100, -1.5, 3., 0.0)
      CALL HBOOK1(22,'CTEH3, Weight W, Pseudosc hyp.',
     &     100, -1.5, 3., 0.0)
      CALL HBOOK1(23,'CTEH3, Chi2, Scalar hyp.', 100, 0., 150., 0.0)
      CALL HBOOK1(24,'CTEH3, Chi2, Pseudo hyp.', 100, 0., 240., 0.0)
      CALL HBOOK1(25,'CTEH3, (Chi2)sc - (Chi2)ps',
     &     100, -140., 60., 0.0)
      CALL HBOOK1(31,'PHI13, Weight W, Scalar hyp.',
     &     100, -1.5, 3., 0.0)
      CALL HBOOK1(32,'PHI13, Weight W, Pseudosc hyp.',
```

```
     &     100, -1.5, 3., 0.0)
      CALL HBOOK1(33,'PHI13, Chi2, Scalar hyp.', 100, 0., 150., 0.0)
      CALL HBOOK1(34,'PHI13, Chi2, Pseudo hyp.', 100, 0., 240., 0.0)
      CALL HBOOK1(35,'PHI13, (Chi2)sc - (Chi2)ps',
     &     100, -140., 60., 0.0)
      CALL HBOOK1(41,'CTEH13, Weight W, Scalar hyp.',
     &     100, -1.5, 3., 0.0)
      CALL HBOOK1(42,'CTEH13, Weight W, Pseudosc hyp.',
     &     100, -1.5, 3., 0.0)
      CALL HBOOK1(43,'CTEH13, Chi2, Scalar hyp.', 100, 0., 150., 0.0)
      CALL HBOOK1(44,'CTEH13, Chi2, Pseudo hyp.', 100, 0., 240., 0.0)
      CALL HBOOK1(45,'CTEH13, (Chi2)sc - (Chi2)ps',
     &     100, -140., 60., 0.0)
      CALL HBOOK1(51,'CTEHWH, Weight W, Scalar hyp.',
     &     100, -1.5, 3., 0.0)
      CALL HBOOK1(52,'CTEHWH, Weight W, Pseudosc hyp.',
     &     100, -1.5, 3., 0.0)
      CALL HBOOK1(53,'CTEHWH, Chi2, Scalar hyp.', 100, 0., 150., 0.0)
      CALL HBOOK1(54,'CTEHWH, Chi2, Pseudo hyp.', 100, 0., 240., 0.0)
      CALL HBOOK1(55,'CTEHWH, (Chi2)sc - (Chi2)ps',
     &     100, -140., 60., 0.0)
      CALL HBOOK1(63,'Sum chi2, Scalar hyp.', 100, 0., 500., 0.0)
      CALL HBOOK1(64,'Sum chi2, Pseudo hyp.', 100, 0., 500., 0.0)
      CALL HBOOK1(65,'Sum (Chi2)sc - (Chi2)ps', 100, -560., 240., 0.0)

C...Open .hook file with distributions for signal and background
      CALL HCDIR('//PAWC',' ')
      CALL HROPEN(50,'SLUGRZ','tford/fhisth.hbook',' ',1024,ISTAT)
      IF(ISTAT.NE.0) print*,' Error from HROPEN!!! ISTAT=',ISTAT

C...Get histo from current working directory
      CALL HCDIR('//SLUGRZ',' ')
      CALL HRGET(301,' ',' ')
      CALL HRGET(302,' ',' ')
      CALL HRGET(303,' ',' ')
      CALL HRGET(304,' ',' ')
      CALL HRGET(305,' ',' ')
      GS=HSUM(301)
      WRITE(*,*) 'GS=', GS
      CALL HUNPAK(301, GHIST1, ' ', 0)
      CALL HUNPAK(302, GHIST2, ' ', 0)
      CALL HUNPAK(303, GHIST3, ' ', 0)
      CALL HUNPAK(304, GHIST4, ' ', 0)
```

```
      CALL HUNPAK(305, GHIST5, ' ', 0)

      CALL HRGET(101,' ',' ')
      CALL HRGET(102,' ',' ')
      CALL HRGET(103,' ',' ')
      CALL HRGET(104,' ',' ')
      CALL HRGET(105,' ',' ')
      FSCS=HSUM(101)
      WRITE(*,*) 'FSCS=', FSCS
      CALL HUNPAK(101, FSCHI1, ' ', 0)
      CALL HUNPAK(102, FSCHI2, ' ', 0)
      CALL HUNPAK(103, FSCHI3, ' ', 0)
      CALL HUNPAK(104, FSCHI4, ' ', 0)
      CALL HUNPAK(105, FSCHI5, ' ', 0)

      CALL HRGET(201,' ',' ')
      CALL HRGET(202,' ',' ')
      CALL HRGET(203,' ',' ')
      CALL HRGET(204,' ',' ')
      CALL HRGET(205,' ',' ')
      FPSS=HSUM(201)
      WRITE(*,*) 'FPSS=', FPSS
      CALL HUNPAK(201, FPSHI1, ' ', 0)
      CALL HUNPAK(202, FPSHI2, ' ', 0)
      CALL HUNPAK(203, FPSHI3, ' ', 0)
      CALL HUNPAK(204, FPSHI4, ' ', 0)
      CALL HUNPAK(205, FPSHI5, ' ', 0)

      CALL HDELET (101)
      CALL HDELET (102)
      CALL HDELET (103)
      CALL HDELET (104)
      CALL HDELET (105)
      CALL HDELET (201)
      CALL HDELET (202)
      CALL HDELET (203)
      CALL HDELET (204)
      CALL HDELET (205)
      CALL HDELET (301)
      CALL HDELET (302)
      CALL HDELET (303)
      CALL HDELET (304)
      CALL HDELET (305)
```

```
C...Close hbook files.
      CALL HREND('SLUGRZ')
      CLOSE (50)

C...Normalize distributions FSC, FPS and G.
      DO IBIN=1,20
         GHIST1(IBIN)=GHIST1(IBIN)/GS
         GHIST2(IBIN)=GHIST2(IBIN)/GS
         GHIST3(IBIN)=GHIST3(IBIN)/GS
         GHIST4(IBIN)=GHIST4(IBIN)/GS
         GHIST5(IBIN)=GHIST5(IBIN)/GS
         FSCHI1(IBIN)=FSCHI1(IBIN)/FSCS
         FSCHI2(IBIN)=FSCHI2(IBIN)/FSCS
         FSCHI3(IBIN)=FSCHI3(IBIN)/FSCS
         FSCHI4(IBIN)=FSCHI4(IBIN)/FSCS
         FSCHI5(IBIN)=FSCHI5(IBIN)/FSCS
         FPSHI1(IBIN)=FPSHI1(IBIN)/FPSS
         FPSHI2(IBIN)=FPSHI2(IBIN)/FPSS
         FPSHI3(IBIN)=FPSHI3(IBIN)/FPSS
         FPSHI4(IBIN)=FPSHI4(IBIN)/FPSS
         FPSHI5(IBIN)=FPSHI5(IBIN)/FPSS
      ENDDO

************************************************************
C...Loop over experiments
      DO 500, IEXP=1, NEXP
C      DO 500, IEXP=1,10
         WRITE(*,*) 'IEXP ', IEXP

C...Choose number of signal and background events after Poisson.
      CALL RNPSSN(AMUS, NSEV, IERR)
      IF(IERR.NE.0) THEN
         WRITE(*,*) 'Error in RNPSSN'
         GOTO 900
      ENDIF
      CALL RNPSSN(AMUB, NBEV, IERR)
      IF(IERR.NE.0) THEN
         WRITE(*,*) 'Error in RNPSSN'
         GOTO 900
      ENDIF
      WRITE(*,*) 'NSEV=', NSEV
      WRITE(*,*) 'NBEV=', NBEV
```

```
C...Book histograms
      PI=PARU(1)
      CALL HBOOK1(1001,'CTHE1', 20, -1., 1., 0.0)
      CALL HBOOK1(1002,'CTHE3', 20, -1., 1., 0.0)
      CALL HBOOK1(1003,'PHI13', 20, 0., PI, 0.0)
      CALL HBOOK1(1004,'CTHE13', 20, -1., 1., 0.0)
      CALL HBOOK1(1005,'CTHEWH', 20, -1., 1., 0.0)

C...Pick process. Loop over CP-even (1), CP-odd (2) or background (3).
      MSEL=0

      DO 300 MODE=1,3
      IF(ISIG.EQ.1.AND.MODE.EQ.2) GOTO 300
      IF(ISIG.EQ.2.AND.MODE.EQ.1) GOTO 300

      WRITE(*,*) 'MODE ', MODE
      MSUB(102)=0
      MSUB(22)=0
C...g + g -> h0
      IF(MODE.NE.3) MSUB(102)=1
C...q + qbar -> Z + Z
      IF(MODE.EQ.3) MSUB(22)=1

C...Choose CP-even or CP-odd.
      IF(MODE.EQ.1) MSTP(25)=1
      IF(MODE.EQ.2) MSTP(25)=2

C...Initialize for LHC.
      CALL PYINIT('cms','p','p',14000D0)

C...Initialize number of events escaping cuts.
      NCUTS=0

C...Loop over events, and generate them. List first few events.
      IEV=0
 150  CONTINUE
        IEV=IEV+1
        CALL PYEVNT
C        IF(IEV.LE.5) WRITE(*,*) 'IEV ', IEV
C        IF(IEV.EQ.500) WRITE(*,*) 'IEV ', IEV
C        IF(IEV.EQ.5000) WRITE(*,*) 'IEV ', IEV
C        IF(IEV.LE.5) CALL PYLIST(1)
```

```
C...Find leptons that satisfy the kinematics
C...cuts pt>7GeV and abs(eta)<2.5.
        NLE=0
        DO ILE=1,10
           ILEPT(ILE)=0
        ENDDO
        DO I=1,N
           IABSK=IABS(K(I,2))
           IF((IABSK.EQ.13.OR.IABSK.EQ.11).AND.K(I,1).LT.20.AND.
     &        PYP(I,10).GT.7D0.AND.ABS(PYP(I,19)).LT.2.5D0) THEN
              NLE=NLE+1
C...Ends program if too many leptons
              IF(NLE.GE.10) THEN
                 WRITE(*,*) 'Number of leptons larger than 10'
                 GOTO 900
              ELSE
                 ILEPT(NLE)=I
              ENDIF
           ENDIF
        ENDDO
C...Throw away events that do not satisfy cuts.
        IF(NLE.LT.4) GO TO 150

C...Satisfy 2 leptons with pt>20GeV
        NLPT=0
        DO ILE=1,NLE
           IF(PYP(ILEPT(ILE),10).GT.20D0) NLPT=NLPT+1
        ENDDO
        IF(NLPT.LT.2) GOTO 150

C...Cuts on invariant masses
        IF(NLE.GT.4) THEN
           WRITE(11,*) 'IEV, NLE: ', IEV, NLE
           GOTO 150
        ENDIF
C...Mass of 4 leptons
        P1=0D0
        P2=0D0
        P3=0D0
        P4=0D0
        DO ILE=1,4
           P1=P1+P(ILEPT(ILE),1)
```

```
            P2=P2+P(ILEPT(ILE),2)
            P3=P3+P(ILEPT(ILE),3)
            P4=P4+P(ILEPT(ILE),4)
         ENDDO
         XM4=P4**2-P1**2-P2**2-P3**2
         IF(XM4.LE.0D0) THEN
            WRITE(*,*) 'XM4^2=', XM4, 'in event ', IEV
            GOTO 900
         ENDIF
         XM4=SQRT(XM4)
C...Cut on 4 lepton invariant mass
         GAMMH=PMAS(25,2)
C         WRITE(*,*) GAMMH
         SIGMH=1.64D0*SQRT((GAMMH/2.36)**2+(0.02*PMAS(25,1))**2)
C         WRITE(*,*) SIGMH
         IF(ABS(XM4-PMAS(25,1)).GE.SIGMH) GOTO 150
C...Make particle-antiparticle pairs and cut on 2 lepton invariant masses
         NPA=0
         DO ILE=1,3
            DO JLE=ILE+1,4
               I1=ILEPT(ILE)
               I2=ILEPT(JLE)
               IF(K(I1,2)+K(I2,2).EQ.0) THEN
                  XM=XM2(I1,I2)
                  SIGMZ=6D0
                  IF(ABS(XM-PMAS(23,1)).LT.SIGMZ) THEN
                     NPA=NPA+1
                     IF(NPA.GT.4) THEN
                        WRITE(*,*) 'NPA=', NPA, ' in event number ', IEV
                        GOTO 900
                     ENDIF
                     IF(K(I1,2).GT.0) THEN
                        IPAIR(NPA,1)=I1
                        IPAIR(NPA,2)=I2
                     ELSEIF(K(I2,2).GT.0) THEN
                        IPAIR(NPA,1)=I2
                        IPAIR(NPA,2)=I1
                     ELSE
                        WRITE(*,*) 'Not particle-antiparticle'
                        GOTO 900
                     ENDIF
                  ENDIF
               ENDIF
```

```
           ENDDO
         ENDDO
         IF(NPA.LT.2) GOTO 150

C...When more than 2 pairs, choose the two best ones
         IF(NPA.GT.2) THEN
            NFMP=0
            XMDB=100D0
            DO IPA=1,NPA-1
               DO 160 JPA=IPA+1,NPA
                  IF(IPAIR(IPA,1).EQ.IPAIR(JPA,1).OR.
     &               IPAIR(IPA,2).EQ.IPAIR(JPA,2)) THEN
                     GOTO 160
                  ELSE
                     NFMP=NFMP+1
                     I1=IPAIR(IPA,1)
                     I2=IPAIR(IPA,2)
                     I3=IPAIR(JPA,1)
                     I4=IPAIR(JPA,2)
                     XMD=ABS(XM2(I1,I2)-PMAS(23,1))+
     &                    ABS(XM2(I3,I4)-PMAS(23,1))
                     IF(XMD.LT.XMDB) THEN
                        XMDB=XMD
                        IFM(1)=I1
                        IFM(2)=I2
                        IFM(3)=I3
                        IFM(4)=I4
                     ENDIF
                  ENDIF
 160           CONTINUE
            ENDDO
            IF(NFMP.EQ.0) GOTO 150
         ELSEIF(NPA.EQ.2) THEN
            IF(IPAIR(1,1).EQ.IPAIR(2,1).OR.
     &         IPAIR(1,2).EQ.IPAIR(2,2)) THEN
               GOTO 150
            ELSE
               IFM(1)=IPAIR(1,1)
               IFM(2)=IPAIR(1,2)
               IFM(3)=IPAIR(2,1)
               IFM(4)=IPAIR(2,2)
               XMDB=ABS(XM2(IFM(1),IFM(2))-PMAS(23,1))+
     &              ABS(XM2(IFM(3),IFM(4))-PMAS(23,1))
```

```
          ENDIF
        ENDIF
        IF(IFM(1).EQ.IFM(3).OR.
     &       IFM(2).EQ.IFM(4)) THEN
          WRITE(*,*) 'Not four distinct fermions in event number ',
     &          IEV
          GOTO 900
        ELSEIF(XMDB.GT.12D0) THEN
          WRITE(*,*) 'XMDB=', XMDB, ' in event number ', IEV
          GOTO 900
        ENDIF
        NCUTS=NCUTS+1


C...Check with "simple" lepton ID that we have chosen "right" pairs
C...Find VV and Higgs positions.
        IHIGG=0
        IWP=0
        IWM=0
        NZ=0
        DO 170 I=1,N
          IF(K(I,1).LT.20) THEN
            IF(K(I,2).EQ.25) IHIGG=I
            IF(K(I,2).EQ.KZ) THEN
              NZ=NZ+1
              IF(NZ.EQ.1) IWP=I
              IF(NZ.EQ.2) IWM=I
            ENDIF
          ENDIF
 170    CONTINUE
        IF(NZ.GT.2) THEN
          WRITE(*,*) 'NZ=', NZ, 'in event number ', IEV
          GOTO 900
        ENDIF
C...Identify fermions (and antifermions) by W+- ancestry.
        IF(MODE.NE.3) NROBO=IHIGG
        IF(MODE.EQ.3) NROBO=MIN(IWP,IWM)
        IFM1=0
        IFM2=0
        IFM3=0
        IFM4=0
        DO 180 I=NROBO+1,N
          IF(K(I,3).EQ.IWP) THEN
```

```
            IF(K(I,2).GT.0) IFM1=I
            IF(K(I,2).LT.0) IFM2=I
          ELSEIF(K(I,3).EQ.IWM) THEN
            IF(K(I,2).GT.0) IFM3=I
            IF(K(I,2).LT.0) IFM4=I
          ENDIF
 180    CONTINUE
C...Check that IFM-pairs are identical with the two methods.
        IF(IFM(1).EQ.IFM1.AND.IFM(2).EQ.IFM2.AND.
     &       IFM(3).EQ.IFM3.AND.IFM(4).EQ.IFM4) THEN
          IWPA=0
        ELSEIF(IFM(1).EQ.IFM3.AND.IFM(2).EQ.IFM4.AND.
     &         IFM(3).EQ.IFM1.AND.IFM(4).EQ.IFM2) THEN
          IWPA=0
        ELSE
          IWPA=1
        ENDIF

C...Boost to f1, f2, f3, f4 COM frame.
        P1=P(IFM(1),1)+P(IFM(2),1)+P(IFM(3),1)+P(IFM(4),1)
        P2=P(IFM(1),2)+P(IFM(2),2)+P(IFM(3),2)+P(IFM(4),2)
        P3=P(IFM(1),3)+P(IFM(2),3)+P(IFM(3),3)+P(IFM(4),3)
        P4=P(IFM(1),4)+P(IFM(2),4)+P(IFM(3),4)+P(IFM(4),4)
        CALL PYROBO(0,0,0D0,0D0,-P1/P4,-P2/P4,-P3/P4)

C...Calculate the angle cos(theta*_W+).
        PP1=P(IFM(1),1)+P(IFM(2),1)
        PP2=P(IFM(1),2)+P(IFM(2),2)
        PP3=P(IFM(1),3)+P(IFM(2),3)
        PABSH=SQRT(P1**2+P2**2+P3**2)
        PABSW=SQRT(PP1**2+PP2**2+PP3**2)
        CTHWH=(P1*PP1+P2*PP2
     &    +P3*PP3)/(PABSH*PABSW)
        CTHWZ=PP3/PABSW

C...Rotate so that W+ is along +z axis.
        PHIWP=PYANGL(PP1,PP2)
        CALL PYROBO(0,0,0D0,-PHIWP,0D0,0D0,0D0)
        PP1=P(IFM(1),1)+P(IFM(2),1)
        PP3=P(IFM(1),3)+P(IFM(2),3)
        THEWP=PYANGL(PP3,PP1)
        CALL PYROBO(0,0,-THEWP,0D0,0D0,0D0,0D0)
```

```
C...Boost the fermions to the rest frame of the respective W.
        PP1=P(IFM(1),1)+P(IFM(2),1)
        PP2=P(IFM(1),2)+P(IFM(2),2)
        PP3=P(IFM(1),3)+P(IFM(2),3)
        PP4=P(IFM(1),4)+P(IFM(2),4)
        PM1=P(IFM(3),1)+P(IFM(4),1)
        PM2=P(IFM(3),2)+P(IFM(4),2)
        PM3=P(IFM(3),3)+P(IFM(4),3)
        PM4=P(IFM(3),4)+P(IFM(4),4)
        CALL PYROBO(IFM(1),IFM(1),0D0,0D0,-PP1/PP4,
     &  -PP2/PP4,-PP3/PP4)
        CALL PYROBO(IFM(2),IFM(2),0D0,0D0,-PP1/PP4,
     &  -PP2/PP4,-PP3/PP4)
        CALL PYROBO(IFM(3),IFM(3),0D0,0D0,-PM1/PM4,
     &  -PM2/PM4,-PM3/PM4)
        CALL PYROBO(IFM(4),IFM(4),0D0,0D0,-PM1/PM4,
     &  -PM2/PM4,-PM3/PM4)
C        IF(IEV.LE.5) CALL PYLIST(1)

C...Calculate relative angles.
        PABS1=SQRT(P(IFM(1),1)**2+P(IFM(1),2)**2+P(IFM(1),3)**2)
        PABS2=SQRT(P(IFM(2),1)**2+P(IFM(2),2)**2+P(IFM(2),3)**2)
        PABS3=SQRT(P(IFM(3),1)**2+P(IFM(3),2)**2+P(IFM(3),3)**2)
        PABS4=SQRT(P(IFM(4),1)**2+P(IFM(4),2)**2+P(IFM(4),3)**2)
        CTH1=P(IFM(1),3)/PABS1
        CTH2=P(IFM(2),3)/PABS2
        CTH3=P(IFM(3),3)/PABS3
        CTH4=P(IFM(4),3)/PABS4
        CTH13=(P(IFM(1),1)*P(IFM(3),1)+P(IFM(1),2)*P(IFM(3),2)+
     &  P(IFM(1),3)*P(IFM(3),3))/(PABS1*PABS3)
        PH13=PYANGL(P(IFM(1),1),P(IFM(1),2))
     &    -PYANGL(P(IFM(3),1),P(IFM(3),2))
        IF(PH13.LT.-PI) PH13=PH13+2D0*PI
        IF(PH13.GT.PI) PH13=PH13-2D0*PI
        IF(PH13.LT.0) PH13=-PH13

C...Set angular variables.
        CTHE1=CTH1
        CTHE3=CTH3
        CTHE13=CTH13
        CTHEWH=CTHWH
        CTHEWZ=CTHWZ
        PHI13=PH13
```

```
C...Fill histograms
      CALL HF1(1001, CTHE1, 1.)
      CALL HF1(1002, CTHE3, 1.)
      CALL HF1(1003, PHI13, 1.)
      CALL HF1(1004, CTHE13, 1.)
      CALL HF1(1005, CTHEWH, 1.)
C      CALL HF2(1006, CTHE13, PHI13, 1.)

C...End of event loop
C        IF(MODE.EQ.1.AND.NCUTS.LT.NSEV) GOTO 150
C        IF(MODE.EQ.2.AND.NCUTS.LT.NPSEV) GOTO 150
         IF(MODE.NE.3.AND.NCUTS.LT.NSEV) GOTO 150
         IF(MODE.EQ.3.AND.NCUTS.LT.NBEV) GOTO 150

         WRITE(*,*) 'IEV ', IEV
         WRITE(*,*) 'NCUTS ', NCUTS

C...End loop over modes (signal and background).
 300  CONTINUE

C...Write histos to file
c      IF(IEXP.EQ.1) THEN
c         CALL HRPUT(1001,NAME//'1.hbook','N')
c         CALL HRPUT(1002,NAME//'1.hbook','U')
c         CALL HRPUT(1003,NAME//'1.hbook','U')
c         CALL HRPUT(1004,NAME//'1.hbook','U')
c         CALL HRPUT(1005,NAME//'1.hbook','U')
c      ENDIF

*****************************************************
C...STATISTICAL ANALYSIS
C...Write histogram H to array.
      HS=HSUM(1001)
      IF(IEXP.LE.5) WRITE(*,*) 'HS= ', HS
      CALL HUNPAK(1001, HHIST1, ' ', 0)
      CALL HUNPAK(1002, HHIST2, ' ', 0)
      CALL HUNPAK(1003, HHIST3, ' ', 0)
      CALL HUNPAK(1004, HHIST4, ' ', 0)
      CALL HUNPAK(1005, HHIST5, ' ', 0)
      CALL HDELET (1001)
      CALL HDELET (1002)
      CALL HDELET (1003)
```

```
      CALL HDELET (1004)
      CALL HDELET (1005)

C...SCALAR hypotesis:
C...Find the denominator of the weight W.
C...Find the numerator, W=WN/WD.
      DO IX=1,5
         WSCD(IX)=0.
         WSCN(IX)=0.
         WSC(IX)=0.
      ENDDO
      DO IBIN=1,20
         IF(HHIST1(IBIN).EQ.0) THEN
            WRITE(*,*) 'Empty bin in HHIST1'
            GOTO 900
         ELSEIF(HHIST2(IBIN).EQ.0) THEN
            WRITE(*,*) 'Empty bin in HHIST2'
            GOTO 900
         ELSEIF(HHIST3(IBIN).EQ.0) THEN
            WRITE(*,*) 'Empty bin in HHIST3'
            GOTO 900
         ELSEIF(HHIST4(IBIN).EQ.0) THEN
            WRITE(*,*) 'Empty bin in HHIST4'
            GOTO 900
         ELSEIF(HHIST5(IBIN).EQ.0) THEN
            WRITE(*,*) 'Empty bin in HHIST5'
            GOTO 900
         ENDIF
         WSCD(1)=WSCD(1)+(HS*FSCHI1(IBIN)-HS*GHIST1(IBIN))**2/
     &        HHIST1(IBIN)
         WSCD(2)=WSCD(2)+(HS*FSCHI2(IBIN)-HS*GHIST2(IBIN))**2/
     &        HHIST2(IBIN)
         WSCD(3)=WSCD(3)+(HS*FSCHI3(IBIN)-HS*GHIST3(IBIN))**2/
     &        HHIST3(IBIN)
         WSCD(4)=WSCD(4)+(HS*FSCHI4(IBIN)-HS*GHIST4(IBIN))**2/
     &        HHIST4(IBIN)
         WSCD(5)=WSCD(5)+(HS*FSCHI5(IBIN)-HS*GHIST5(IBIN))**2/
     &        HHIST5(IBIN)
         WSCN(1)=WSCN(1)+(HHIST1(IBIN)-HS*GHIST1(IBIN))*
     &        (HS*FSCHI1(IBIN)-HS*GHIST1(IBIN))/HHIST1(IBIN)
         WSCN(2)=WSCN(2)+(HHIST2(IBIN)-HS*GHIST2(IBIN))*
     &        (HS*FSCHI2(IBIN)-HS*GHIST2(IBIN))/HHIST2(IBIN)
         WSCN(3)=WSCN(3)+(HHIST3(IBIN)-HS*GHIST3(IBIN))*
```

```
     &        (HS*FSCHI3(IBIN)-HS*GHIST3(IBIN))/HHIST3(IBIN)
         WSCN(4)=WSCN(4)+(HHIST4(IBIN)-HS*GHIST4(IBIN))*
     &        (HS*FSCHI4(IBIN)-HS*GHIST4(IBIN))/HHIST4(IBIN)
         WSCN(5)=WSCN(5)+(HHIST5(IBIN)-HS*GHIST5(IBIN))*
     &        (HS*FSCHI5(IBIN)-HS*GHIST5(IBIN))/HHIST5(IBIN)
      ENDDO
C...The weight W.
      DO IX=1,5
         IF(WSCD(IX).EQ.0.) THEN
            WRITE(*,*) 'WSCD(IX)=0'
            GOTO 900
         ENDIF
         WSC(IX)=WSCN(IX)/WSCD(IX)
      ENDDO
C...Use the w from CTHEWH
C...Chi^2
      DO IX=1,5
         CH2SC(IX)=0.
      ENDDO
      DO IBIN=1,20
         IF(HHIST3(IBIN).EQ.0) THEN
            WRITE(*,*) 'Empty bin in HHIST3'
            GOTO 900
         ENDIF
         CH2SC(1)=CH2SC(1)+
     &        (HHIST1(IBIN)-WSC(5)*HS*FSCHI1(IBIN)-
     &        (1-WSC(5))*HS*GHIST1(IBIN))**2/HHIST1(IBIN)
         CH2SC(2)=CH2SC(2)+
     &        (HHIST2(IBIN)-WSC(5)*HS*FSCHI2(IBIN)-
     &        (1-WSC(5))*HS*GHIST2(IBIN))**2/HHIST2(IBIN)
         CH2SC(3)=CH2SC(3)+
     &        (HHIST3(IBIN)-WSC(5)*HS*FSCHI3(IBIN)-
     &        (1-WSC(5))*HS*GHIST3(IBIN))**2/HHIST3(IBIN)
         CH2SC(4)=CH2SC(4)+
     &        (HHIST4(IBIN)-WSC(5)*HS*FSCHI4(IBIN)-
     &        (1-WSC(5))*HS*GHIST4(IBIN))**2/HHIST4(IBIN)
         CH2SC(5)=CH2SC(5)+
     &        (HHIST5(IBIN)-WSC(5)*HS*FSCHI5(IBIN)-
     &        (1-WSC(5))*HS*GHIST5(IBIN))**2/HHIST5(IBIN)
      ENDDO
C...Take the sum over all chi2, except CTHEWH:
      CH2SCA=0.
      DO IX=1,4
```

```
         CH2SCA=CH2SCA+CH2SC(IX)
      ENDDO
      WRITE(*,*) 'CH2SCA=', CH2SCA

C...PSEUDOSCALAR hypotesis:
C...Find the denominator of the weight W.
C...Find the numerator, W=WN/WD.
      DO IX=1,5
         WPSD(IX)=0.
         WPSN(IX)=0.
         WPS(IX)=0.
      ENDDO
      DO IBIN=1,20
         IF(HHIST1(IBIN).EQ.0) THEN
            WRITE(*,*) 'Empty bin in HHIST1'
            GOTO 900
         ELSEIF(HHIST2(IBIN).EQ.0) THEN
            WRITE(*,*) 'Empty bin in HHIST2'
            GOTO 900
         ELSEIF(HHIST3(IBIN).EQ.0) THEN
            WRITE(*,*) 'Empty bin in HHIST3'
            GOTO 900
         ELSEIF(HHIST4(IBIN).EQ.0) THEN
            WRITE(*,*) 'Empty bin in HHIST4'
            GOTO 900
         ELSEIF(HHIST5(IBIN).EQ.0) THEN
            WRITE(*,*) 'Empty bin in HHIST5'
            GOTO 900
         ENDIF
         WPSD(1)=WPSD(1)+(HS*FPSHI1(IBIN)-HS*GHIST1(IBIN))**2/
     &        HHIST1(IBIN)
         WPSD(2)=WPSD(2)+(HS*FPSHI2(IBIN)-HS*GHIST2(IBIN))**2/
     &        HHIST2(IBIN)
         WPSD(3)=WPSD(3)+(HS*FPSHI3(IBIN)-HS*GHIST3(IBIN))**2/
     &        HHIST3(IBIN)
         WPSD(4)=WPSD(4)+(HS*FPSHI4(IBIN)-HS*GHIST4(IBIN))**2/
     &        HHIST4(IBIN)
         WPSD(5)=WPSD(5)+(HS*FPSHI5(IBIN)-HS*GHIST5(IBIN))**2/
     &        HHIST5(IBIN)
         WPSN(1)=WPSN(1)+(HHIST1(IBIN)-HS*GHIST1(IBIN))*
     &        (HS*FPSHI1(IBIN)-HS*GHIST1(IBIN))/HHIST1(IBIN)
         WPSN(2)=WPSN(2)+(HHIST2(IBIN)-HS*GHIST2(IBIN))*
     &        (HS*FPSHI2(IBIN)-HS*GHIST2(IBIN))/HHIST2(IBIN)
```

```
          WPSN(3)=WPSN(3)+(HHIST3(IBIN)-HS*GHIST3(IBIN))*
     &         (HS*FPSHI3(IBIN)-HS*GHIST3(IBIN))/HHIST3(IBIN)
          WPSN(4)=WPSN(4)+(HHIST4(IBIN)-HS*GHIST4(IBIN))*
     &         (HS*FPSHI4(IBIN)-HS*GHIST4(IBIN))/HHIST4(IBIN)
          WPSN(5)=WPSN(5)+(HHIST5(IBIN)-HS*GHIST5(IBIN))*
     &         (HS*FPSHI5(IBIN)-HS*GHIST5(IBIN))/HHIST5(IBIN)
       ENDDO
C...The weight W.
       DO IX=1,5
          IF(WPSD(IX).EQ.0.) THEN
             WRITE(*,*) 'WPSD(IX)=0'
             GOTO 900
          ENDIF
          WPS(IX)=WPSN(IX)/WPSD(IX)
       ENDDO
C...Use w from CTHEWH
C...Chi^2
       DO IX=1,5
          CH2PS(IX)=0.
       ENDDO
       DO IBIN=1,20
          IF(HHIST3(IBIN).EQ.0) THEN
             WRITE(*,*) 'Empty bin in HHIST3'
             GOTO 900
          ENDIF
          CH2PS(1)=CH2PS(1)+
     &         (HHIST1(IBIN)-WPS(5)*HS*FPSHI1(IBIN)-
     &         (1-WPS(5))*HS*GHIST1(IBIN))**2/HHIST1(IBIN)
          CH2PS(2)=CH2PS(2)+
     &         (HHIST2(IBIN)-WPS(5)*HS*FPSHI2(IBIN)-
     &         (1-WPS(5))*HS*GHIST2(IBIN))**2/HHIST2(IBIN)
          CH2PS(3)=CH2PS(3)+
     &         (HHIST3(IBIN)-WPS(5)*HS*FPSHI3(IBIN)-
     &         (1-WPS(5))*HS*GHIST3(IBIN))**2/HHIST3(IBIN)
          CH2PS(4)=CH2PS(4)+
     &         (HHIST4(IBIN)-WPS(5)*HS*FPSHI4(IBIN)-
     &         (1-WPS(5))*HS*GHIST4(IBIN))**2/HHIST4(IBIN)
          CH2PS(5)=CH2PS(5)+
     &         (HHIST5(IBIN)-WPS(5)*HS*FPSHI5(IBIN)-
     &         (1-WPS(5))*HS*GHIST5(IBIN))**2/HHIST5(IBIN)
       ENDDO
C...Take the sum over all chi2, except CTHEWH:
       CH2PSA=0.
```

```
      DO IX=1,4
         CH2PSA=CH2PSA+CH2PS(IX)
      ENDDO
      WRITE(*,*) 'CH2PSA=', CH2PSA

C...Fill histos
      DO IX=1,5
         CALL HF1(10*IX+1, WSC(IX), 1.)
         CALL HF1(10*IX+2, WPS(IX), 1.)
         CALL HF1(10*IX+3, CH2SC(IX), 1.)
         CALL HF1(10*IX+4, CH2PS(IX), 1.)
         CALL HF1(10*IX+5, (CH2SC(IX)-CH2PS(IX)), 1.)
      ENDDO
      CALL HF1(63, CH2SCA, 1.)
      CALL HF1(64, CH2PSA, 1.)
      CALL HF1(65, (CH2SCA-CH2PSA), 1.)


C...End loop over experiments.
 500  CONTINUE

 900  CONTINUE
C...Save histograms.
      CALL HRPUT(0,NAME//'.hbook','N')

 999  END
```

Bibliography

[1] A. Gurtu, *Invited talk at 30th International Conference on High energy physics (ICHEP 2000)*, Osaka, Japan, 27 July–2 August 2000.
Published in "Osaka 2000, Proceedings of the 30th International Conference on High energy physics" **vol. 1**, 107-118

[2] S. L. Glashow, *Nucl. Phys.* **22** (1961) 579 ; S. Weinberg, *Phys. Rev. Lett.* **19** (1967) 1264 ; A. Salam, in *Elementary Particle Theory: Relativistic Groups and Analyticity (Nobel Symposium No. 8)*, edited by N. Svartholm (Almqvist and Wiksell, Stockholm, 1968), p. 367; S. L. Glashow, J. Iliopoulos and L. Maiani, *Phys. Rev.* **D2** (1970) 1285

[3] F. Mandl and G. Shaw, *Quantum Field Theory* (Revised Edition), John Wiley and Sons Ltd, 1993

[4] J. F. Gunion, H. E. Haber, G. Kane and S. Dawson, *The Higgs Hunters Guide*, Perseus Books, 1990

[5] F. Zwirner, *Invited talk at 20th International Symposium on Lepton and Photon Interactions at High Energies (Lepton Photon 01)*, Rome, Italy, 23-28 Jul 2001, [arXiv:hep-ph/0112130]

[6] A. Pilaftsis and C. E. M. Wagner, *Nucl. Phys.* **B553** (1999) 3

[7] C. N. Yang, *Phys. Rev.* **77** (1950) 242; N. M. Kroll and W. Wada, *Phys. Rev.* **98** (1955) 1355

[8] M. J. Duncan, G. L. Kane and W. W. Repko, *Phys. Rev. Lett.* **55** (1985) 773

[9] C. A. Nelson, *Phys. Rev.* **D37** (1988) 1220

[10] A. Skjold and P. Osland, *Phys. Lett.* **B311** (1993) 261-265; **B329** (1994) 305-311; *Nucl. Phys.* **B453** (1995) 3-16

[11] H. Pois, T. J. Weiler and T. C. Yuan, *Phys. Rev.* **D47** (1993) 3886

[12] D. Chang, W-Y. Keung and I. Phillips, *Phys. Rev.* **D48** (1993) 3225

[13] V. Barger, K. Cheung, A. Djouadi, B. A. Kniehl and P. M. Zerwas, *Phys. Rev.* **D49** (1994) 79

[14] M. Krämer, J. Kühn, M. L. Stong and P. M. Zerwas, *Z. Phys.* **C64** (1994) 21-30

[15] J. F. Gunion and X-H. He, *Phys. Rev. Lett.* **76** (1996) 4468

[16] P. Osland, *Act. Phys. Pol.* **B30** (1999) 1967

[17] C. A. Bøe, O. M. Ogreid, P. Osland, Jian-zu Zhang, *Eur. Phys. J.* **C9** (1999) 413

[18] G. R. Bower, T. Pierzchała, Z. Wąs and M. Worek, *arXiv:hep-ph/0204292*

[19] M. E. Peskin and D. V. Schroeder, *An Introduction to Quantum Field Theory*, Perseus Books Publishing, L.L.C., 1995

[20] N. Cabibbo, *Phys. Rev. Lett.* **10** (1963) 531;
M. Kobayashi and T. Maskawa, *Prog. Theor. Phys.* **49** (1973) 652

[21] Particle Data Group (D.E. Groom et al.), *Review of Particle Physics, Particle Data Group*, Eur. Phys. J. **C15** (2000) 1-878

[22] A. C. Hearn, *REDUCE User's Manual 3.6*, Konrad-Zuse-Zentrum Berlin, 1993

[23] A. Skjold, *Higgs Boson Production within the Standard Model*, Cand. Scient. Thesis in Theoretical Particle Physics, University of Bergen, 20 Feb, 1992

[24] I. S. Gradshteyn and I. M. Ryzhik, *Table of Integrals, Series and Products* (Corrected and Enlarged Edition), Academic Press, 1980

[25] E. L. Stiefel, *An Introduction to Numerical Mathematics*, Academic Press, 1963

[26] T. Sjöstrand, L. Lönnblad and S. Mrenna, *PYTHIA 6.2, Physics and Manual*, 2001

[27] T. Sjöstrand, P. Edén, C. Friberg, L. Lönnblad, G. Miu, S. Mrenna and E. Norrbin, *Computer Physics Commun.* **135** (2001) 238

[28] *ATLAS Detector and Physics Performance, Technical Design Report*, Volume I, CERN/LHCC/99-14, ATLAS TDR 14, 25 MAY 1999

[29] *ATLAS Detector and Physics Performance, Technical Design Report*, Volume II, CERN/LHCC/99-15, ATLAS TDR 15, 25 MAY 1999

[30] E. W. N. Glover and J. J. Van Der Bij, *Phys. Lett.* **B219** (1989) 488; *Nucl. Phys.* **B321** (1989) 561;

[31] R. W. Brown and K. O. Mikaelian, *Phys. Rev.* **D19** (1979) 922

[32] E. Richter-Wąs, D. Froidevaux, F. Gianotti and L. Poggioli, *ATLAS Internal Note*, Phys-NO-048, 17/07/1995

[33] E. Accomando et al., *Phys. Rept.* **299** (1998) 1-78

[34] W. T. Eadie, D. Drijard, F. E. James, M. Roos, B. Sadoulet, *Statistical Methods in Experimental Physics*, North-Holland, 1971